

**Preparation and Characterisation of Polymer Films from  
Polymerizable Microemulsions**

Miles R Porter MChem

University of Hull

March 2004



For Louise

# ACKNOWLEDGEMENTS

I would like to thank my supervisors Professors Bernie Binks and Paul Fletcher for their guidance and support throughout this Ph.D. Thanks also to Dr. John Clint for several useful discussions.

I would also like to thank Avecia Ltd, Blackley, UK and E. P. S. R. C. for the CASE award that funded this project and in particular Dr. Tom Annable and Dr. Steve Yeates from Avecia for continued interest and many useful discussions on this project.

I would also like to thank many members of the Surfactant and Colloid Group for their friendship and support and for making my time in the group so enjoyable.

I would like to thank my parents, Ray and Margaret, whose early encouragement and faith allowed me to choose the academic paths I have followed.

Last but not least I would like to thank my wife Louise, without whose unending support, understanding and encouragement, neither this thesis nor the work inside it would exist.

# *ABSTRACT*

# ABSTRACT

This thesis is concerned with the microemulsion phase behaviour of polymerizable surfactants with polymerizable oils and water, and the effect of various properties and characteristics of the equilibrium microemulsion phases and their components on the structure of solid polymers prepared by polymerisation of the liquid microemulsion phases. The polymerizable surfactants each contain a polymerizable methacrylate group in one of two possible locations. In two of the surfactants, the methacrylate group is located on the head group of the surfactant and on one the methacrylate group is located on the surfactant tail group. Three oils were used, each possessing an acrylate polymerizable group at either end of the oil molecule.

The characterisation of polymerizable surfactants in aqueous/ polymerizable oil systems at low [surfactant] was observed initially. It was found that the solubility of the surfactants is similarly low in each of the three oils and each surfactant was found to be soluble in water. Stable o/w emulsions were prepared using each of the surfactants with no evidence of phase inversion with temperature observed in any system but phase inversion with electrolyte was observed in some systems. Salt was found to affect the partitioning of each surfactant between water and oil and C<sub>3/11</sub>-M surfactant was found to exhibit an electrolytic effect of its own. Winsor I microemulsion systems were prepared at low [salt] and Winsor II microemulsions were prepared at high [salt] for systems containing HDDA or DPGDA oils for each of

the surfactants. The effects of each of the components present in each system on surfactant partitioning and cmc in water and oil and were observed.

High surfactant concentration microemulsion phases were then prepared using each of the three surfactants with each of the three oils (nine systems) so that the effect of surfactant and oil molecular structure on phase equilibration (location of aggregates, equilibrium phase composition etc.) could be determined. A broad range of phase types were observed, dependent on the structures of the surfactant and oil molecules. Phase inversion due to increasing initial [surfactant] alone (i.e. no added salt) was observed in several systems. The possibility of control of equilibrium water content of the equilibrium microemulsion phases with surfactant concentration was studied. Systems that did not demonstrate phase inversion with initial [surfactant] displayed control of equilibrium water content of the equilibrium microemulsion phases with initial [surfactant]. It was thought that control of porosity of the solid polymers may be possible by controlling the equilibrium water content of the liquid microemulsion.

Solid polymer films were prepared by polymerisation of equilibrium microemulsion phases containing high initial [surfactant] using a photopolymerisation method. 0.1 min using 1 wt. % Darocur 1173 initiator was sufficient UV irradiation time to prepare solid films. The opacity of the polymer films was seen to increase with increasing water content of the parent microemulsion. The strength of the films was seen to decrease with increasing water content of the parent microemulsion. Three different microstructures of polymer films were observed by SEM and were dependent on the structures of the surfactants and oils in the microemulsion. The pore

volume fraction of the polymers was found to be dependent on the microemulsion phase type, including surfactant and oil types and was controllable in several cases by equilibrium water content of the parent microemulsion, therefore by initial [surfactant] in the microemulsion.

# CONTENTS

<b>Chapter 1</b>	<b><u>Introduction</u></b>	<b>1</b>
1.1	Introduction and industrial relevance	1
1.2	Surfactant properties	2
	<i>1.2.1 General surfactant structure</i>	2
	<i>1.2.2 Surfactant adsorption at interfaces</i>	5
	<i>1.2.3 Surfactant aggregation</i>	8
	1.2.3.1 Formation of micelles	8
	1.2.3.2 Structures of microemulsions and relation to preferred monolayer curvature	11
	<i>1.2.4 Relationship between macroemulsion and microemulsion         phase behaviour</i>	18
1.3	<i>Polymerisation of (meth)acrylate species</i>	19
	<i>1.3.1 Monomer structure</i>	19
	<i>1.3.2 Initiators</i>	21
	<i>1.3.3 Polymerisation</i>	23
	<i>1.3.4 Surfactant and oil polymer structures</i>	25
1.4	Review of relevant literature	27
1.5	Aims of the present study	32
1.6	Presentation of this thesis	33
1.7	References	34



<b>Chapter 2</b>	<b><u>Experimental</u></b>	<b>38</b>
2.1	Materials	38
	2.1.1 <i>Water</i>	38
	2.1.2 <i>Polymerizable surfactants</i>	38
	2.1.3 <i>Polymerizable oils</i>	39
	2.1.4 <i>Other chemicals used in emulsions/ microemulsions</i>	40
	2.1.5 <i>Structural materials</i>	41
	2.1.6 <i>General chemicals</i>	41
2.2	Preparation of glassware	43
2.3	Surfactant characterisation	43
	2.3.1 <i>Determination of solubility of surfactants in water and oils</i>	43
	2.3.2 <i>Determination of surfactant purity</i>	44
2.4	Emulsions – preparation and characterisation	44
	2.4.1 <i>Emulsion preparation</i>	44
	2.4.2 <i>Variation of electrolyte concentration</i>	45
	2.4.3 <i>Variation of temperature</i>	45
	2.4.4 <i>Conductivity measurements</i>	45
	2.4.5 <i>Drop test</i>	46
2.5	Preparation of microemulsions – low initial [surfactant]	46
	2.5.1 <i>Variation of electrolyte concentration</i>	46
	2.5.2 <i>Variation of initial surfactant concentration</i>	47
2.6	Preparation of microemulsions – high initial [surfactant]	47
	2.6.1 <i>Systems containing surfactant C<sub>3/11-M</sub> – variation of initial [surfactant]</i>	47
	2.6.2 <i>Systems containing surfactants C<sub>10</sub> or C<sub>12</sub> – variation of initial [surfactant concentration]</i>	48
2.7	Microemulsion phase characterisation	48
	2.7.1 <i>Determination of equilibrium surfactant concentration</i>	

	<i>by Epton titration</i>	48
2.7.2	<i>Determination of equilibrium water content by Karl Fischer titration</i>	50
2.7.3	<i>Calculation of microemulsion phase composition</i>	51
2.8	Purification of surfactant C <sub>3/11-M</sub>	51
2.8.1	<i>Method provided by Avecia</i>	51
2.8.2	<i>Enhanced method</i>	53
2.9	Polymerisation by photo-initiation	53
2.9.1	<i>Polymerisation of oil</i>	53
2.9.2	<i>Polymerisation of C<sub>3/11-M</sub> surfactant solutions</i>	54
2.9.3	<i>Polymerisation cell design</i>	55
	2.9.3.1 Selection of suitable glass	55
	2.9.3.2 Selection of spacer material	55
	2.9.3.3 Determination of absorbance of incident UV by cell	56
2.9.4	<i>Polymerisation of microemulsion phases</i>	56
2.10	Characterisation of polymer films	57
	2.10.1 <i>Visual inspection/ handling</i>	57
	2.10.2 <i>Scanning Electron Microscopy (S.E.M.)</i>	57
	2.10.3 <i>Determination of pore volume fraction of polymer films</i>	58
2.11	References	59
<b>Chapter 3</b>	<b><u>Characterisation of polymerizable surfactants in aqueous/ polymerizable oil systems</u></b>	<b>60</b>
3.1	Introduction	60
3.2	Solubility of surfactants in water and oils	61
3.3	Macroemulsion phase behaviour	63

3.3.1	<i>Emulsion type versus temperature</i>	63
3.3.2	<i>Emulsion type versus salt concentration</i>	66
3.4	Partitioning of surfactant with respect to added electrolyte	67
3.5	Partitioning of surfactant with respect to initial surfactant concentration	70
3.6	Conclusions	79
3.7	References	81
<b>Chapter 4</b>	<b><u>Characterisation of microemulsion systems containing high surfactant concentration</u></b>	<b>83</b>
4.1	Introduction	83
4.2	Microemulsions prepared with H <sub>2</sub> O	84
4.3	Microemulsions prepared with D <sub>2</sub> O in absence of salt	87
4.3.1	<i>Purity issues with surfactant C<sub>3/11-M</sub></i>	87
4.3.1.1	Problems resulting from impurities present in C <sub>3/11-M</sub>	88
4.3.1.1.1	<i>Microemulsion phase equilibration</i>	88
4.3.1.1.2	<i>Purity gradient in sample vessel</i>	88
4.3.1.2	Purification of surfactant C <sub>3/11-M</sub>	90
4.3.1.2.1	<i>Effects on phase equilibration using Avecia method</i>	90
4.3.1.2.2	<i>Modification of purification method</i>	91
4.3.2	<i>Equilibrium phase appearance and partitioning of surfactant</i>	93
4.3.3	<i>Phase composition</i>	97
4.4	Conclusions	108

4.5	References	110
<b>Chapter 5</b>	<b><u>Characterisation of polymer films prepared by polymerisation of equilibrium microemulsion phases</u></b>	<b>112</b>
5.1	Introduction	112
5.2	Polymerisation by photo-initiation	113
	5.2.1 <i>Polymerisation of HDDA oil</i>	114
	5.2.2 <i>Polymerisation of C<sub>3/11-M</sub> aqueous solutions</i>	114
	5.2.3 <i>Polymerisation cell</i>	117
	5.2.3.1 Absorbance of UV by glass	118
	5.2.3.2 Polymerisation cell design	118
	5.2.3.3 Absorbance of incident UV by polymerisation cell containing HDDA oil with initiator	120
5.3	Appearance and strength of polymer films	121
5.4	Microstructure of polymer films	123
	5.4.1 <i>Appearance of films by electron microscopy</i>	123
	5.4.2 <i>Pore volume fraction of polymer films by water absorption</i>	125
6.6	Conclusions	131
6.7	References	134
<b>Chapter 6</b>	<b><u>Conclusions</u></b>	<b>136</b>
6.1	Phase behaviour of polymerizable methacrylate surfactants with polymerizable acrylate oils	136
6.2	Phase equilibration in high surfactant concentration polymerizable	

surfactant and oil systems	138
6.3 Characteristics of polymer films from microemulsions containing polymerizable surfactants and oils	139
<b>Future Work</b>	<b>142</b>
<b>Appendix 1</b> Data presented in Chapter 3	
<b>Appendix 2</b> Data presented in Chapter 4	
<b>Appendix 3</b> Data presented in Chapter 5	

# *CHAPTER 1*

# CHAPTER 1

## INTRODUCTION

### 1.1 Introduction and industrial relevance

This thesis is concerned with the microemulsion phase behaviour of polymerizable surfactants and polymerizable oils and water, and the resulting structure of solid polymer materials formed by polymerisation of the parent liquid microemulsions. Polymerisation of microemulsion systems stabilised by either non-polymerizable or polymerizable surfactants or a mixture of both have been reported in the past with several resulting polymer structures including dispersed latexes and particles,<sup>1-5</sup> polymerised micellar solutions<sup>6-9</sup> and solid polymer films,<sup>10-21</sup> which may be porous depending on the structure of the parent polymerizable microemulsion.<sup>10,11,22-24</sup> A thorough investigation of the microemulsion phase behaviour of the surfactants and oils is of great importance as the structure of the parent microemulsion affects various physical properties of the resulting polymer including opacity, strength and porosity.<sup>6-24</sup> These structural features of the polymer may need to be controlled, which may be achieved by adjustment of the parent microemulsion composition, so that polymers of desired physical properties can be prepared reproducibly.

The work described in this thesis, which was sponsored in part by Avecia Ltd. (Blackley), was initiated by their commercial interest in the coatings used on acetate sheets which allow inkjet printing inks to be deposited on the acetate sheets with a standard, commercially available inkjet printer. These coatings are rough in texture and cause some scattering of light from the projector bulb resulting in a slightly dimmed image. In addition, the cost of acetate sheets for inkjet printing is undesirably high. Polymerizable microemulsions represent an attractive solution to the current problems with ink jet acetate coatings mentioned above, as in some cases, polymers formed by polymerisation of microemulsions are optically transparent, smooth and highly porous,<sup>11,13-15,17-21</sup> which may allow the deposition of ink jet printing ink with desirable results. Avecia have patented the synthesis of several polymerizable surfactants, as commercially available polymerizable surfactants are prohibitively expensive. This thesis describes work using the Avecia surfactants with commercially available polymerizable oils.

In this first chapter, an introduction to relevant surfactant phenomena and polymerisation chemistry is presented together with a section describing the project aims and presentation of this thesis.

## **1.2 Surfactant Properties**

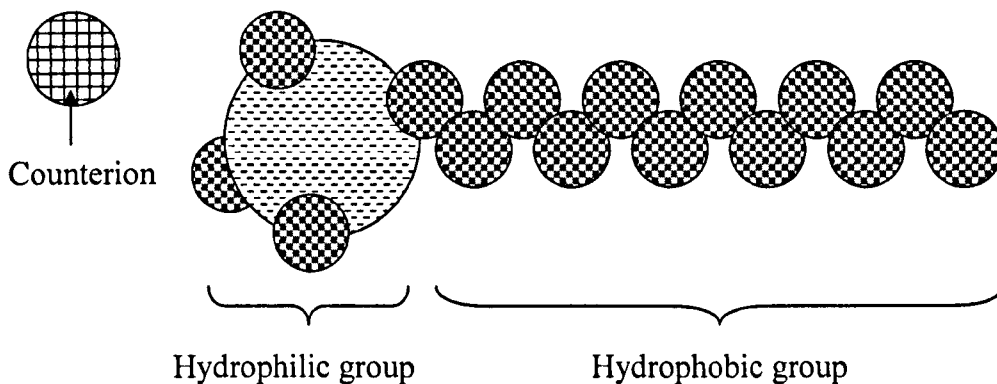
### **1.2.1 General surfactant structure**

The acronym surfactant is derived from the characteristic tendency of these molecules to orient themselves at interfaces (surfaces) and modify the properties of

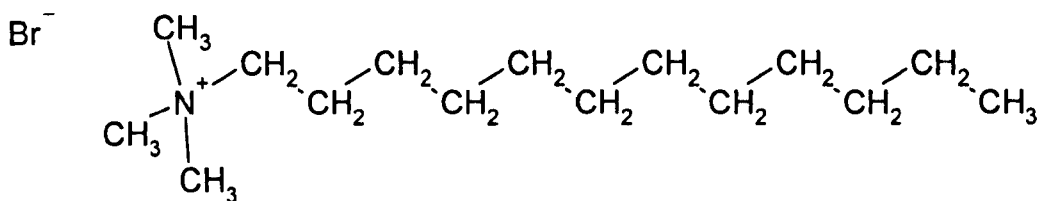


the interface at which they are adsorbed, i.e. SURFace ACTive AgeNT. This tendency to adsorb at interfaces is a result of their amphiphilic nature: part of the surfactant molecule is hydrophilic so will preferably partition into a highly polar environment e.g. water and part of the surfactant molecule is hydrophobic so will preferably partition out of a highly polar environment into e.g. oil. A schematic diagram of a typical surfactant molecule is shown in Figure 1.1 with the molecular structure of this particular surfactant molecule shown in Figure 1.2.

**Figure 1.1. Schematic representation of an ionic surfactant molecule**



**Figure 1.2. Molecular structure of surfactant shown in Figure 1.1**



The hydrophobic part, termed the tail group is usually a single (although a surfactant can contain more than one) aliphatic hydrocarbon chain. The hydrophilic part, termed the head group, can be one of many hundreds of examples some of which are given below. Surfactant types are divided into four main categories based on the chemical properties and charge nature of the hydrophilic head group.<sup>25,26</sup>

### *Nonionic*

These are most commonly of the polyoxyethylene-n-chain ether type and are abbreviated to  $C_nE_m$  where n is the number of carbon atoms in the hydrophobic tail and m is the number of oxyethylene groups on the hydrophilic head, e.g. Penta-oxyethylene-n-dodecyl ether, abbreviated to  $C_{12}E_5$ . Nonionic surfactants are used in many applications including detergents and as emulsifiers.

### *Anionic*

This class of surfactant includes the original carboxylate ( $-CO_2^-$ ) soaps and early sulphonate ( $-SO_3^-$ ) detergents. Anionic surfactants are still used in commercial soaps and detergents today and industrially are a very important class of surfactants.

### *Cationic*

This class of surfactants includes quaternary ammonium salts (the type used in this thesis), imidazolinium and alkyl pyridinium compounds. The positive charge that they carry on the head group leads to considerable adsorption on to negatively charged surfaces such as cotton fibres and hair<sup>25</sup> and for this reason they are used extensively as fabric and hair conditioners.

### *Zwitterionic*

Also referred to as amphoteric surfactants, these include the betaines ( $-\text{N}^+(\text{CH}_3)_2\text{CH}_2\text{CO}_2^-$ ) which are milder on the skin than ionic surfactants<sup>25</sup> and so are used in sensitive personal care products.

Any of the above mentioned classes of surfactant may also contain other functional groups for use in particular applications. Examples include fluorocarbon groups<sup>27,28</sup> or fluorescent groups<sup>29,30</sup> for use in e.g. surfactant molecule adsorption studies<sup>31</sup> and polymerizable groups as described in detail in this thesis. The addition of another functional group, for example a methacrylate polymerizable group, should not significantly alter the surface activity of the surfactant compared to a similar surfactant without this group. This has been demonstrated previously.<sup>32</sup> The additional functional groups may be present on either the head or the tail groups. In the case of polymerizable surfactants, polymerizable groups on the head group (sometimes referred to as H-type) and on the tail group (sometimes referred to as T-type) have been studied. The position of the polymerizable group is shown to affect the structure of the resulting polymer.<sup>33-35</sup> The surfactants used in this study include two H-type surfactants (differing in alkyl tail length) and one T-type (containing a C<sub>11</sub> chain).

#### **1.2.2 Surfactant adsorption at interfaces**

The amphiphilic nature of a surfactant molecule results in unique phenomena when it is placed in solution in (e.g.) water. The hydrophilic part of the surfactant molecule will preferably reside in an aqueous environment and the hydrophobic part will preferably reside out of the aqueous environment. This leads to adsorption at

aqueous/ air (or aqueous/ oil) interfaces where the surfactant molecule can orient itself in an energetically favourable configuration, where the hydrophilic head group is in the aqueous phase and the hydrophobic tail group is in the air (or oil) phase. This process of adsorption at interfaces is driven by the increased ordering of water around the hydrophobic tail group as it resides in an aqueous phase, which results in increased hydrogen bonding of water around the tail and is termed the hydrophobic effect.<sup>36</sup> This increased ordering is energetically unfavourable and so migration of the surfactant molecule to the interface is spontaneous resulting in a decrease in free energy of the system, which is achieved by a lowering of the surface tension at the interface.<sup>25</sup> Surface tension is defined as the reversible work required to form a unit area of surface at constant temperature, pressure and composition.<sup>25</sup> The relation between the amount of surfactant adsorbed under these conditions and the resulting change in surface tension is given by the Gibbs adsorption equation (equation 1.1a)<sup>37</sup>

$$-d\gamma = \sum_i \Gamma_i d\mu_i \quad (1.1a)$$

where  $\gamma$  = the surface tension ( mN m<sup>-1</sup>)

$\Gamma_i$  = the surface excess concentration of species i. Surface excess is defined as the extra amount of species i adsorbed at the surface over and above that which would be present if the bulk concentration was to continue right up to the surface

$\mu_i$  = the chemical potential of species i

$\sum_i$  = the summation for all species i

Assuming ideal behaviour, the position of the surface such that the surface excess concentration of solvent is zero and the presence of only one surface active species (the surfactant  $s$ ), equation 1.1a becomes

$$-d\gamma = \Gamma_s d\mu_s \quad (1.1b)$$

but for changes in surfactant concentration and assuming that surfactant activity is equal to concentration (valid for dilute solutions)<sup>25</sup> the change in surface tension with surfactant concentration ( $c_s$ ) for a nonionic surfactant or an ionic surfactant in the presence of excess electrolyte is given by

$$-d\gamma = \Gamma_s RT d\ln c_s \quad (1.1c)$$

Due to the adsorption of counterions in the case of an ionic surfactant in the absence of excess electrolyte equation 1.1c becomes<sup>37</sup>

$$-d\gamma = \Gamma_s 2RT d\ln c_s \quad (1.1d)$$

Thus, the surface tension is lowered with increasing surfactant concentration. This relation continues until the maximum amount of adsorbed surfactant at the surface is reached, whereupon further increase in [surfactant] will result in aggregation of surfactant in the bulk solution. The [surfactant] where the maximum surface adsorption is reached is called the critical micelle concentration (cmc).

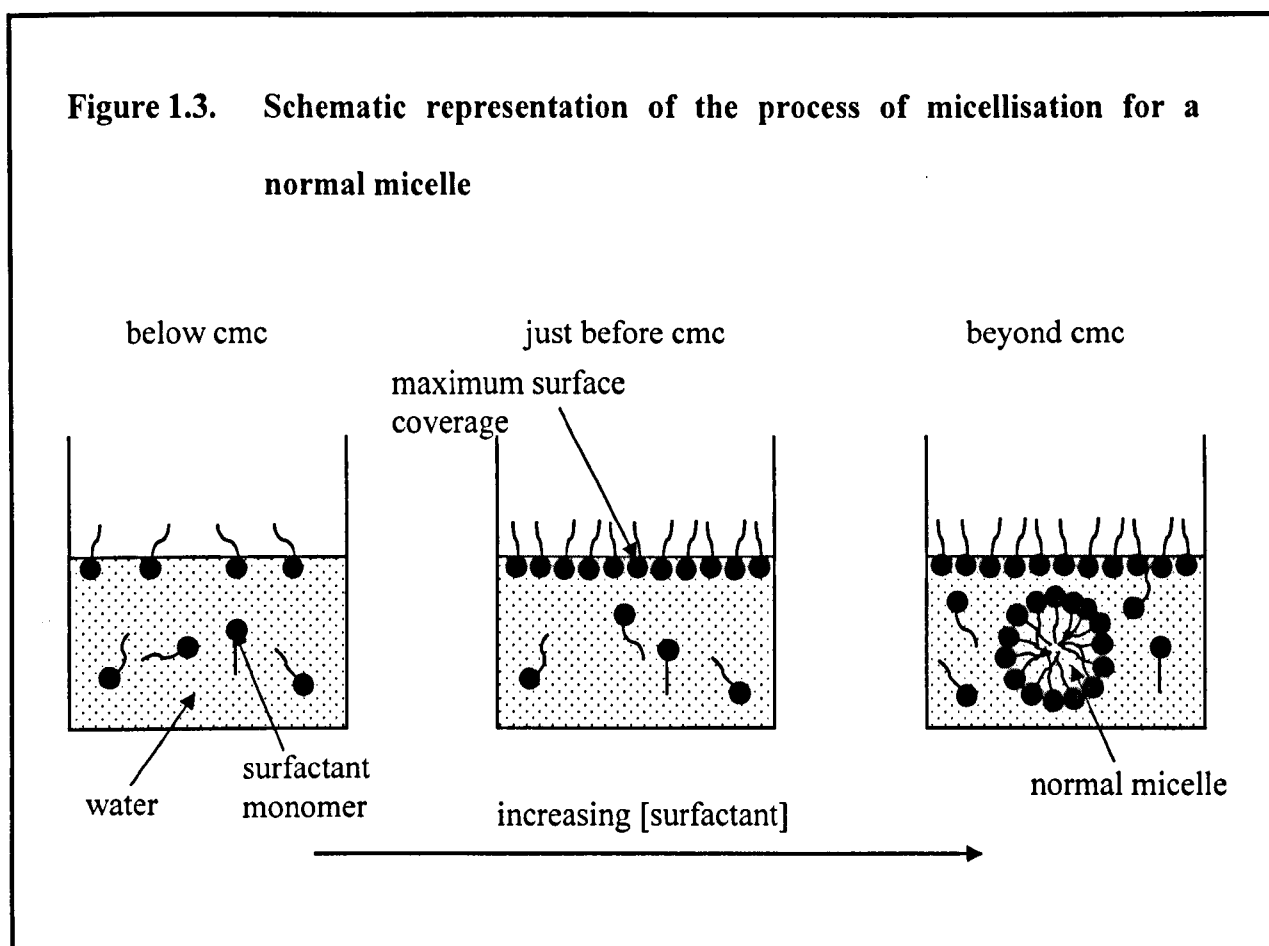
### 1.2.3 Surfactant aggregation

#### 1.2.3.1 Formation of micelles

Once the concentration of surfactant in a solution has reached the cmc, all further surfactant added will aggregate to form structures where the surfactant molecules are arranged such that the head groups will reside in an aqueous like environment and the tail groups will reside in an oil like environment. These structures are called micelles.<sup>25,38,39</sup> The driving force for this phenomenon is the same as that for the case of surfactant adsorption at surfaces i.e. the hydrophobic effect. The free energy of transfer of a hydrocarbon chain (the surfactant tail) from an oil like phase into water is large and positive, reflecting the fact that hydrocarbons have a very low solubility in water.<sup>25</sup> If the surfactant molecules cannot arrange themselves at a surface they will aggregate to form an internal hydrocarbon environment comprised of the surfactant tail groups with the hydrophilic head groups pointing outwards into the water, forming a normal micelle. If the solvent is an oil, then the surfactant molecules will aggregate to form a structure where the hydrophilic head groups form an internal aqueous like environment and the tail groups will point out into the oil, forming a reverse micelle. This process for a normal micelle is shown schematically in Figure 1.3.

The cmc value of a surfactant is related to its hydrophobicity,<sup>25,37</sup> which is itself related to the number of CH<sub>2</sub> groups on the surfactant (tail) chain<sup>40</sup> and for an ionic surfactant with a particular counter-ion, the [counter-ion] in the surfactant solution.<sup>41,42</sup> It has been observed for several different surfactant types that the cmc of

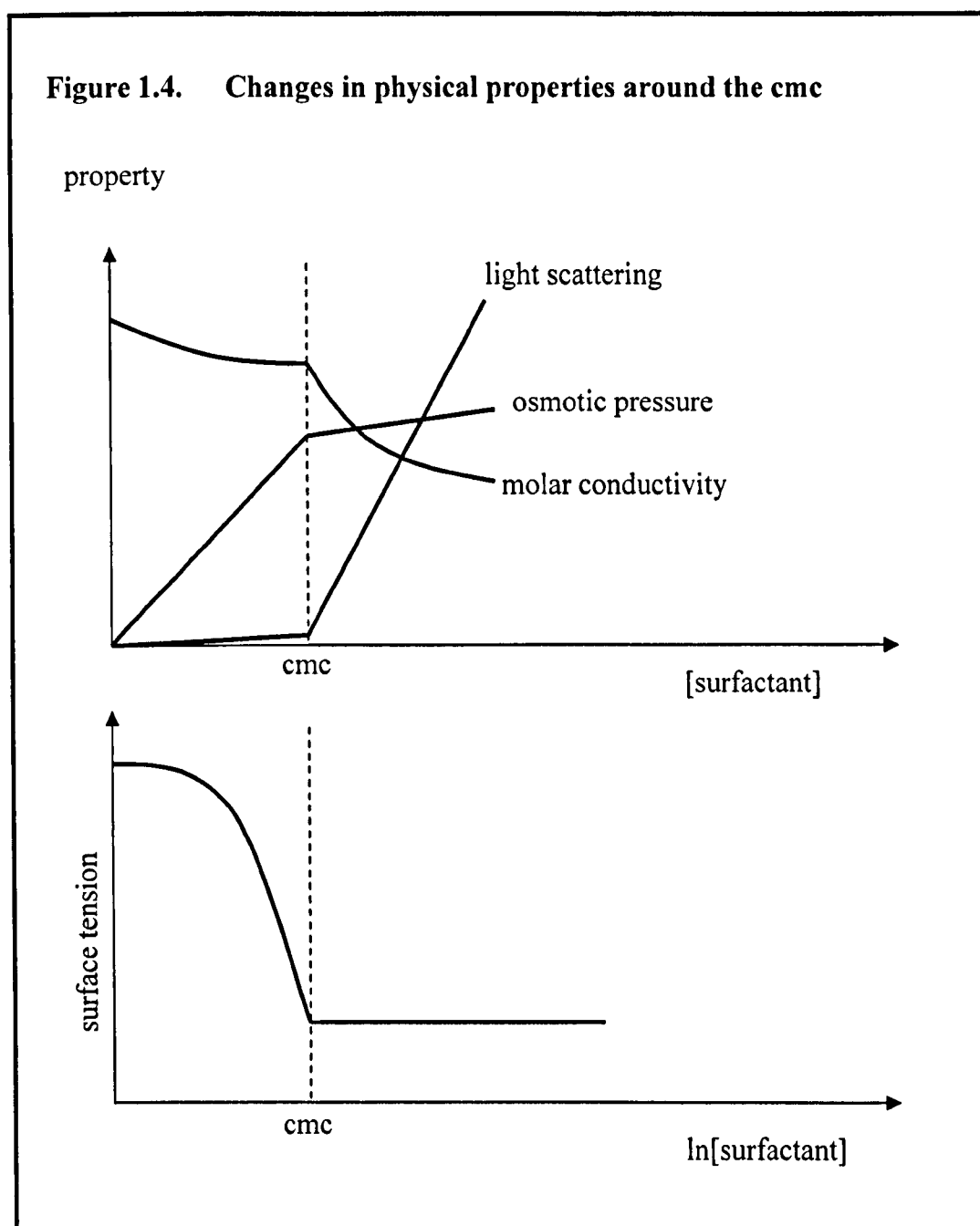
a surfactant decreases by a factor of  $\sim 2$  for each additional  $\text{CH}_2$  group in the surfactant chain.



It has also been observed for several different ionic surfactants (for which the cmc is also affected by chain length) that the cmc for a particular surfactant decreases with [counter-ion] in the aqueous surfactant solution. The standard free energy of micellisation ( $\Delta G_m^\circ$ ) is related to the cmc of the surfactant<sup>25</sup> as shown in equation 1.2

$$\Delta G_m^\circ = RT \ln(\text{cmc}) \quad (1.2)$$

which shows that as cmc decreases (i.e. hydrophobicity of the surfactant increases)  $\Delta G_m^0$  decreases, suggesting that the standard free energy of micellisation decreases with increasing hydrophobicity (increasing tail length) of the surfactant. This has been demonstrated experimentally and a typical reduction in  $\Delta G_m^0$  for each  $\text{CH}_2$  group in the surfactant tail is  $\sim 3 \text{ kJ mol}^{-1}$ .<sup>43,44</sup> A number of physical properties of a surfactant solution change abruptly at the cmc. Figure 1.4 shows a selection of these properties.





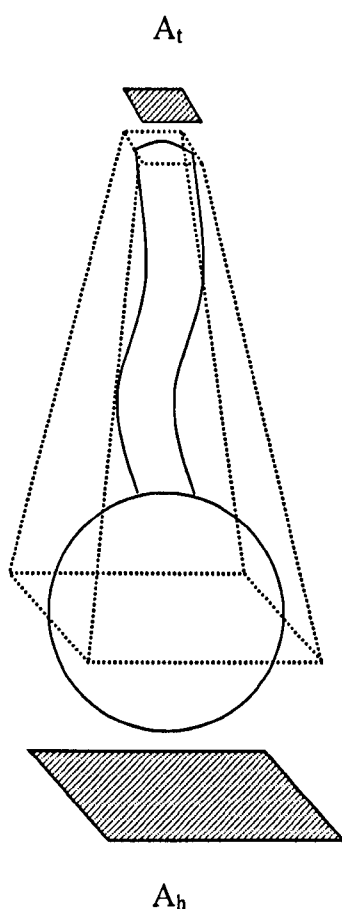
The extent of light scattering increases significantly beyond the cmc as micelles are much larger than surfactant monomers and so scatter light photons to a much greater extent. Osmotic pressure is proportional to the number of particles present in solution and so increases to a much lesser extent with increasing [surfactant] after the cmc, as additional surfactant molecules form micelles containing many surfactant molecules, rather than individual monomers. For ionic surfactants, the molar conductivity shows a break after the cmc as a result of the lower conductivity of micellised surfactant due to the relatively large size and slow movement of micelles. The change in surface tension with increasing [surfactant] is described in 1.2.2.

### ***1.2.3.2 Structures of microemulsions and relation to preferred monolayer curvature***

The type of structure that a particular surfactant will form in a ternary mixture of oil, water and the surfactant is dependent on the structure of the surfactant and in particular the relative cross-sectional areas of the head and tail groups -  $A_h$  and  $A_t$  respectively. Figure 1.5 shows a schematic representation of  $A_h$  and  $A_t$  on a surfactant molecule which is represented as a truncated square pyramid.  $A_h$  and  $A_t$  are generally not equal for a curved monolayer. The packing parameter  $P$ , which is a concept developed by Mitchell and Ninham,<sup>45</sup> is often used to characterise the tendency of a surfactant monolayer to curve. Equation 1.3 defines the packing parameter  $P$ .

$$P = \frac{A_t}{A_h} \quad (1.3)$$

**Figure 1.5. Schematic representation of the relative cross-sectional areas of the surfactant head and tail groups,  $A_h$  and  $A_t$**



The parameter  $P$  is not determined solely by the molecular structure of the surfactant molecule, as if this was the case, a particular surfactant would always form a monolayer with a very specific curvature. This is not the case and monolayer curvature has been shown to be affected by a variety of solution conditions such as temperature,<sup>46</sup> and particularly in the case of ionic surfactants, electrolyte concentration.<sup>26,41,42,47</sup>  $P$ , therefore, is determined by the *effective*  $A_h$  and  $A_t$  of the surfactant which depends on intermolecular interactions *in-situ* in the monolayer, such

as electrostatic and steric forces. If  $P$  is  $<1$ , i.e.  $A_t < A_h$ , then the monolayer curvature is such that the tail groups point towards the centre of the curve and the head groups point outwards (termed positive curvature). This will form normal micelles. If  $P > 1$ , i.e.  $A_t > A_h$ , then the monolayer curvature is such that the head groups will point towards the centre of the curve and the tail groups will point outwards (termed negative curvature). This will form reverse micelles. If  $P \sim 1$  then the monolayer curvature is approximately zero and intermediate structures may form.

If a second phase is present, e.g. oil, with an aqueous surfactant solution above the cmc, then the second phase (termed the dispersed phase) can be solubilised into the core of the micelles present in the first phase (termed the continuous phase) forming a microemulsion. A microemulsion is defined as a thermodynamically stable dispersion of one phase in another phase in which it would be otherwise immiscible. It is important to note that these are thermodynamically stable dispersions and require no energy input in order to form. If the micelles are normal micelles (i.e. positive surfactant monolayer curvature) located in a continuous phase of water, then oil can be solubilised in the hydrocarbon tail core forming an oil-in-water (o/w) microemulsion. If sufficient oil is present such that the surfactant cannot solubilise all of the oil into the micelle cores and the o/w microemulsion phase is in equilibrium with excess oil, then the system is termed a Winsor I microemulsion (WI).<sup>49,50</sup> If the micelles are reverse micelles (i.e. negative surfactant monolayer curvature) located in a continuous phase of oil, then water can be solubilised into the micelle core consisting of the surfactant head groups, forming a water-in-oil (w/o) microemulsion. If sufficient water is present such that the surfactant cannot solubilise all of the water and the w/o microemulsion phase is in equilibrium with an excess water phase, then

the system is termed a Winsor II microemulsion (WII).<sup>49,50</sup> An intermediate structure is possible ( zero net curvature) consisting of domains of water and oil separated by a surfactant monolayer. This forms a sponge-like structure which does not possess definite continuous or dispersed phases and is termed bicontinuous. If the bicontinuous phase is in equilibrium with excess oil and water phases, then the resulting three phase system is termed a Winsor III microemulsion (WIII).<sup>49,50</sup> Figure 1.6 shows the structure of these microemulsion types and Figure 1.7 shows the Winsor phase system of classification.

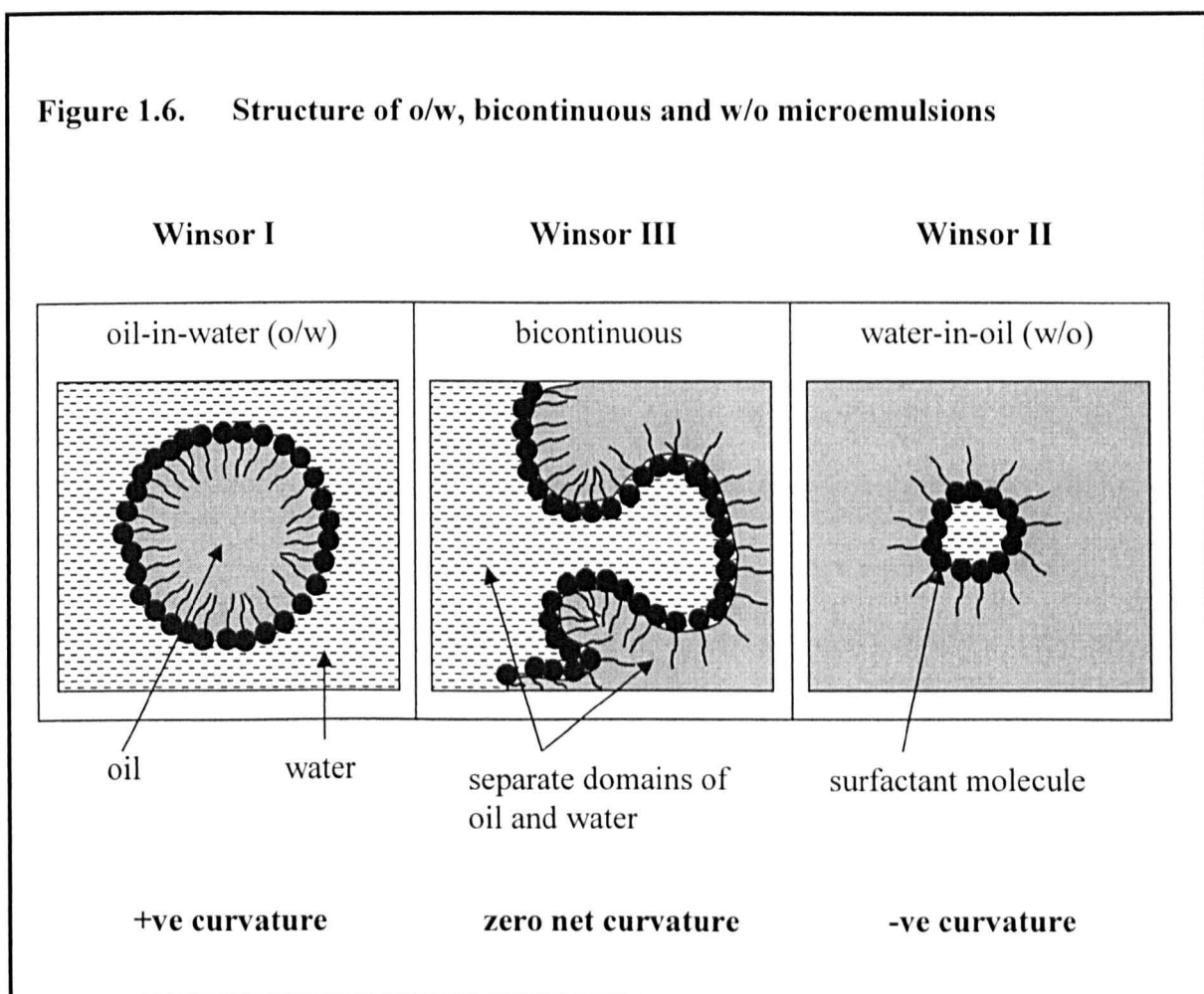
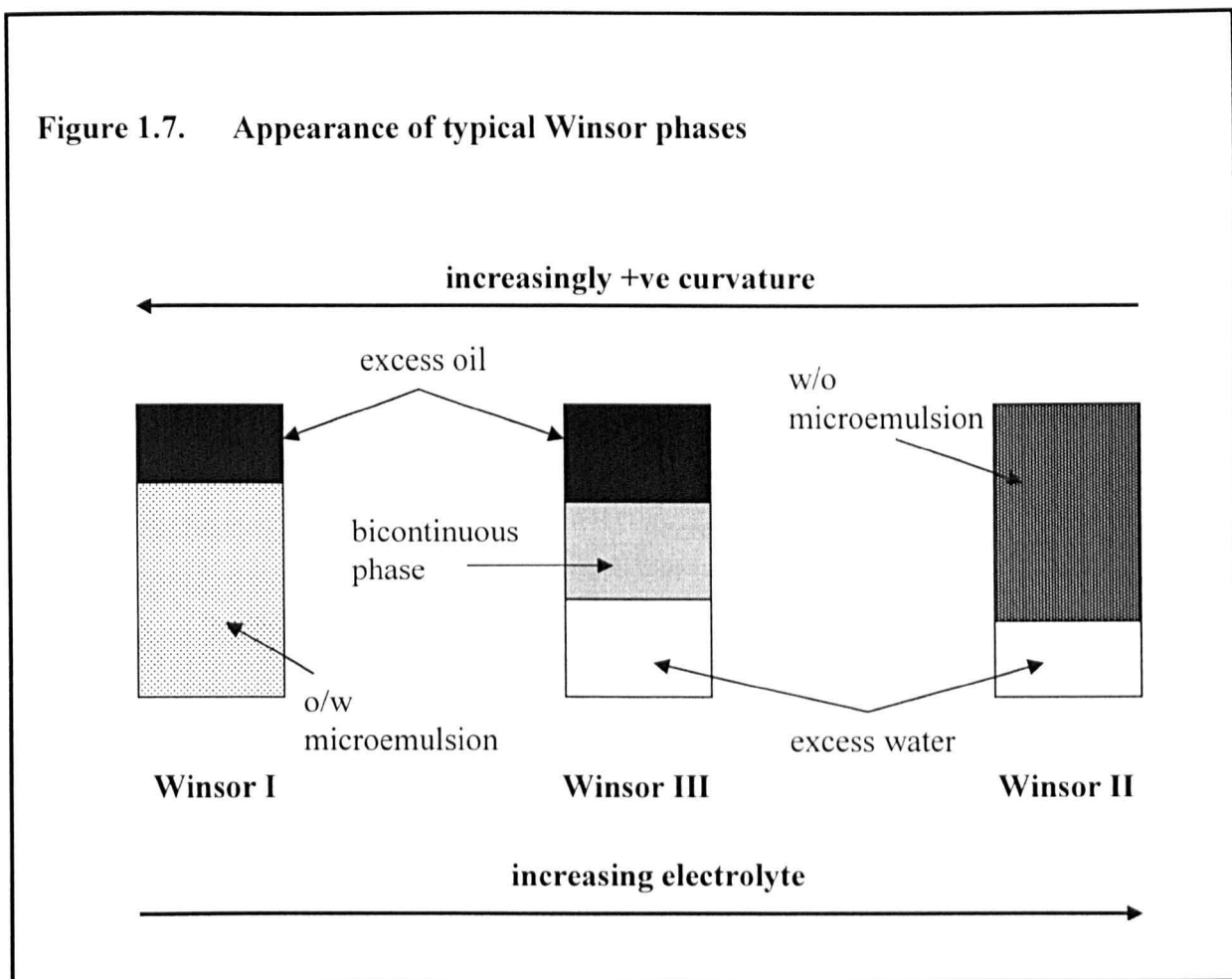
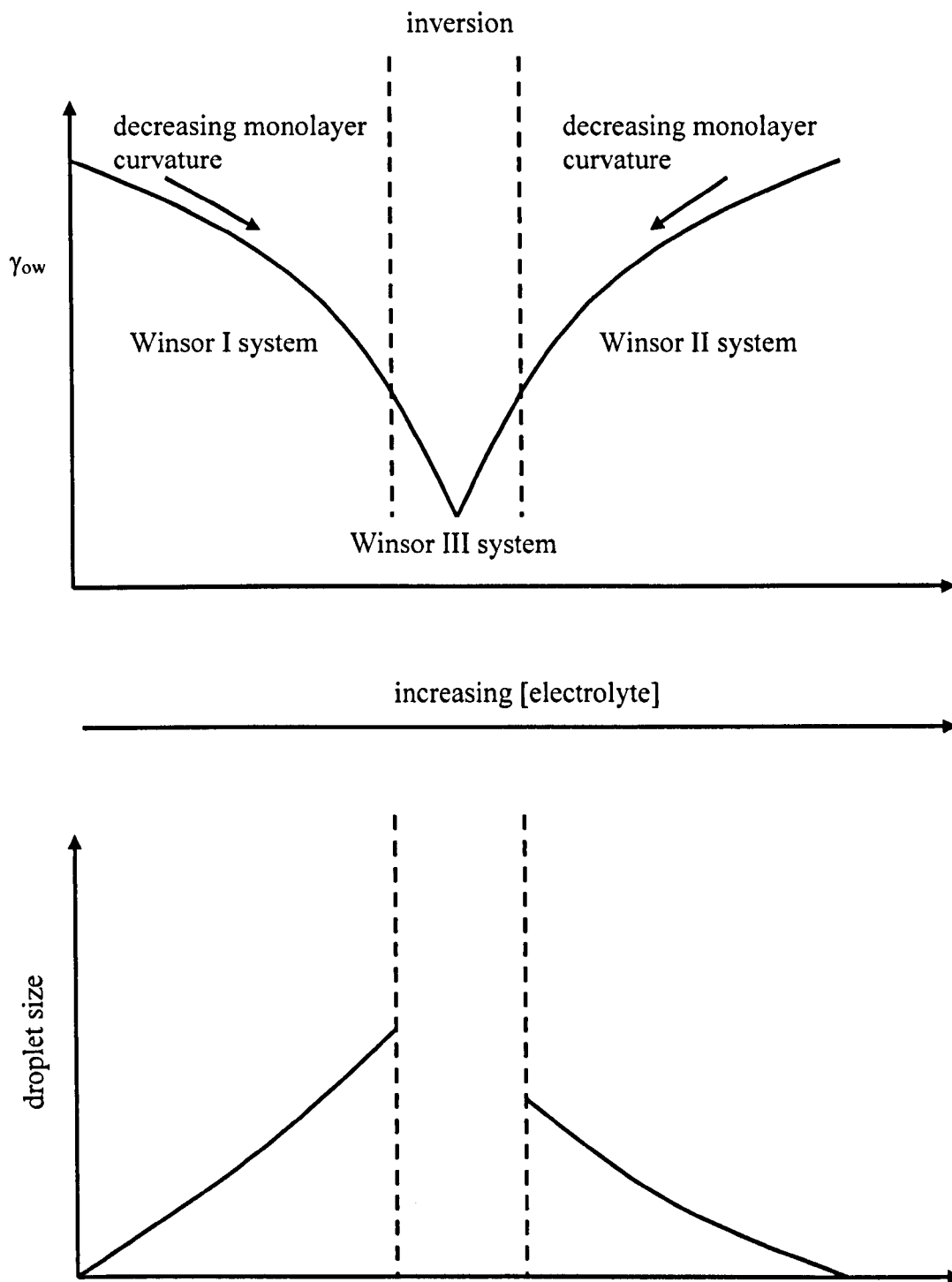


Figure 1.7. Appearance of typical Winsor phases



The ratio  $A_h/A_t$  and therefore the surfactant monolayer curvature can be controlled for a system containing an ionic surfactant by adjustment of the total electrolyte concentration in the aqueous phase in a system of oil, water, ionic surfactant and electrolyte.<sup>26,41,42,46-47</sup> It has been shown that the surfactant itself can act as a weak electrolyte resulting in changing monolayer curvature with [surfactant] alone,<sup>48,51</sup> but in most cases the electrolyte is present as an additional salt, e.g. NaCl. Electrolyte produces this effect by screening the electrostatic repulsion that exists between charged surfactant head groups allowing them to further close pack, thus decreasing the effective size, therefore decreasing  $A_h$ .<sup>26</sup> This decreases  $P$  so the curvature becomes less positive. If sufficient electrolyte is added,  $A_h$  will become smaller than  $A_t$  and the surfactant monolayer curvature will change from positive to

Figure 1.8. Effect of [electrolyte] on oil-water interfacial tension ( $\gamma_{ow}$ ), monolayer curvature, Winsor type and droplet radius ( $r_c$ ) for an ionic surfactant stabilised system



negative, therefore inverting the microemulsion phase type from o/w through bicontinuous and on to w/o. The microemulsion droplet size ( $r_c$ ),<sup>52</sup> tension of the interface between oil and water phases ( $\gamma_{ow}$ )<sup>53</sup> and Winsor type are all dependent on the surfactant monolayer curvature, which is affected by [electrolyte] as shown in Figure 1.8.

The thermodynamically favourable formation of a microemulsion is dependent on the free energy of microemulsion formation ( $\Delta G_m$ ).<sup>53-55</sup> There are two main contributions to this term. The first contribution is from the free energy associated with the increase in interfacial area between the droplet core and the continuous phase as a result of the curvature of the interface. This term is equal to the product of the tension of the curved interface ( $\gamma_{ow}$ ) and the increase in interfacial area ( $\Delta A_{ow}$ ). This is a positive free energy term and therefore disfavours microemulsion formation. The second contribution arises from the change in entropy due to dispersion of the droplets ( $\Delta S$ ) and is equal to the product of absolute temperature (T) and  $\Delta S$ . This is a negative and therefore favourable free energy term. The total free energy of microemulsion formation is given by the difference between these two terms and is shown in equation 1.4.

$$\Delta G_m = \gamma_{ow} \Delta A_{ow} - T \Delta S \quad (1.4)$$

Microemulsion drops are typically around 5 - 100 nm in diameter and scatter light weakly. Assuming spherical, monodisperse drops, equation 1.5 gives the relationship between the radius of the droplet core ( $r_c$ ) and the microemulsion composition,

$$r_c = \frac{3V_{dc}}{A_s} \left( \frac{[\text{dispersed component}]}{[\text{surfactant}] - \text{cmc}} \right) \quad (1.5)$$

where  $V_{dc}$  is the molecular volume of the dispersed component and  $A_s$  is the area per surfactant molecule at the surface of the droplet. This model predicts that the droplet diameter is proportional to the ratio of molar concentration of the dispersed phase to that of the surfactant, i.e. to the extent of solubilisation of the dispersed phase. This means that as  $[\text{surfactant}]$  is increased in a system, unless the ratio of molar concentration of dispersed phase to surfactant is kept constant, the droplet size should decrease. This simple model does not take into account any secondary effect of increase in  $[\text{surfactant}]$  such as additional electrolytic effect for a charged surfactant.

#### **1.2.4 Relationship between macroemulsion and microemulsion phase behaviour**

Macroemulsions are thermodynamically unstable but can be kinetically stable dispersions of oil in water (or *vice versa*) stabilised by a surfactant monolayer (or particles)<sup>56-58</sup>, with droplet sizes in the micrometer range.<sup>59</sup> The droplets cause considerable scattering of light and as a result are opaque and white. Over time the emulsion will phase separate into two or more equilibrium phases. This is in contrast to microemulsions, which are thermodynamically stable dispersions with droplet sizes in the nanometer range also stabilised by a surfactant monolayer and scatter light weakly so are generally optically clear or blueish. It is frequently observed that the phase behaviour of macro and microemulsions stabilised by the same surfactant is



very similar in relation to continuous phase<sup>60,61</sup> and phase inversion values with temperature and [electrolyte].<sup>41,47</sup> A common example is with phase type. If an o/w (WI) microemulsion system is homogenised, the resulting macroemulsion will consist of micrometer sized oil drops in a continuous phase of an o/w microemulsion, i.e both micro and macroemulsions possess a water continuous phase.<sup>60,61</sup> Another example is the [salt] at which a system will invert from o/w to w/o, which is frequently found to be similar for macro and microemulsions stabilised by the same surfactant.<sup>41,55</sup> A number of studies have developed the understanding of how the macroemulsion and microemulsion types are related and it is likely that the spontaneous curvature of the surfactant monolayer is central to this correlation.<sup>62-64</sup>

### **1.3 Polymerisation of (meth)acrylate species**

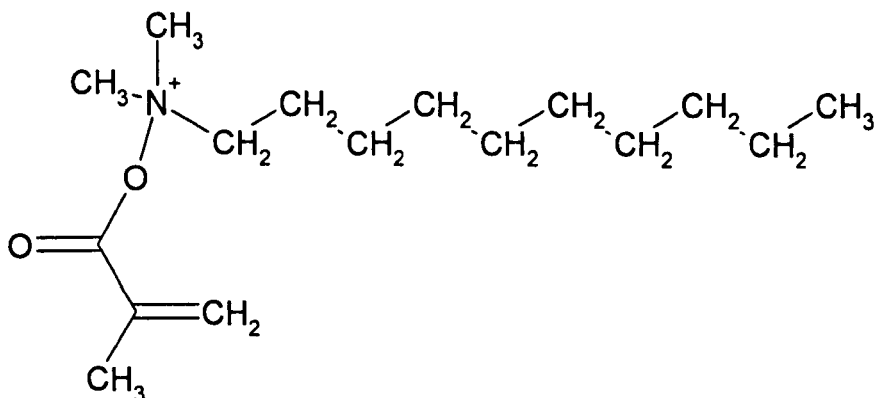
The surfactants and oils used for emulsion and microemulsion preparation in this thesis are polymerizable due to the presence of a methacrylate group in the surfactant molecules and two acrylate groups in the oil molecules. This section describes some common features of methacrylate and acrylate polymerisation and the separate steps involved in a free radical addition polymerisation reaction.

#### **1.3.1 Monomer structure**

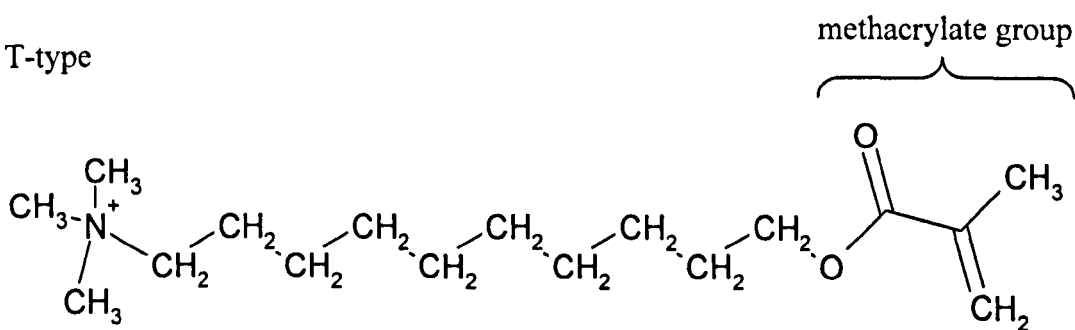
The surfactant monomers used in this study contain a polymerizable methacrylate group on either the head group (H-type) or the tail group (T-type) of the surfactant. These two examples are shown in Figure 1.9a. The oil monomers used in

**Figure 1.9a. Location and structure of a methacrylate group on H-type and T-type surfactants**

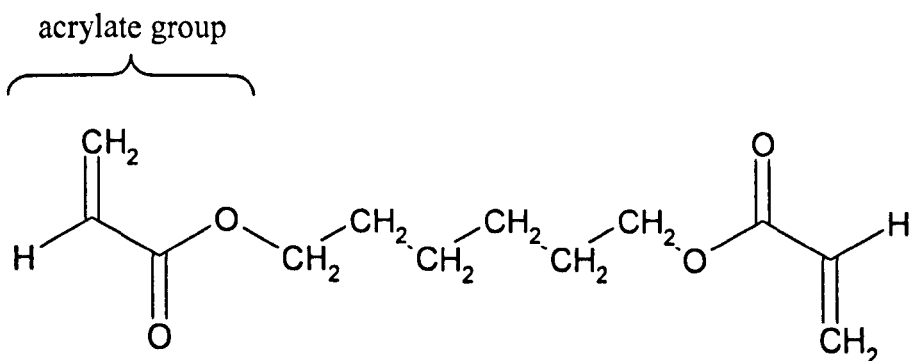
H-Type



T-type



**Figure 1.9b. Location and structure of acrylate group on polymerizable oils**

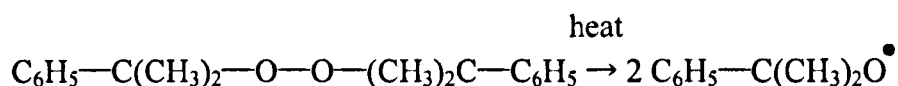


this study contain an acrylate polymerizable group at either end of the oil molecule. This is shown in Figure 1.9b. The polymerizable group consists of a carbon-carbon  $\pi$  bond with one of the carbons  $\sigma$  bonded to a second carbon atom bonded to two oxygen atoms which are strongly electron withdrawing. This arrangement makes the carbon-carbon double bond susceptible to rearrangement if activated by free radical or ionic initiators.<sup>67</sup> This results in a free radical active centre which will propagate a chain reaction resulting in polymer chain growth until the active centre is deactivated by a termination reaction. This process is described in detail later. The structure of the resulting polymer is of the same composition as the monomer but multiplied n times where n is the number of monomer units bonded to form the polymer. The electrons in the carbon-carbon  $\pi$  bond within each monomer are simply rearranged to account for the  $\sigma$  bonding between monomer units.

### 1.3.2 Initiators

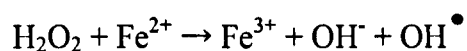
Several methods of producing free radical initiators are possible and include thermal decomposition, redox reactions, ionising radiation and photolysis. The choice of reaction type depends on the polymerizable species and desired polymer structure.

- (i) thermal decomposition (e.g. dicumyl peroxide)



(ii) redox reaction

A radical is produced by the simultaneous reduction of one species in its reaction with another to yield a free radical molecule e.g. addition of an iron<sup>(II)</sup> salt to hydrogen peroxide results in oxidation of the iron to iron<sup>(III)</sup> and reduction of the peroxide to an OH<sup>-</sup> ion and a free radical OH<sup>•</sup> molecule:



(iii) ionising radiation

Strong particular (e.g.  $\alpha$  or  $\beta$ ) or electromagnetic (e.g.  $\gamma$  or X-rays) radiation can be used to produce radicals in a three stage process involving ejection of an electron from an initiator molecule followed by dissociation of the initiator and electron capture of the polymerizable material to produce a propagating radical molecule.

(iv) photolysis

This method involves the irradiation using UV of an initiator molecule, which decomposes to form two radical containing molecules, which then initiate the polymerisation reaction e.g. photolysis of Darocur 1173:

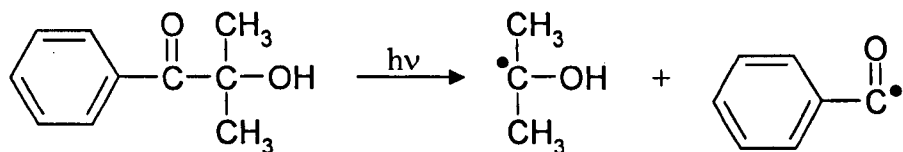


Photo-initiation was the method chosen for this study as the other methods require either reaction conditions or the presence of highly reactive species that would disturb the microemulsion equilibrium to a significant extent and may prevent the microstructure of the microemulsions from being retained during the polymerisation process.

### 1.3.3 Polymerisation

Polymerisation by free radical addition can be separated into three distinct stages:

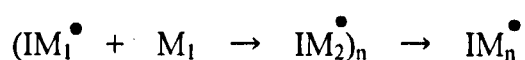
#### (i) Initiation

As described above, the polymerisation reaction is initiated by a source of radicals produced according to necessary reaction conditions. Usually, an initiator molecule (I) is required and should be chosen so as not to interfere with any equilibrium which is desired to be maintained during the polymerisation reaction. The initiator radical reacts with a polymerizable monomer (M) to form a monomer radical ( $\text{IM}^\bullet$ ). Once this initial source of free radicals has been produced, the polymerisation chain reaction should sustain itself. Photo-initiation is used as an example below:



(ii) Propagation

The monomer radical then reacts with a second polymerizable monomer to form a dimer radical. This chain propagation proceeds by addition, forming a polymer chain. This chain reaction can lead to polymers containing over 1000 units, so the presence of the initiator molecule at the end of the chain has little or no consequence to the overall polymer structure.



This continues until a termination reaction occurs.

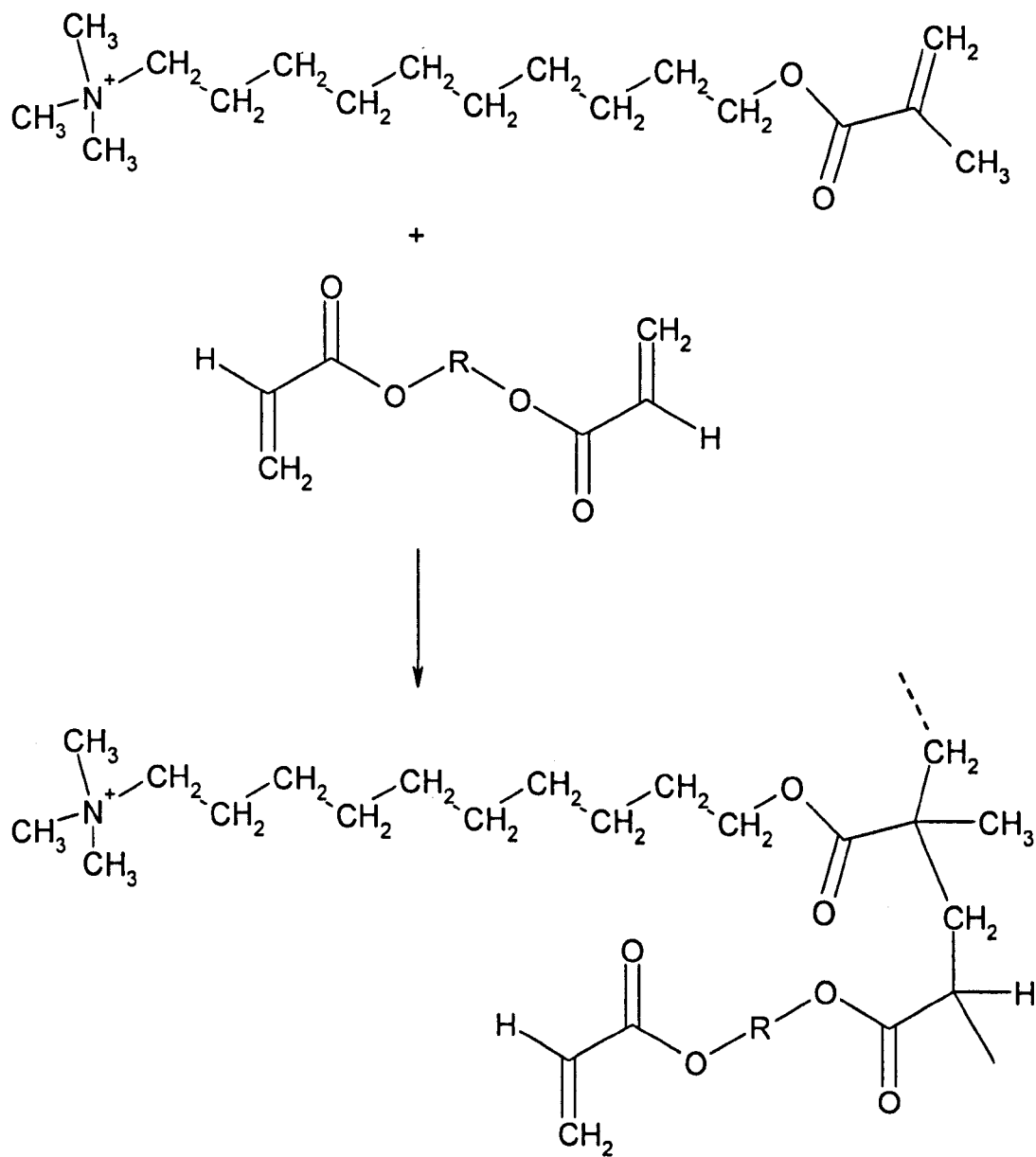
(iii) Termination

The chain propagation reaction of a single growing polymer chain in radical addition polymerisation is terminated long before all the reactive monomer in solution is used up by the growing polymer chain. This is a result of the high reactivity of radical species which quickly react to form inactive covalent bonds. Several termination reactions are possible: a) the combination of two growing chain ends, b) the combination of a growing polymer chain end and an active initiator molecule, c) transfer of the active centre to the solvent, or d) interaction of the radical with inhibitors (e.g. oxygen). The length of the final polymer chain is inversely proportional to the concentration of active radical species present in a particular system<sup>65</sup> due to the increased number of termination reactions possible, so low concentrations of initiator are necessary to produce long polymer chains.

### 1.3.4 Surfactant and oil polymer structures

The surfactants and oils used in the work described in this thesis are copolymerizable. The acrylate groups of the oils can polymerise with the methacrylate groups of the surfactant and acrylate groups of other oil molecules giving rise to many possible oil-surfactant polymer arrangements. Figure 1.10 shows one such possible reaction between a diacrylate oil (HDDA) and a T-type methacrylate surfactant C<sub>3/11-M</sub> (see Chapter 2).

**Figure 1.10. A possible polymer repeating unit of a diacrylate oil and methacrylate T-type surfactant**



The second acrylate group in the oil may react with either another oil acrylate group or a second surfactant methacrylate group.



## 1.4 Review of relevant literature

Several authors have described the preparation of porous polymeric materials from the direct polymerisation of microemulsions. The effects of several factors have been investigated on the control of the opacity and porosity of the polymers. The adjustment of amount and type of monomer oil and water content of the parent microemulsion has been studied by Gan and co-workers<sup>11,19-21,66</sup> in systems consisting of a polymerisable zwitterionic surfactant ((acryloyloxy)undecyldimethylammonium-acetate, AUDMAA), methyl methacrylate (MMA) and water with 2 wt. % cross-linking agent ethylene glycol dimethacrylate (EGDMA). It was found that increasing the [MMA] from 40 to 60 wt. % and reducing the water content from 30 to 20 wt. %, the resulting polymers moved from clear to turbid although the pre-cursor bicontinuous microemulsion used in each case was clear. The pore sizes of the turbid polymers were not given but the bicontinuous structure-like channels in the clear polymers range from 50-70 nm in width and 100-200 nm in length. Chew et al.<sup>21</sup> observed the effect of adding a different monomer oil to a system on polymer pore size. The system consisted of water (30 wt. %), MMA oil (42 wt. %) and polymerizable surfactant AUDMAA (26.46 wt. %) with 1.54 wt. % cross-linker (EGDMA) and a polymerisation initiator. It was found that the addition of 2-hydroxyethyl methacrylate (HEMA) oil up to 12.6 wt. % was found to reduce the pore size of the resulting polymers from 40-50 nm with no HEMA, to 20-25 nm with 4.2 wt. % HEMA and to 1.6 nm with 12.6 wt. % HEMA. The pre-cursor microemulsions were bicontinuous in structure and this structure was observed to be preserved in the final polymer.

The adjustment of water content in pre-cursor microemulsions has been shown to have a marked effect on pore size and appearance of the final polymers. Liu et al.<sup>19</sup> describe adjustment of water content from 25 to 45 wt. % in a system consisting of water, polymerisable surfactant macromonomer  $\omega$ -methoxy-poly(ethylene oxide)<sub>40</sub>-undecyl- $\alpha$ -methacrylate (C<sub>1</sub>-PEO-C<sub>11</sub>-MA-40) at concentrations of 26.25-19.25 wt. %, and an oil monomer mixture consisting of 95 wt. % MMA plus HEMA (1:1) and 5 wt. % EGDMA from 48.75 to 35.75 wt. %. The increase in water content was found to increase the pore size from 1.1 nm at 25 wt. % water to 3.6 nm at 45 wt. % water. The pre-cursor microemulsions were again bicontinuous in structure and this was preserved to yield a bicontinuous structured clear polymer. This data agrees with that in a similar system.<sup>11</sup>

The [surfactant] in the pre-cursor microemulsion has also been shown to have an effect on pore size and appearance of the final polymer.<sup>11,13,19,67</sup> Chieng et al.<sup>13</sup> describe this effect in a system containing water (54-48 wt. %), MMA (8 wt. %), HEMA (32 wt. %), non-polymerizable surfactant DTAB (6-12 wt. %), cross-linker EGDMA (4 wt. %) and initiator dibenzyl ketone (DBK, 0.3 wt. %). The microemulsions used were bicontinuous but this structure was not preserved on polymerisation. The resulting porous polymers consisted of latex particles coagulated together to form interconnected globules and the [surfactant] was found to affect the size of these globules and hence the pore size. The system with 6 wt. % DTAB produced an opaque polymer with pore sizes between 1-3  $\mu$ m. Increasing [DTAB] to 12 wt. % resulted in a clear polymer with pore sizes in the range 50-200 nm. This is because a higher surfactant concentration can stabilise a greater number of oil-water domains, so the average size of these decreases as their number increases. Chieng et

al.<sup>66</sup> describe a system of 18 wt. % MMA, 42 wt. % HEMA, 33.2-28.0 wt. % water and DTAB surfactant 6.8-12 wt. %. The opacity of the final polymer was found to decrease on increasing DTAB content in the pre-cursor microemulsions. The microemulsions were bicontinuous and clear and it was found that this structure was not preserved in systems of low DTAB concentration (6.8-8 wt. %) but was preserved in systems with 10-12 wt. % DTAB. The pore sizes of the polymers were not given but electron micrographs of the polymers show the pore sizes to be in the  $\mu\text{m}$  range in systems with low DTAB concentration but in the nm range for systems with high DTAB concentration. The type of surfactant was also investigated in this paper and a system very similar to that described above but with non-polymerizable anionic surfactant sodium dodecyl sulphate (SDS) at 4-10 wt. % in place of cationic DTAB was polymerised and the appearance of the final polymers was observed using electron microscopy. Again the pre-cursor microemulsions were bicontinuous but this structure was not seen to be preserved at any of the SDS concentrations used with all resulting polymers being opaque. It is thought that the higher flexibility of the DTAB monolayer film compared to that of SDS and the strong interaction with copolymers of MMA and HEMA may be responsible for the higher stability of these systems, which leads to the formation of globular aggregates with smaller pore sizes in the DTAB polymers.

The effect of long and short alkyl chain length cationic surfactants on polymer structure has also been investigated.<sup>66</sup> Bicontinuous microemulsions consisted of MMA and HEMA with weight ratio maintained at 1:4 at a total concentration of 50 wt. % and an aqueous solution of 20 % surfactant mixture of hexyltrimethylammonium bromide ( $\text{C}_6\text{TAB}$ ), dodecyltrimethylammonium bromide

(C<sub>12</sub>TAB) and cetyltrimethylammonium bromide (C<sub>16</sub>TAB) also at a total concentration of 50 wt. %. It was found that increasing the ratio of short chain surfactant to long chain surfactant reduced the pore size in both systems. In the system with C<sub>16</sub>TAB and C<sub>12</sub>TAB the pore size of the resulting polymer was reduced from 50-300 nm with 25 % C<sub>12</sub>TAB to 50-100 nm with equal amounts of C<sub>12</sub>TAB and C<sub>16</sub>TAB to 20-100 nm with 100% C<sub>12</sub>TAB. In the system with C<sub>16</sub>TAB and C<sub>6</sub>TAB this effect was even more pronounced with the pore size reducing from 0.2-1.0 µm with 20 % C<sub>6</sub>TAB to 50-200 nm with 40 % C<sub>6</sub>TAB. This is thought to be due to the effect of a shorter chain on the surfactant producing smaller aggregates in the microemulsion that polymerise to produce a polymer with smaller pores. It was found that good control over the pore size could be achieved with mixing short and long chain surfactants in the pre-cursor microemulsion.

The effect of salt in a pre-cursor microemulsion on the appearance of the resulting polymer was studied by Chew et al.<sup>21</sup> in a system containing 40 wt. % aqueous solution of NaCl, 32.29 wt. % AUDMAA, 26.24 wt. % MMA, 1.17 wt. % EGDMA and 0.12 wt. % DMPA. Bicontinuous microemulsions were produced and polymerised with the concentration of salt in the aqueous solution increasing from 0-3.0 wt. %. The pore size of resulting polymers was found to increase with salt from 40-60 nm with no salt to 50-70 nm with 1 wt. % salt to pore sizes in the micrometer range with 3.0 wt. % giving polymers with a hazy appearance. This is due to the effect of an electrolyte on de-stabilising the bicontinuous structure of a microemulsion as phase inversion is approached.

Much of the work described in the literature describes the polymerisation of bicontinuous microemulsions<sup>11,13,15-18,20,21,66</sup> as the preservation of this sponge-like structure leads to a polymer consisting of nm sized channels. The factors described above can alter this structure and thus alter the structure of the final polymeric material providing a means of controlling the structure of the polymer. The literature also suggests that a polymerisable surfactant capable of copolymerisation with the oil is necessary to achieve preservation of the bicontinuous structure although this has not been investigated in depth.

Detailed studies of the effect of molecular structure of a series of similar surfactants and independently the effect of molecular structure of a series of similar polymerizable oils on the phase equilibration of microemulsions containing the surfactants, water and the oils have not been carried out. In particular, the effect of various parameters such as [surfactant] and type, oil type and overall composition of the microemulsion system has not been related to Winsor phase behaviour of systems containing polymerizable surfactants and oils. While some work on the effect of composition of microemulsion phases on the structure of the resulting polymers has been reported, the work does not describe broad ranges of [surfactant], oil content and water content either for one particular system or a range of similar systems. Most of the work reported in the preparation of solid polymers from microemulsions is concerned with the polymerisation of bicontinuous phases. This thesis describes the effects of microemulsion properties mentioned above on various physical properties of the resulting polymers and describes the polymerisation of several microemulsion phase types.

## 1.5 Aims of the present study

The aim of the work described in this thesis has been twofold:

(a) To gain an increased understanding of the phase equilibration of systems of water, each of the polymerizable oils and each of the polymerizable surfactants at low and high initial [surfactant]. Although polymerizable surfactants have been used with polymerizable oils for the polymerisation of microemulsions in the past, very little work has been done on the characterisation of ternary systems of water, oil and surfactant with polymerizable species. A sound knowledge of the partitioning data, cmcs in water and oils, and phase inversion characteristics is required before reproducible microemulsion phases can be prepared with desired characteristics such as aggregate type and composition.

(b) To polymerise microemulsion phases and determine the characteristic features of the parent liquid microemulsion which yields polymers with desired properties such as optical clarity, strength and porosity. Fine tuning of the microemulsion composition may be required to prepare microemulsions which would polymerise to form polymers with all of the desired properties as it is possible that the microemulsion properties which result in one particular desirable polymer property may prevent polymers with a second desirable property from being produced. It was necessary to determine how the interaction of particular features of the parent microemulsions affects the overall properties of the solid polymer.

## 1.6 Presentation of this thesis

Chapter 2 describes the experimental procedures used to collect the data presented in the thesis and describes all chemicals and materials used. Chapter 3 describes the characterisation of the polymerizable surfactants in aqueous/polymerizable oil systems at low surfactant concentration. The solubility of the surfactants in water and the three oils, macroemulsion trends and partitioning characteristics of the surfactants between water and the oils is described. Chapter 4 describes microemulsion equilibration using the nine surfactant-oil combinations with high surfactant content. The aggregate type, phase equilibration in relation to Winsor type and composition of the equilibrium phases prepared is discussed. Chapter 5 describes the polymerisation of the equilibrium phases described in Chapter 4 and relates the features of the parent microemulsions to characteristic features of the polymers. The effect of aggregate type, composition and equilibrium water content of the microemulsion phases on optical clarity, strength and pore volume fraction is discussed. Chapter 6 draws the conclusions of the previous chapters together in an attempt to correlate the equilibrium polymerizable microemulsion properties with the solid polymer properties.

## 1.7 References

- <sup>1</sup> F. Candau, M. Pabon and J. Anquetil, *Colloids Surfaces A*, **153**, 47 (1999).
- <sup>2</sup> M. E. Treviño, R. G. López, R. D. Peralta, F. Becerra, E. Mendizabal and J. E. Puig, *Polymer Bulletin*, **42**, 411 (1999).
- <sup>3</sup> X. J. Xu, C. H. Chew, K. S. Siow, M. K. Wong and L. M. Gan, *Langmuir*, **15**, 8067 (1999).
- <sup>4</sup> C. Larpent and T. F. Tadros, *Colloid Polym. Sci.*, **269**, 1171 (1991).
- <sup>5</sup> M. Summers, J. Eastoe and S. Davis, *Langmuir*, **18**, 5023 (2002).
- <sup>6</sup> M. Summers and J. Eastoe, *Langmuir*, **19**, 6357 (2003).
- <sup>7</sup> M. Summers, J. Eastoe, S. Davis, Z. Du, R. M. Richardson, R. K. Heenan, D. Steytler and I. Grillo, *Langmuir*, **17**, 5388 (2001).
- <sup>8</sup> M. Summers, J. Eastoe, R. K. Heenan, D. Steytler and I. Grillo, *J. Disp. Sci. Technol.*, **22**, 597 (2001).
- <sup>9</sup> C. Larpent, E. Bernard, J. Richard and S. Vaslin, *Macromolecules*, **30**, 354 (1997).
- <sup>10</sup> W. Palani Raj, M. Sasthav and H. M. Chung, *Langmuir*, **7**, 2586 (1991).
- <sup>11</sup> L. M. Gan, T. D. Li, C. H. Chew and W. K. Teo, *Langmuir*, **11**, 3316 (1995).
- <sup>12</sup> M. Sasthav and H. M. Chung, *Langmuir*, **7**, 1378 (1991).
- <sup>13</sup> T. H. Chieng, L. M. Gan, C. H. Chew, L. Lee, S. C. Ng, K. L. Pey and D. Grant, *Langmuir*, **11**, 3321 (1995).
- <sup>14</sup> W. Palani Raj, M. Sasthav and H. M. Chung, *Langmuir*, **7**, 2586 (1991).
- <sup>15</sup> T. H. Chieng, L. M. Gan, C. H. Chew, S. C. Ng and K. L. Pey, *Langmuir*, **12**, 319 (1996).
- <sup>16</sup> W. Xu, K. S. Siow, Z. Gao, S. Y. Lee, P. Y. Chow and L. M. Gan, *Langmuir*, **15**, 4812 (1999).



- <sup>17</sup> T. D. Li, L. M. Gan, C. H. Chew, W. K. Teo and L. H. Gan, *Langmuir*, **12**, 5863 (1996).
- <sup>18</sup> C. H. Chew, L. M. Gan, L. H. Ong, K. Zhang, T. D. Li, T. P. Loh and P. M. MacDonald, *Langmuir*, **13**, 2917 (1997).
- <sup>19</sup> J. Liu, L. M. Gan, C. H. Chew, W. K. Teo and L. H. Gan, *Langmuir*, **13**, 6421 (1997).
- <sup>20</sup> T. D. Li, L. M. Gan, C. H. Chew, W. K. Teo and L. H. Gan, *J. Membr. Sci.*, **133**, 177 (1997).
- <sup>21</sup> C. H. Chew, T. D. Li, L. H. Gan, C. H. Queck and L. M. Gan, *Langmuir*, **14**, 6068 (1998).
- <sup>22</sup> F. M. Menger, T. Tsuno and G. S. Hammond, *J. Am. Chem. Soc.*, **112**, 1263 (1990).
- <sup>23</sup> M. Antonietti, R. Basten and F. Gröhn, *Langmuir*, **10**, 2498 (1994).
- <sup>24</sup> A. Aguiar, S. González-Villegas, M. Rabelero, E. Mendezabal, J. E. Ping, J. M. Dominguez and I. Katime, *Macromolecules*, **32**, 6767 (1999).
- <sup>25</sup> J. H. Clint, 'Surfactant Aggregation', Blackie, London (1992).
- <sup>26</sup> M. J. Rosen, 'Surfactants and Interfacial phenomena', Wiley, New York (1998).
- <sup>27</sup> J. Eastoe, A. Paul, A. Rankin, R. Wat, J. Penfold, J. R. P. Webster, *Langmuir*, **17**, 7873 (2001).
- <sup>28</sup> J. Eastoe, A. Rankin, R. Wat, C. D. Bain, D. Styrkas and J. Penfold, *Langmuir*, **19**, 7734 (2003).
- <sup>29</sup> P. Taylor, C. Xu, P. D. I. Fletcher and V. N. Paunov, *Chem. Commun.*, 1732 (2003).
- <sup>30</sup> O. Cayre, V. N. Paunov and O. D. Velev, *J. Mat. Chem.*, **13**, 2445 (2003).
- <sup>31</sup> O. Cayre, V. N. Paunov and O. D. Velev, *Chem. Commun.*, 2296 (2003).
- <sup>32</sup> A. Bumajdad, J. Eastoe, R. K. Heenan, J. R. Lu, D. C. Steytler and P. Timmins, *Langmuir*, **15**, 5271 (1998).

- <sup>33</sup> M. Dreja and B. Tieke, *Macromol. Rapid Commun.*, **17**, 825 (1996).
- <sup>34</sup> M. Dreja, W. Pyckhout-Hintzen and B. Tieke, *Macromolecules*, **31**, 272 (1998).
- <sup>35</sup> M. Pyrasch and B. Tieke, *Colloid Polym. Sci.*, **278**, 375 (2000).
- <sup>36</sup> C. Tanford, 'The Hydrophobic Effect: Formation of Micelles and Biological Membranes', 2nd Ed., Wiley, New York (1980).
- <sup>37</sup> R. Aveyard, D. A. Haydon, 'An Introduction to the Principles of Surface Chemistry', Cambridge University Press, Cambridge (1973).
- <sup>38</sup> G. S. Hartley, 'Aqueous solutions of Paraffin Chain salts', Hermann & Cie, Paris (1936).
- <sup>39</sup> D. J. Shaw, Introduction to Colloid and Surface Chemistry (4<sup>th</sup> edition), Butterworth-Heinemann, Oxford (1992).
- <sup>40</sup> P. Mukerjee, K. J. Mysels, 'Critical Micelle Concentrations of Aqueous Surfactant Systems', National Bureau of Standards, Washington (1971).
- <sup>41</sup> B. P. Binks, *Colloids and Surfaces A*, **71**, 167 (1993).
- <sup>42</sup> R. Aveyard, B. P. Binks, S. Clark, P. D. I. Fletcher, H. Giddings, P. A. Kingston and A. Pitt, *Colloids and Surfaces*, **59**, 97 (1991).
- <sup>43</sup> J. M. Corkill, J. F. Goodmann and J. R. Tate, *Trans. Faraday Soc.*, **60**, 996 (1964).
- <sup>44</sup> L. Benjamin, *J. Phys. Chem.*, **68**, 3575 (1964).
- <sup>45</sup> D. J. Mitchell and B. W. Ninham, *J. Chem. Soc. Faraday Trans. II*, **77**, 601 (1981).
- <sup>46</sup> R. Aveyard, B. P. Binks and J. Mead, *J. Chem. Soc. Faraday Trans. I*, **81**, 2169 (1985).
- <sup>47</sup> B. P. Binks, J. Dong and N. Rebolj, *Phys. Chem. Chem. Phys.*, **1**, 2335 (1999).
- <sup>48</sup> R. Aveyard, B. P. Binks, P. J. Dowding, P. D. I. Fletcher, C. E. Rutherford and B. Vincent, *Phys. Chem. Chem. Phys.*, **1**, 1971 (1999).
- <sup>49</sup> P. A. Winsor, 'Solvent Properties of Amphiphilic Compounds', Butterworths,

London (1954).

- <sup>50</sup> P. A. Winsor, *Trans. Faraday Soc.*, **44**, 376 (1948).
- <sup>51</sup> P. D. I. Fletcher, *J. Chem. Soc. Faraday Trans. I*, **83**, 1493 (1987).
- <sup>52</sup> B. P. Binks, J. Meunier, O. Abillon and D. Langevin, *Langmuir*, **5**, 415 (1989).
- <sup>53</sup> R. Aveyard, *Chemistry & Industry*, 474 (1987).
- <sup>54</sup> M. E. Cates, D. Andelman, S. A. Safran and D. Roux, *Langmuir*, **4**, 802 (1988).
- <sup>55</sup> E. Ruckenstein, *J. Colloid Int. Sci.*, **114**, 173 (1986).
- <sup>56</sup> S. U. Pickering, *J. Chem. Soc.*, **91**, 2001 (1907).
- <sup>57</sup> B. P. Binks and S. O. Lumsdon, *Langmuir*, **16**, 2539 (2000).
- <sup>58</sup> B. P. Binks and J. A. Rodrigues, *Langmuir*, **19**, 4905 (2003).
- <sup>59</sup> B. P. Binks (Ed), 'Modern Aspects of Emulsion Science', Royal Society of Chemistry, Cambridge (1998).
- <sup>60</sup> H. Kunieda and K. Shinoda, *J. Colloid Int. Sci.*, **106**, 107 (1985).
- <sup>61</sup> J. L. Salager, G. López-Castellanos, M. Miñana-Peréz, C. Parra, C. Cucuphat, A. Graciaa and J. Lachaise, *J. Disp. Sci. Technol.*, **12**, 59 (1991).
- <sup>62</sup> R. Aveyard, B. P. Binks, T. A. Lawless and J. Mead, *J. Chem. Soc. Faraday Trans. I*, **81**, 2155 (1995).
- <sup>63</sup> H. Smith, G. C. Covatch and K. H. Lim, *J. Phys. Chem.*, **95**, 1463 (1991).
- <sup>64</sup> A. Kabalnov and H. Wennerström, *Langmuir*, **12**, 276 (1996).
- <sup>65</sup> J. M. G. Cowie, 'Polymers: Chemistry and Physics of Modern Materials', 2<sup>nd</sup> Ed., Blackie Academic, Glasgow (1991).
- <sup>66</sup> T. H. Chieng, L. M. Gan, C. H. Chew, S. C. Ng and K. L. Pey, *Polymer*, **37**, 4823 (1996).
- <sup>67</sup> T. H. Chieng, L. M. Gan, W. K. Teo and K. L. Pey, *Polymer*, **37**, 5917 (1996).

# *CHAPTER 2*

# CHAPTER 2

## EXPERIMENTAL

### 2.1 Materials

#### 2.1.1 Water

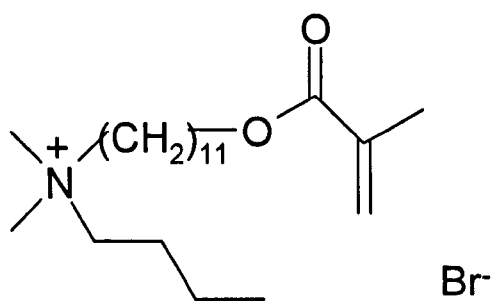
All water used in the study was purified firstly by reverse osmosis (Elgastat Prima – Elga) and then with a Milli-Q reagent water system (Millipore). After this purification, its surface tension was  $71.9 \pm 0.1 \text{ mN m}^{-1}$  at  $25 \text{ }^\circ\text{C}$  which is in good agreement with literature values,<sup>1</sup> indicating the absence of surface active impurities.

#### 2.1.2 Polymerizable surfactants

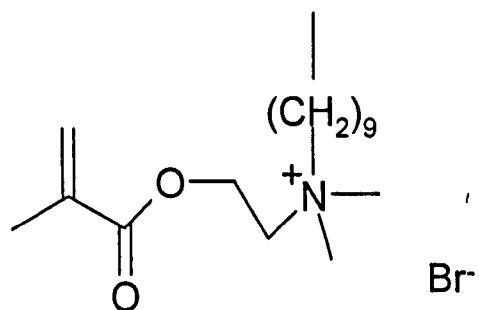
All polymerizable surfactants used in this work are quaternary ammonium salts and were synthesised and supplied by AVECIA Ltd., Blackley, Manchester, UK. Each surfactant molecule contains a polymerizable methacrylate group. Table 2.1 lists the purities as supplied and the appearance of each surfactant along with the batch numbers. The purities were measured by Epton titration.<sup>2</sup> Figure 2.1 shows the molecular structure of each surfactant.<sup>3</sup> Surfactants C<sub>10</sub> and C<sub>12</sub> are structurally similar in that the polymerizable methacrylate group is located on the hydrophilic head group. The difference between C<sub>10</sub> and C<sub>12</sub> is the length of the hydrophobic tail group as

**Figure 2.1. Molecular structures of the three polymerizable surfactants used in this study**

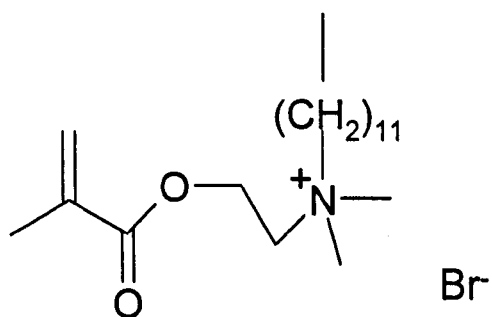
**C<sub>3/11</sub>-M**



**C<sub>10</sub>**



**C<sub>12</sub>**



shown in Figure 2.1. Surfactant C<sub>3/11-M</sub> has a quite different structure to C<sub>10</sub> and C<sub>12</sub> surfactants. C<sub>3/11-M</sub> contains a four carbon chain on the hydrophilic head group and the polymerizable methacrylate group is located at the end of the 11 carbon hydrophobic tail.

**Table 2.1. Purity, appearance and batch numbers of polymerizable surfactants**

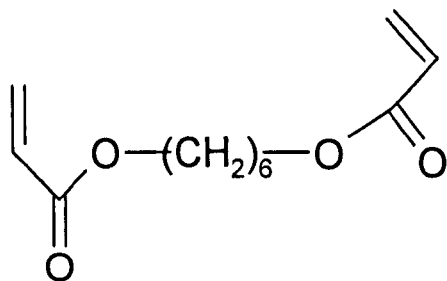
<b>Surfactant</b>	<b>Purity (as supplied) / %</b>	<b>Appearance</b>	<b>Batch number</b>
C <sub>10</sub>	99	White powder	NBZ-1206/39
C <sub>12</sub>	99	White powder	6/6/00
C <sub>3/11-M</sub>	82 - 89	Brownish oil	NBZ-1877-77 and 17/5/01

### 2.1.3 Polymerizable oils

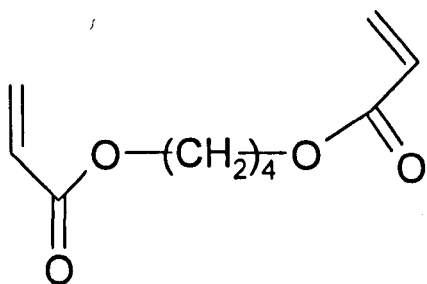
The polymerizable oils used were selected by Avecia Ltd. from many commercially available polymerizable oils due to their acrylate polymerizable groups present which can co-polymerise satisfactorily with the methacrylate group present on the polymerizable surfactant molecules.<sup>4</sup> Table 2.2 lists the source, purity and the batch number of each oil. Figure 2.2 shows the molecular structure of each oil.

**Figure 2.2. Molecular structures of the three polymerizable oils used in this study**

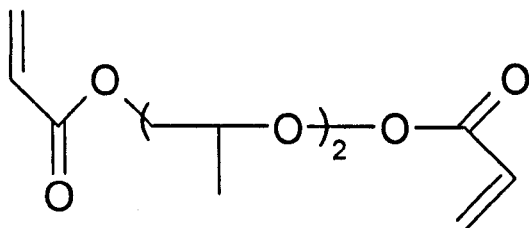
**1,6-hexanedioldiacrylate (HDDA)**



**1,4-butanedioldiacrylate (BDDA)**



**Dipropyleneglycoldiacrylate (DPGDA)**





**Table 2.2. Source, purity and batch numbers of polymerizable oils**

<b>Oil</b>	<b>Source</b>	<b>Purity</b>	<b>Batch number</b>
HDDA	Union Chimique Belge (UCB)	High Grade	61002785
BDDA	Aldrich	Tech (>90 %)	06318 MU
DPGDA	UCB	High Grade	61003418

#### 2.1.4 Other chemicals used in emulsions/ microemulsions

Several other materials have been used in this work for the preparation of emulsions and microemulsions in addition to water and the polymerizable oils and surfactants. Table 2.3 lists these materials along with their source, purity and relevant notes.

**Table 2.3. Name, source, purity and notes for other materials used in the preparation of emulsions and microemulsions**

<b>Chemical</b>	<b>Source</b>	<b>Purity</b>	<b>Batch</b>
NaBr	BDH	Specially pure ( $\geq 99.9\%$ )	392499/1
D <sub>2</sub> O	Aldrich	99.9 %	10156
D <sub>2</sub> O	Apollo Scientific	> 99 %	0210

### 2.1.5 Structural materials

In addition to the chemicals described above several structural materials were used in this work, mainly for the polymerisation study. The materials along with their source, purity and relevant notes are given in Table 2.4.

**Table 2.4. Name, source, purity and notes for structural materials**

<b>Material</b>	<b>Source</b>	<b>Purity</b>	<b>Notes</b>
Glass slide 1	Menzel-Glaser	-	Extra-white glass
Glass slide 2	Chance Propper	-	Blue star 1.2 mm
Cover slip	Chance Propper	-	No. 1 <sup>1</sup> / <sub>2</sub>
Aluminium foil	Aluchef	> 99 %	12.0 ± 0.5 µm thick
Aluminium foil	Goodfellows	> 99 %	50.0 µm thick

### 2.1.6 General chemicals

Chemicals used in this work for purposes other than the preparation of emulsions or microemulsions are given, along with their source, purity and relevant notes in Table 2.5. Where possible, the same batch of a particular chemical was used throughout the work.

**Table 2.5. Name, source, purity and notes for general chemicals used in this work for purposes other than the preparation of emulsions/microemulsions**

<b>Chemical</b>	<b>Source</b>	<b>Purity</b>	<b>Notes/ batch</b>
Sodium Dodecyl Sulphate (SDS)	BDH	Specially pure ( $\geq 99.9\%$ )	0567028K
CHCl <sub>3</sub>	Fisher	>99%	0240014, 0249926
HCl s.g. 1.83	Fisher	98%	0083042
TTAB	Sigma	>99%	Purified
Dimidium bromide	Sigma	>99%	19H3600
Disulphine blue	Sigma	>99%	105H3410
Darocur 1173	Ciba	99 %	Kept out of sunlight
Hexane	Fisher	HPLC	9953582 509
Ethanol	Fisher	AR Grade	0240255
Diethyl ether	Fisher	Analysis	0240041
Methanol	Fisher	HPLC grade	0132861
Hydranal Coulomat CG (Karl Fischer)	Riedel-de Haën	N/A	Lot 2031 C
Hydranal Coulomat AG (Karl Fischer)	Riedel-de Haën	N/A	Lot 12130
Silica, Merck grade 9385, 230-400 mesh, 60 angstrom	Aldrich	N/A	507527-071
Filter agent Celite 521	Aldrich	N/A	03717LO

## **2.2 Preparation of glassware**

Prior to use, all glassware was firstly washed in warm soapy water then rinsed thoroughly with water purified by reverse osmosis using the Elgastat reverse osmosis setup. Following this, glassware was cleaned by submerging and rinsing several times in alcoholic potassium hydroxide, followed by thorough rinsing with water purified by reverse osmosis and a final rinse with Milli-Q water. The glassware was then dried in an oven.

## **2.3 Surfactant characterisation**

### **2.3.1 Determination of solubility of surfactants in water and oils**

#### *Method 1*

Using 5 ml ampoules, an accurately weighed (using a Precisa balance XT220A) mass of surfactant was placed in 1 ml of water or the oil being used as the solvent and the ampoule was sealed using a Bunsen flame. This was then placed in the well of a thermostatted Grant LTD 6G water bath and left for 20 minutes at each temperature to allow a reasonable time for the surfactant to dissolve. The temperature was increased in 5 °C increments and the sample was observed to see if dissolution had occurred at the end of each 20 minute period.

## *Method 2*

Accurately weighed (using a Precisa balance XT220A) amounts of surfactant C<sub>12</sub> were placed in the solvent (water or oil) in a small, stoppered test tube. Concentrations from 0.2 – 5.0 wt. % were used. These were left to dissolve with gentle stirring in a thermostatted water bath at 25 °C for several days (i.e. constant temperature) and the extent of dissolution observed visually.

### **2.3.2 Determination of surfactant purity**

An accurately weighed (using a Precisa balance XT220A) amount of the surfactant of interest was placed in a large sample tube (Quickfit 150 mm, B24). This was then titrated against SDS using the standard Epton titration procedure (see 2.7.1) and the purity calculated as total cationic species present. This measurement was repeated a further two times and the average of the three values taken.

## **2.4 Emulsions – preparation and characterisation**

### **2.4.1 Emulsion preparation**

From a stock solution of 1 wt. % surfactant dissolved in Milli-Q water, 4 ml was added to a small (i.d.12 mm, length 50 mm) specimen tube followed by 4 ml of the monomer oil. The mixture was then homogenised using an Ultra Turrax T25 homogeniser at 11,000 rpm equipped with a small (8 mm) head for 2 minutes. This method has been reported as a suitable method of emulsion preparation.<sup>5</sup>

#### **2.4.2 Variation of electrolyte concentration**

For variation of salt concentration, the method described in 2.4.1 was slightly altered. 2 ml of 2 wt. % aqueous surfactant solution was added to a small specimen tube, followed by 2 ml of aqueous NaBr solution at double the concentration required in the total aqueous phase (made from dilution of a stock salt solution). This mixture was then shaken and 4 ml of the monomer oil added, followed by homogenisation as described above.

#### **2.4.3 Variation of temperature**

The method of emulsion preparation described in 2.4.1 was followed (i.e. fixed electrolyte concentration). The conductivity of the emulsions was measured as described in 2.4.4 below with the temperature increased in 5 °C increments between measurements. The emulsion mixture was equilibrated in the water bath for 5 minutes at each desired temperature then re-homogenised as described above before the conductivity of the emulsion was measured.

#### **2.4.4 Conductivity measurements**

Once the emulsion had been formed, the sample tube containing it was placed directly in the well of a Grant LTD 6G thermostatted water bath at a set temperature and left for 5 minutes to equilibrate. The exact temperature of the emulsion was checked using a glass bulb mercury thermometer to 0.1°C. The emulsion was re-homogenised and the conductivity of the emulsion measured using a PTI – 18 digital conductivity meter (later changed to a Jenway 4310 digital conductivity meter)

equipped with a glass bodied Pt-Pt black electrode. Emulsions were re-homogenised for 2 minutes before each conductivity measurement. The conductivity of a 0.1 M solution of KCl in Milli-Q water was measured using the equipment described above and gave a value of  $12.88 \text{ mS cm}^{-1}$ , which agrees well with literature values.<sup>6</sup>

#### **2.4.5 Drop test**

Using a Pasteur pipette, a small drop ( $\sim 0.05 \text{ ml}$ ) of emulsion (or microemulsion) was dropped into a small beaker containing one of the possible continuous phases of the emulsion or microemulsion (water,  $\text{D}_2\text{O}$  or one of the three polymerizable oils). If the droplet is seen to disperse immediately in the liquid contained in the beaker then the continuous phase of the emulsion or microemulsion is likely to be the same as this liquid. If a water continuous emulsion or microemulsion droplet is placed into oil then the droplet remains intact. If  $\text{D}_2\text{O}$  is used as the continuous phase, the droplet will sink to the bottom. If an oil continuous emulsion or microemulsion is dropped into water (or  $\text{D}_2\text{O}$ ) then the droplet will rapidly spread along the surface and then disperse into the water.

### **2.5 Preparation of microemulsions – low initial [surfactant]**

#### **2.5.1 Variation of electrolyte concentration**

2 ml of 2 wt. % aqueous surfactant was placed in a small test tube (13 x 75 mm internal diameter) containing a small magnetic stirrer bar. 2 ml of double the concentration of NaBr required initially in the aqueous phase was then added. This

produced 4 ml of 1 wt. % surfactant with the required NaBr concentration. This was then shaken well and 4 ml of the monomer oil was then added very gently down the side of tube so as not to cause any initial mixing of the two phases. Six of these tubes were then placed in a beaker filled with water which was itself placed in a water tank thermostatted by a Grant LTD 6G water bath at 25 °C above a Variomag V15 magnetic stirrer set on the slowest setting. This was then left for 7 days to equilibrate.

### **2.5.2 Variation of initial surfactant concentration**

2 ml of a solution of surfactant at double the concentration required in the initial aqueous phase (from stock solution dilution) was placed in a small sample tube containing a small magnetic stirrer bar, followed by 2 ml of NaBr solution at double the concentration required in the initial aqueous phase (also from stock solutions). This produced a 4 ml solution of surfactant and salt at the required concentrations. The rest of the procedure was carried out as described in 2.5.1.

## **2.6 Preparation of microemulsions – high initial [surfactant]**

### **2.6.1 Systems containing surfactant C<sub>3/11-M</sub> – variation of initial [surfactant]**

The samples were prepared by adding a portion of stock solution of 1.30 M C<sub>3/11-M</sub> in D<sub>2</sub>O to a small sample tube, then diluting with D<sub>2</sub>O and shaken to produce 4.00 ml of initial aqueous phase at the required surfactant concentration. 4.00 ml of oil was then added very gently down the side of the sample tube along with a small magnetic flea. The sample tubes were placed in a two-walled water tank connected to



a Grant LTD 6G water bath at 25 °C. The tank was positioned on a Camlab Variomag electronically HP15 stirrer set at 100 r.p.m. and the system left to equilibrate for 7 days.

## **2.6.2 Systems containing surfactants C<sub>10</sub> or C<sub>12</sub> – variation of initial [surfactant]**

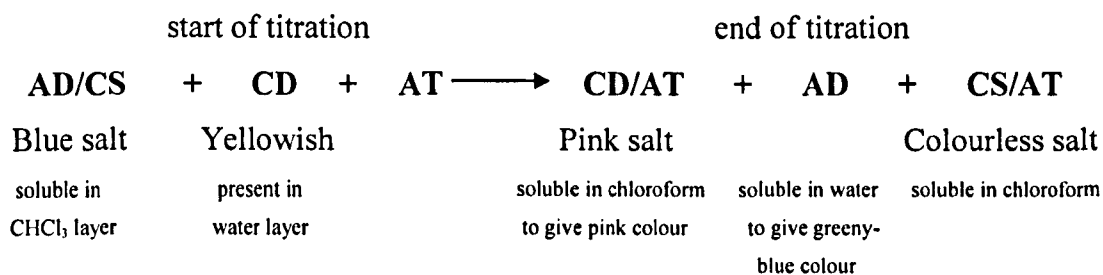
Concentrations of C<sub>10</sub> or C<sub>12</sub> in wt. % similar to those of C<sub>3/11-M</sub> used previously were calculated and added to equal amounts of oil and D<sub>2</sub>O (in wt. %) to give a series of samples with equal ratios of water to oil but varying surfactant concentration. The D<sub>2</sub>O was added to a small sample tube first with a small magnetic flea followed by the dry surfactant then the oil. This left the solid surfactant at the interface between the oil and D<sub>2</sub>O phases where it would form aggregates without needing to dissolve greatly in either phase first. The samples were equilibrated as described in 2.6.1.

## **2.7 Microemulsion phase characterisation**

### **2.7.1 Determination of equilibrium surfactant concentration by Epton titration**

In order to determine the partitioning of surfactant in equilibrium systems a two-phase titration<sup>2</sup> was used to measure the amount of surfactant present in each phase of a microemulsion system. The indicator solution used in the titration contains both an anionic dye (disulphine blue) and a cationic dye (dimidium bromide). When this is used with a two-phase system of water and chloroform as the titration mixture,

a colour change is observed in the chloroform layer which is pink with excess anionic species and blue with excess cationic species. Thus, the amount of cationic species in a sample (i.e. polymerizable surfactant) can be calculated by titration with an anionic titrant. This is known as the Epton titration.<sup>7, 8</sup>



where AD = anionic dye, CD = cationic dye, AT = anionic titrant and CS = cationic sample.

10 ml of chloroform, 5 ml of Milli-Q water and 5 ml of mixed indicator solution containing the above dyes were placed into a large test tube. Using an SGS glass syringe, an accurately measured volume of equilibrium phase was withdrawn from the sample tube and added to the titration mixture. The mixture was then thoroughly shaken and titrated against the anionic surfactant SDS of known concentration until a light pink colour was seen in the chloroform layer. This enabled the calculation of cationic surfactant present in each phase of the equilibrium system.

It was decided to confirm the concentration of the SDS stock solution using the surfactant TTAB. Using a 1 ml Gilson Pipetteman, 1 ml of accurately prepared aqueous  $1 \times 10^{-2}$  M TTAB solution was added to a large sample tube containing 5 ml H<sub>2</sub>O, 10 ml CHCl<sub>3</sub> and 5 ml of mixed indicator solution. This mixture was then

shaken and titrated against  $1 \times 10^{-2}$  M SDS stock. This was repeated three times and the average taken as the titre value. This titration was carried out for each SDS stock solution prior to use as the titrant for equilibrium phases.

### **2.7.2 Determination of equilibrium water content by Karl Fischer titration**

The water content of equilibrium phases was determined using the Karl Fischer technique.<sup>9</sup> A Denver Instruments 275 KF Karl Fischer auto titrator controlled by a Denver Instruments 260 Titration Controller was used. The titrator module contains a glass chamber for the catholyte reagent with a glass frit at the bottom across which is a cell electrode. This chamber is placed in a second glass chamber containing the anolyte reagent, which contains a second electrode, which measures the flow of current in the anolyte solution. The frit separates the anolyte and catholyte reagents and the cell electrode controls the amount of catholyte reagent that can cross the frit, which is determined by the flow of current through the anolyte solution containing the sample. The titrator maintains the flow of current through the anolyte solution at a particular value (620 – 90 mA depending on the condition of the anolyte reagent). The flow of current through the solution is affected by the water content of the sample added to the anolyte chamber; thus the water content of the sample can be calculated using the flow of current across the cell electrode required to maintain the flow of current through the anolyte solution. A 20  $\mu$ l sample was extracted from each microemulsion phase using a 25  $\mu$ l SGS syringe and the mass of this sample inputted into the titration controller. The titration is then run from the controller and the water content in wt. % is calculated from the titration results (in  $\mu$ g water) by the controller. An average from three measurements was taken for each equilibrium phase.

### 2.7.3 Calculation of microemulsion phase composition

The surfactant content was determined by Epton titration, which is used to determine the surfactant concentration in mol dm<sup>-3</sup>. Using the density of the microemulsion phase the surfactant concentration in wt. % can be calculated. The density was measured by taking the mass (using a Precisa balance XT220A) of an accurately measured volume (20 µl using an SGS glass syringe) of equilibrium phase. The water content, also in wt. %, was measured by Karl Fischer titration and the oil content in wt. % was calculated by subtracting the sum of the surfactant (corrected for surfactant purity) and water contents (in wt. %) from 100 assuming all mass present in the microemulsion phase was surfactant (plus surfactant impurities), water and oil. For the phases containing added electrolyte, the composition calculation is less accurate as the amount of salt in wt. % is not measured. However, the total concentration of salt in the initial aqueous phase for the highest salt concentration sample (0.069 M NaBr in initial aqueous phase) has been calculated to be ~0.7 wt. %. The salt does not partition into the oil so the salt content in the total equilibrium microemulsion phases containing surfactant and oil will be very much less than this.

## 2.8 Purification of surfactant C<sub>3/11-M</sub>

### 2.8.1 Method provided by Avecia

As the producers of the surfactant C<sub>3/11-M</sub>, Avecia provided a purification method using the following chemicals:

Ether	As needed: 1st washing ~1900 ml other washings ~950 ml each
Methanol	As needed: 1st washing ~100 ml other washings ~50 ml each
Phenothiazine	0.0168 g
4-Methoxyphenol	0.0168 g

The method is summarised as:

1. Approximately 100g of C<sub>3/11-M</sub> is poured into a 2 litre beaker and made up to 2000 ml with ether/methanol 95/5. It is then mixed using a magnetic stirrer plate for 30 mins.
2. The beaker is then placed in a bucket of ice/water for 30 mins.
3. The mix is filtered using a Buchner funnel and silica grade 9385 230-400mesh and Celite 521 filter aids. The filter aids are washed in ether/methanol 95/5 mix for 30 mins, cooled for 30 mins, filtered, and filtrates added together.
4. The inhibitors are added.
5. The solvents are removed by rotary vacuum (using dry ice/acetone in the cold finger of the rotary evaporator).
6. When all solvent is removed the oil is re-dispersed in 1litre of ether/methanol 95/5 and mixed for 30 mins.
7. Steps 2 and 3 and then step 5 are repeated to give the final product.

In order to purify the C<sub>3/11-M</sub>, this purification method was used for 25 g of C<sub>3/11-M</sub> with the following minor modifications designed to remove the solvent more effectively. The vacuum pumping was performed in two stages. The first stage used a Büchi Rotavapor 46 rotary evaporator diaphragm pump, which brings the pressure down to 8 mmHg. To remove further solvent a Speedivac High Vacuum oil pump was used which brings the pressure down to 0.5 mmHg.

### **2.8.2 Enhanced method**

The method described in 2.8.1 was used as described except that the inhibitors were not added until the end of step 3 following step 7, i.e. after the final filtration but before evaporation of solvents. The surfactant was kept from exposure to light throughout using aluminium foil.

## **2.9 Polymerisation by photo-initiation**

Photo-initiation of the polymerisation of acrylates by UV radiation has been reported<sup>10</sup> and was the method used for this work.

### **2.9.1 Polymerisation of oil**

Darocur 1173 UV initiator was used to initiate the polymerisation of HDDA oil using UV light from a UVP spot cure SCL1-2 lamp equipped with an automatic shutter. The light was transmitted via a liquid filled UV wand, with the tip positioned 20 mm from a glass slide onto which the material to be polymerised was placed.

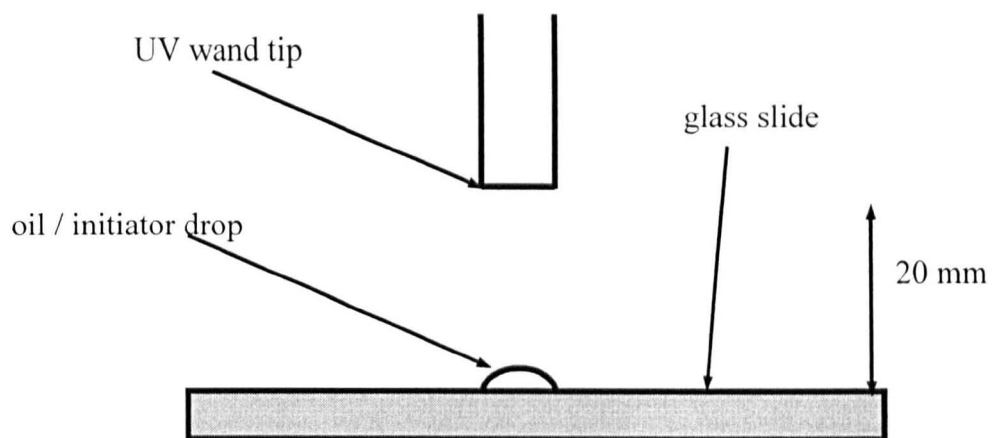
Darocur 1173 solutions in HDDA (1 – 4 wt. %) were prepared. These solutions were stirred well and placed away from sunlight. A small drop of one of these solutions was then placed on a microscope slide and exposed to UV light for a set period of time. The exposure time and initiator concentrations were varied. The concentrations of initiator in HDDA oil solutions prepared were 1.0, 2.0, 3.0 and 4.0 wt. %, named HD1, HD2, HD3 and HD4 respectively. A diagram of the set-up used is shown in Figure 2.3.

A second set-up was designed so that the termination effects of atmospheric oxygen on the polymerisation process for this particular system could be studied. This was very similar to the set-up above except a rubber ring 2 mm deep was placed on the glass slide and filled with HD 2. This was irradiated with UV light for 0.2 min.

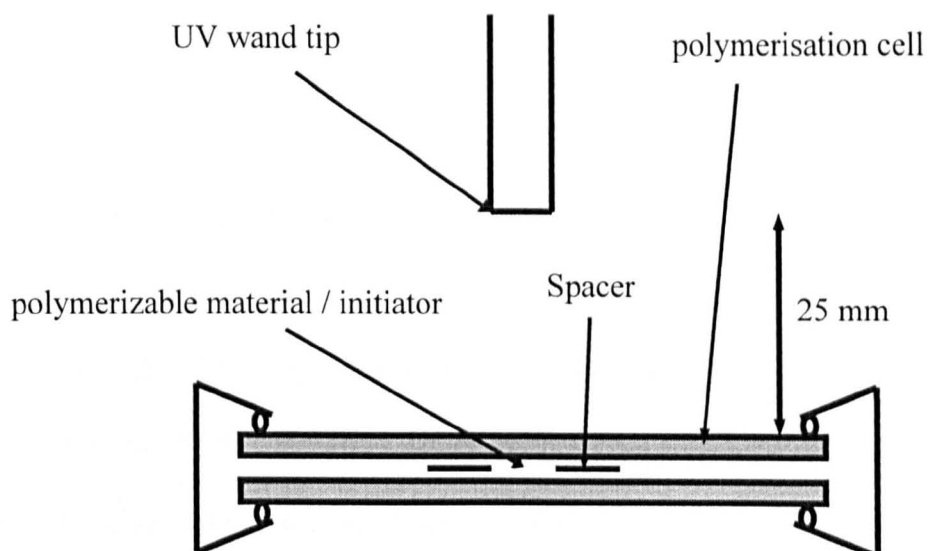
### **2.9.2 Polymerisation of C<sub>3/11-M</sub> surfactant solutions**

0.6439 g of C<sub>3/11-M</sub> batch 17/5/01 (brown-yellow oil at room temperature) was placed into a small sample bottle and to it 0.0146 g Darocur 1173 was added leaving a 2.2 wt. % solution of Darocur in C<sub>3/11-M</sub>. This was mixed thoroughly and a small droplet of the surfactant / Darocur mixture placed on top of a single glass slide. Pure C<sub>3/11-M</sub> with 2 wt. % initiator was polymerised using the set-up shown in Figure 2.3 followed by a series of solutions of surfactant in Milli-Q water also containing 2 wt. % Darocur. The concentrations of surfactant present in these solutions were: 0.23, 0.45, 0.72, 0.90 and 1.08 M.

**Figure 2.3.** Position of UV wand tip in relation to initiator/ oil droplet on glass slide during polymerisation of HDDA oil



**Figure 2.4.** Design of polymerisation cell and configuration of the UV wand





### **2.9.3 Polymerisation cell design**

In order to prepare reproducible polymer films of a pre-determined thickness and to minimise termination effects of the polymerisation process due to atmospheric oxygen,<sup>11</sup> it was decided to design a polymerisation cell. A droplet of material to be polymerised would be added to the cell and after polymerisation the polymer film could be removed for examination and analysis.

#### ***2.9.3.1 Selection of suitable glass***

In order to select a suitable glass for the top of the cell through which the UV light would pass, the UV absorption spectra of two brands of glass slide and a cover slip were measured so that a glass could be selected which would not absorb most of the UV emitted by the spot cure instrument. The UV transmission spectrum of the instrument was obtained from the manufacturer. UV/Vis spectra were obtained using an ATI Unicam UV3 200-UV spectrophotometer. The instrument was initially zeroed with empty sample and reference cuvette holders. To record the spectra, the glass slide or coverslip was mounted (using Sellotape) vertically against the sample beam cuvette holder.

#### ***2.9.3.2 Selection of spacer material***

It was decided to try aluminium foil as the spacer material. A 1 cm<sup>2</sup> hole was cut into a piece of foil which was sandwiched between two glass slides held together with a clip. This was positioned 25 mm under the UV wand giving complete coverage

of the sample by the UV beam. Samples of HD 1 were then irradiated for 0.1 min using this system. This was repeated using multiple layers of foil of two thicknesses to study the maximum possible thickness of polymer film and their reproducibility. The polymerisation set-up using the cell is shown in Figure 2.4.

### ***2.9.3.3 Determination of absorbance of incident UV by cell***

UV/Vis absorbance spectra of the polymerisation cell and of samples for polymerisation were determined in order to ensure that sufficient intensity of UV light from the UV wand is transmitted through the samples. UV/Vis spectra were obtained using an ATI Unicam UV3 200-UV spectrophotometer. The instrument was initially zeroed with empty sample and reference cuvette holders. To record the spectra, the polymerisation cell was mounted (using Sellotape) vertically against the sample beam cuvette holder. A polymerisation cell with a 50  $\mu\text{m}$  spacer was filled with HDDA oil containing Darocur 1173 at 1 wt. %. The UV/Vis absorption spectra were measured from 190 to 700 nm. This was repeated with an empty polymerisation cell and this spectrum subtracted from the filled cell spectra. This allows the separate contributions of absorption of UV from both the cell and its contents to be measured.

### **2.9.4 Polymerisation of microemulsion phases**

Microemulsion phases were polymerised using the polymerisation cell as described in 2.9.3.2. Using the density of each phase and the density of the initiator (Darocur 1173) suitable volumes of each phase and Darocur were calculated such that

a solution of Darocur at 2 wt. % in each phase could be prepared by addition of the Darocur directly to the microemulsion phase.

## **2.10 Characterisation of polymer films**

### **2.10.1 Visual inspection/ handling**

Initial characterisation of the polymer films was by direct optical observation and mechanical handling. This was to provide a relative measure of the optical clarity of the films and their strength. The films were observed after polymerisation and removal from the polymerisation cell and drying by exposure to the atmosphere. The films were handled using Fontax Taxal inox no mag number 4 tweezers and were gently bent until the film fractured. The stiffness and brittleness of the films was recorded.

### **2.10.2 Scanning Electron Microscopy (SEM)**

Images produced by the Hull University SEM Service used a Cambridge Instruments Stereoscan 360 SEM instrument operating at 20 kV. Samples were prepared by coating with carbon. The films were fractured at room temperature prior to coating.

### 2.10.3 Determination of pore volume fraction of polymer films

A square piece of polymer film was carefully cut using a scalpel blade and the length of the sides measured using a micrometer screw gauge (Mitutoyo No.293-766-30). The thickness of the film was then measured using the same screw gauge so that the total film volume could be calculated. The films were then dried using a vacuum dessiccator containing silica gel (BDH self indicating, lot K28029975 047) for 48 hours. After this time the films were removed from the dessiccator and weighed using a five figure analytical balance (Sartorius 1712, 30/160g) set at 30 g maximum. This gave the dry weight of the films. The films were then placed in a small sample bottle, which was filled with Milli-Q water and left to absorb water for 48 hours. The films were then removed and blotted using blue kimwipe paper to remove excess water droplets and re-weighed on the Sartorius balance. This gave the fully absorbed wet weight. To allow for any expansion of the films during the water absorption process, the film dimensions were measured while wet i.e. with water fully absorbed. The wet dimensions were used to calculate pore volume fraction as the pore volume fraction by water uptake is the quantity being investigated. It was checked that re-immersion of the polymer films in the Milli-Q water for a further 48 hours did not give additional water absorption, i.e. full absorption occurs within 48 hours.

## 2.11 References

- <sup>1</sup> International critical tables, McGraw-Hill, London, **4**, 447 (1928).
- <sup>2</sup> V. W. Reid, G. F. Longman and E. Heinerth, *Tenside*, **4**, 293 (1967).
- <sup>3</sup> Structural analysis report, Analytical services, Avecia Ltd (2000).
- <sup>4</sup> E. Andrzejewska, L. A. Linden and J. F. Rabeck, *Polymer International*, **42**, 179 (1997).
- <sup>5</sup> See for example, B. P. Binks and J. Dong, *Colloids and Surfaces A*, **132**, 289 (1998).
- <sup>6</sup> Y. C. Wu, K. W. Pratt and W. F. Koch, *Journal of Solution Chemistry*, **18**, 515 (1989).
- <sup>7</sup> S. R. Epton, *Nature*, London, **160**, 795 (1947).
- <sup>8</sup> S. R. Epton, *Trans. Faraday. Soc.*, **44**, 226 (1948).
- <sup>9</sup> K. Fischer, *Angew. Chem.*, **48**, 394 (1935).
- <sup>10</sup> See for example, W. R. Palain Raj, M. Sasthav and H. M. Cheung, *Langmuir*, **7**, 2586 (1991).
- <sup>11</sup> H. de Bruyn, R. G. Gilbert and B. S. Hankett, *Polymer*, **41**, 8633 (2000).

# *CHAPTER 3*

# CHAPTER 3

## CHARACTERISATION OF POLYMERIZABLE SURFACTANTS IN AQUEOUS/ POLYMERIZABLE OIL SYSTEMS

### 3.1 Introduction

The surfactants used in this study are all quaternary ammonium surfactants containing a methacrylate polymerizable group. They are all novel surfactants prepared by Avecia Ltd. and as a result there is no data on them (e.g. solubility in water and oil, cmc values etc.) available in the literature. Prior to any studies on microemulsion phase behaviour and subsequent phase polymerisation, it was necessary to measure certain characteristics of the surfactants in water and the three oils. The solubility of the surfactants in water and the oils was determined so that a suitable protocol for adding the surfactant to water and oil could be established for the preparation of microemulsion phases. Macroemulsion type versus temperature and salt concentration was measured as macroemulsion phase behaviour has been shown to be closely related to microemulsion phase behaviour in surfactant systems.<sup>1-7</sup> Using this information, the effects of salt concentration and initial surfactant concentration on the partitioning of the surfactants between water and oil have been studied, to determine phase inversion behaviour and cmc values in water and oil.

The information provided by this work was used to prepare microemulsion systems with suitable formulations such that the microemulsion phase behaviour of the three surfactants with the three oils and water could be studied in detail.

### 3.2 Solubility of surfactants in water and oils

In order to determine in which phase (oil or water) it would be preferable to initially place the surfactants in systems containing water and oil, the solubility of the surfactants at various temperatures in each of the oils and water was measured. Cationic surfactants dissolve typically to fairly high concentrations in highly polar solvents such as water. The solubility of a surfactant in water is dependent on several factors, including type of headgroup, charge on headgroup and length and type of hydrophobic tail. From the structures of the surfactants shown in Chapter 2, Figure 2.1, one would expect the order of solubility of the surfactants in water to be:  $C_{3/11-M} > C_{10} > C_{12}$ . This is because the hydrophobic tail in  $C_{3/11-M}$  has a highly polar methacrylate group at the end which will increase the polarity of the tail and thus result in increased solubility in water.  $C_{10}$  and  $C_{12}$  both contain an un-modified straight chain hydrocarbon tail. The two carbon increase in length of the  $C_{12}$  tail will make the surfactant less soluble than  $C_{10}$ . The solubility of cationic surfactants in oil will depend on the nature of the head and tail groups of the surfactant and also on the polarity of the oil.<sup>8</sup> Cationic surfactants do not dissolve very well in non-polar oils such as dodecane. A more polar oil may allow the surfactant to dissolve to a small extent. The order of polarity of the oils follows: DPGDA > BDDA > HDDA so one would expect each surfactant to dissolve in the oils according to the order of oil polarity and within each oil in the order of surfactant tail polarity.



The work on the  $C_{10}$  and  $C_{12}$  surfactants was performed by Ashby et al.<sup>9</sup> and it was found that both were much more preferentially soluble in water where they dissolved at room temperature although for  $C_{12}$  some heat input was required at concentrations above 2.0 wt. %. Both surfactants dissolved more preferably in DPGDA than BDDA with neither dissolving in HDDA at any concentration measured (down to 0.2 wt. %). Overall  $C_{10}$  was found to be more soluble than  $C_{12}$ . Figures 3.1 to 3.4 show the temperatures at which various concentrations of  $C_{3/11-M}$  dissolve in water and in the three monomer oils.

The results show that  $C_{3/11-M}$  dissolved more preferably in water than the oils with the solubility in the three oils being very similar for each oil, which is in agreement with the data collected for the surfactants  $C_{10}$  and  $C_{12}$ . This is due to the ionic nature of the surfactants. A polar solvent such as water solvates ionic species well due to the interaction of the dipole in a water molecule with the charge of an ionic species. Hydrogen bonding is also possible between water and the surfactants. The dipole in the monomer oil molecule is weak compared to that in water and hydrogen bonding between a monomer oil molecule and a surfactant molecule is not possible at all. An increase in temperature leads to an increase in the solubility of the surfactants in all cases.

The  $C_{12}$  surfactant was found to be very sparingly soluble in water and insoluble in HDDA in the above work. High concentrations of  $C_{12}$  would be required to prepare polymerizable microemulsion phases and it was doubtful following the above solubility work that  $C_{12}$  could be added in sufficient amounts as a surfactant solution. It was decided to carry out more accurate solubility experiments using

Figure 3.1. Temperature of dissolution of surfactant  $C_{3/11-M}$  vs. wt. % of  $C_{3/11-M}$  in water

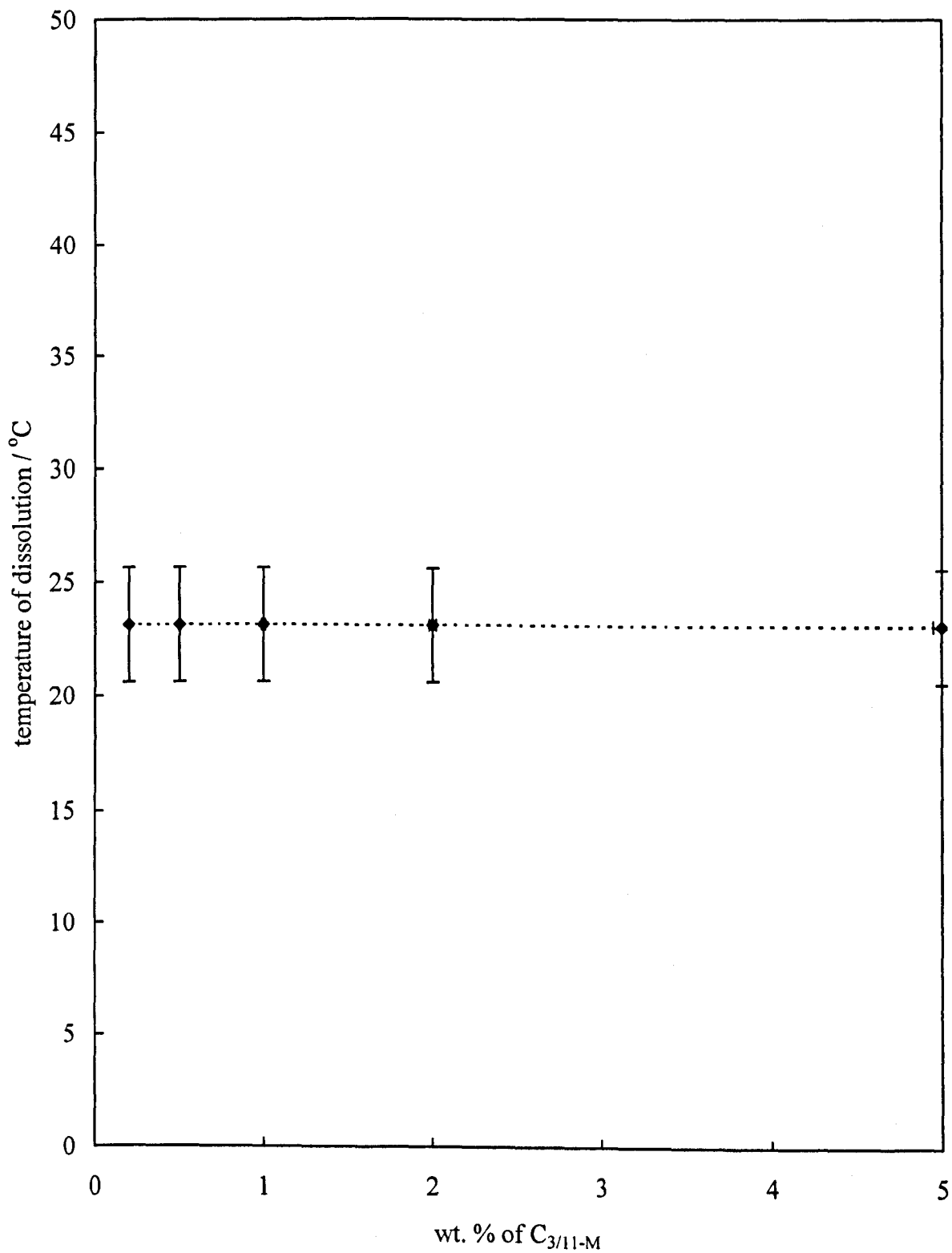


Figure 3.2. Temperature of dissolution of surfactant  $C_{3/11-M}$  vs. wt. % of  $C_{3/11-M}$  in HDDA oil

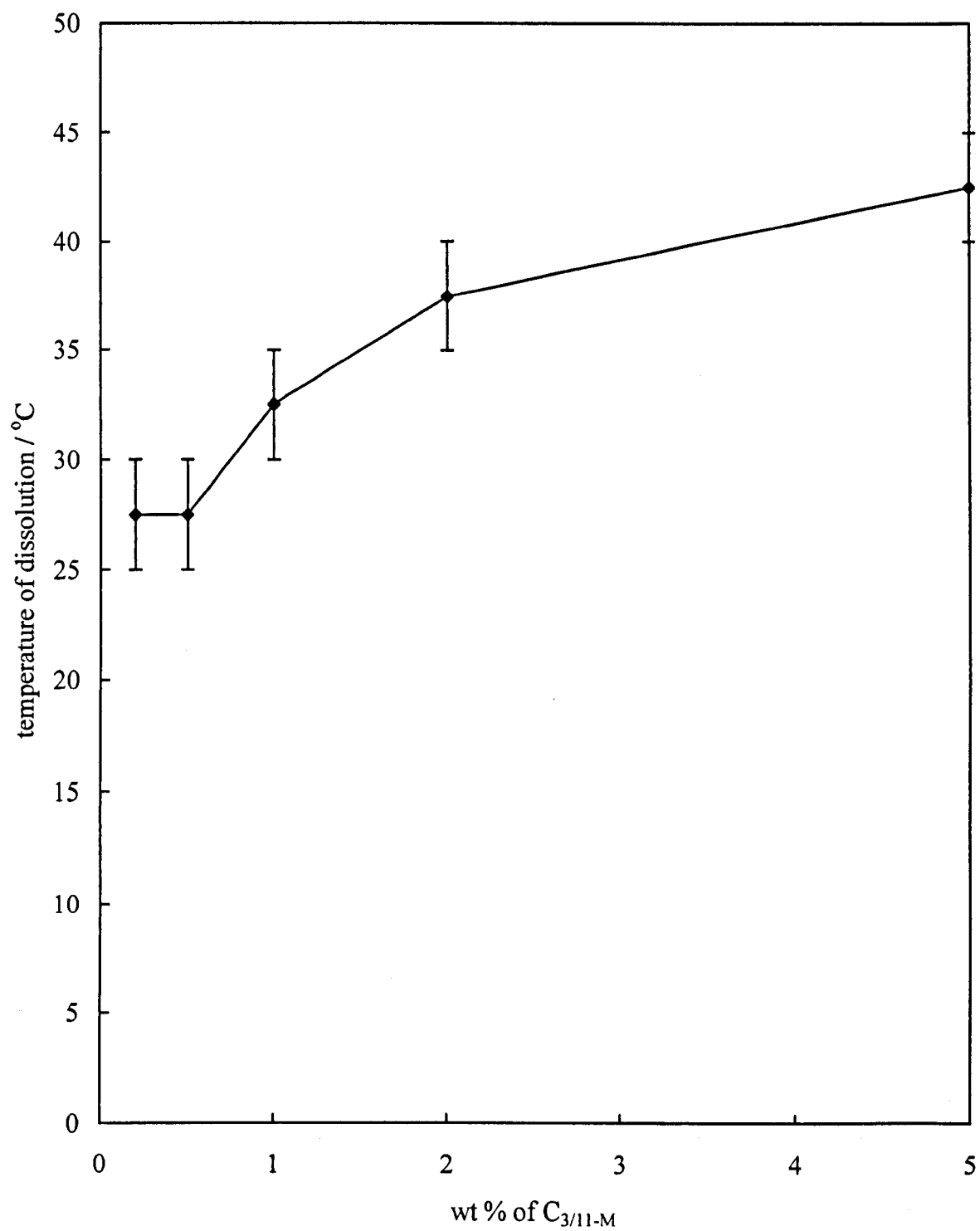


Figure 3.3. Temperature of dissolution of surfactant  $C_{3/11-M}$  vs. wt. % of  $C_{3/11-M}$  in BDDA oil

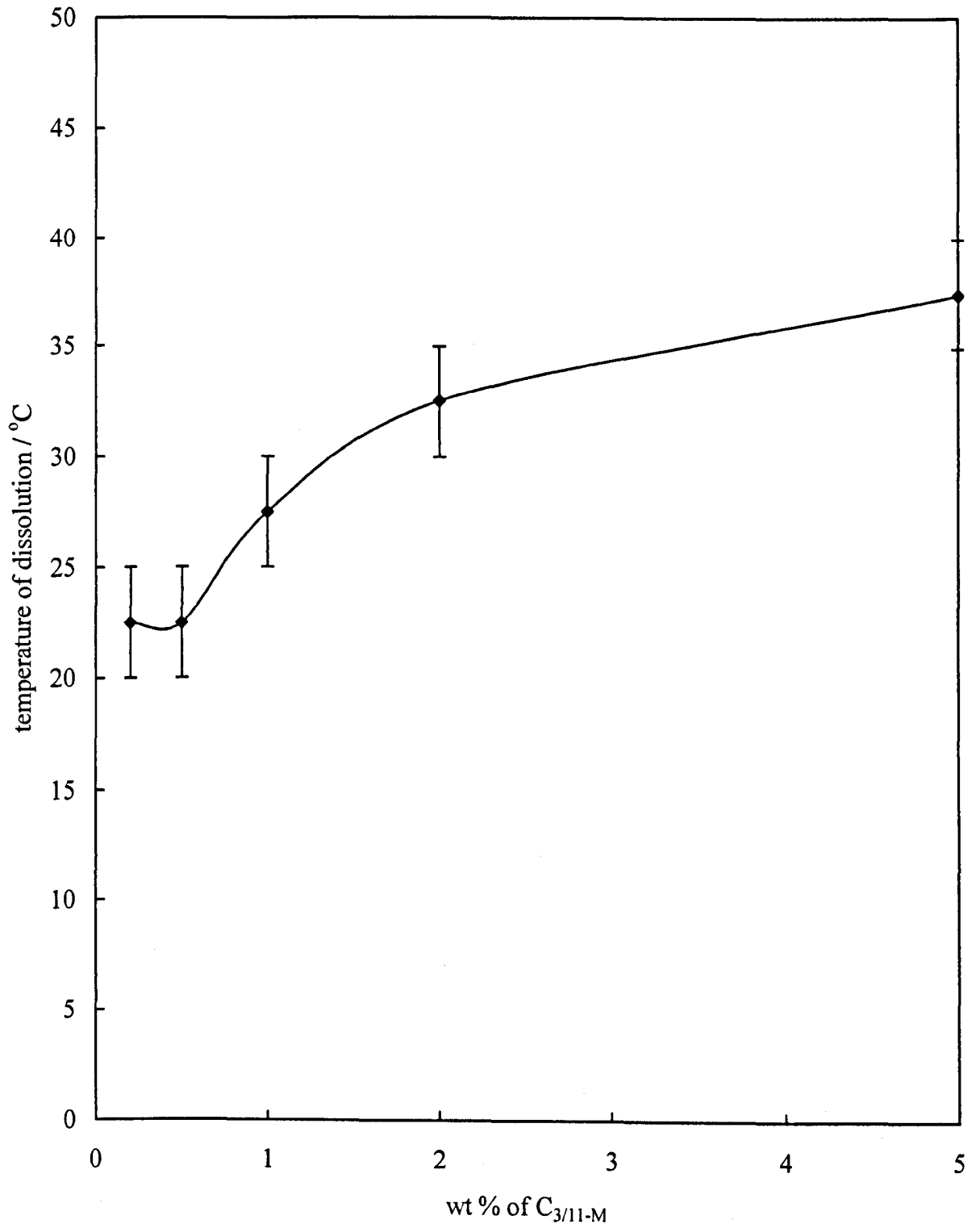
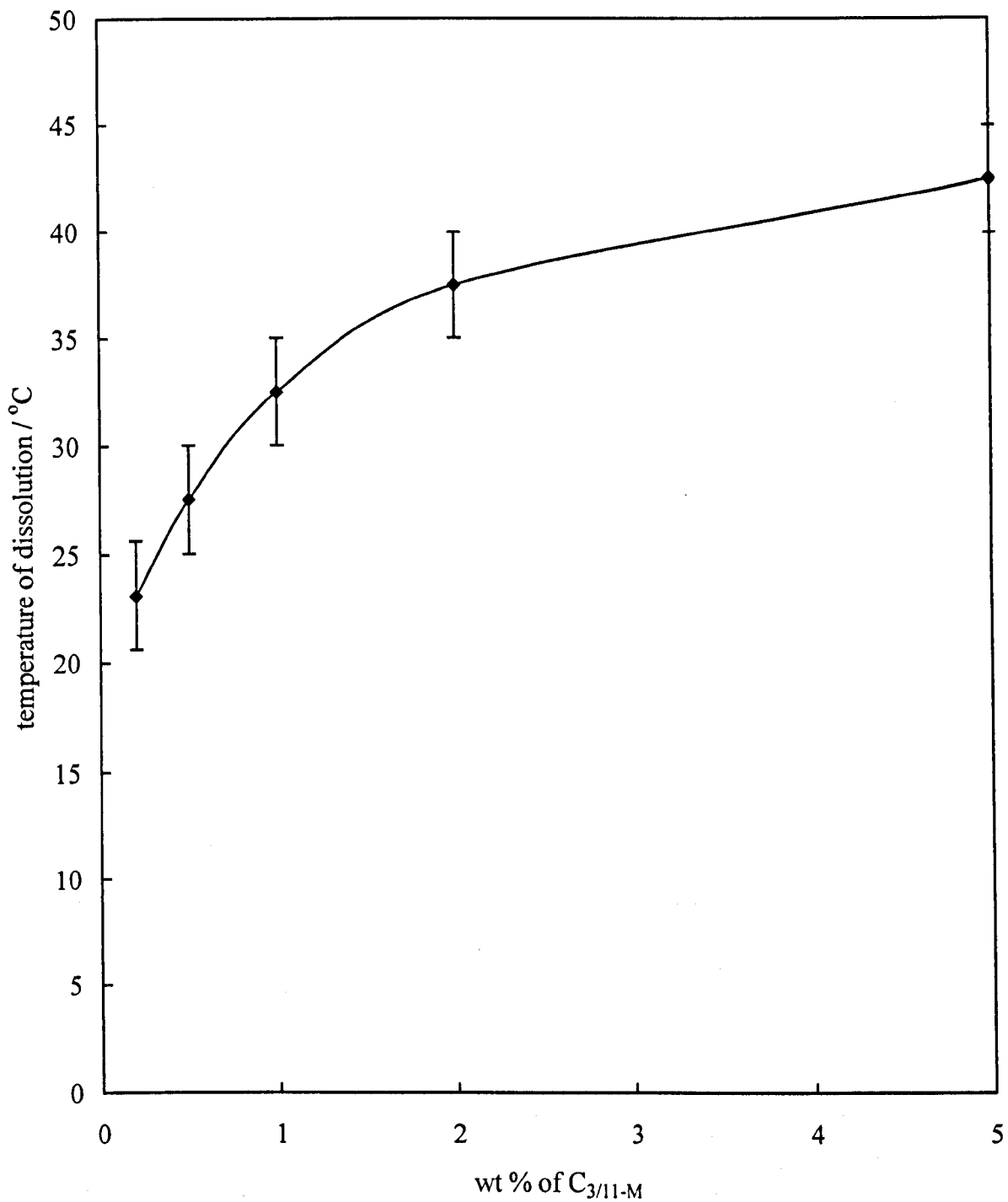


Figure 3.4. Temperature of dissolution of surfactant  $C_{3/11-M}$  vs. wt. % of  $C_{3/11-M}$  in DPGDA oil



accurately weighed (using a precise balance XT220A) amounts of surfactant and placing the surfactant with the solvent in a sample tube as described in Chapter 2. The results of this experiment are shown in Table 3.1 along with the solvents used and the quantities of surfactant.

Table 3.1 shows that the surfactant will, in fact, dissolve in HDDA more easily than in water over time. It is quite possible that this is in fact a micellar solution rather than a surfactant monomer solution, due to the time required for the surfactant to disperse into the oil. High concentrations of surfactant are needed to prepare microemulsions suitable for polymerisation. Concentrations much higher than 5 wt % C<sub>12</sub>, which showed some undissolved surfactant, will be needed; thus a method of preparing the microemulsions without introducing the surfactant as a solution was required.

### **3.3 Macroemulsion phase behaviour**

#### **3.3.1 Emulsion type versus temperature**

Using the data above, emulsions were prepared and their conductivity measured at various temperatures. Temperature is known to have an effect on the emulsion type in nonionic surfactant-stabilised systems – above a certain temperature phase inversion may occur and the emulsion type will change from one type to the other e.g. oil-in-water to water-in-oil.<sup>2,10</sup> The temperature at which this occurs is called the Phase Inversion Temperature (PIT). In these experiments there was no added electrolyte present. The work on surfactants C<sub>10</sub> and C<sub>12</sub> was performed by

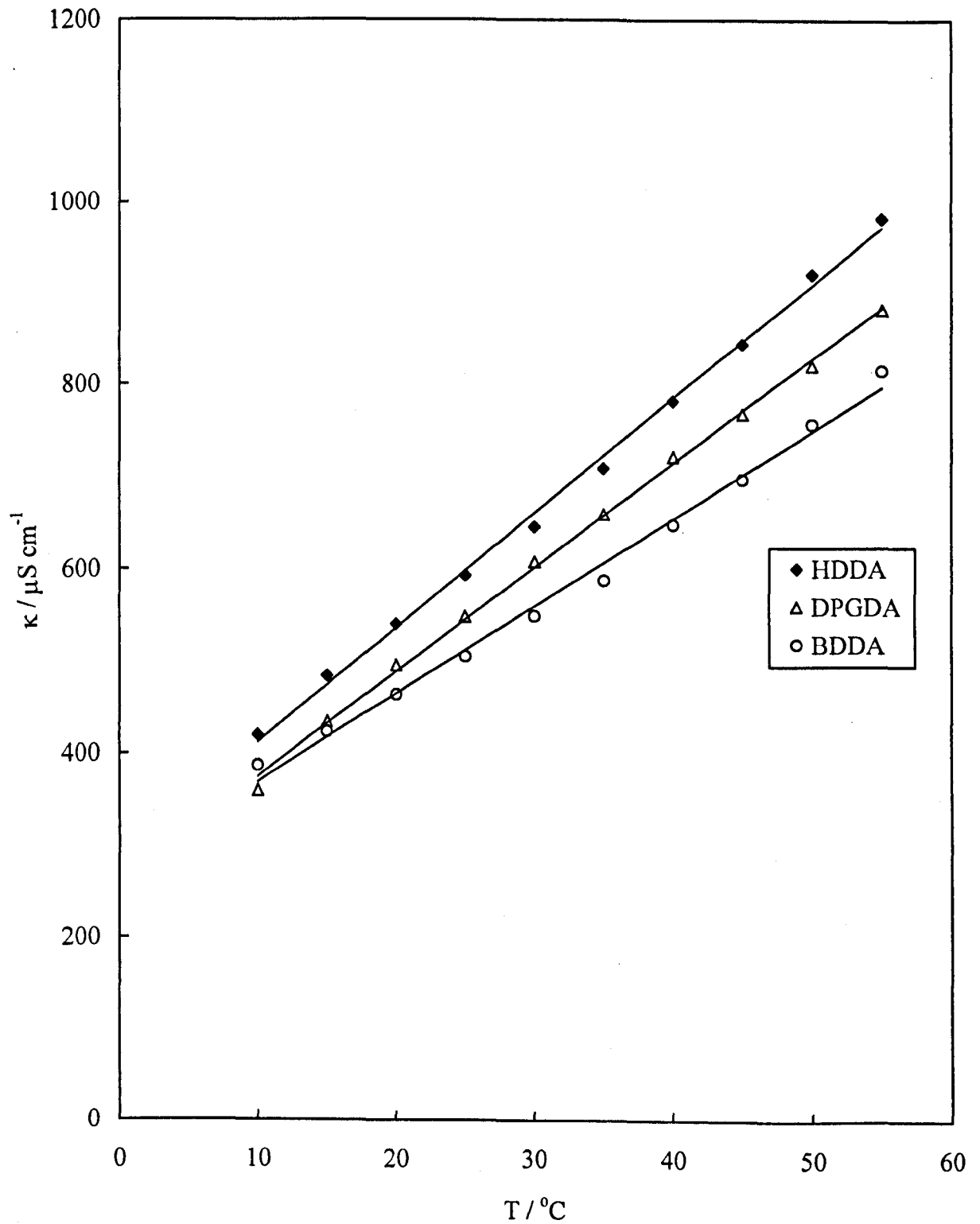
**Table 3.1. Solubility of surfactant C<sub>12</sub> in water and HDDA**

<b>Amount of C<sub>12</sub>/wt. %</b>	<b>Solvent</b>	<b>Time left to dissolve</b>	<b>Appearance of sample tube</b>
0.2	H <sub>2</sub> O	3 days	Surfactant dissolved
0.5	H <sub>2</sub> O	3 days	Few small undissolved particles
1.0	H <sub>2</sub> O	3 days	More particles than above
2.0	H <sub>2</sub> O	3 days	Mostly undissolved
5.0	H <sub>2</sub> O	3 days	Mostly undissolved
0.2	HDDA	3 days	Surfactant dissolved
0.5	HDDA	3 days	Undissolved particles, slight cloudiness
1.0	HDDA	3 days	More particles and more cloudy
2.0	HDDA	3 days	V. cloudy, many more particles
5.0	HDDA	3 days	Opaque emulsion like appearance
0.2	H <sub>2</sub> O	3 weeks	Surfactant dissolved
0.5	H <sub>2</sub> O	3 weeks	Few small undissolved particles
1.0	H <sub>2</sub> O	3 weeks	More particles than above
2.0	H <sub>2</sub> O	3 weeks	Mostly undissolved
5.0	H <sub>2</sub> O	3 weeks	Mostly undissolved
0.2	HDDA	3 weeks	Surfactant dissolved
0.5	HDDA	3 weeks	Surfactant dissolved
1.0	HDDA	3 weeks	Surfactant dissolved
2.0	HDDA	3 weeks	Surfactant dissolved
5.0	HDDA	3 weeks	Very few small undissolved particles

Ashby et al.<sup>9</sup> and it was found that all emulsions were highly conducting indicating an o/w emulsion<sup>4,11</sup> and no phase inversion was seen up to 55 °C, beyond which the monomer oils can self polymerise. Figure 3.5 shows the conductivity of 1:1 volume ratio emulsions of water and each of the monomer oils stabilised by surfactant C<sub>3/11-M</sub>. All emulsions are highly conducting indicating o/w emulsions and phase inversion cannot be induced by temperature up to 55 °C. As the temperature increases, so does the conductivity of the emulsions. This is to be expected as raising the thermal energy of a system will increase the ion mobility and thus conductivity will increase.<sup>12</sup> It is possible that a system may phase invert at a higher temperature but the monomer oils are known to be unstable and may self-polymerise at temperatures above 55 °C. However, increasing the temperature in ionic surfactant-stabilised systems has been shown to have the opposite effect to that seen in nonionic surfactant systems.<sup>13</sup> Increasing the temperature in ionic surfactant systems actually makes the surfactant monolayer curvature more positive by increasing the counter-ion dissociation from the head group. This increases repulsive forces between head groups, thus making their effective size increase. The conductivities of emulsions with the same surfactant but different oils are very similar. This could suggest that the droplet sizes for each oil with a particular surfactant are similar, as the conductivity of an emulsion is affected by the size of emulsion drops.<sup>14</sup> Since phase inversion could not be effected by temperature, we decided to investigate the effect of salt concentration on the conductivity of the emulsions as salt is also known to cause phase inversion in emulsion systems stabilised by ionic surfactants.<sup>8,15</sup>



**Figure 3.5.** Effect of temperature (T) on conductivity ( $\kappa$ ) for a 1:1 volume ratio emulsion of oil and aqueous solution of 1 wt. % surfactant  $C_{3/11-M}$



### 3.3.2 Emulsion type versus salt concentration

Using the data above, a surfactant concentration of 1 wt. % was used to prepare emulsions at 25 °C with varying salt concentration in the aqueous phase. The conductivity of an emulsion will increase with added salt because of the increased concentration of electrolyte in the system.<sup>12</sup> At a certain concentration of salt, the emulsion type may invert from o/w to w/o and this will be accompanied by a sudden and significant change (lowering) of the conductivity of the emulsion. This is because the continuous phase changes from a highly conducting surfactant/salt solution to a non-conducting oil phase containing very little free conducting material. The work on C<sub>10</sub> and C<sub>12</sub> surfactants was carried out by Ashby et al.<sup>9</sup> and it was found that HDDA systems phase invert to produce w/o emulsions at 0.1 M NaBr. BDDA and DPGDA systems do not phase invert to produce stable emulsions, although the o/w emulsions break at 0.1 M NaBr for the C<sub>12</sub> surfactant and at 0.05 M NaBr for the C<sub>10</sub> surfactant. Figures 3.6 to 3.8 show the effect of salt concentration on the conductivity and type of emulsions for 1:1 volume ratio emulsions of water and each of the monomer oils stabilised by C<sub>3/11-M</sub> surfactant. In all cases the conductivity increases sharply up to the phase inversion salt concentration where the system becomes w/o and the conductivity drops to a minimum value. The figures show that in the DPGDA and HDDA systems phase inversion occurs at 0.05 M NaBr, whereas in the BDDA system phase inversion occurs at 0.04 M NaBr. The salt concentration required for phase inversion with C<sub>3/11-M</sub> surfactant systems is therefore independent of oil type as expected. It was found that for some systems near phase inversion multi-phase emulsions were produced which were water continuous (possibly w/o/w) before phase inversion and oil continuous (possibly o/w/o) after phase inversion. Phase inversion

**Figure 3.6. Effect of [NaBr] on conductivity ( $\kappa$ ) and type of emulsion for 1:1 volume ratio emulsions of HDDA and aqueous solution of 1 wt. % surfactant  $C_{3/11-M}$ .  $T = 25^\circ\text{C}$ , time to onset of phase separation is given**

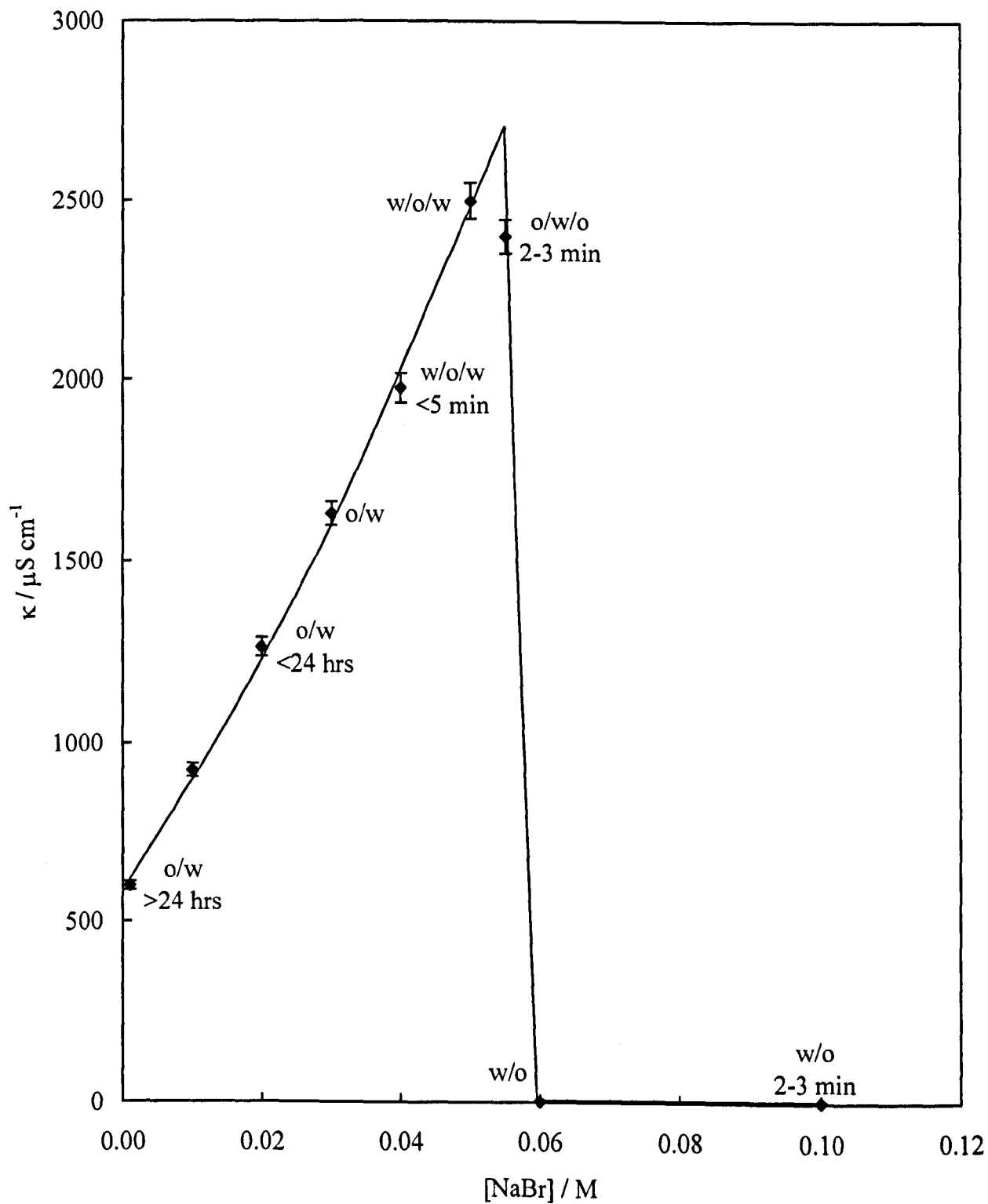
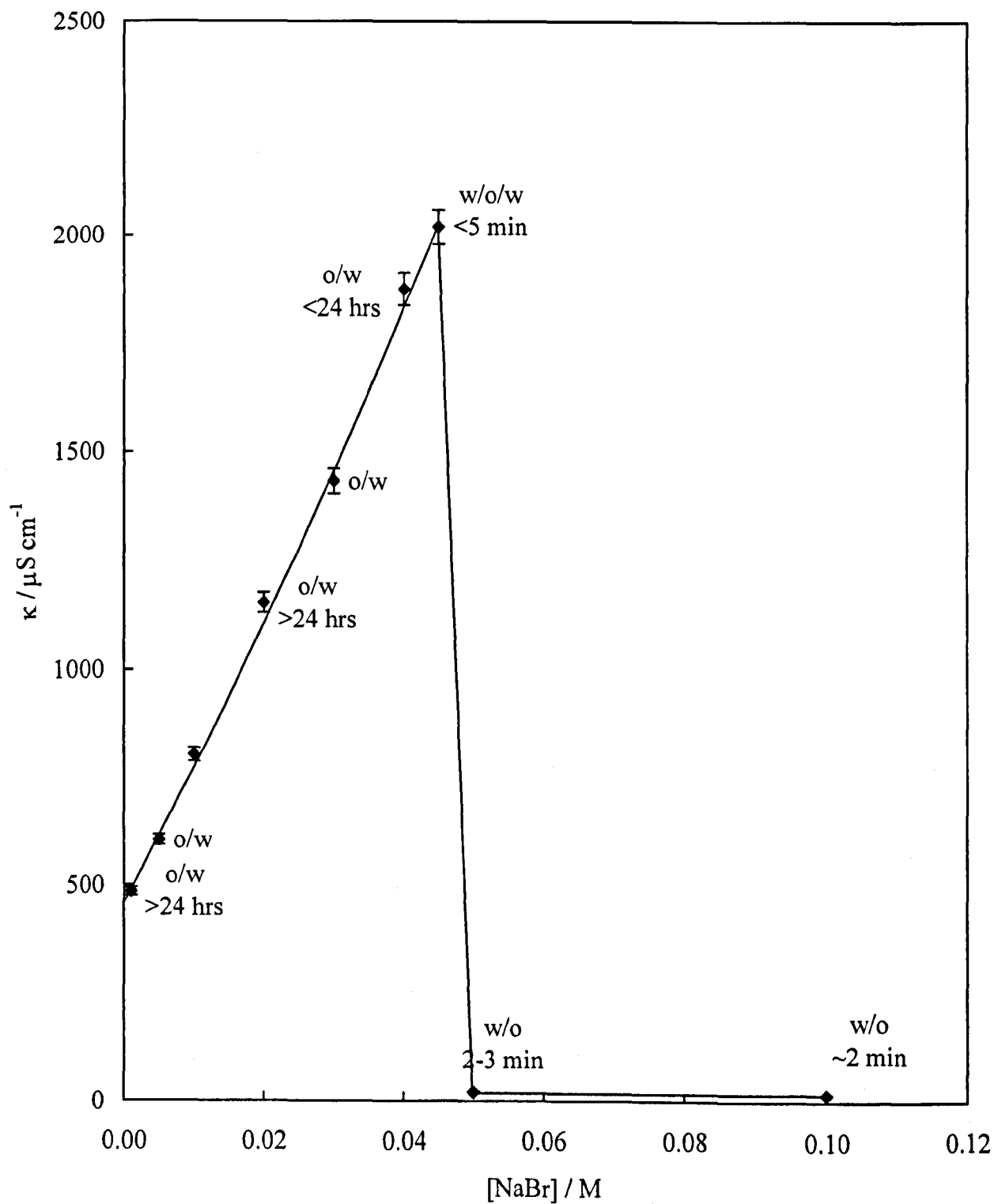
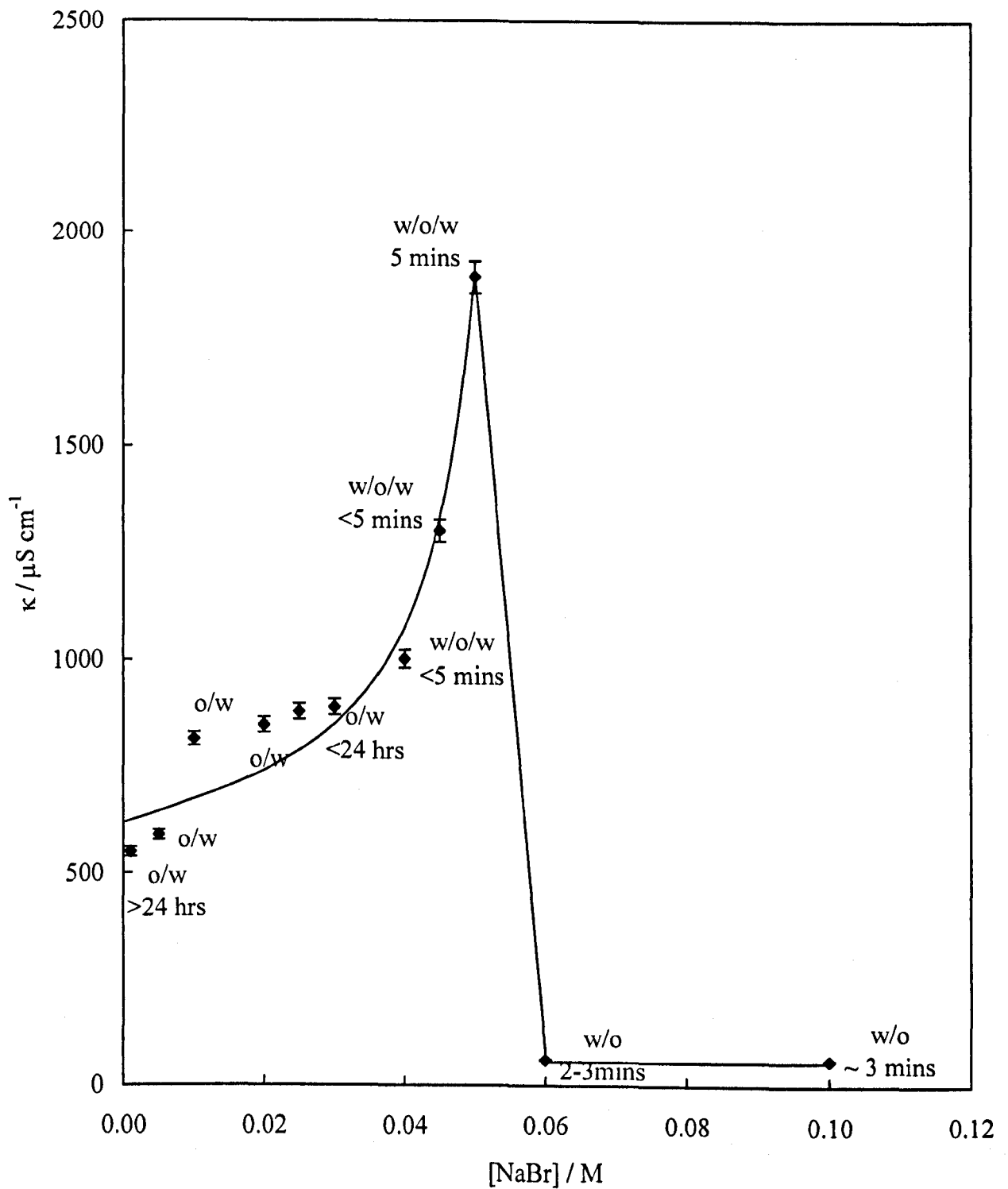


Figure 3.7. Effect of [NaBr] on conductivity ( $\kappa$ ) and type of emulsion for 1:1 volume ratio emulsions of BDDA and aqueous solution of 1 wt. % surfactant  $C_{3/11-M}$ .  $T = 25^\circ\text{C}$ , time to onset of phase separation is given



**Figure 3.8. Effect of [NaBr] on conductivity ( $\kappa$ ) and type of emulsion for 1:1 volume ratio emulsions of DPGDA and aqueous solution of 1 wt. % surfactant  $C_{3/11-M}$ .  $T = 25^\circ C$ , time to onset of phase separation is given**



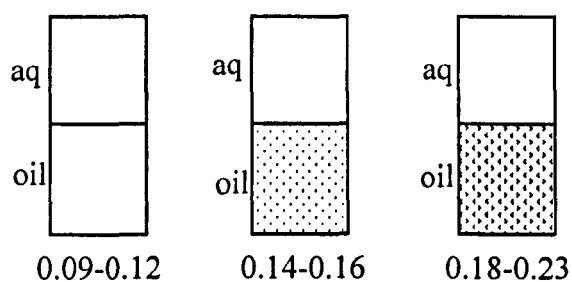
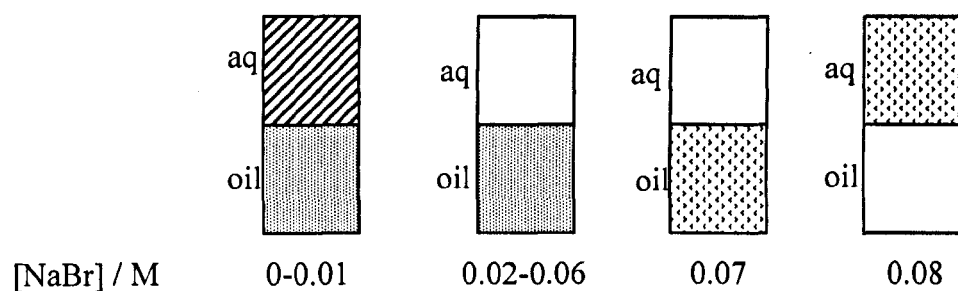
occurs with added salt in an ionic emulsion system because one of the ions of the salt interacts with the ionic head group of the surfactant.<sup>8,16</sup> In this case, the anionic Br<sup>-</sup> ion screens the repulsions between head groups. The effective head group size becomes smaller than the tail group and the preferred curvature of the monolayer is reversed.

### 3.4 Partitioning of surfactant with respect to added electrolyte

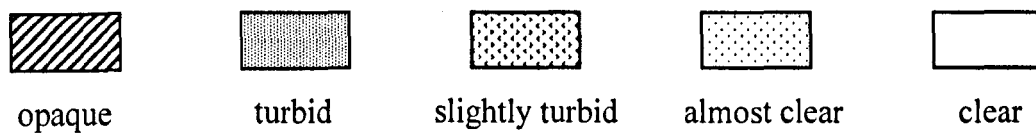
When two immiscible liquids are added together, e.g. water and oil, and a surfactant is added to the system, after a certain period of time the surfactant will distribute (partition) between the two phases reaching an equilibrium partitioning. Surfactant partitioning is a particularly simple but useful method of microemulsion characterisation, as a sample can be taken from each phase and the amount of surfactant partitioned in each phase can be determined. It should be noted that monomer and aggregated surfactant (e.g. micelles) may partition differently between water and oil. The partitioning of an ionic surfactant between two phases is affected by the presence of dissolved electrolyte in either phase.<sup>17</sup> The aim of this experiment was to see to what extent salt would affect this partitioning behaviour.

Ashby et al.<sup>9</sup> carried out the partitioning of surfactants C<sub>10</sub> and C<sub>12</sub> between water and the two oils BDDA and HDDA. It was found that the phase that the surfactants partitioned in most favourably switched from water to oil at salt concentrations of approximately 0.05 M. Figures 3.9 and 3.10 refer to the partitioning of surfactant C<sub>3/11-M</sub> between HDDA and water at 25 °C. Figure 3.10 shows the effect of salt concentration on the partitioning with Figure 3.9 showing the appearance of the sample tubes prior to sampling for analysis. Figures 3.11 and 3.12 are the equivalent

**Figure 3.9.** Appearance of equilibrium phases for a system of water and HDDA oil (1:1, v:v) stabilised by surfactant  $C_{3/11-M}$  at 21.5 mM in initial aqueous phase, with various salt concentrations at 25 °C



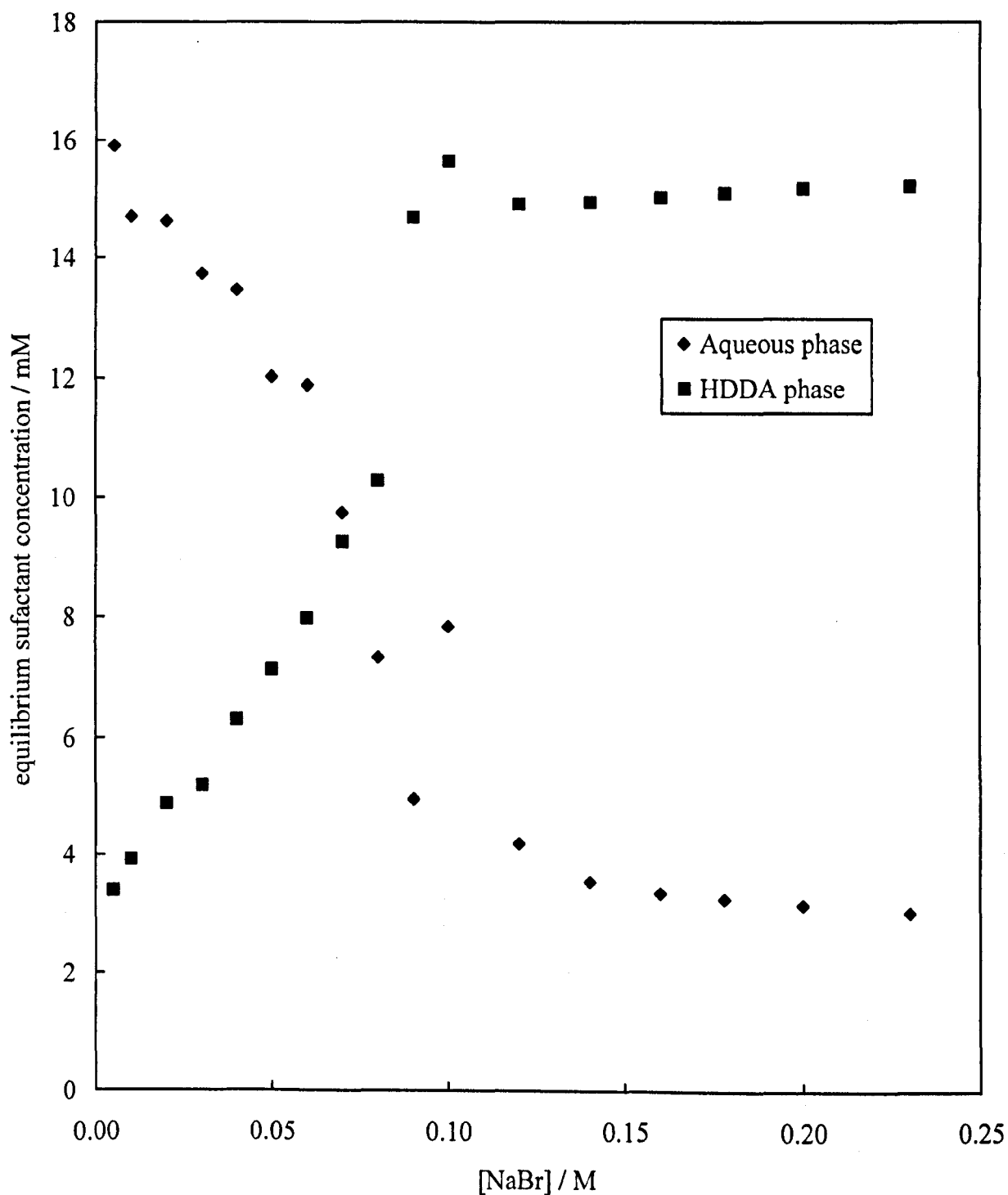
Key:



aq or oil denotes continuous phase

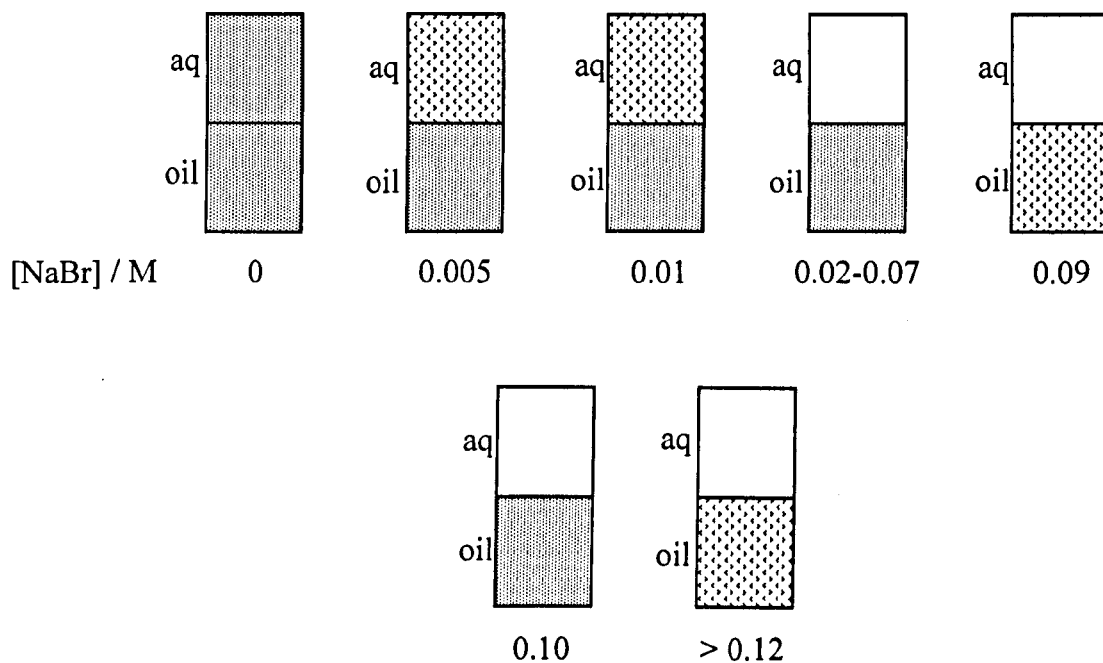
*photo?*

Figure 3.10. Concentration of  $C_{3/11-M}$  against initial  $[NaBr]$  in aqueous phase at equilibrium. Temperature =  $25^{\circ}C$ ,  $\phi_o = 0.5$ , oil phase = HDDA, aqueous phase =  $H_2O$ , initial [surfactant] = 21.52 mM in aqueous phase

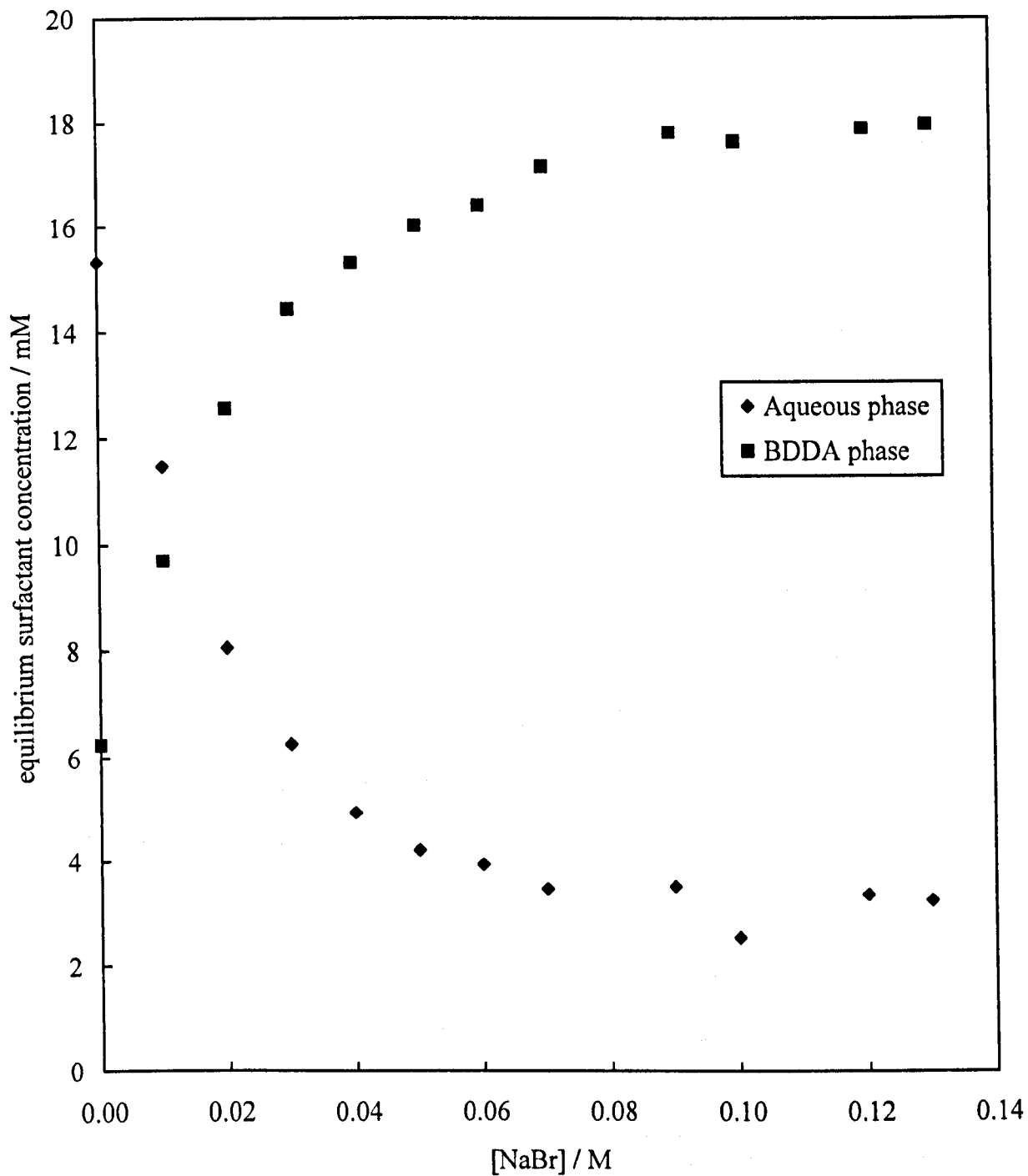




**Figure 3.11.** Appearance of equilibrium phases for a system of water and BDDA oil (1:1, v:v) stabilised by surfactant C<sub>3/11-M</sub> at 21.5 mM in initial aqueous phase with various salt concentrations at 25 °C



**Figure 3.12.** Concentration of  $C_{3/11-M}$  against initial  $[NaBr]$  in aqueous phase at equilibrium. Temperature =  $25^{\circ}C$ ,  $\phi_o = 0.5$ , oil phase = BDDA, aqueous phase =  $H_2O$ , initial [surfactant] = 21.52 mM in aqueous phase



figures with BDDA in place of HDDA. It can be seen from the plots that salt does indeed greatly affect the partitioning of surfactant and causes the preferential partitioning of surfactant to switch from water to oil at concentrations as low as 0.01 M NaBr ( $C_{3/11-M}$ , BDDA). It is important to understand that this partitioning data does not distinguish between monomer and aggregated surfactant partitioning.

Figures 3.9 and 3.11 show that as salt concentration is increased the stable emulsion that forms in the aqueous phase becomes less stable until at high salt concentrations the aqueous phase is clear. Once the concentration of surfactant in a phase has reached the cmc, all additional surfactant will be present as micelles, possibly as a microemulsion.<sup>16</sup> At low salt concentration, the surfactant curvature is such that an o/w microemulsion will form, and all surfactant above the cmc in each phase will partition in the water phase as micelles. At high salt concentration however, the curvature of the surfactant above the cmc is such that a w/o microemulsion will form and all additional surfactant above the cmc's of each phase will partition in the oil phase to form reverse micelles. It is interesting to note that phase inversion of the macroemulsion occurs at a similar salt concentration to the surfactant partitioning inversion for microemulsions. This is due to the same factors affecting each case, i.e. the charge on the electrolyte affecting effective head group size of the surfactant. The effect seen here agrees well with reports in the literature.<sup>6,7</sup>

It was decided to study the effect of initial surfactant concentration on the partitioning of surfactant with respect to salt. A higher initial surfactant concentration than that used previously was selected since the surfactant is charged and can act as a weak salt (weakly dissociating), which may reduce the salt concentration required for

phase inversion.<sup>6,18</sup> The effect of surfactant concentration on the extent of partitioning of surfactant in oil at low salt concentration (at which one of the values for cmc was determined – see section 3.5) was studied. Figure 3.13 shows the appearance of the equilibrium phases for a system prepared using surfactant C<sub>3/11-M</sub> at 100 mM initial surfactant with HDDA oil and aqueous solutions of NaBr. Figure 3.14 shows the partitioning of the surfactant with added NaBr.

It can be seen from Figure 3.14 that the salt concentration at which the preferential phase of surfactant partitioning changed from water to oil, was lower for the 100 mM initial surfactant concentration (~ 0.02 M NaBr) compared with that for the 21.5 mM initial surfactant concentration (~ 0.06 M NaBr) seen in Figure 3.10. This suggests that the surfactant itself does indeed act as a weak salt. This effect must be taken into account when selecting systems where the surfactant curvature is to be controlled with electrolyte addition at high initial surfactant concentrations. It can also be seen that the surfactant concentration in the oil phase at 0.01 M NaBr for the 100 mM initial surfactant concentration is much higher (~ 35 mM) than the cmc in oil for a system at this salt concentration (3.8 mM). At 0.01 M NaBr the system was found to be o/w - see later, which suggests that the surfactant concentration in oil should not increase beyond the cmc value for an ideal system. The much higher surfactant concentration found in the oil phase for the 100 mM initial surfactant concentration series at 0.01 M salt, is due to the higher overall electrolyte concentration in the system. This shields the charge on the head group of the surfactant, thus making the head less hydrophilic and shifting the HLB to lower values.<sup>5</sup> The droplets seen in the sample tubes at 0.02 and 0.04 M NaBr may indicate the presence of a third phase as this is around phase inversion, where surfactant monolayer curvatures close to zero

**Figure 3.13.** Appearance of equilibrium phases for a system of water and HDDA oil (1:1, v:v) stabilised by surfactant  $C_{3/11-M}$  at 100.0 mM in initial aqueous phase with various salt concentrations at 25 °C

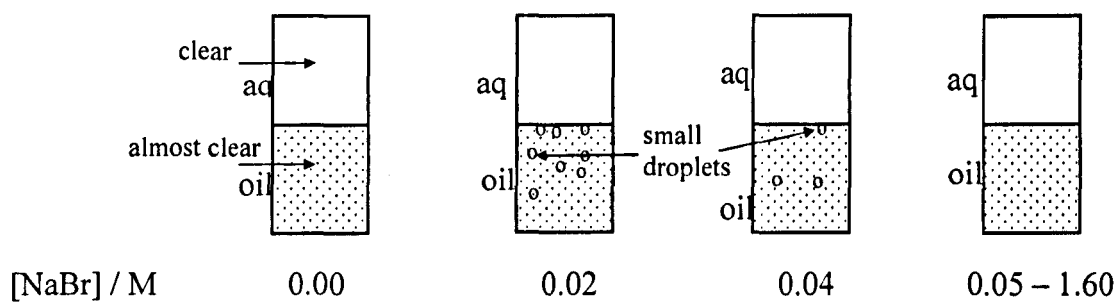
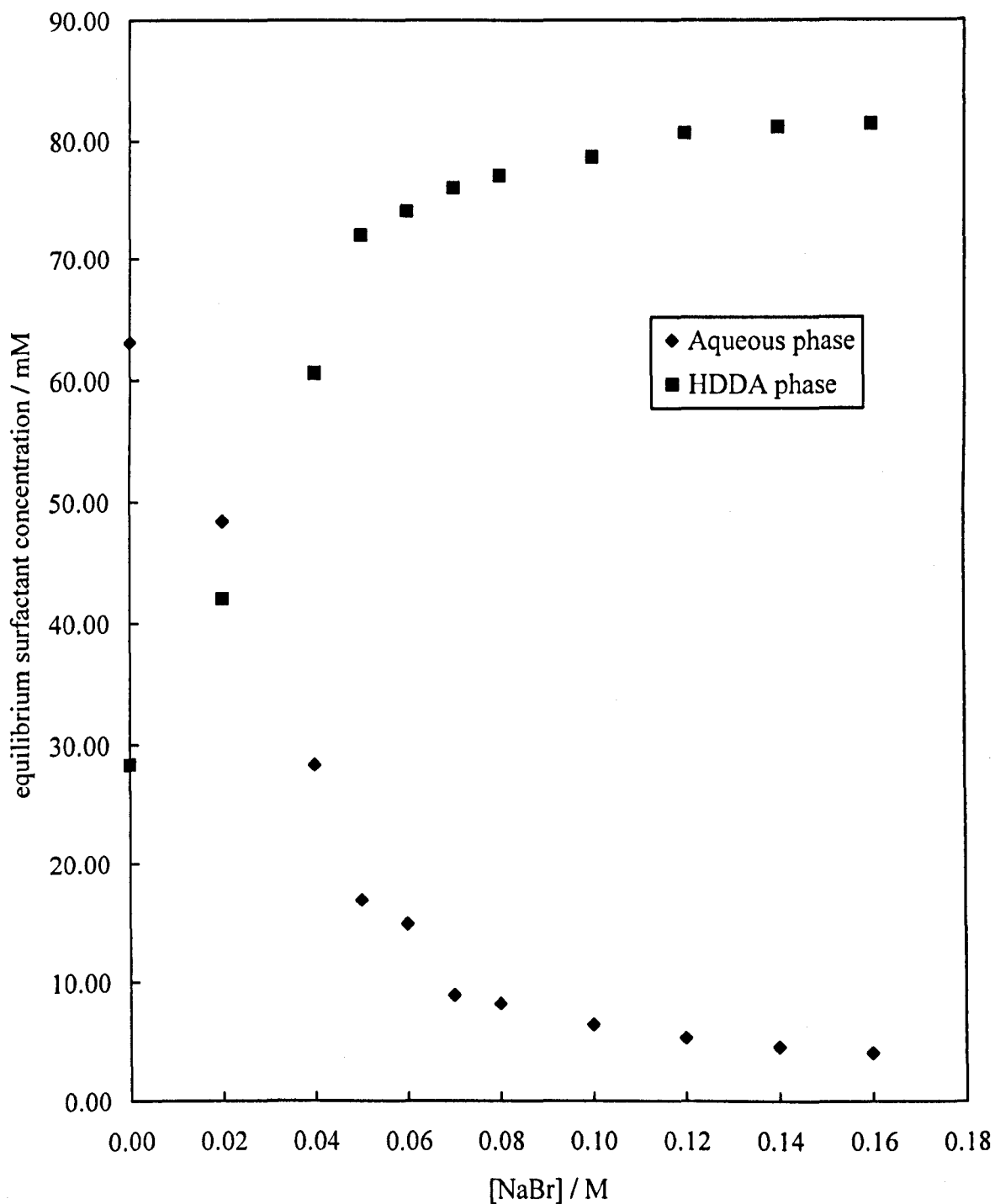


Figure 3.14. Concentration of  $C_{3/11-M}$  against initial  $[NaBr]$  in aqueous phase at equilibrium. Temperature =  $25^{\circ}C$ ,  $\phi_o = 0.5$ , oil phase = HDDA, aqueous phase =  $H_2O$ , initial [surfactant] = 100.0 mM in aqueous phase



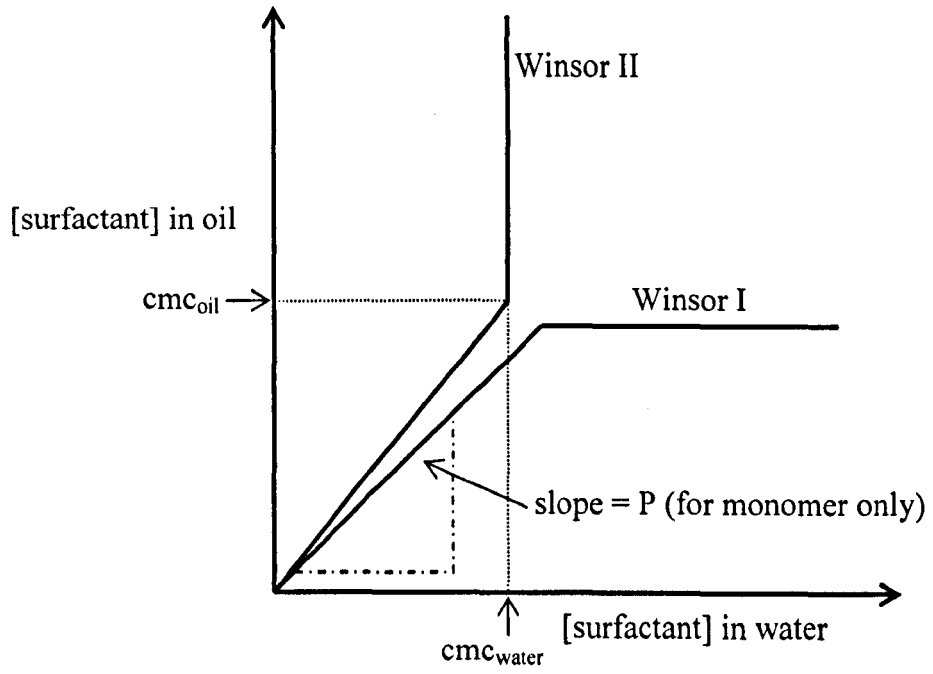
would be expected. This could result in a bicontinuous phase, which at these low surfactant levels would only be present as a very small phase volume.

The above data was used along with that collected by Ashby et al.<sup>9</sup> to decide on suitable salt concentrations to use in order to measure the cmc of the surfactants in two phase systems consisting of water and each of the oils. It was desirable to choose a salt concentration far below that of phase inversion (0.01 M) and one far above that of phase inversion (0.50 M) for each system so that cmc's in both o/w and w/o systems could be determined.

### **3.5 Partitioning of surfactant with respect to initial surfactant concentration**

When the initial concentration of surfactant in a water and oil system is increased, the equilibrium concentration in each phase will increase at constant ratio until the cmc in each phase is reached. Beyond this point all additional surfactant will form micelles in the phase of preferred partitioning.<sup>19</sup> Thus, if an o/w microemulsion (Winsor I)<sup>20</sup> forms then all additional surfactant beyond the cmc will reside in the water phase and so the concentration of surfactant in that phase will rise, whereas the concentration of surfactant in the oil phase will remain constant. The reverse is expected if a w/o microemulsion (Winsor II)<sup>20</sup> forms. The equilibrium surfactant concentrations in each phase can be plotted as surfactant concentration in oil vs. surfactant concentration in water. Figure 3.15 shows the expected curves for Winsor I and Winsor II systems, along with the methods for measuring cmc and the partition coefficient  $P$ , defined as:

**Figure 3.15. Expected curves of equilibrium surfactant concentration in each phase for Winsor I and II systems**





**Figure 3.16. Partitioning of surfactant C<sub>3/11-M</sub> at equilibrium. [NaBr] = 0.01 M, temperature = 25°C,  $\phi_o = 0.5$ , oil phase = HDDA, aqueous phase = water**

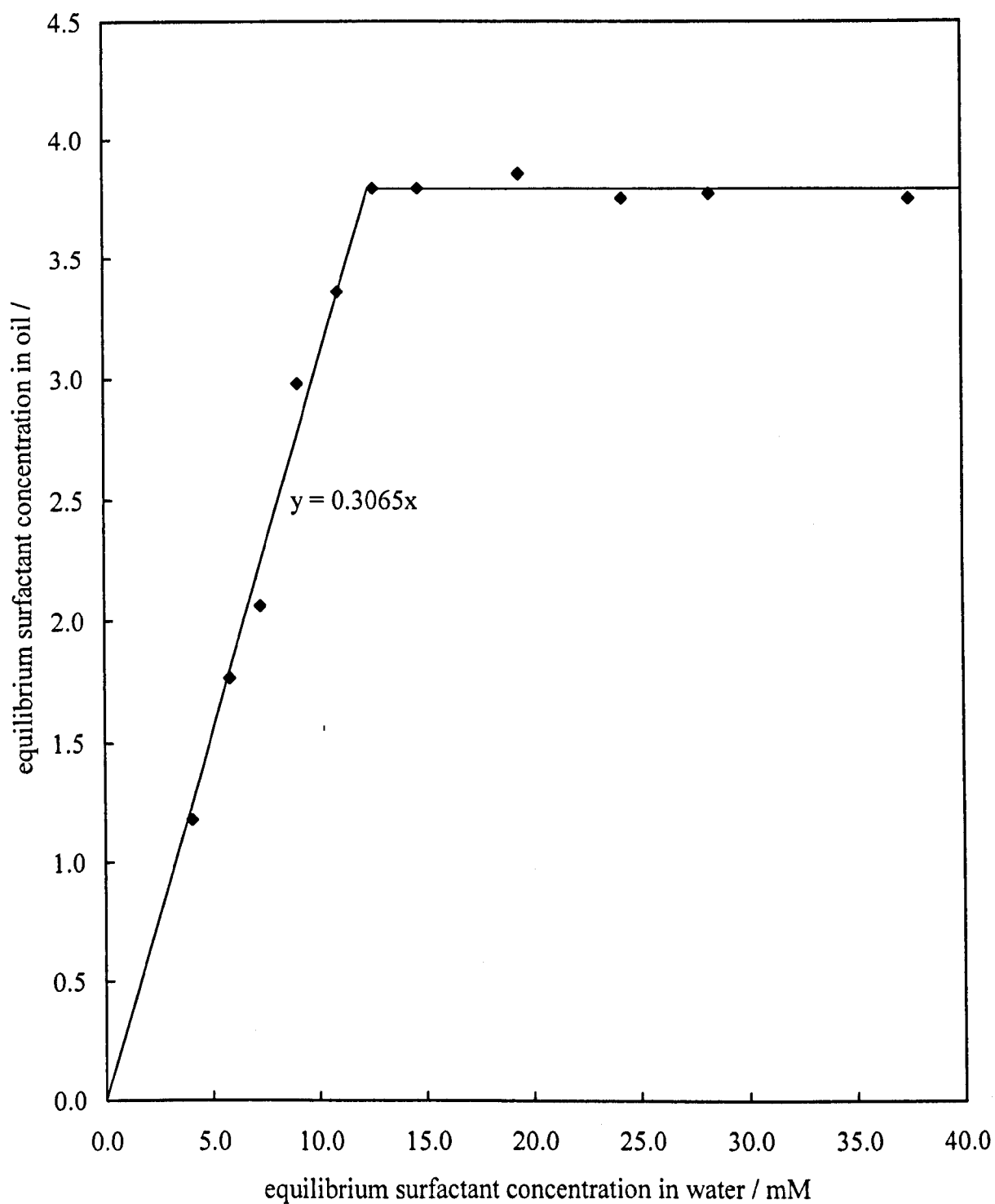


Figure 3.17. Partitioning of surfactant  $C_{3/11-M}$  at equilibrium.  $[NaBr] = 0.5\text{ M}$ , temperature =  $25^{\circ}\text{C}$ ,  $\phi_o = 0.5$ , oil phase = HDDA, aqueous phase = water

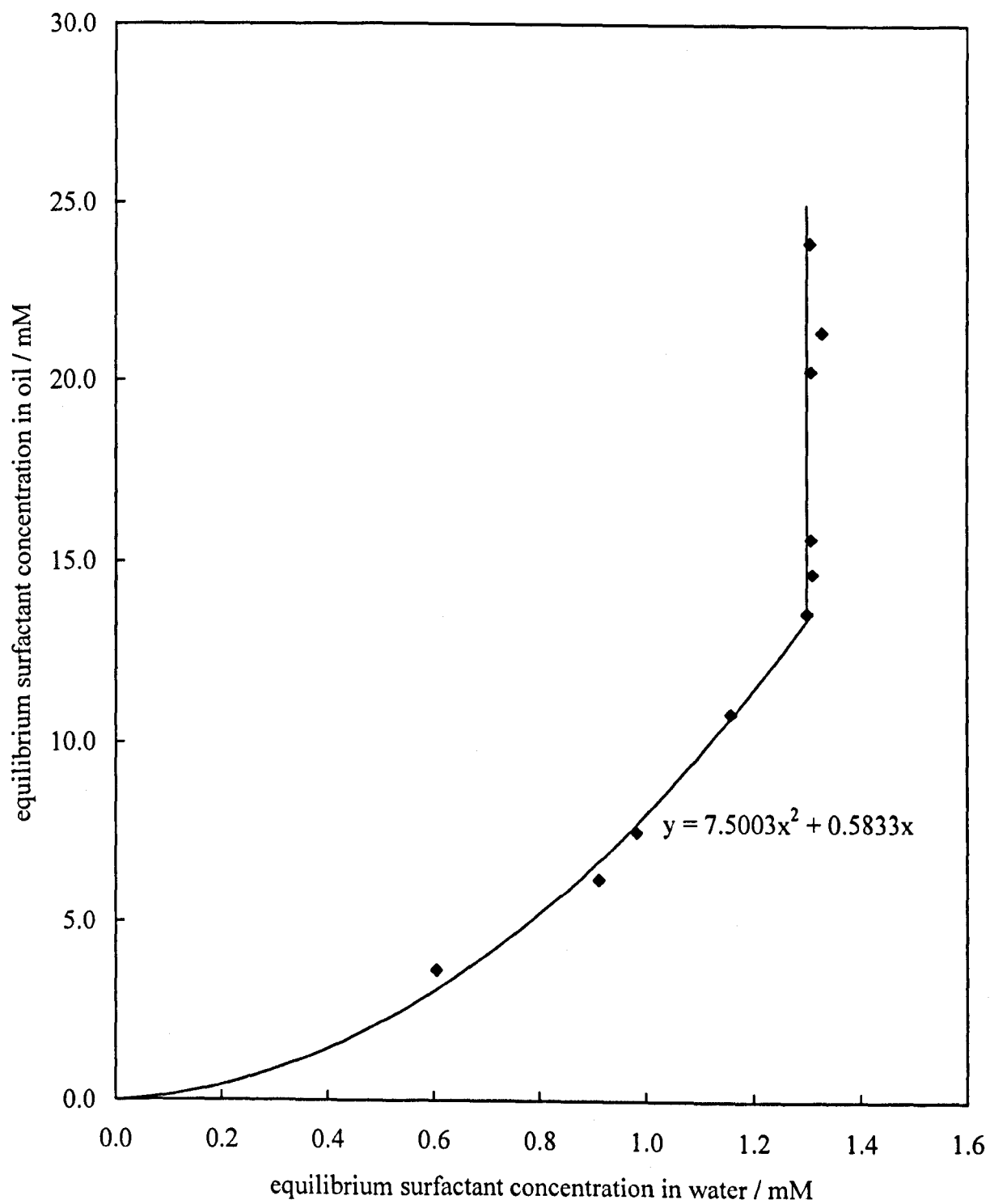
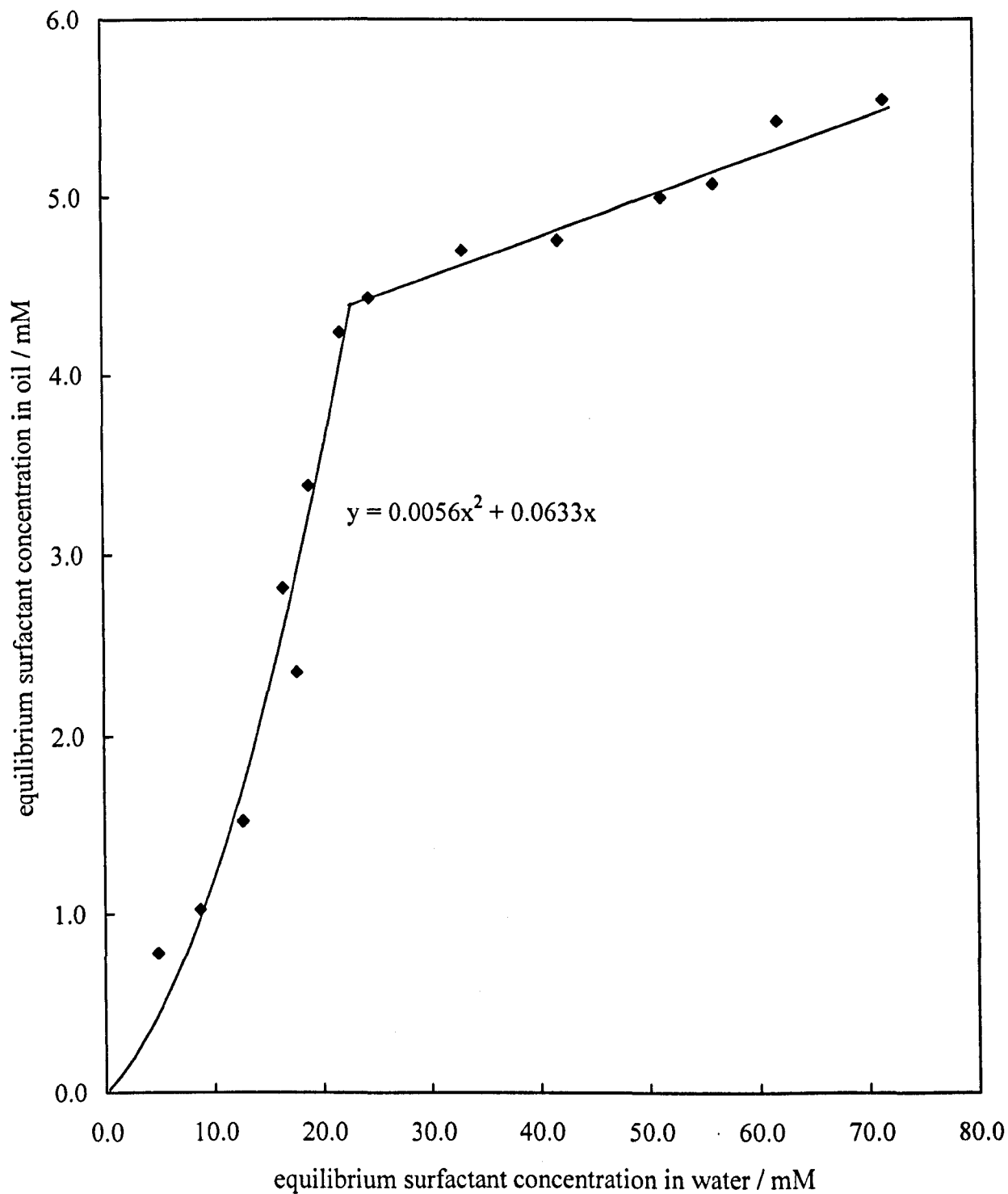


Figure 3.18. Partitioning of surfactant C<sub>10</sub> at equilibrium. [NaBr] = 0.01 M, temperature = 25°C,  $\phi_o = 0.5$ , oil phase = HDDA, aqueous phase = water



**Figure 3.19. Partitioning of surfactant C<sub>10</sub> at equilibrium. [NaBr] = 0.5 M, temperature = 25°C,  $\phi_o = 0.5$ , oil phase = HDDA, aqueous phase = water**

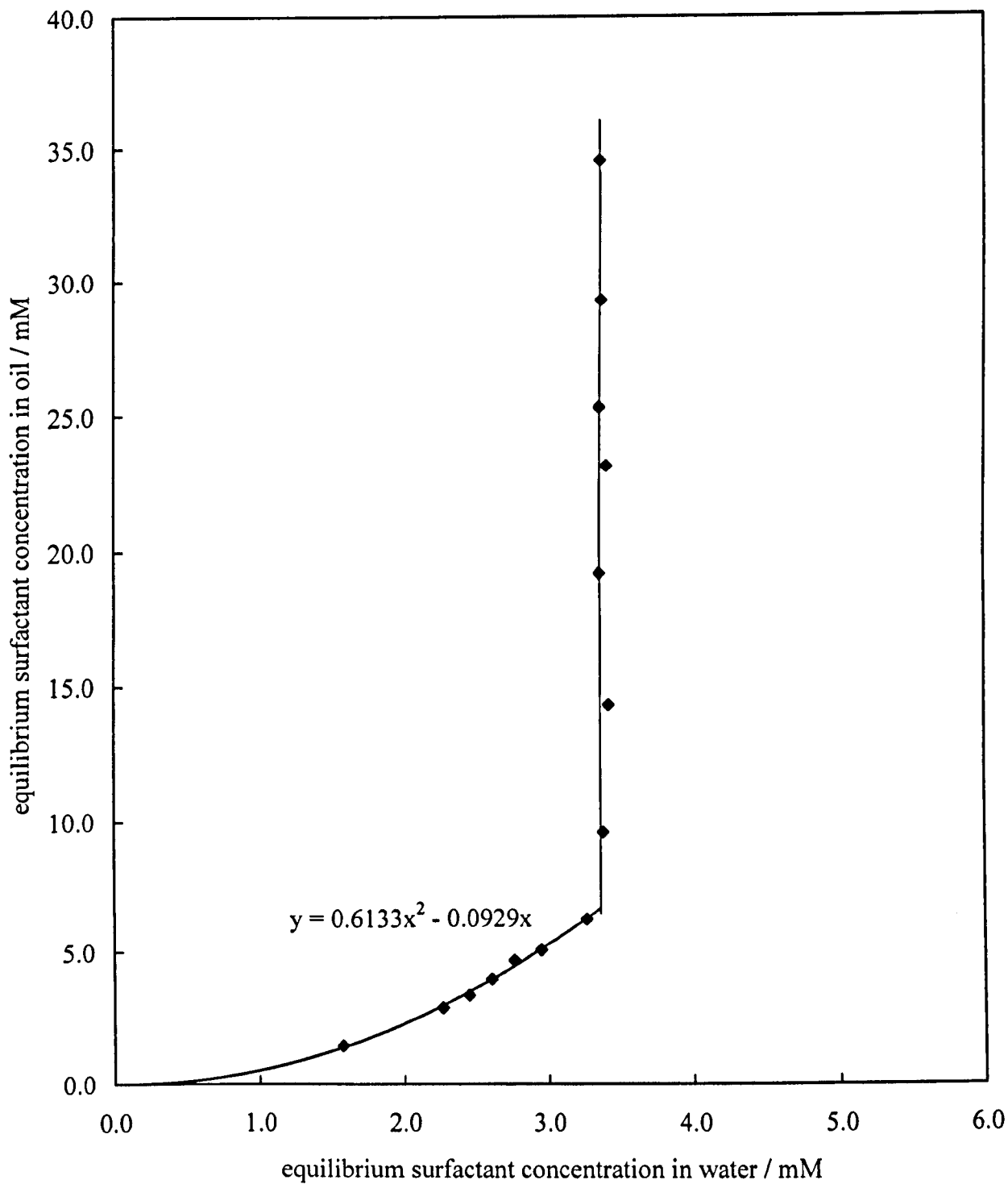


Figure 3.20. Partitioning of surfactant  $C_{12}$  at equilibrium.  $[NaBr] = 0.01\text{ M}$ , temperature =  $25^{\circ}\text{C}$ ,  $\phi_o = 0.5$ , oil phase = HDDA, aqueous phase = water

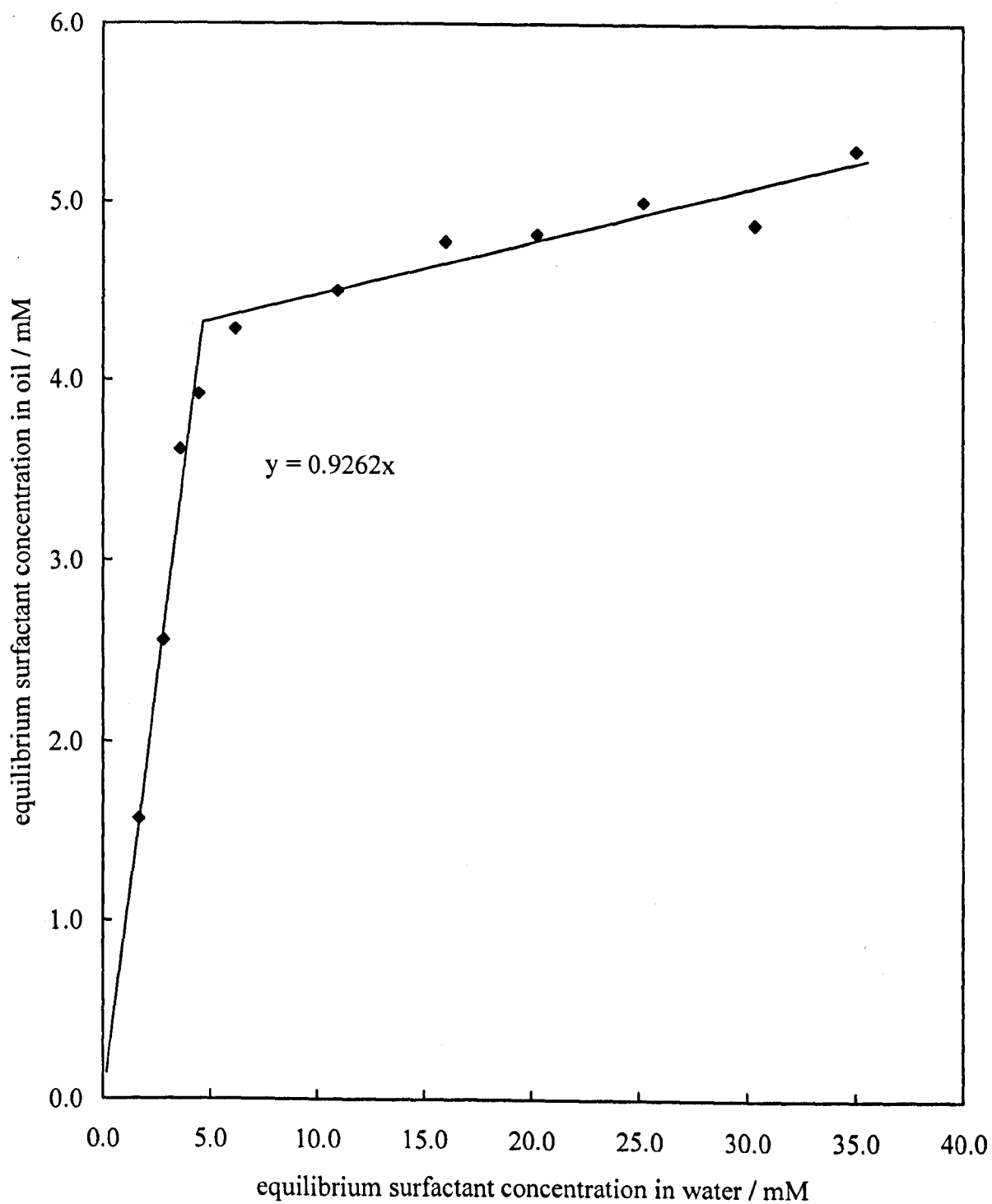


Figure 3.21. Partitioning of surfactant  $C_{12}$  at equilibrium.  $[NaBr] = 0.5 \text{ M}$ , temperature =  $25^\circ\text{C}$ ,  $\phi_o = 0.5$ , oil phase = HDDA, aqueous phase = water

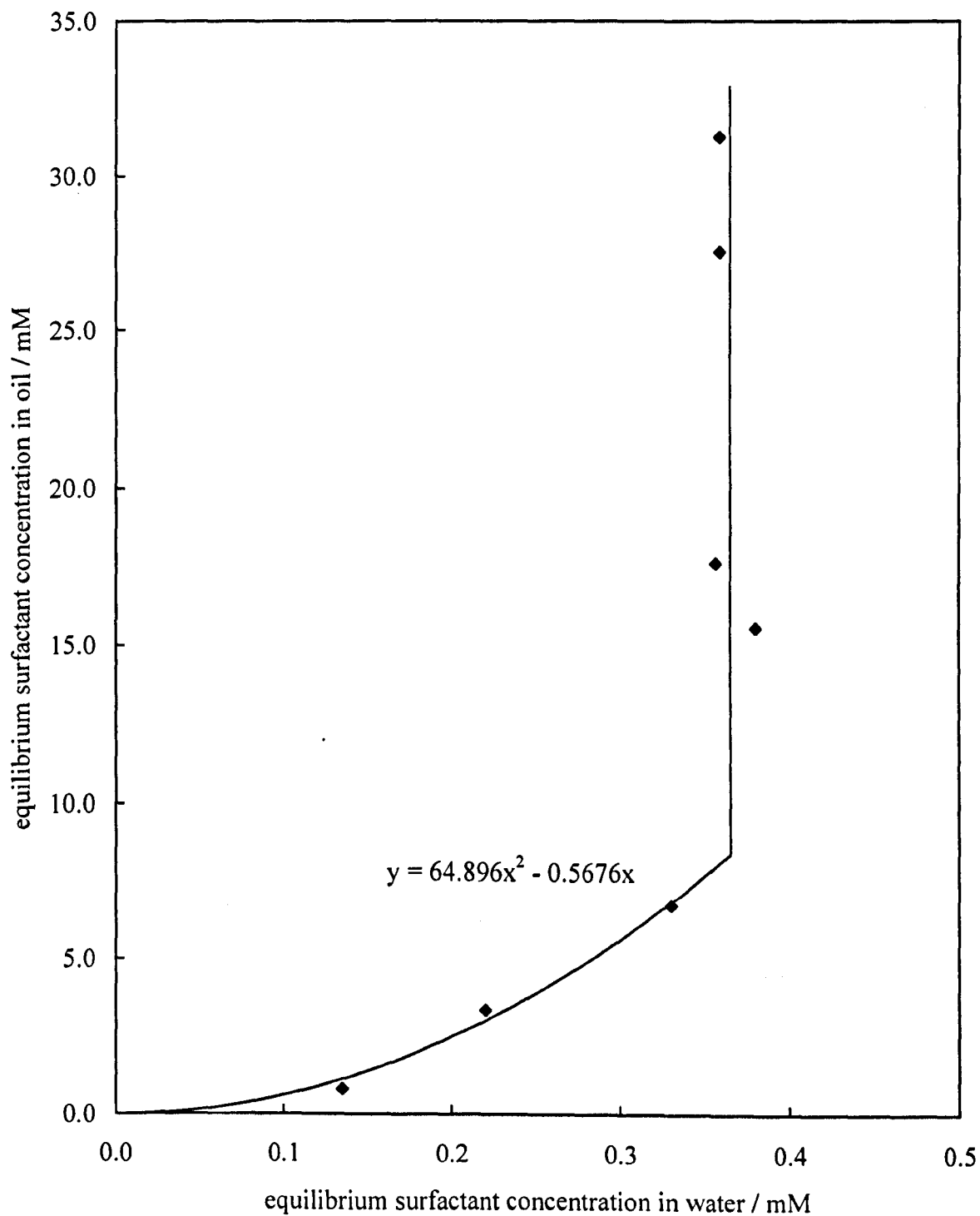


Figure 3.22. Partitioning of surfactant  $C_{3/11-M}$  at equilibrium.  $[NaBr] = 0.01\text{ M}$ , temperature =  $25^\circ\text{C}$ ,  $\phi_o = 0.5$ , oil phase = DPGDA, aqueous phase = water

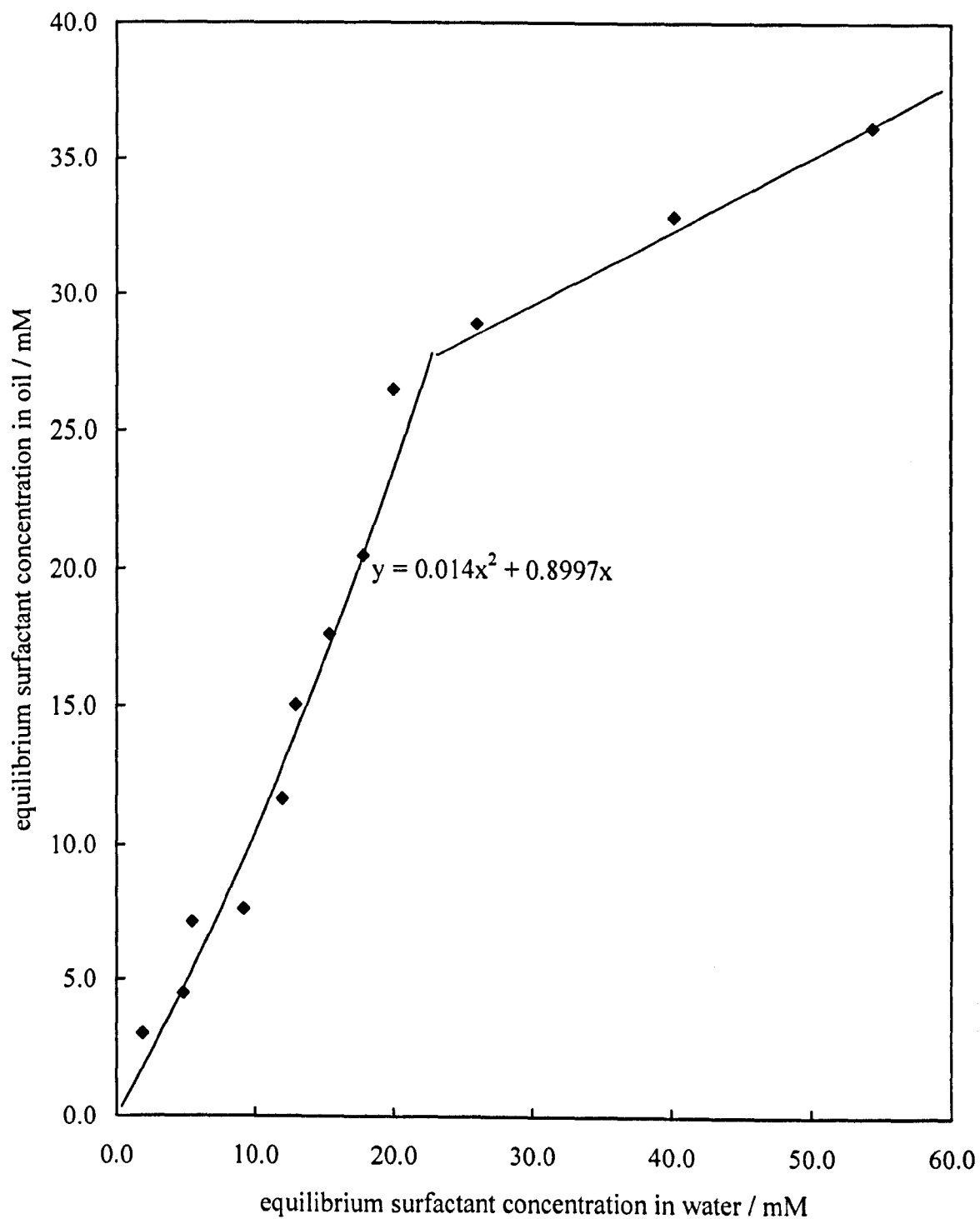


Figure 3.23. Partitioning of surfactant  $C_{3/11-M}$  at equilibrium.  $[NaBr] = 0.5 M$ , temperature =  $25^{\circ}C$ ,  $\phi_o = 0.5$ , oil phase = DPGDA, aqueous phase = water

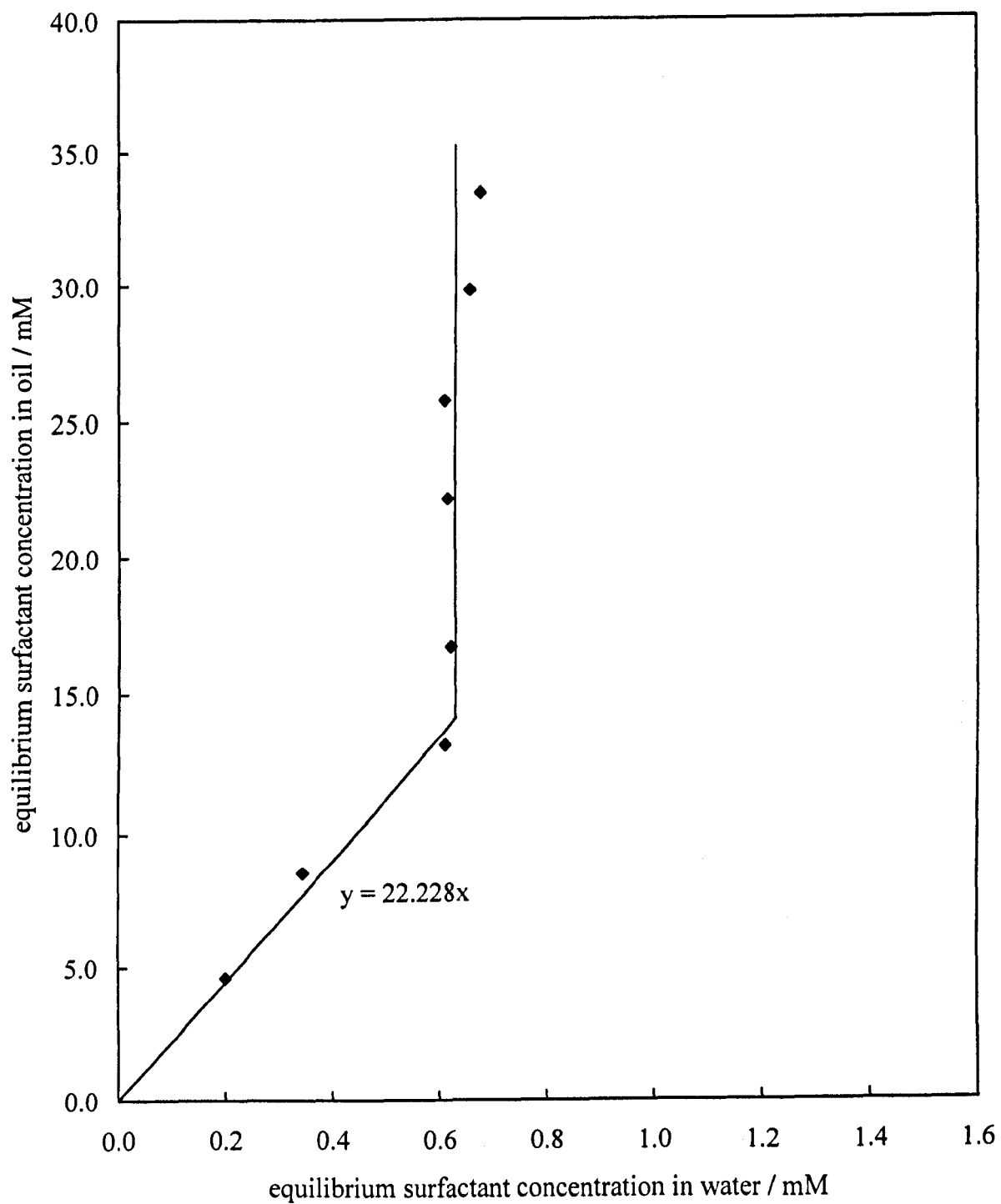




Figure 3.24. Partitioning of surfactant C<sub>10</sub> at equilibrium. [NaBr] = 0.01 M, temperature = 25°C,  $\phi_o = 0.5$ , oil phase = DPGDA, aqueous phase = water

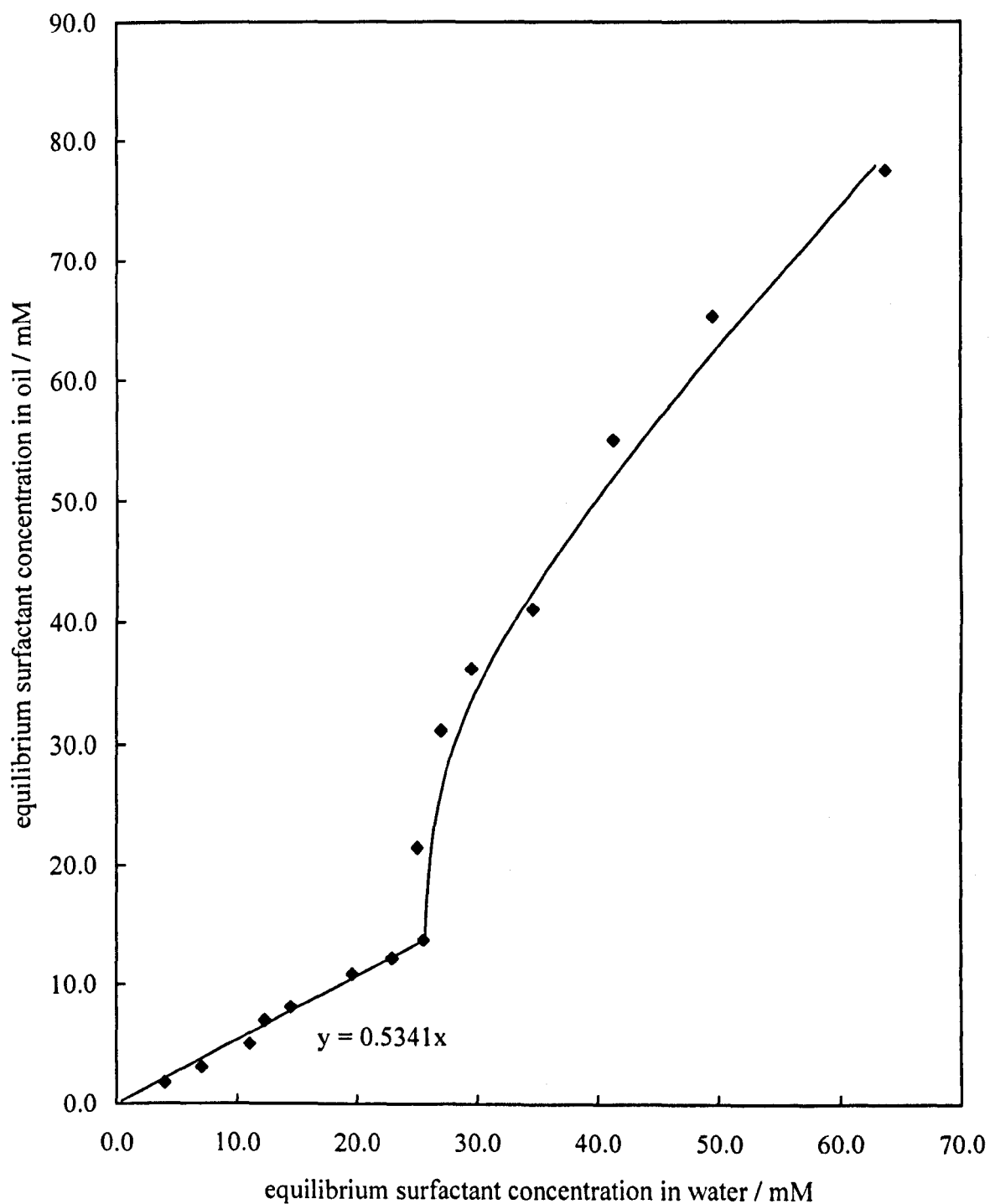


Figure 3.25. Partitioning of surfactant  $C_{10}$  at equilibrium.  $[NaBr] = 0.5\text{ M}$ , temperature =  $25^\circ\text{C}$ ,  $\phi_o = 0.5$ , oil phase = DPGDA, aqueous phase = water

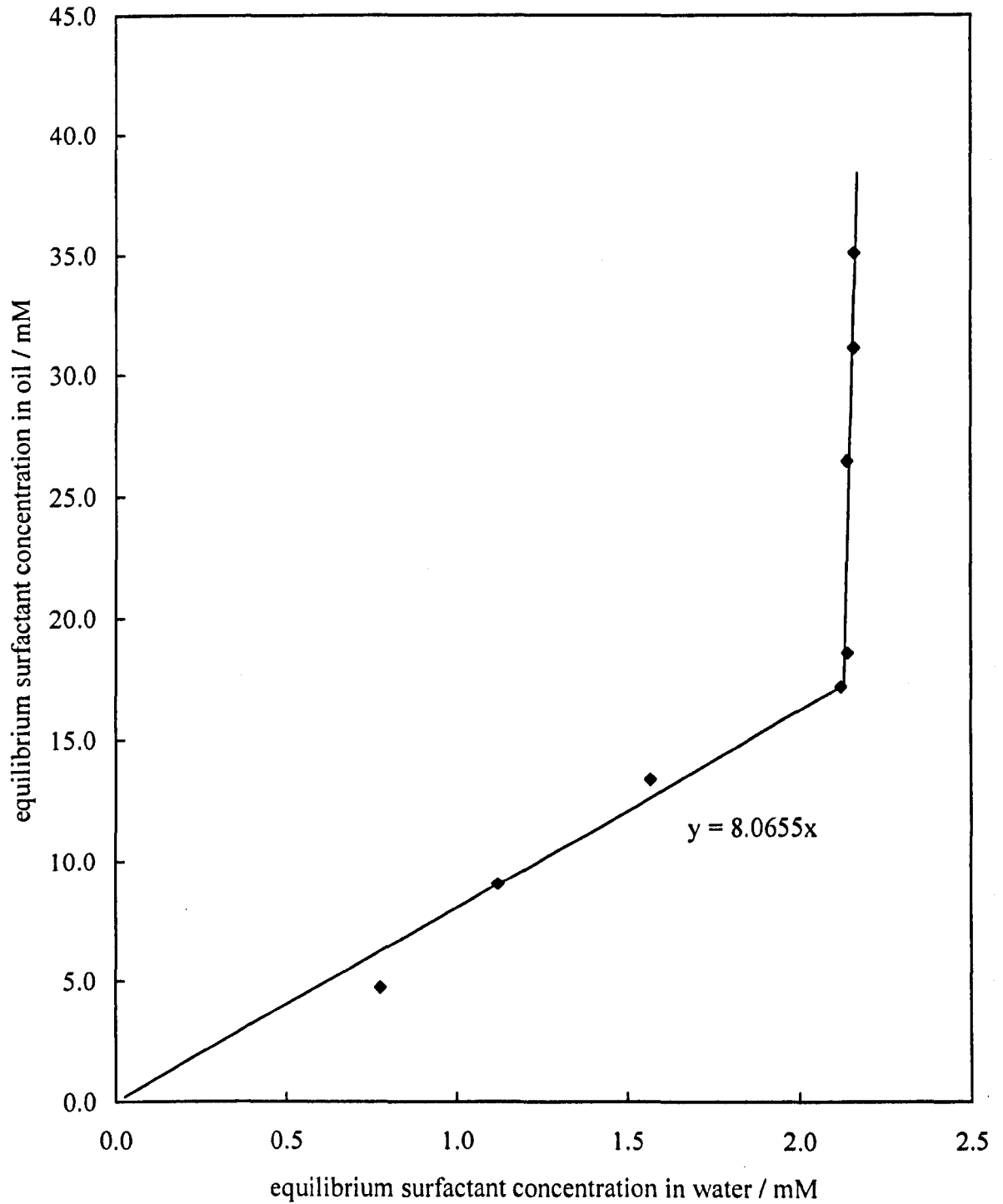


Figure 3.26. Partitioning of surfactant  $C_{12}$  at equilibrium.  $[NaBr] = 0.01\text{ M}$ , temperature =  $25^\circ\text{C}$ ,  $\phi_o = 0.5$ , oil phase = DPGDA, aqueous phase = water

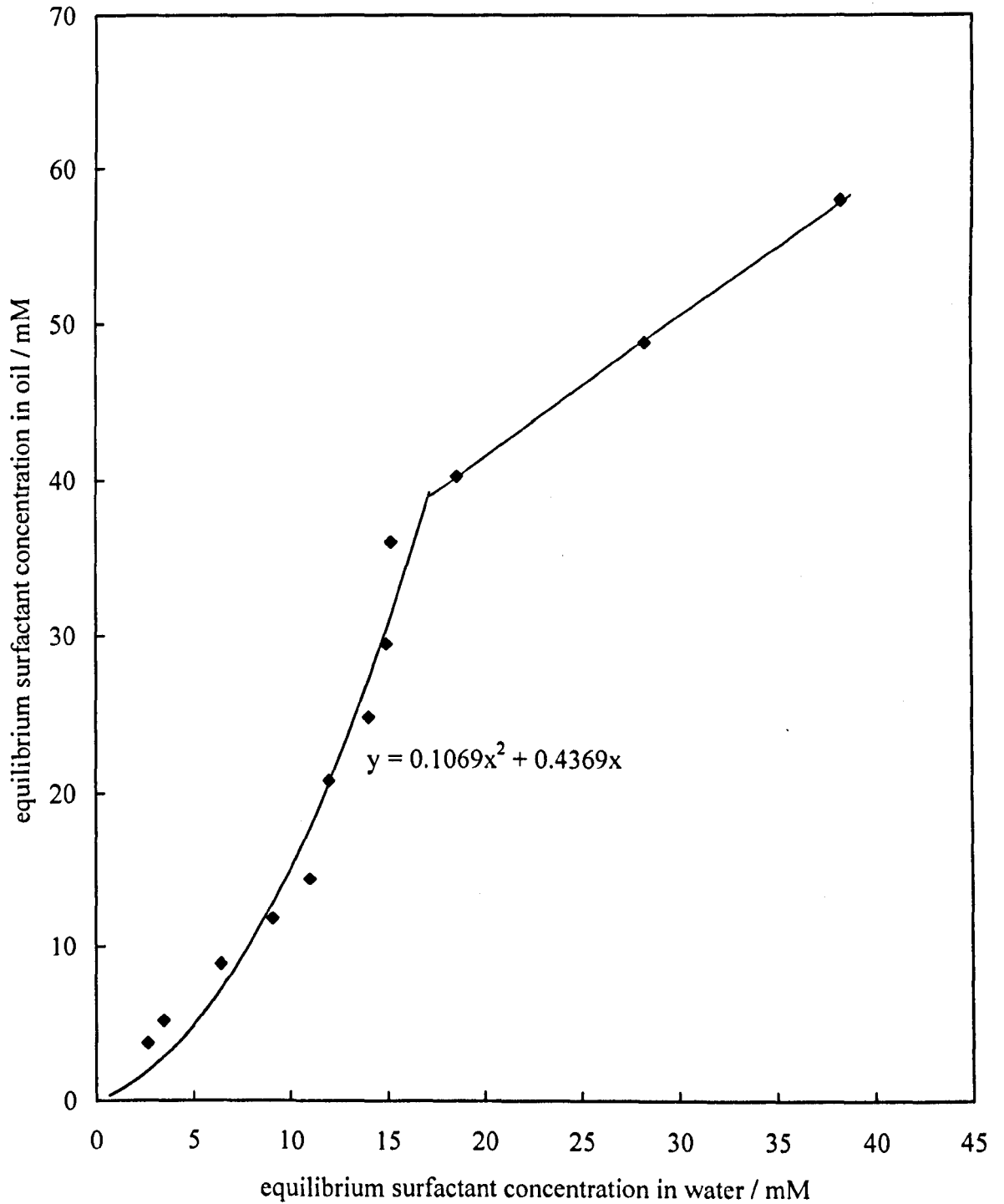
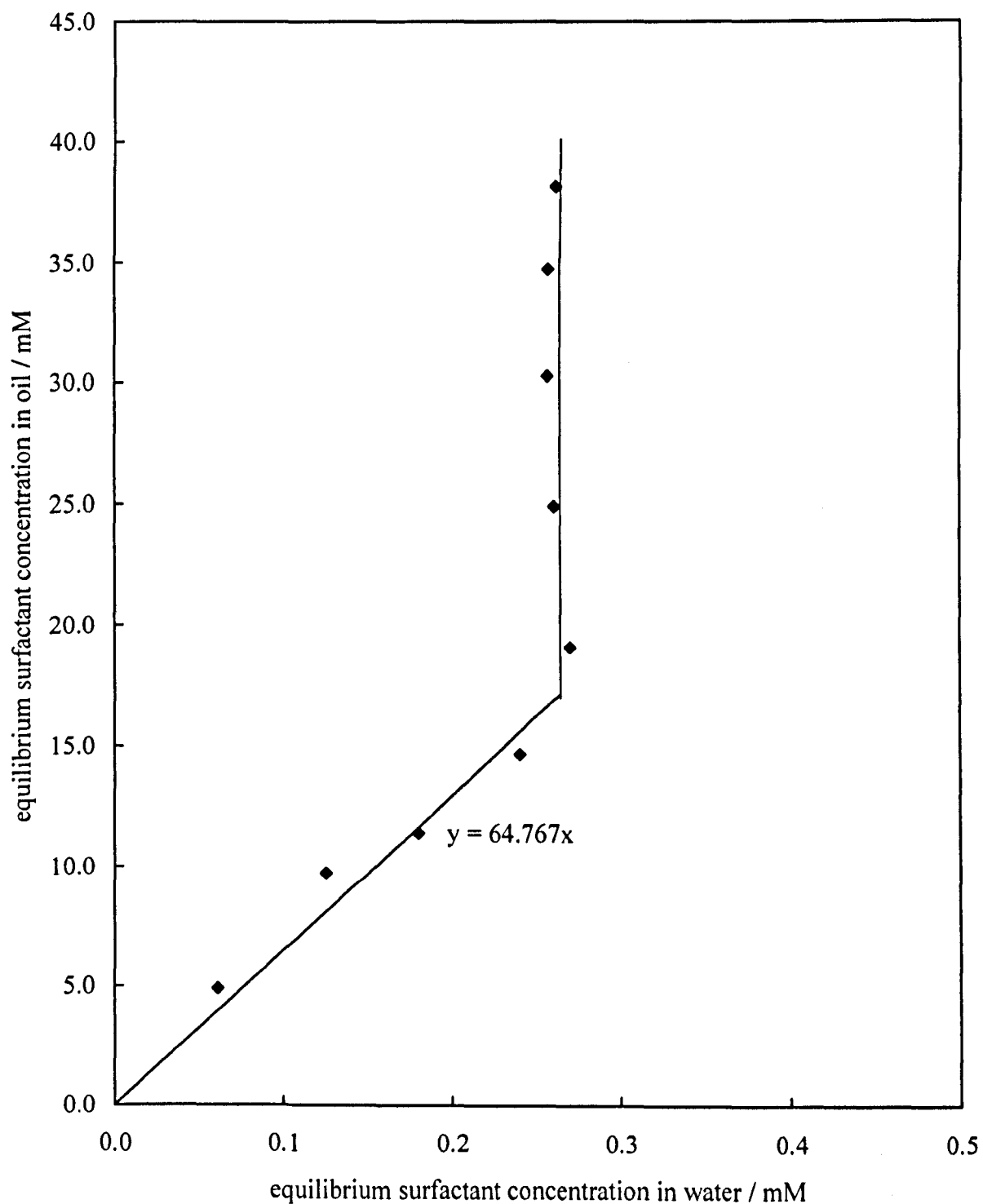


Figure 3.27. Partitioning of surfactant  $C_{12}$  at equilibrium.  $[NaBr] = 0.5\text{ M}$ , temperature =  $25^{\circ}\text{C}$ ,  $\phi_0 = 0.5$ , oil phase = DPGDA, aqueous phase = water



$$P = \frac{[\text{surfactant}] \text{ in oil}}{[\text{surfactant}] \text{ water}}$$

The partitioning of surfactant between water and oil has been studied for all three surfactants with HDDA oil and DPGDA oil at 0.01 M NaBr (below phase inversion) and 0.50 M NaBr (above phase inversion) to yield cmc values in water and oil and partition coefficients for Winsor I and II systems. This enables the effect of surfactant structure on cmc and partition coefficients to be studied for the two different oils. Figures 3.16 – 3.27 show the effect of initial surfactant concentration on the partitioning of surfactant between water and oil phases. It can be seen from these plots that Winsor I systems are produced at the low salt concentration in most cases and Winsor II systems are observed for the high salt concentration samples in all cases. Some non-ideal characteristics are seen in some systems where either the distribution of surfactant up to the cmc (Figures 3.17, 3.18, 3.19, 3.21, 3.22 and 3.26) or the distribution after the cmc (Figure 3.24) is non-linear, or surfactant is seen to partition into both water and oil after the cmcs are reached (Figures 3.18, 3.20, 3.22, 3.24 and 3.26). In some cases, a second order polynomial curve was fitted to the data up to the cmc. In these cases the value of P is dependent on the initial [surfactant] in the system, thus making direct comparison of overall P values difficult. Table 3.2 gives a summary of the Winsor type, partition coefficients, ideality of the system pre and post cmc and cmc values in water and oil for each of the systems studied.

**Table 3.2. Location of aggregates, partition coefficients and cmc values in water and oil for systems studied at 25 °C**

Surfactant / oil	[NaBr] / M	Winsor type	P <sup>a</sup>	Ideal partitioning post-cmc	cmc <sub>water</sub> / mM	cmc <sub>oil</sub> / mM
C <sub>3/11-M</sub> / HDDA	0.01	I	0.31	✓	12.3	3.8
C <sub>3/11-M</sub> / HDDA	0.50	II	-	✓	1.3	13.6
C <sub>10</sub> / HDDA	0.01	I	-	-	23.0	4.4
C <sub>10</sub> / HDDA	0.50	II	-	✓	3.4	6.7
C <sub>12</sub> / HDDA	0.01	I	0.93	-	4.8	4.3
C <sub>12</sub> / HDDA	0.50	II	-	✓	0.36	8.2
C <sub>3/11-M</sub> / DPGDA	0.01	I	-	-	22.7	27.6
C <sub>3/11-M</sub> / DPGDA	0.50	II	22.3	✓	0.62	13.8
C <sub>10</sub> / DPGDA	0.01	II	0.53	-	25.5	13.7
C <sub>10</sub> / DPGDA	0.50	II	8.07	✓	2.1	17.3
C <sub>12</sub> / DPGDA	0.01	I	-	-	17.0	39.0
C <sub>12</sub> / DPGDA	0.50	II	64.8	✓	0.26	17.0

<sup>a</sup> A dash (-) indicates non-ideal monomer surfactant partitioning.

### *Effect of components on ideality of surfactant monomer partitioning*

No obvious effect of surfactant chain length or position of methacrylate polymerizable group on the surfactant molecule is observed. Generally, DPGDA systems exhibit more ideal monomer partitioning than HDDA systems. The only exceptions to this are with low salt  $C_{3/11-M}$  and  $C_{12}$  surfactant systems, where the monomer partitioning in the HDDA system is ideal but is non-ideal in the equivalent system containing DPGDA. All Winsor II systems with DPGDA oil show ideal monomer partitioning. No trend is observed with  $[NaBr]$  for the HDDA systems. High salt systems (Winsor II) and the low salt Winsor II system with DPGDA shows ideal monomer partitioning whereas the low salt Winsor I systems are non-ideal for this oil.

### *Effect of components on ideality of post-cmc surfactant partitioning*

No effect of surfactant chain length on the post-cmc surfactant partitioning is observed. Positioning the polymerizable methacrylate group on the end of the hydrophobic tail ( $C_{3/11-M}$ ) appears to improve the ideality of post-cmc partitioning at low salt concentrations, as the  $C_{3/11-M}$  / HDDA system is the only low salt system to exhibit ideal surfactant partitioning beyond the cmc. Oil type has little effect other than with the low salt  $C_{3/11-M}$  system described above.  $[NaBr]$  appears to have a significant effect on post-cmc surfactant partitioning, as all high salt Winsor II systems show ideal partitioning whereas all low salt systems (mostly Winsor I) show non-ideal partitioning (except  $C_{3/11-M}$  HDDA low salt). This pattern suggests that post-cmc, non-ideal partitioning in the low salt systems is a result of the electrolytic effect of the surfactant. As the initial  $[surfactant]$  is increased, the total electrolytic effect of

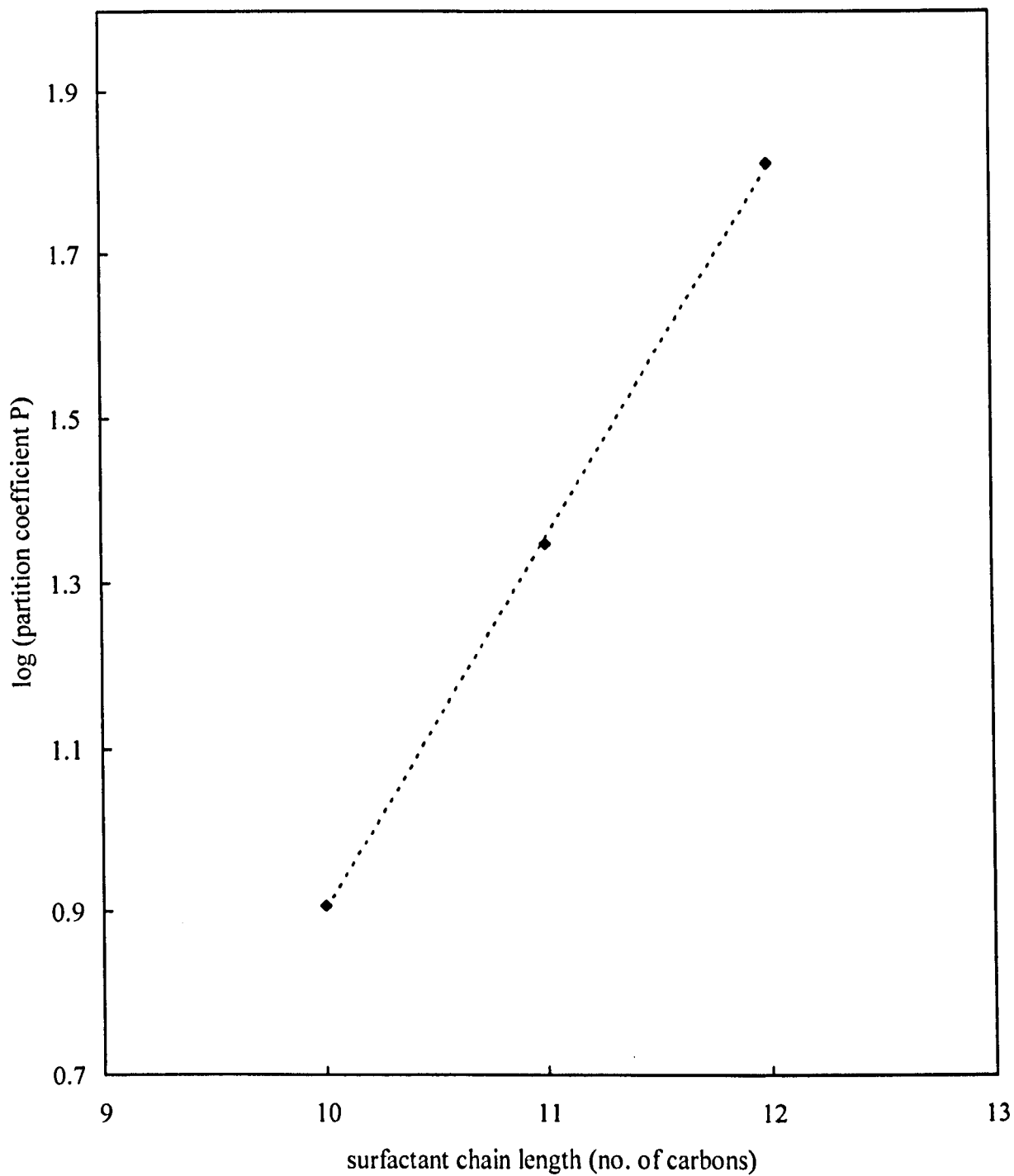
the surfactant increases, resulting in increasing surfactant partitioning into the oil phase in a WI system post-cmc. In WII systems, already at high [electrolyte], increasing the initial [surfactant] post-cmc (although increasing total [electrolyte] in the system further) will not affect partitioning post-cmc as the [electrolyte] at 0.50 M NaBr is already at a level such that all surfactant after the cmc partitions into the oil phase.

#### *Effect of components on partition coefficient P*

The high salt DPGDA systems and low salt HDDA systems show that increasing the chain length of the surfactant results in an increase in the partition coefficient  $P$ . This is expected, as the hydrophobicity of the surfactant increases with tail length and so the surfactant would be expected to partition into oil more readily with increasing tail length. One may have expected  $C_{3/11-M}$  to have the lowest value of  $P$  as the presence of the polar methacrylate group on the end of the hydrophobic tail should make the tail less hydrophobic than if the tail was a simple  $C_{11}$  hydrocarbon chain. Figure 3.28 shows a plot of  $\log(P)$  vs. the number of carbons in the hydrocarbon chain part of the tail. This figure shows that the presence of the polar methacrylate group on the end of the tail in the case of  $C_{3/11-M}$  does not lower the value of  $P$ , as the data point for  $C_{3/11-M}$  follows a linear relationship with those for  $C_{10}$  and  $C_{12}$ . This conclusion relies on a linear relationship between  $\log$  of the partition coefficient and surfactant tail length. It is likely that this is the case, as the length of the surfactant tail has a linear effect on the  $\log$  of the cmc of the surfactant<sup>16</sup> which is related to the hydrophobicity of the surfactant. The hydrophobic effect is likely to affect  $P$  in a similar manner. Comparing the high and low salt  $C_{10}$  / DPGDA systems,



Figure 3.28. Log (monomer partition coefficient P) vs surfactant chain length, where  $P = [\text{surfactant}]_{\text{oil}} / [\text{surfactant}]_{\text{aqueous}}$  for 1:1 v/v mixtures of water and DPGDA oil.  $[\text{NaBr}]$  in initial aqueous phase = 0.50 M

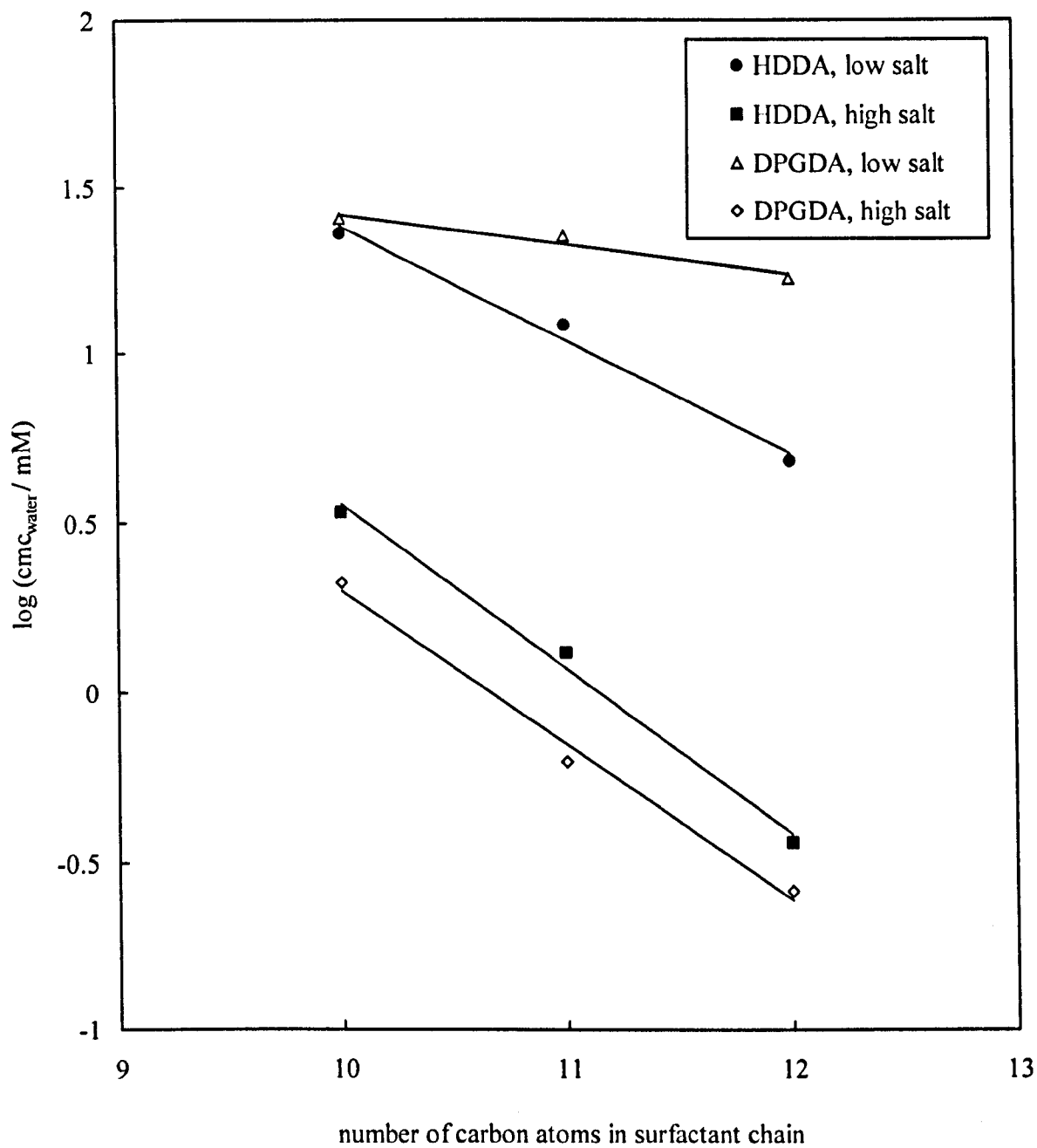


an increase in [NaBr] causes an increase P, which is likely to be due to the charge shielding effect of electrolyte on charged surfactants. This reduces the effective charge on the surfactant head group, which will allow the surfactant to partition more easily into oil. Due to the non-ideal monomer partitioning of surfactant in some of the systems it is not possible to determine the effect of oil type on P from this data.

#### *Effect of components on cmc values*

The cmc in water of the surfactants is seen to decrease by a factor of  $\sim 2$  for each additional  $\text{CH}_2$  group on the hydrophobic surfactant chain. This agrees well with literature values<sup>16,21</sup> and is due to the hydrophobic effect (see Chapter 1, section 1.2.2). Figure 3.29 shows the relationship between  $\log(\text{cmc}_{\text{water}})$  and the surfactant tail length for the two oil systems at high and low [NaBr]. In most cases, positioning the polymerizable methacrylate group on the hydrophobic tail slightly lowers the cmc in relation to the linear relationship between surfactant tail length and  $\text{cmc}_{\text{water}}$ . An increase in the polarity of the oil used has an opposite effect on  $\text{cmc}_{\text{water}}$  for the low salt systems to that for the high salt systems. The use of DPGDA (more polar) in the low salt systems causes a factor of  $\sim 2$  increase in  $\text{cmc}_{\text{water}}$  compared to the values obtained for the HDDA (less polar) systems. In the high salt systems, the use of DPGDA instead of HDDA causes a factor of  $\sim 2$  decrease in the  $\text{cmc}_{\text{water}}$  values obtained. This effect of oil polarity in the low salt WI systems can be explained by considering the free energy of transfer of the hydrophobic tail from an aqueous phase to an oil phase. The magnitude of this value is dependent on the difference in polarity between the oil and aqueous phases, so increasing the polarity of the oil will decrease the difference in polarity between the phases, therefore, decrease the free energy of

**Figure 3.29. Variation of  $\log(\text{cmc}_{\text{water}})$  with surfactant chain length for 1:1 v/v systems containing various salt concentrations in the initial aqueous phase with HDDA or DPGDA oil**



transfer. According to equation 3.1, the standard free energy of transfer ( $\Delta G^\circ$ ) is inversely proportional to the cmc:

$$\Delta G^\circ = RT \ln cmc \quad (3.1)$$

Therefore, a decrease in the free energy of transfer will result in an increase in cmc. Increasing [electrolyte] causes a reduction in  $cmc_{water}$  in all cases due to the charge shielding effect of electrolyte on an ionic surfactant allowing the surfactant headgroups to pack closer together. This allows smaller micelles to form, thus requiring fewer surfactant monomers.<sup>6,21</sup> The micelles that form at high salt in these systems are reverse micelles, as these systems are W II i.e. w/o. The largest reduction is seen in the more polar oil systems and the order of the magnitude of the reduction in  $cmc_{water}$  with [salt] for both oil systems with respect to surfactant type is:  $C_{12} > C_{3/11-M} > C_{10}$ .

Surfactant tail length has a complex relationship with  $cmc_{oil}$ , which seems to depend on the oil type and salt concentration of a particular system. The cmc in oil does not increase or decrease with surfactant tail length for any low salt WI or high salt WII system. The position of the polymerizable methacrylate group on the surfactant molecule is not observed to have a clear effect on  $cmc_{oil}$ . The polarity of the oil used does affect  $cmc_{oil}$  as higher  $cmc_{oil}$  values are observed for the more polar DPGDA oil than those for equivalent HDDA systems in all cases. In the case of aggregation in aqueous systems, micellisation is driven by the free energy of transfer of a hydrocarbon chain from a polar aqueous environment into a non-polar oil environment. This energy of transfer is large and negative reflecting the fact that

hydrocarbon chains would rather reside in a non-polar phase than a polar one. Aggregation in oil systems, i.e. micellisation in oil, may be driven by the hydrophilic head groups aggregating out of the oil phase and into an aqueous-like environment of the surfactant head groups in a similar manner to hydrocarbon tails aggregating out of water. The free energy of transfer of a hydrophilic head group from oil to aqueous-like environment must be negative reflecting the fact that the head group would rather reside in an aqueous-like environment than in oil. If the surfactant type is fixed and oils of different polarity are used, then the magnitude of the free energy of transfer will depend on the polarity of the oil. A more polar oil will result in lower values for the energy of transfer as the surfactant would partition more preferably into a more polar oil than a less polar one. A lower free energy of transfer will result in a higher value for the cmc as the driving force for micellisation, which is dependent on the magnitude of the free energy of transfer, will be reduced, thus the onset of micellisation will occur at a higher monomer surfactant concentration. As [NaBr] increases from 0.01 to 0.5 M in each system,  $cmc_{oil}$  increases in the HDDA systems and decreases in the DPGDA systems showing a transition from W I to W II. The effect seen in the DPGDA systems will be due to closer packing of the hydrophilic head groups due to reduced electrostatic repulsions as seen with  $cmc_{water}$ . The increase in  $cmc_{oil}$  with increasing [electrolyte] seen in the HDDA systems is more difficult to explain but could be due to the added salt ions reducing the effective charge on the head group. This will reduce their tendency to aggregate so that the head groups are out of the oil phase, i.e. decrease  $\Delta G^\circ$ , therefore increasing the  $cmc_{oil}$ . There appears to be a balance between a decrease in  $cmc_{oil}$  due to reduced electrostatic repulsion of headgroups and an increase in  $cmc_{oil}$  due to decreased desire of headgroups to

aggregate out of the oil phase (i.e. decrease in  $\Delta G^\circ$ ). The equilibrium position of this balance depends on the polarity of the oil present.

#### *Effect of [NaBr] on Winsor type*

Increasing the [NaBr] in the initial aqueous phase from 0.01 to 0.50 M inverts the systems from W I to W II in all systems with one exception. Addition of electrolyte to an ionic surfactant system reduces the effective charge on the surfactant due to the electrolyte counterions shielding the charge on the surfactant. This reduces the electrostatic repulsion of the surfactant head groups, therefore reducing their effective charge, shifting the HLB value of the surfactant to lower values and reversing the surfactant monolayer curvature. The exception to this is the C<sub>10</sub> / DPGDA system, where it is believed even at 0.01 M salt a w/o system is formed.

### 3.6 Conclusions

The preparation and characterisation of emulsions, microemulsions and surfactant solutions of the nine systems using the three surfactants and the three oils has been described. The effects of temperature and added electrolyte on the macroemulsions and the effects of added electrolyte and initial concentration of surfactant on the partitioning of surfactant between the two phases in microemulsion systems have been studied.

(a) All surfactants are most soluble in water with the solubility in the three oils being similar for each surfactant. In general, the order of extent to which the surfactants dissolve in each solvent is:  $H_2O \gg DPGDA > BDDA > HDDA$ . The order of solubility of the surfactants in each solvent is:  $C_{3/11-M} > C_{10} > C_{12}$ .

(b) It has been shown that stable o/w emulsions can be produced in all nine systems and that no phase inversion occurs with temperature up to 55°C in any system.

(c) Oil-in-water emulsion breaking occurs at high salt concentrations in all systems with phase inversion to produce w/o emulsions occurring in all systems containing  $C_{3/11-M}$  and all systems containing HDDA.

(d) At a certain concentration of salt, the partitioning of surfactant between oil and water changes from mostly in water to mostly in oil in all systems as the preferred curvature of surfactant changes from positive to negative.

(e) The salt concentration at which the preferential phase of surfactant partitioning changes from water to oil decreases as the surfactant concentration in the initial aqueous phase increases, suggesting that the surfactant itself acts as a weak salt. This also increases the amount of surfactant that will partition into the oil phase for an o/w system as the charge on the head group of the surfactant is shielded more effectively, thus shifting the HLB for the surfactant towards lower values.

(f) Winsor I microemulsion systems have been produced at low salt concentration and Winsor II systems are observed at high salt concentration for systems containing HDDA or DPGDA for each of the three surfactants.

(g) Increasing surfactant chain length increases the monomer partition coefficient  $P$ . Low salt, Winsor I systems show non-ideal surfactant partitioning post-cmc whereas high salt systems show ideal surfactant partitioning post-cmc.

(h) The cmc in water of the surfactants is seen to decrease by a factor of  $\sim 2$  for each additional  $\text{CH}_2$  group on the hydrophobic surfactant chain.  $\text{cmc}_{\text{water}}$  for a particular surfactant increases with increasing polarity of the oil used for low salt systems but decreases with increasing polarity of the oil used for high salt systems. Increasing [electrolyte] decreases  $\text{cmc}_{\text{water}}$  in all systems.

(i) Increasing polarity of the oil increases  $\text{cmc}_{\text{oil}}$  for a particular surfactant. Increasing electrolyte increases  $\text{cmc}_{\text{oil}}$  with HDDA and decreases  $\text{cmc}_{\text{oil}}$  for DPGDA.



### 3.7 References

- <sup>1</sup> A. Kabalnov and H. Wennerström, *Langmuir*, **12**, 276 (1996).
- <sup>2</sup> K. Shinoda and S. Friberg, 'Emulsions and Solubilisation', Wiley, New York (1986).
- <sup>3</sup> D. N. Petsev, N. D. Denkov and P. A. Kralchevsky, *J. Colloid Interface Sci*, **176**, 201 (1995).
- <sup>4</sup> B. P. Binks, *Langmuir*, **9**, 25 (1993).
- <sup>5</sup> B. P. Binks (Ed), 'Modern Aspects of Emulsion Science', Royal Society of Chemistry, Cambridge (1998).
- <sup>6</sup> B. P. Binks, *Colloids and Surfaces A*, **71**, 167 (1993).
- <sup>7</sup> B. P. Binks, J. Dong and N. Rebolj, *Phys. Chem. Chem. Phys.*, **1**, 2335 (1999).
- <sup>8</sup> M. J. Rosen, 'Surfactants and Interfacial phenomena', Wiley, New York (1998).
- <sup>9</sup> N. P. Ashby, B. P. Binks and P. D. I. Fletcher, Report to Avecia Ltd., August 2000.
- <sup>10</sup> K. Shinoda and H Arai, *J. Phys. Chem.*, **68**, 3485 (1964).
- <sup>11</sup> R. Aveyard, B. P. Binks, P. D. I. Fletcher, X. Ye and J. R. Lu, in J. Sjöblom (Ed.), 'Emulsions – A Fundamental and Practical Approach', Kluwer, Amsterdam, pp. 97 (1992).
- <sup>12</sup> P. W. Atkins, *Physical Chemistry* (5<sup>th</sup> edition), Oxford University Press, Oxford (1994).
- <sup>13</sup> D. J. Shaw, *Introduction to Colloid and Surface Chemistry* (4<sup>th</sup> edition), Butterworth-Heineman, Oxford (1992).
- <sup>14</sup> R. J. Hunter, *Foundations of Colloid Science* (2<sup>nd</sup> edition), Oxford University Press, New York (2001).
- <sup>15</sup> R. Aveyard, B. P. Binks and P. D. I. Fletcher, in E. Wyn-Jones and D. Bloor

- (Eds.), 'Structure, Dynamics and Equilibrium Properties of Colloidal Systems', Kluwer, Amsterdam, pp. 557 (1990).
- <sup>16</sup> J. H. Clint, 'Surfactant Aggregation', Blackie, London (1992).
- <sup>17</sup> P. Swansbury, PhD Thesis, University of Hull (1993).
- <sup>18</sup> R. Aveyard, B. P. Binks, P. J. Dowding, P. D. I. Fletcher, C. E. Rutherford and B. Vincent, *Phys. Chem. Chem. Phys.*, **1**, 1971 (1999).
- <sup>19</sup> B. P. Binks, PhD Thesis, University of Hull (1986).
- <sup>20</sup> P. A. Winsor, 'Solvent Properties of Amphiphilic Compounds', Butterworths, London (1954).
- <sup>21</sup> R. Aveyard, B. P. Binks, S. Clark, P. D. I. Fletcher, H. Giddings, P. A. Kingston and A. Pitt, *Colloids and Surfaces*, **59**, 97 (1991).

# *CHAPTER 4*

# CHAPTER 4

## CHARACTERISATION OF MICROEMULSION SYSTEMS CONTAINING HIGH SURFACTANT CONCENTRATION

### 4.1 Introduction

Following work on the characterisation of microemulsion systems containing the polymerizable surfactants and oils, with surfactant concentrations at most only a few times that of the cmc for each particular system, microemulsion systems with high initial [surfactant] were prepared. There are two reasons for this:

(i) It is known that microemulsion phases can be polymerised to form polymer films.<sup>1-10</sup> The sponge-like structure of bicontinuous microemulsions in particular (domains of water and oil separated by surfactant monolayers)<sup>11-14</sup> polymerises very well to form a microstructurally ordered polymer film.<sup>1-7</sup> If the oil and surfactant are polymerizable, the oil domains and surfactant monolayers can polymerise leaving a solid structure from which the water contained in the microemulsion can drain or evaporate; thus, a porous polymer will be produced.<sup>15</sup> Bicontinuous phases are surfactant rich and require [surfactant] far in excess of the cmc to stabilise large volume fractions in an equilibrium system.<sup>16</sup>

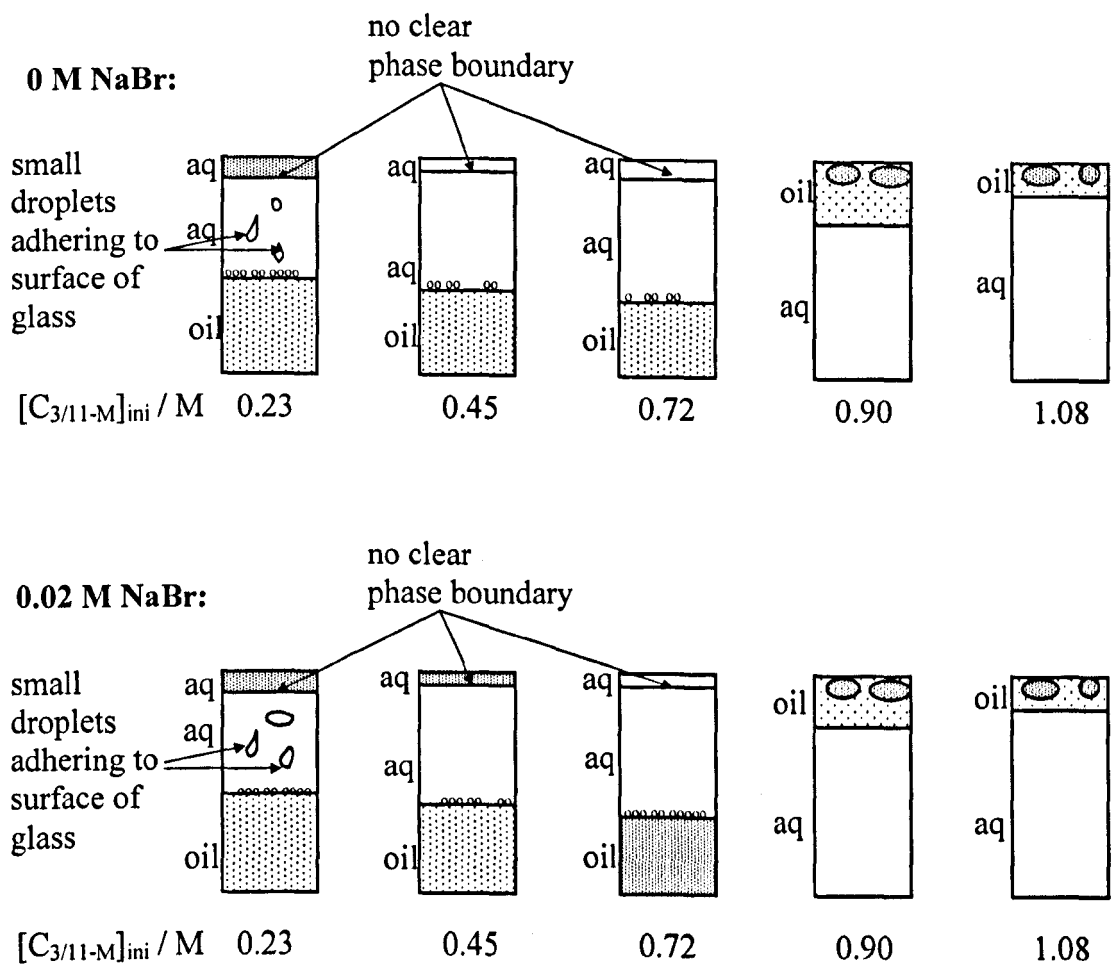
(ii) Micellar phases can also polymerise but in an o/w system are unlikely to form a polymer film at low initial [surfactant]. This is because in order to produce a solid film, significant polymer linking between separate micelles needs to occur during the polymerisation process.<sup>17</sup> This can only take place if the quantity of micelles is high enough to result in sufficient micelle-micelle interactions during the polymerisation process. Increasing the overall [surfactant] in a system increases the number of micelles at equilibrium allowing sufficient micelle-micelle interactions to form a polymer structure.

## 4.2 Microemulsions prepared with H<sub>2</sub>O

Water has been used as the aqueous phase in the work described in Chapter 3, so it was decided to prepare microemulsion phases using high initial [surfactant] also using water as the aqueous phase, as it is cheap and readily available in purified form.


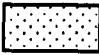


Following the appearance of an apparent third phase shown in Chapter 3, Figure 3.13, an equilibrium system using C<sub>3/11-M</sub> surfactant and HDDA oil with a high initial surfactant concentration ( $[\text{surfactant}]_{\text{ini}}$ ) was prepared at 0 and 0.02 M NaBr. It was thought that if a third phase was present, an increase in  $[\text{surfactant}]_{\text{ini}}$  would increase the volume fraction of the droplets seen in Figure 3.13 producing a definite third phase. The [NaBr] of 0 M and 0.02 M in the initial aqueous phase were selected because most droplets were seen in the system containing 0.02 M NaBr. A system containing no added electrolyte was also prepared because it was thought that the electrolytic effect of the surfactant, described in Chapter 3, may stabilise a third phase at very high  $[\text{surfactant}]_{\text{ini}}$ . Figure 4.1 shows the appearance of the equilibrium phases

**Figure 4.1.** Appearance of equilibrium phases for a system containing HDDA oil and H<sub>2</sub>O stabilised by various [C<sub>3/11-M</sub>]<sub>ini</sub> at 0.00 M and 0.02 M initial [NaBr]



[C<sub>3/11-M</sub>]<sub>ini</sub> is the surfactant concentration in the initial aqueous phase prior to equilibration, corrected for surfactant purity.

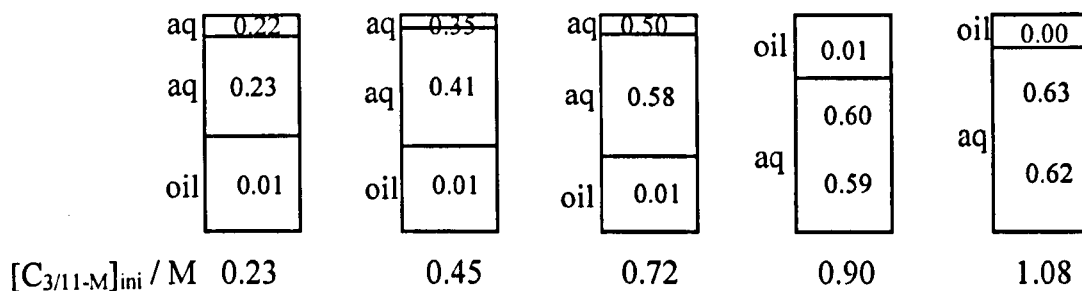
**Key:**

			
clear	almost clear	slightly turbid	turbid

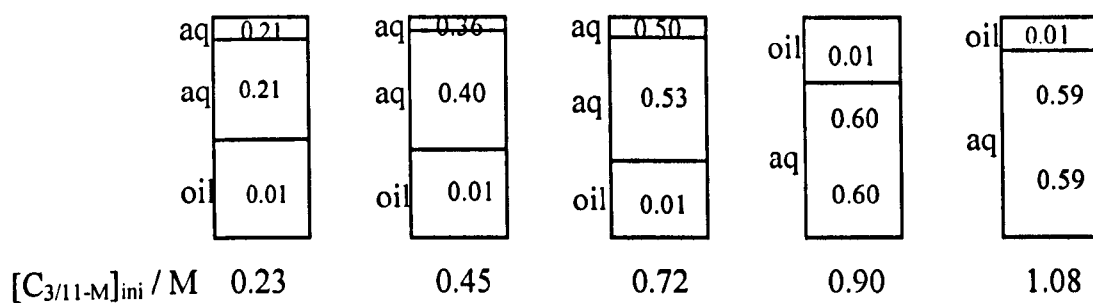
prior to sampling. Figure 4.2 shows the [surfactant] present in each equilibrium phase, calculated from Epton titrations of the phases. These figures are corrected to account for the purity of the surfactant. Note that the numbers will not necessarily add up to the [surfactant]<sub>ini</sub> value below each tube as this value is for the initial aqueous phase, which is half the original total phase volume. Changes in aqueous phase volume and surfactant partitioning into oil phases during equilibration need to be taken into account when calculating mass balance. Above 0.72 M [surfactant]<sub>ini</sub>, the relative densities of the aqueous and oil phases invert. Solubilisation of oil into the aqueous phase increases steadily with increasing surfactant concentration, which would be expected for o/w systems, as the greater the concentration of surfactant the more micelles are formed and more oil can be solubilised into the normal micelle core.<sup>16,18</sup> It is thought that as there is no clear phase boundary between the two aqueous phases in the samples containing 0.23, 0.45 and 0.72 M [surfactant]<sub>ini</sub>, they are actually one phase with the equilibrium [surfactant] increasing slightly down the tube, possibly as a result of a gradient under gravity, in equilibrium with an oil continuous phase. Figure 4.2 shows that the aggregates in the equilibrium systems are located in the aqueous phase only for both salt concentrations making this a Winsor I-like system. Higher salt concentrations would be necessary to produce a Winsor III system<sup>16,19</sup> consisting of a surfactant-rich bicontinuous phase in equilibrium with excess oil and water phases. In order to determine the nature of the droplets seen in the samples at 0.90 and 1.08 M [C<sub>3/11-M</sub>]<sub>ini</sub>, a calculation of proportion of added surfactant accounted for by Epton titration was made. Table 4.1 shows the number of moles of surfactant added initially and the number of moles calculated from the titrations. It can be seen that all of the surfactant is accounted for within the errors except the sample with 0.92

**Figure 4.2. [Surfactant] / M of equilibrium phases for a system containing HDDA oil and H<sub>2</sub>O stabilised by various [C<sub>3/11-M</sub>]<sub>ini</sub> at 0.00 M and 0.02 M initial [NaBr]**

**0 M NaBr:**



**0.02 M NaBr:**





$\times 10^{-3}$  moles of surfactant added initially, which is close to the error limit, suggesting that the small droplets seen in the sample tubes do not contain a surfactant-rich phase.

**Table 4.1. Moles of surfactant added initially and number of moles calculated from titrations after equilibrium. Oil = HDDA**

<b>[NaBr] / M</b>	<b>[C<sub>3/11-M</sub>]<sub>ini</sub> / M</b>	<b>No. of moles of surfactant added to sample (<math>\times 10^{-3}</math>)<sup>a</sup></b>	<b>No. of moles calculated from titrations (<math>\times 10^{-3}</math>)<sup>a</sup></b>	<b>Mass balance / %</b>
0.00	0.23	0.92	1.01	+9.8
0.00	0.45	-	-	-
0.00	0.72	2.89	2.91	+5.8
0.00	0.90	3.60	3.42	-5.6
0.00	1.08	4.32	4.35	+0.7
0.02	0.23	0.92	0.97	+4.6
0.02	0.45	1.80	1.87	+3.9
0.02	0.72	2.89	2.81	-2.8
0.02	0.90	3.60	3.42	-5.0
0.02	1.08	4.32	4.07	-5.8

<sup>a</sup> The errors in these figures were calculated to be 6% in the aqueous phase and 9% in the oil phase.

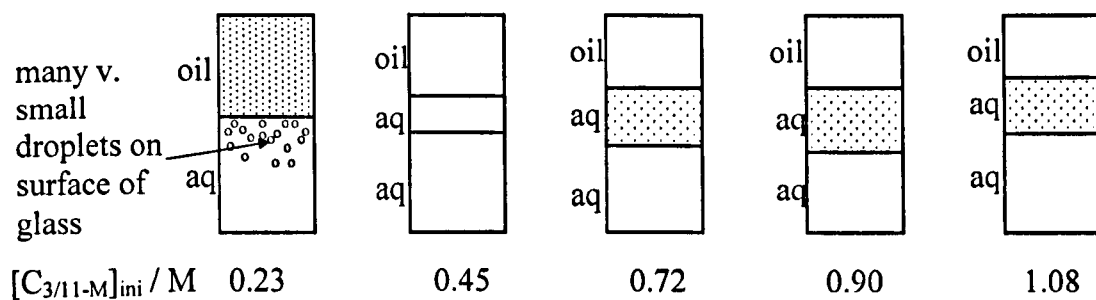
### 4.3 Microemulsions prepared with D<sub>2</sub>O in the absence of salt

In the work described in 4.2 it was thought that the similarity in density of water and HDDA may be contributing to the unclear phase boundaries and no definite third phase seen, as one would expect to see a third phase in systems with high [surfactant]<sub>ini</sub> such as these. It was therefore decided to prepare samples with the same series of initial surfactant concentrations as those in Figures 4.1 and 4.2, but using D<sub>2</sub>O in place of H<sub>2</sub>O to increase the density difference between the oil and aqueous phases. This should enable formation of a third phase with a density of sufficient difference to the oil and aqueous phases to produce clear phase boundaries. The samples were equilibrated in the same way as those in section 4.2.1 using the same batches and purity of C<sub>3/11-M</sub> surfactant and HDDA oil. Figure 4.3 shows the appearance of these phases at equilibrium. The use of D<sub>2</sub>O in place of H<sub>2</sub>O clearly has a significant effect on the equilibration of the microemulsion phases resulting in three phase systems with clear phase boundaries.

#### 4.3.1 Purity issues with surfactant C<sub>3/11-M</sub>

During analysis of the phases shown in Figure 4.3 it was noted that the microemulsion phases were not stable following extraction of small portions of the equilibrium phases and the phase equilibration was not reproducible. The extraction of small portions of phase from a system at equilibrium should not affect the equilibrium position of the system i.e. the composition of each equilibrium phase should remain the same; only the relative phase volumes should change. It was thought that the purity of the surfactant might be the cause of this non-reproducible equilibration, as it

**Figure 4.3. Appearance of equilibrium phases for a system containing HDDA oil and D<sub>2</sub>O stabilised by various [C<sub>3/11-M</sub>]<sub>ini</sub> (batch NBZ-1877-77) prior to extraction of portion of phases**



is well known that impurities can affect the formation and stability of microemulsion phases.

#### ***4.3.1.1 Problems resulting from impurities present in C<sub>3/11-M</sub>***

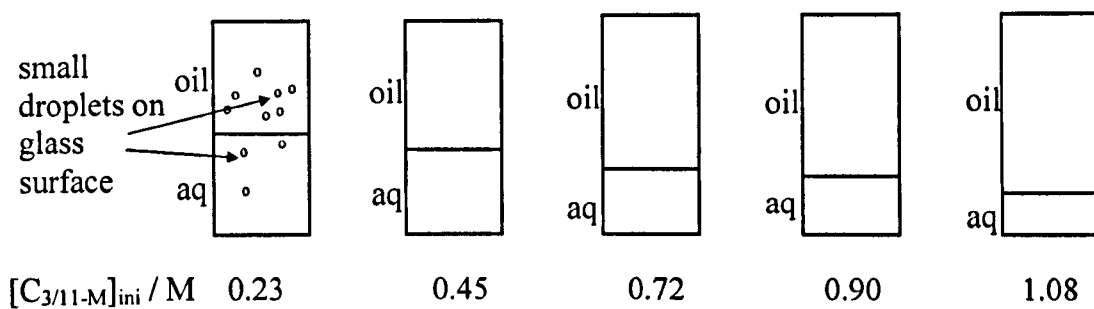
##### **4.3.1.1.1 Microemulsion phase equilibration**

The appearance of the equilibrium phases in Figure 4.3 following the extraction of portions of each of the phases is shown in Figure 4.4. In order to check the reproducibility of the preparation, it was decided to prepare another series of the samples prepared exactly as those shown in Figure 4.3. Batch 17/5/01 of C<sub>3/11-M</sub> surfactant was used for the repeat preparation of these phases, as batch NBZ-1877-77 was no longer available in sufficient quantities. It was found that a third phase could no longer be produced in any sample. The preparation was repeated but again no third phase resulted in any sample, although the solubilisation of water into oil increases with increasing [surfactant]<sub>ini</sub>. Figure 4.5 shows the appearance of the phases prepared with batch 17/5/01 of C<sub>3/11-M</sub> surfactant.

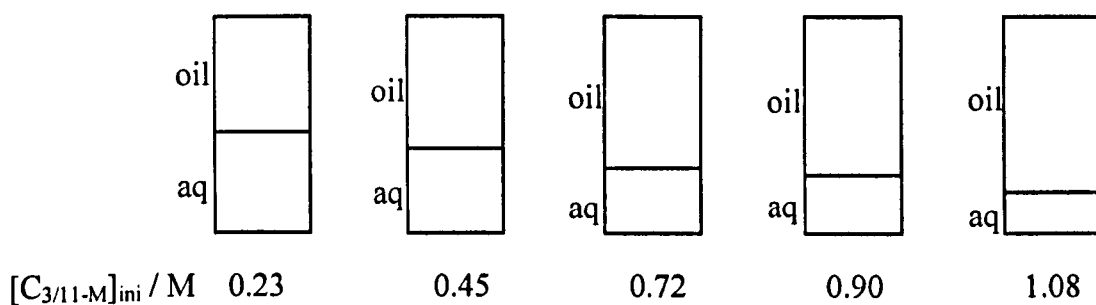
##### **4.3.1.1.2 Purity gradient in sample vessel**

It was thought that the lack of reproducibility of preparation of three phase systems could be due to differences in the level of impurities present in the two surfactant batches. The surfactant is a brown oil when first prepared and undergoes a phase transition over time to a light brown wax. It is possible that any impurities will rise or settle within the sample bottle before this transition occurs, so the purity of.

**Figure 4.4.** Appearance of equilibrium phases for a system containing HDDA oil and D<sub>2</sub>O stabilised by various [C<sub>3/11-M</sub>]<sub>ini</sub> (batch NBZ-1877-77) after extraction of portion of phases



**Figure 4.5.** Appearance of equilibrium phases for a system containing HDDA oil and D<sub>2</sub>O stabilised by various [C<sub>3/11-M</sub>]<sub>ini</sub> using batch 17/5/01 of C<sub>3/11-M</sub>



C<sub>3/11-M</sub> surfactant batch 17/5/01 was measured at certain points in the sample bottle provided by Avecia.. Table 4.2 shows the results of the study

**Table 4.2. Purity of surfactant C<sub>3/11-M</sub> in relation to position in sample bottle**

Distance from top of sample bottle / mm	Surfactant added to Epton mixture / x10 <sup>-3</sup> moles	Surfactant calculated from Epton titration / x10 <sup>-3</sup> moles	Surfactant purity / % ± 1.5
5	5.23	4.67	89.3
5	5.30	4.62	87.2
40	5.80	4.95	85.3
40	4.25	3.70	85.1
65	6.61	5.50	83.2
65	5.28	4.34	82.2

It can be seen from Table 4.2 that there is some small difference in the purity of the surfactant depending on the position of the sample in the sample vessel. This may affect the reproducibility of equilibration of microemulsion phases prepared with this surfactant.

#### 4.3.1.2 Purification of surfactant C<sub>3/11-M</sub>

To enable the reproducible preparation of high surfactant concentration microemulsion phases using C<sub>3/11-M</sub> surfactant a method of surfactant purification was developed.

##### 4.3.1.2.1 Effects on phase equilibration using Avecia method

A sample of C<sub>3/11-M</sub> batch 17/5/01 was purified using the method provided by Avecia described in detail in Chapter 2, section 2.8.1. The purity was measured by Epton titration before purification and after steps 5 and 7 of the purification method. The purity of the surfactant is shown in Table 4.3.

**Table 4.3. Purity of C<sub>3/11-M</sub> batch 17/5/01 before and after purification**

<b>Stage of purification</b>	<b>Purity / % ± 1.5</b>
unpurified	88.7
after step 5	96.8
after step 7	96.1

Table 4.3 shows that maximum purification is reached after step 5 and that purification using this procedure has a significant effect on the purity of the surfactant. A series of microemulsion samples have been prepared using an identical method to

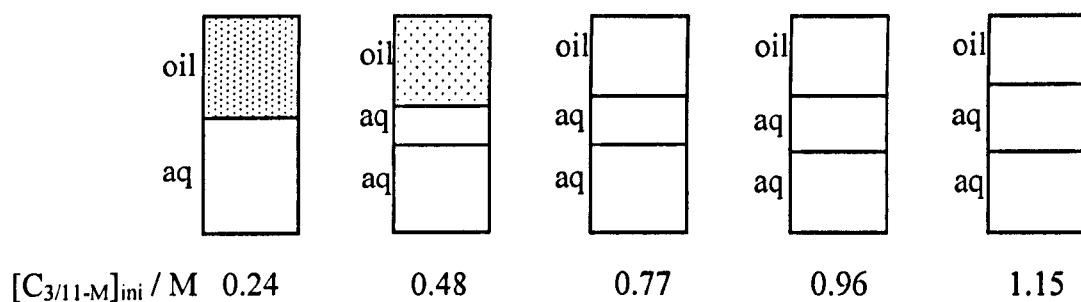
those shown in Figure 4.3. The appearance of these phases is shown in Figure 4.6. Following purification a third phase is produced in all samples from 0.48 M  $[C_{3/11-M}]_{ini}$ . Thus, the purification of the surfactant enables production of a third phase. It is noted that the phase boundaries are more defined than has been observed in previous samples.

#### 4.3.1.2.2 Modification of purification method

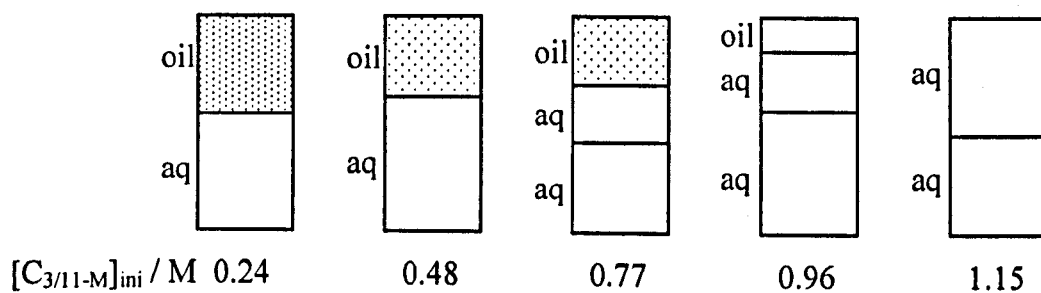
Following the purification of  $C_{3/11-M}$  surfactant and subsequent preparation of microemulsion phases shown in Figure 4.6, a second set of phases were prepared exactly as those in Figure 4.6 but the purified surfactant had been standing for 4 weeks. The appearance of these tubes after equilibration is shown in Figure 4.7. Figure 4.7 shows that there is some difference in the phase behaviour of the purified surfactant after standing. It has been noted previously that the surfactant changes from a dark brown oil to a light brown paste suggesting there is a time dependent phase transition of the surfactant. This process takes several months. However, the purified surfactant was seen to become lighter in colour after standing for only two weeks. It was thought that this may be due to the surfactant self-polymerising to some extent due to insufficient inhibition following the purification process, which removes the inhibitors at the filtration stage. The presence of polymers in a microemulsion system is known to affect the phase equilibration of a system<sup>20,21</sup> and has been shown to lead to enhanced solubilisation of oil.<sup>22-25</sup> This explains the increased solubilisation of the excess oil phase seen in Figure 4.6 into the two aqueous phases in the two samples at 0.96 and 1.15 M  $[C_{3/11-M}]_{ini}$  seen in Figure 4.7. Complete solubilisation of the excess oil phase is seen in the sample at 1.15 M  $[C_{3/11-M}]_{ini}$ .



**Figure 4.6.** Appearance of equilibrium phases for a system containing HDDA oil and D<sub>2</sub>O stabilised by various [C<sub>3/11-M</sub>]<sub>ini</sub> using batch 17/5/01 of C<sub>3/11-M</sub> purified using Avecia method, prepared immediately after purification



**Figure 4.7.** Appearance of equilibrium phases for a system containing HDDA oil and D<sub>2</sub>O stabilised by various [C<sub>3/11-M</sub>]<sub>ini</sub> using batch 17/5/01 of C<sub>3/11-M</sub> purified using Avecia method, prepared 4 weeks after purification

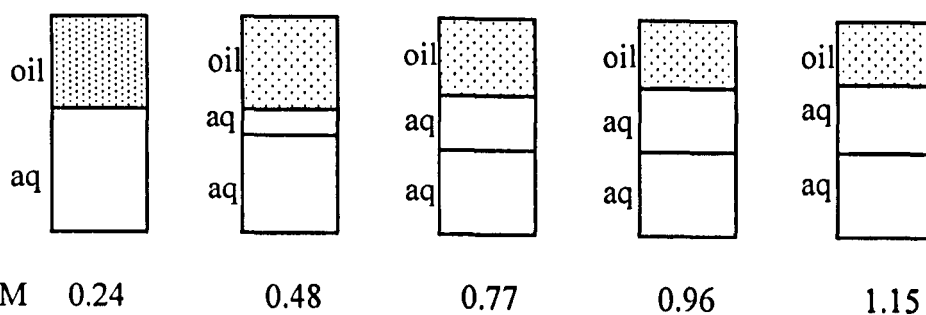


The purification method was modified to prevent the surfactant from degrading over short (~ 4 week) periods of time following purification. The purification method described previously was used, except the polymerisation inhibitors were added after the final washing stage but before the rotary evaporation of the solvents as described in detail in Chapter 2, section 2.8.2. This ensured that all the inhibitors remained in the liquid surfactant after the purification process and would prevent the surfactant from self-polymerising. Two sets of microemulsion samples were prepared, similar to those shown in Figures 4.3 to 4.7 but with  $C_{3/11-M}$  purified using the modified method. The first set of microemulsion phases was prepared immediately following purification and the second set four weeks later. The appearance of the equilibrium microemulsion phases is shown in Figure 4.8, which clearly shows that the modified method of  $C_{3/11-M}$  purification greatly improves the reproducibility of the surfactant over a time period of four weeks.

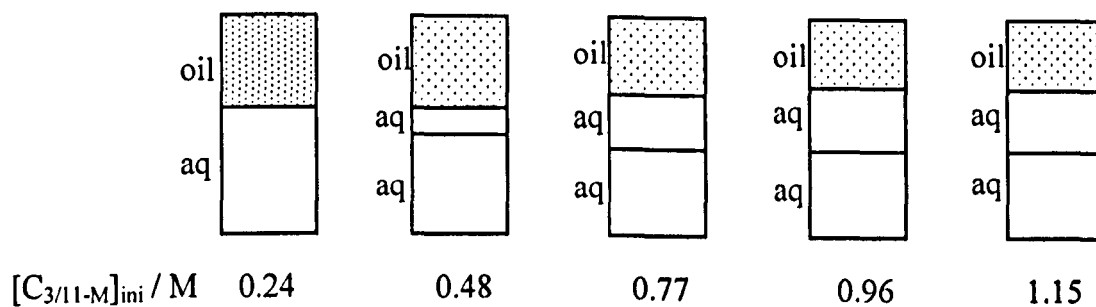
Microemulsion phases using high  $[\text{surfactant}]_{\text{ini}}$  were prepared using the nine surfactant-oil combinations with  $D_2O$  as the aqueous phase in each case. Purified  $C_{3/11-M}$  surfactant was used in all systems containing  $C_{3/11-M}$  surfactant with  $D_2O$ . The following sections in this chapter describe the appearance and composition of these equilibrium systems. For ease of reference,  $D_2O$  is referred to as water and the  $D_2O$  continuous phases referred to as aqueous or water continuous in sections 4.3.2 and 4.3.3.  $C_{10}$  and  $C_{12}$  surfactant purities were measured prior to the preparation of equilibrium phases and were 99.5 % pure.

**Figure 4.8.** Appearance of equilibrium phases for a system containing HDDA oil and D<sub>2</sub>O stabilised by various [C<sub>3/11-M</sub>]<sub>ini</sub> using batch 17/5/01 of C<sub>3/11-M</sub> purified using modified method. Set 1 was prepared immediately following purification. Set 2 was prepared four weeks after purification

**Set 1**



**Set 2**

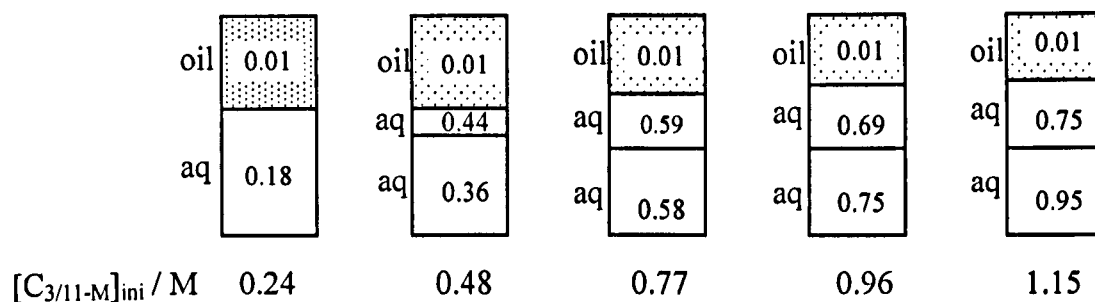


### 4.3.2 Equilibrium phase appearance and partitioning of surfactant

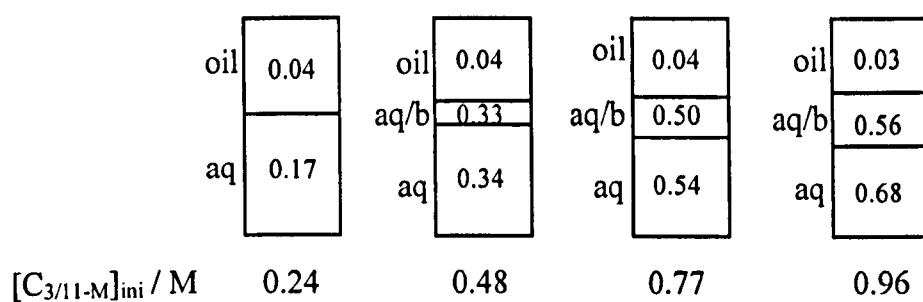
For systems containing  $C_{3/11-M}$  surfactant,  $[\text{surfactant}]_{\text{ini}}$  in the initial aqueous phase is given in M. As described in Chapter 2, the system is made up of equal volumes of surfactant solution and pure oil. Thus, while the oil content is 50 vol. % in each sample, the water content decreases as the surfactant content increases. For systems containing  $C_{10}$  or  $C_{12}$  surfactants, the initial  $[\text{surfactant}]$  in the system are given in wt. %. It should be noted that in these systems, the oil:water weight ratio is 1:1 in each sample and makes up the remaining wt. % of the sample after the surfactant. The number in each phase is the equilibrium  $[\text{surfactant}]$  in M, measured by Epton titration. The cmc values presented in Chapter 3 vary between each system from 0.3 – 40 mM. Therefore equilibrium  $[\text{surfactant}]$  in any phase significantly higher than 0.04 M suggests the presence of aggregates.

The appearance and  $[\text{surfactant}]$  of the equilibrium phases for each system are given in Figures 4.9 to 4.17. None of the systems described in section 4.3 contain added electrolyte. The labels oil/aq/b describe the continuous phase of the equilibrium phase (b denotes bicontinuous). Figure 4.9 shows that for a system containing  $C_{3/11-M}$  surfactant, HDDA oil and  $D_2O$ , as  $[\text{surfactant}]_{\text{ini}}$  is increased, a middle phase forms, which is seen to increase in volume at the expense of the upper and lower phases. This suggests that the middle phase is a surfactant-rich phase.<sup>16</sup> The continuous phase was determined using the drop test method and appeared to be aqueous continuous. The equilibrium  $[\text{surfactant}]$  figures show that the middle and lower phases (both aqueous) contain the aggregates. This is a Winsor I-like system but with two aggregate containing aqueous phases in equilibrium with one excess oil phase (containing

**Figure 4.9. Appearance and [surfactant] of equilibrium phases for a system containing HDDA oil and D<sub>2</sub>O for various initial [C<sub>3/11-M</sub>]**



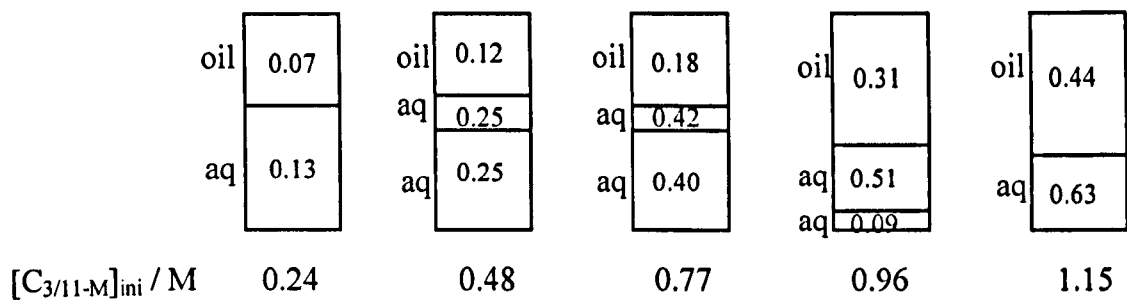
**Figure 4.10. Appearance and [surfactant] of equilibrium phases for a system containing BDDA oil and D<sub>2</sub>O for various initial [C<sub>3/11-M</sub>]**



All phases were clear. The middle and lower phases showed a very slight yellow tint.

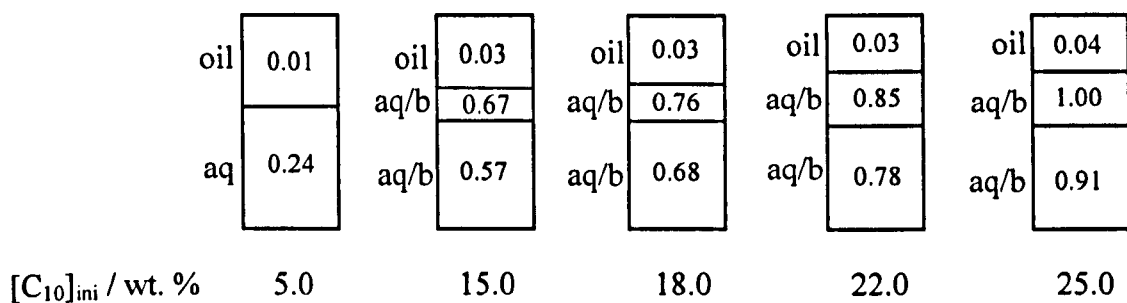
slightly more surfactant than the cmc, which is expected as post-cmc partitioning in this system is non-ideal). We shall refer to this type of system as Winsor I\* (WI\*). In the system shown in Figure 4.9, the middle and lower phases contain a similar amount of surfactant but with higher [surfactant] in the lower phase. Figure 4.10 shows a similar system to that in Figure 4.9 but with BDDA used in place of HDDA. Again, as [surfactant]<sub>ini</sub> is increased a middle phase forms which is seen to increase in volume at the expense of the upper and lower phases suggesting a surfactant-rich middle phase. The continuous phase of the middle phase was difficult to determine using the drop test method but appeared to be aqueous or bicontinuous. The equilibrium [surfactant] figures show that the middle and lower phases (either aqueous or bicontinuous) contain the aggregates. This is another example of a WI\* system, with the middle and lower phases containing similar equilibrium [surfactant]. Figure 4.11 shows that a quite different trend in phase volume with increasing [surfactant]<sub>ini</sub> is seen for systems containing DPGDA oil with C<sub>3/11-M</sub> surfactant. A third phase is seen above 0.24 M [C<sub>3/11-M</sub>]<sub>ini</sub> as seen before but the volume of the upper oil phase is seen to increase as the lower aqueous phase volume decreases with increasing [surfactant]<sub>ini</sub>. The equilibrium [surfactant] figures show that as [surfactant]<sub>ini</sub> is increased, the equilibrium [surfactant] in both the upper (oil continuous) and middle (aqueous) phases increases. The lower aqueous phase becomes fully absorbed into the middle phase between 0.96 M and 1.15 M [surfactant]<sub>ini</sub>. It appears that the increasing [surfactant]<sub>ini</sub> is causing an inversion of aggregate-containing phase, the early stages of which are seen in this system. This effect of inversion of aggregate-containing phase usually occurs with increasing added electrolyte concentration,<sup>16</sup> however, reduction of the surfactant monolayer curvature towards the Winsor I/III boundary has been reported with increasing concentration of ionic surfactant (AOT) alone.<sup>18,26</sup> The

**Figure 4.11. Appearance and [surfactant] of equilibrium phases for a system containing DPGDA oil and D<sub>2</sub>O for various [C<sub>3/11-M</sub>]<sub>ini</sub>**



All phases were clear and colourless. The middle and lower phases showed a slight yellow tint.

**Figure 4.12. Appearance and [surfactant] of equilibrium phases for a system containing HDDA oil and D<sub>2</sub>O for various [C<sub>10</sub>]<sub>ini</sub>**



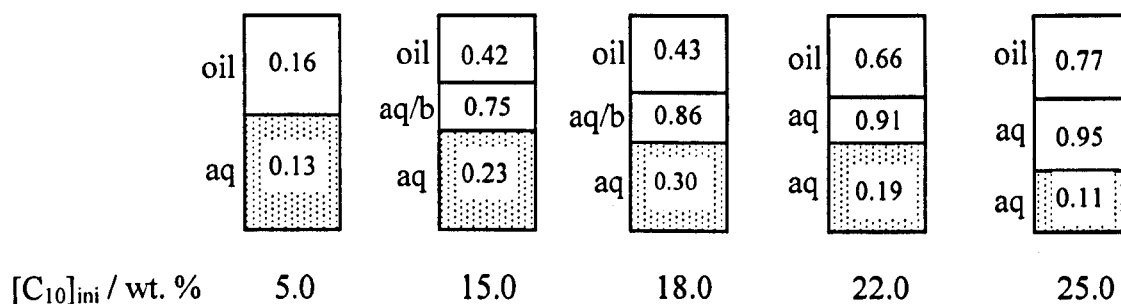
All phases were clear and colourless.

aggregate-containing phase inversion in the case shown in Figure 4.11 is due to the increase in  $[C_{3/11-M}]_{ini}$  alone, causing self-inversion. The self-inversion process is not complete and in the samples prepared with the highest  $[\text{surfactant}]_{ini}$ , an aggregate-containing oil continuous phase is in equilibrium with an aggregate-containing water continuous phase. We shall refer to this self-inverting from a WI type of system to WII type as WI<sup>i</sup>.

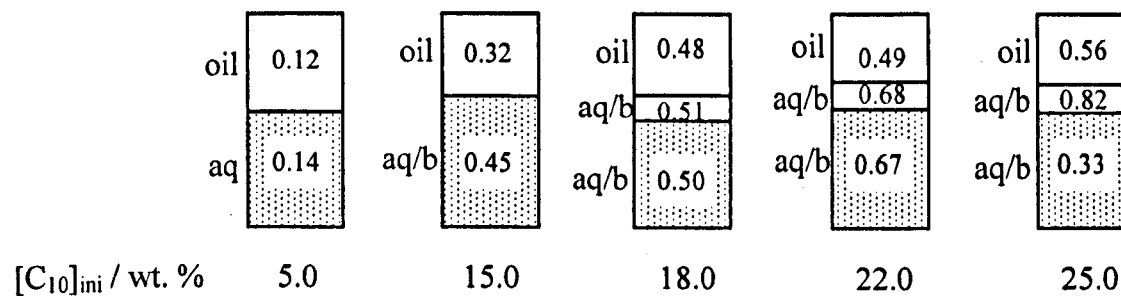
Figures 4.12 to 4.14 show a similar series of systems to those seen in figures 4.9 to 4.11 but using  $C_{10}$  surfactant in place of  $C_{3/11-M}$ . Figure 4.12 shows a similar trend for  $C_{10}$  with HDDA to that seen previously with  $C_{3/11-M}$  surfactant with HDDA and BDDA, in that beyond a certain  $[\text{surfactant}]_{ini}$  a third phase is seen, which increases in volume at the expense of the upper and lower phases with increasing  $[\text{surfactant}]_{ini}$ . The continuous phase of the middle and lower phases for the three phase systems appears not to be entirely water continuous and may be bicontinuous. The equilibrium  $[\text{surfactant}]$  in each phase shows that these samples are WI\* systems although in this case the middle phase has a higher equilibrium  $[\text{surfactant}]$  than that of the lower phase. Figure 4.13 shows a very interesting WI<sup>i</sup> system. In this case there are three phases, one oil continuous and two aqueous/ bicontinuous as seen in WI\* systems but the equilibrium  $[\text{surfactant}]$  figures show that all of the phases are aggregate containing phases, with the middle phase showing a much higher equilibrium  $[\text{surfactant}]$  than the upper or lower phases. The concentration of surfactant in the upper phase is always higher than that of the lower phase but this difference is seen to increase with increasing  $[\text{surfactant}]_{ini}$  beyond 18 wt. %, suggesting self-inversion similar to that seen in Figure 4.11.  $C_{10}$  surfactant with



**Figure 4.13. Appearance and [surfactant] of equilibrium phases for a system containing BDDA oil and D<sub>2</sub>O for various [C<sub>10</sub>]<sub>ini</sub>**



**Figure 4.14. Appearance and [surfactant] of equilibrium phases for a system containing DPGDA oil and D<sub>2</sub>O for various [C<sub>10</sub>]<sub>ini</sub>**

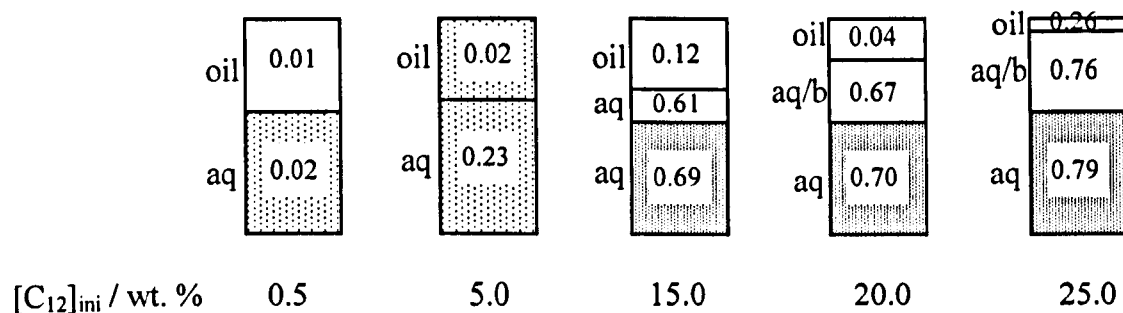


DPGDA oil seen in Figure 4.14 shows another WI<sup>i</sup> system with the equilibrium [surfactant]<sub>ini</sub> highest in the middle phase.

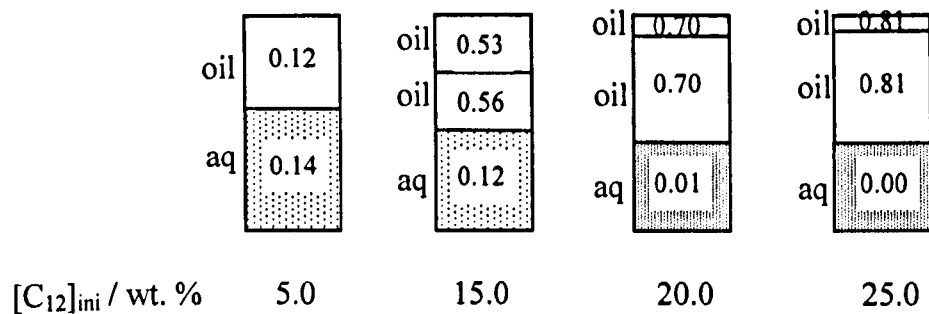
Figures 4.15 to 4.17 show another series of systems but using C<sub>12</sub> surfactant. With C<sub>12</sub> and HDDA as seen in Figure 4.15, a WI<sup>i</sup> system is produced. At the highest [surfactant]<sub>ini</sub> (25 wt. %) the equilibrium [surfactant] of the upper (oil) phase is seen to increase over that at 20 wt. % [surfactant]<sub>ini</sub> suggesting that self-inversion may have started but at these high concentrations of surfactant it is unlikely that sufficient surfactant could be added to cause complete phase inversion. If BDDA oil and C<sub>12</sub> surfactant are used, shown in Figure 4.16, a different progression of phases is seen to those seen previously. In this case, once sufficient initial surfactant is present to form three phases, rapid self inversion occurs with further increase in [surfactant]<sub>ini</sub>, such that at 20 wt. % and 25 wt. % Winsor II-like systems are formed, but with two oil continuous aggregate-containing phases in equilibrium with an excess water phase. We shall refer to this type of system where complete inversion is achieved as WII\*. Figure 4.17 (C<sub>12</sub> with DPGDA) shows another WI<sup>i</sup> system similar to that seen in Figure 4.13 for C<sub>10</sub> with BDDA; however, the occurrence of a third phase in system in Figure 4.17 requires a higher [surfactant]<sub>ini</sub>.

Figures 4.9 to 4.17 show that the structures of the surfactant and oil do affect the microemulsion phase equilibration and formation. A broad range of phase types can be prepared from Winsor I-like water continuous phases, through bicontinuous and on to Winsor II-like oil continuous phases by selection of suitable surfactants and oils. It is interesting that none of the surfactant/ oil combinations seem to produce definite three-phase Winsor III systems, even those that exhibit self-inversion. The

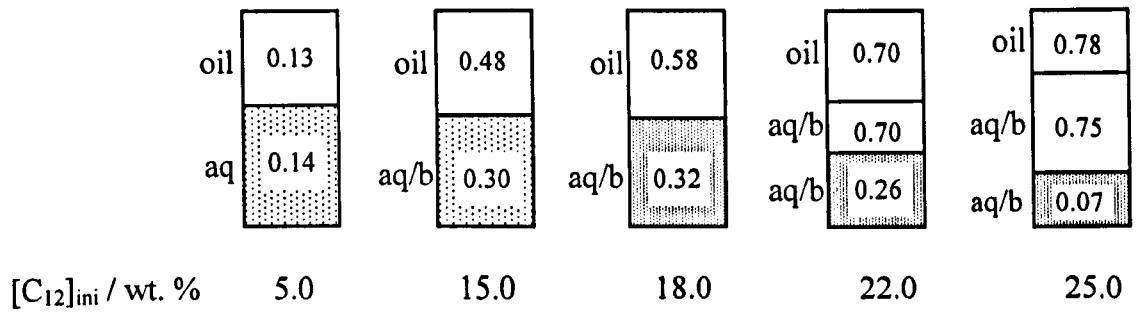
**Figure 4.15. Appearance and [surfactant] of equilibrium phases for a system containing HDDA oil and D<sub>2</sub>O for various [C<sub>12</sub>]<sub>ini</sub>**



**Figure 4.16. Appearance and [surfactant] of equilibrium phases for a system containing BDDA oil and D<sub>2</sub>O for various [C<sub>12</sub>]<sub>ini</sub>**



**Figure 4.17. Appearance and [surfactant] of equilibrium phases for a system containing DPGDA oil and D<sub>2</sub>O for various [C<sub>12</sub>]<sub>ini</sub>**



systems shown here seem to go from a Winsor I-like to Winsor II-like system with the occurrence of a highly concentrated middle phase in equilibrium with aggregate-containing water and oil continuous phases. It is not surprising that non-ideal phase equilibration is observed with respect to formation of ideal Winsor I, WII or WIII phases because non-ideal surfactant partitioning post-cmc was observed in all systems except C<sub>3/11-M</sub> / HDDA as described in Chapter 3. One could argue that because the electrolyte causing phase inversion comes from the surfactant, an increase in [electrolyte] will be accompanied by an increase in [surfactant], which could upset the phase equilibrium with respect to phase type. This is unlikely, as increases in [surfactant] and electrolyte have been shown to have separate, independent effects (increase in surfactant-rich phase volume and phase inversion respectively).<sup>16</sup> The phases were also observed through cross-polarized filters to check for optical anisotropy. All phases were found to be optically isotropic, therefore none of the phases were lamella or liquid crystalline.<sup>27</sup>

### 4.3.3 Phase composition

Following work on the appearance and [surfactant] of the equilibrium microemulsion phases, the composition of each equilibrium phase was determined for oil, water and surfactant content in wt. %. This would present a more complete picture of each phase and would show the effect of [surfactant]<sub>ini</sub> on the composition of each phase. The aim was to attempt to correlate the water content of the microemulsion phases with the porosity of polymer films prepared by polymerisation of the equilibrium phases, as the water content of the pre-cursor microemulsion has been shown to affect the porosity of the resulting polymer.<sup>2</sup> The surfactant content was

determined by Epton titration. Using the density of the microemulsion phase (determined by taking the mass of a known volume of microemulsion phase) the surfactant content in wt. % can be calculated. The water content also in wt. % was measured by Karl Fischer titration. The oil content in wt. % was calculated by subtracting the sum of the surfactant and water contents (in wt. %) from 100 assuming all mass present in the microemulsion phase was surfactant (plus any surfactant impurities), water and oil. The composition of each equilibrium phase for each system was determined and the change in composition with increasing  $[\text{surfactant}]_{\text{ini}}$  is shown in Figures 4.18 to 4.44.

$$\phi_o \text{ is defined as: } \frac{\text{Volume of oil}}{\text{Volume of oil} + \text{Volume of initial aqueous phase}}$$

(In systems containing surfactant  $C_{3/11-M}$  the initial aqueous phase contains the surfactant. In systems containing surfactants  $C_{10}$  and  $C_{12}$  the initial aqueous phase is pure  $D_2O$ .)

#### **$C_{3/11-M}$ , HDDA, $D_2O$ :**

Figure 4.18 shows that as  $[\text{surfactant}]_{\text{ini}}$  increases, the composition of the upper (oil continuous) phase remains approximately constant. This is expected, as the  $[\text{surfactant}]$  remains fairly constant as seen in Figure 4.9, so the upper phase is excess oil. Figure 4.19 shows that as equilibrium  $[\text{surfactant}]$  increases in the middle phase, the proportions of water and oil cross at between  $\sim 0.7$  M and  $\sim 0.8$  M  $[C_{3/11-M}]_{\text{ini}}$  as the proportion of water decreases and that of oil increases. This occurs as the increase in surfactant concentration allows more oil to be solubilised into the aqueous phase.

Figure 4.18. Composition of upper equilibrium phase vs. surfactant concentration in initial aqueous phase ( $[\text{surfactant}]_{\text{ini}}$ ) for system containing  $\text{C}_{3/11}\text{-M}$ , HDDA and  $\text{D}_2\text{O}$ .  $\phi_0 = 0.5$ ,  $T = 25^\circ\text{C}$

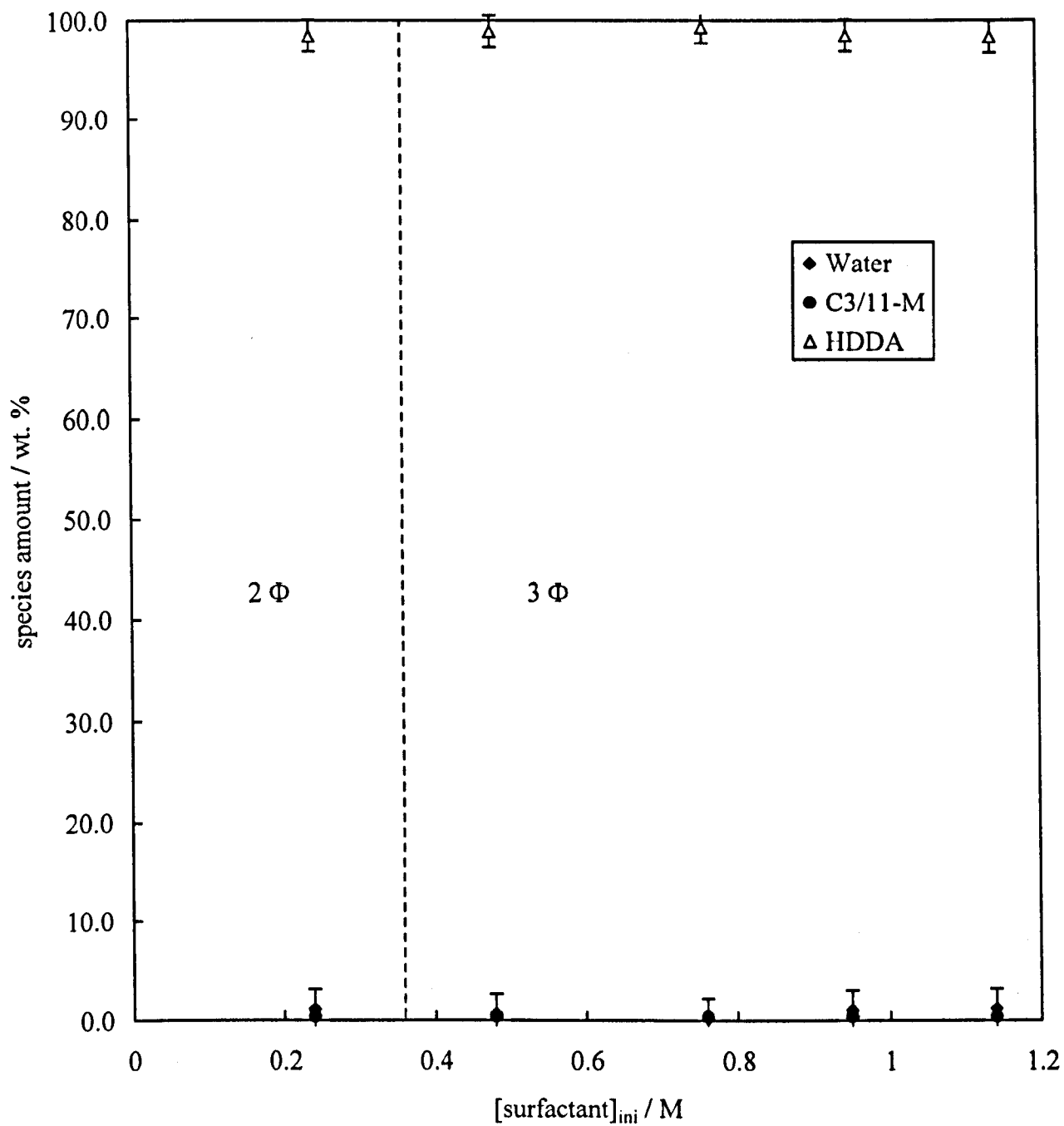


Figure 4.19. Composition of middle equilibrium phase vs. surfactant concentration in initial aqueous phase ( $[\text{surfactant}]_{\text{ini}}$ ) for system containing  $\text{C}_{3/11-\text{M}}$ , HDDA and  $\text{D}_2\text{O}$ .  $\phi_0 = 0.5$ ,  $T = 25^\circ\text{C}$

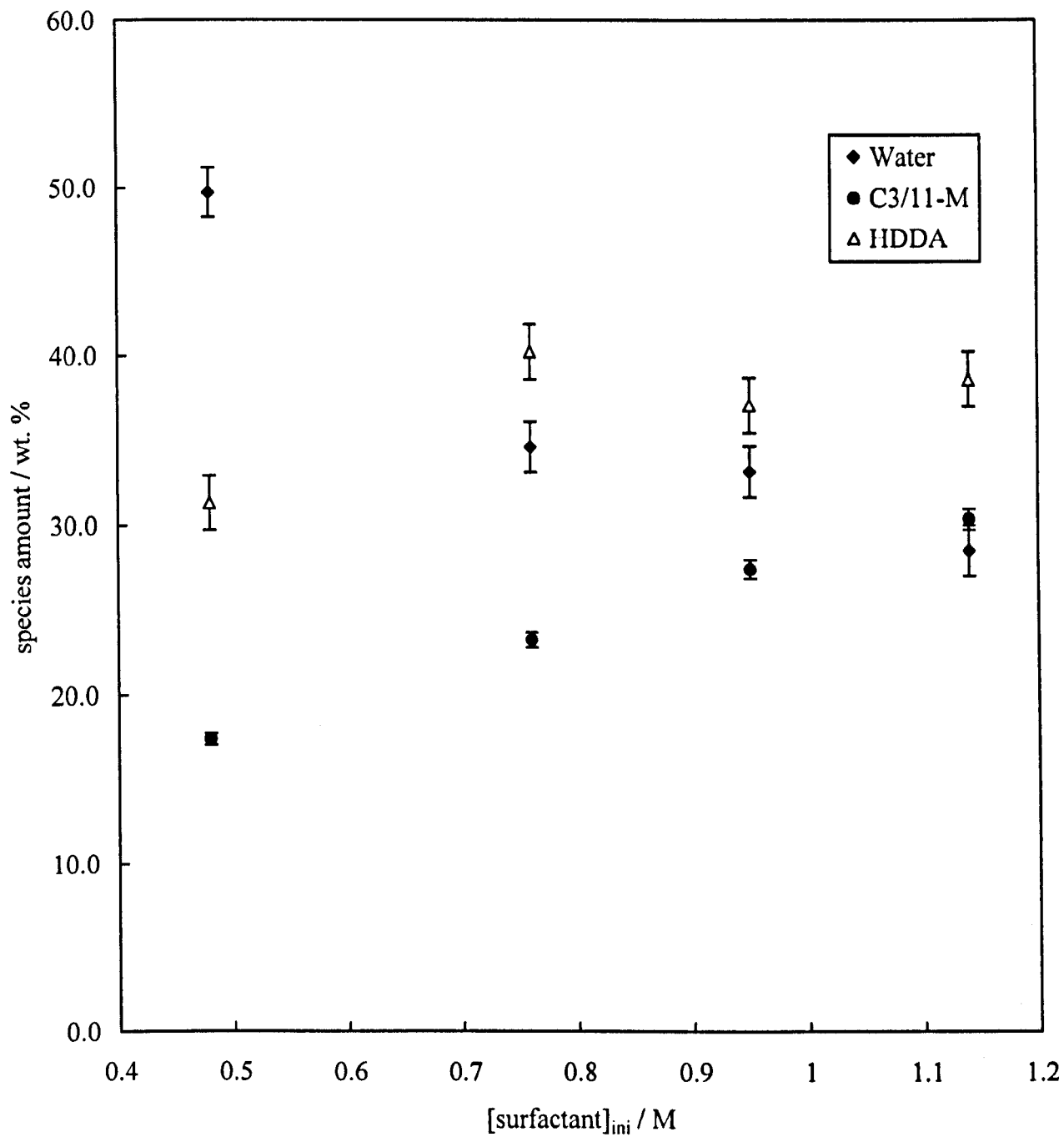
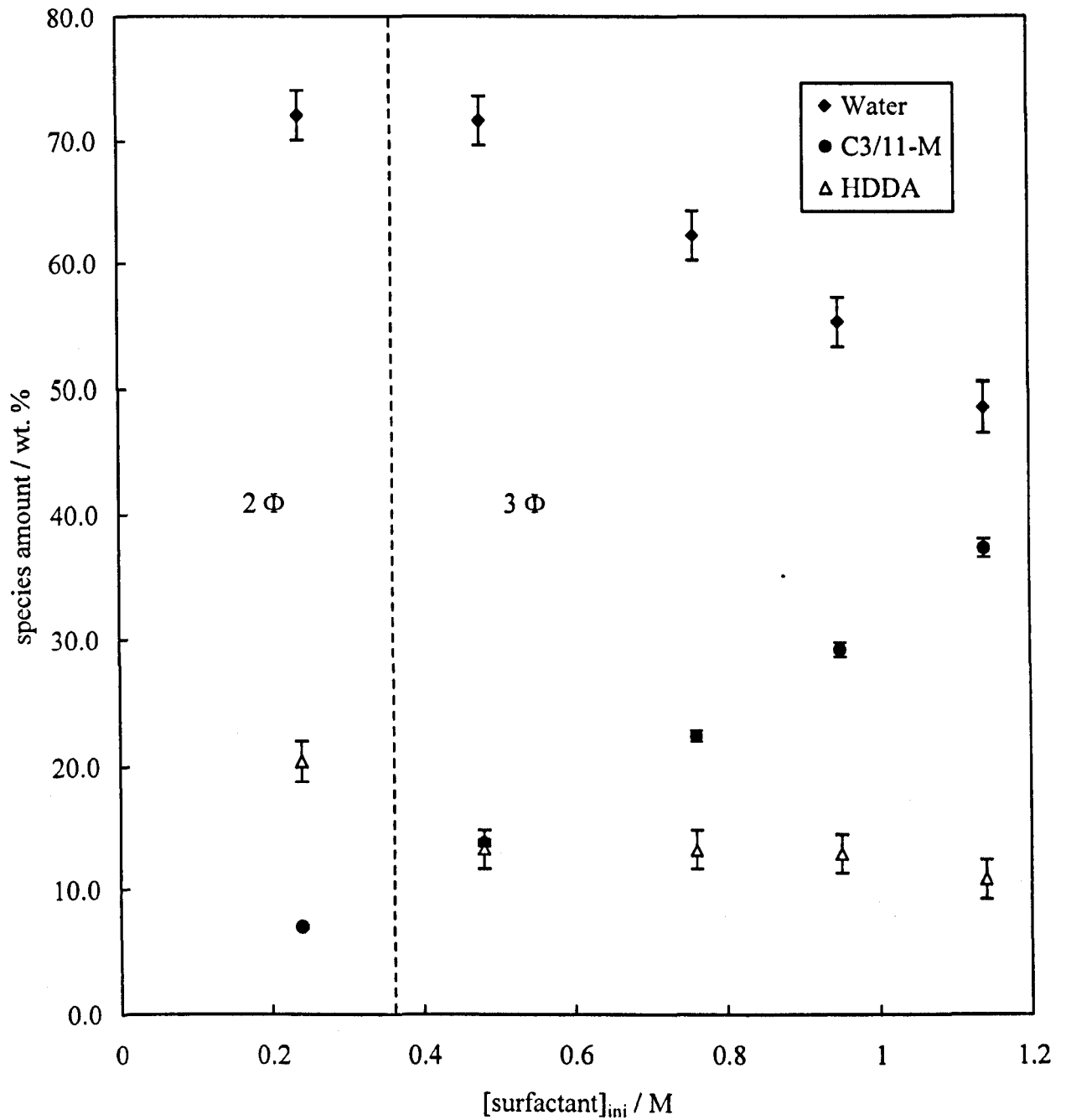




Figure 4.20. Composition of lower equilibrium phase vs. surfactant concentration in initial aqueous phase ( $[\text{surfactant}]_{\text{ini}}$ ) for system containing  $\text{C}_{3/11}\text{-M}$ , HDDA and  $\text{D}_2\text{O}$ .  $\phi_0 = 0.5$ ,  $T = 25^\circ\text{C}$



As the proportion of surfactant increases in the lower phase, shown in Figure 4.20, the amount of water decreases more rapidly at higher  $[\text{surfactant}]_{\text{ini}}$  and the amount of oil also decreases but very gradually. The equilibrium  $[\text{surfactant}]$  is seen to increase to a greater extent with increasing  $[\text{surfactant}]_{\text{ini}}$  in the lower phase, such that the proportions of  $\text{D}_2\text{O}$  and surfactant tend towards equality. Figures 4.19 and 4.20 show that the equilibrium  $[\text{surfactant}]$  increases linearly with  $[\text{surfactant}]_{\text{ini}}$  in both aggregate-containing phases in this system. Water content in both aggregate-containing phases can be controlled by  $[\text{surfactant}]_{\text{ini}}$ .

### **$\text{C}_{3/11}\text{-M}$ , BDDA, $\text{D}_2\text{O}$ :**

Figure 4.21 shows that the upper phase consists mainly of excess oil with low concentrations of water and surfactant. Figure 4.22 shows that the middle phases contain a high proportion of surfactant and roughly similar amounts of oil and water, confirming that this is an aggregate-containing phase. The relative proportions of water and oil cross at approximately 0.62 M  $[\text{surfactant}]_{\text{ini}}$  and a fairly small increase in  $[\text{surfactant}]_{\text{ini}}$  causes a large change in phase composition. Figure 4.23 shows that the lower phase is also an aggregate-containing phase as there is a large proportion of oil present in each phase (~20%). This will be present as solubilised oil. The amount of oil remains fairly constant with increasing  $[\text{surfactant}]_{\text{ini}}$  but the water content decreases significantly. The water content remains higher than that of the oil content in each phase. Figures 4.22 and 4.23 show that the equilibrium  $[\text{surfactant}]$  increases linearly with  $[\text{surfactant}]_{\text{ini}}$  in both aggregate-containing phases in this system. Water content in both aggregate-containing phases can be controlled by  $[\text{surfactant}]_{\text{ini}}$ .

Figure 4.21. Composition of upper equilibrium phase vs. surfactant concentration in initial aqueous phase ( $[\text{surfactant}]_{\text{ini}}$ ) for system containing  $\text{C}_{3/11}\text{-M}$ , BDDA and  $\text{D}_2\text{O}$ .  $\phi_0 = 0.5$ ,  $T = 25^\circ\text{C}$

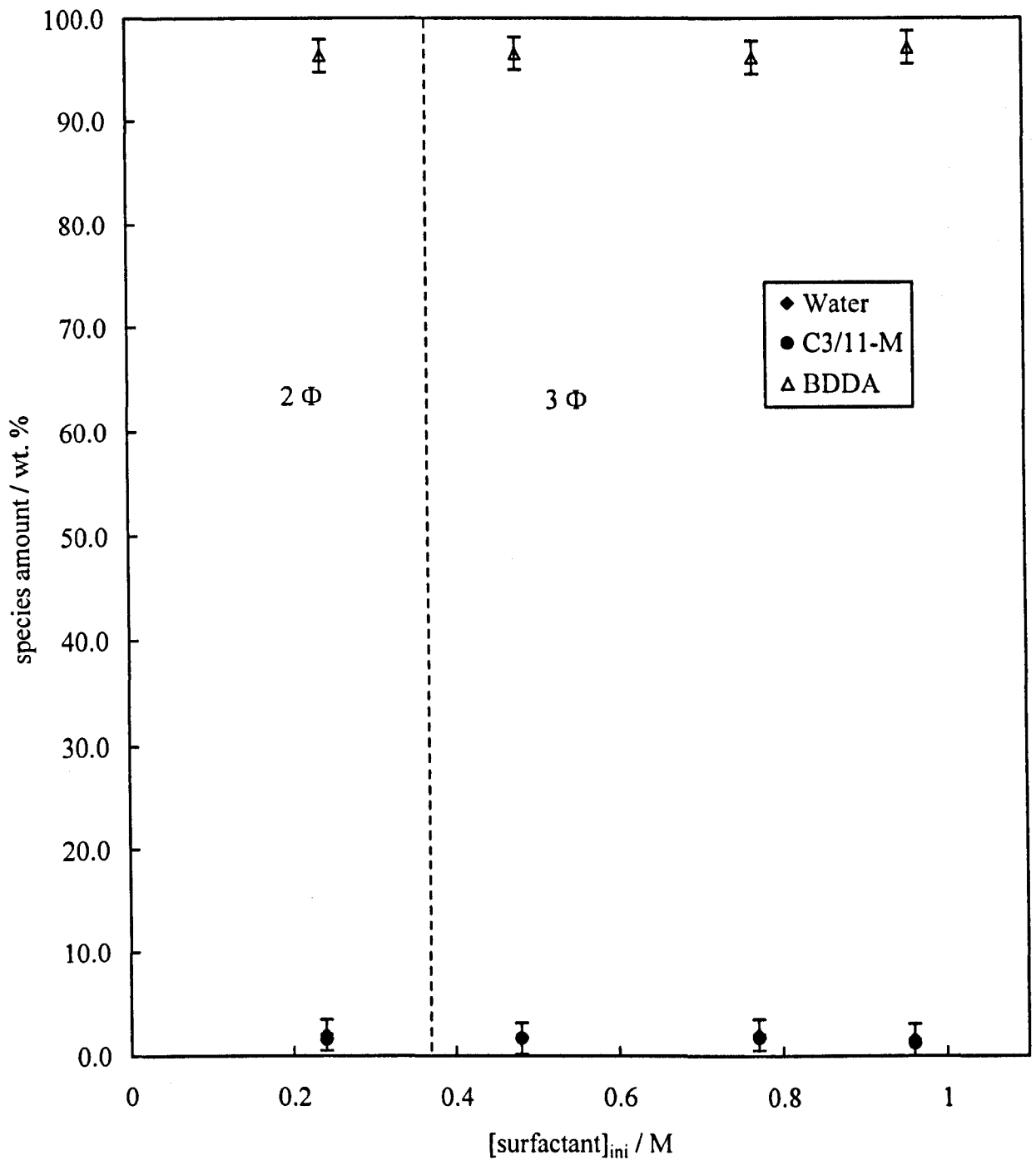
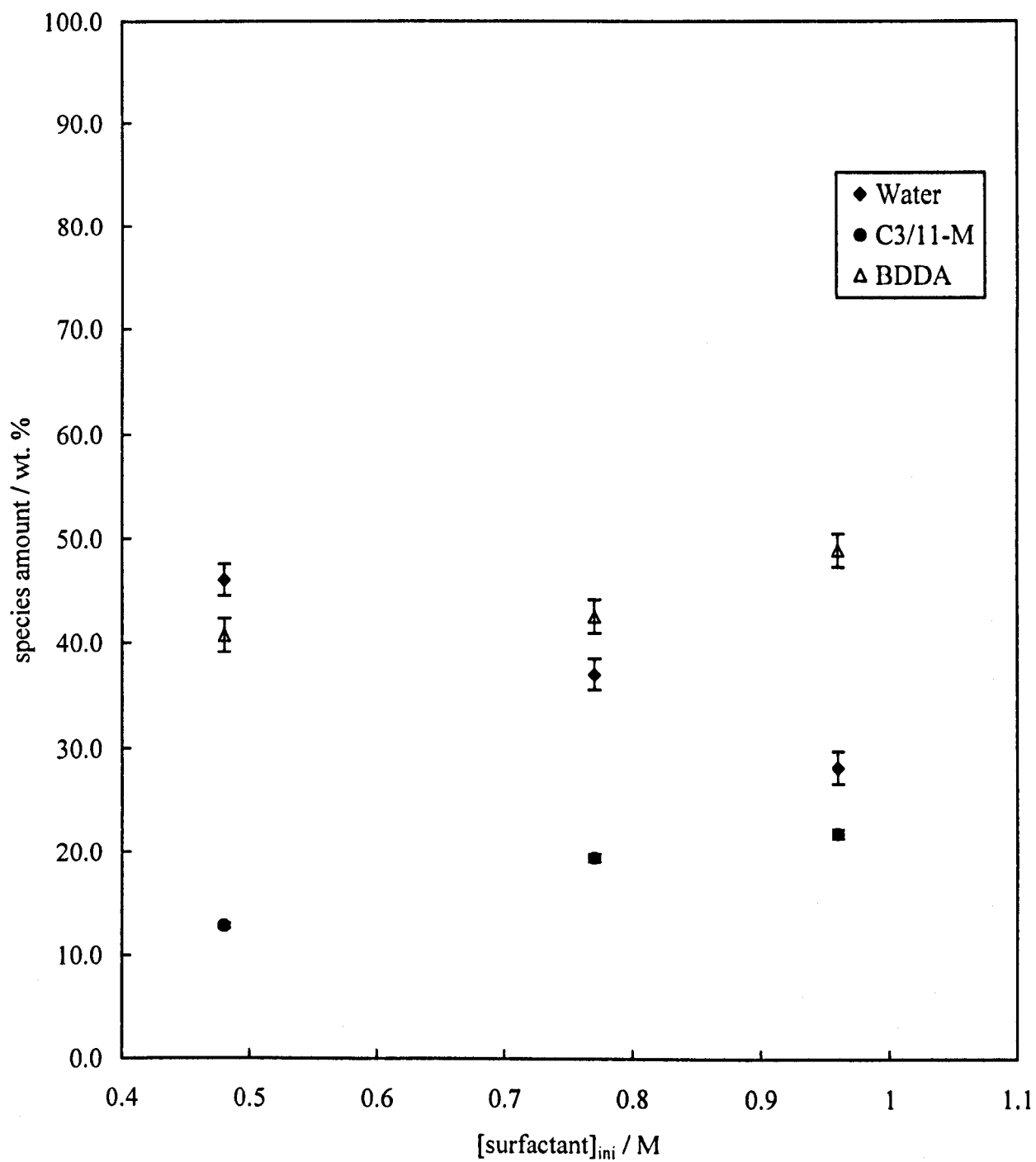
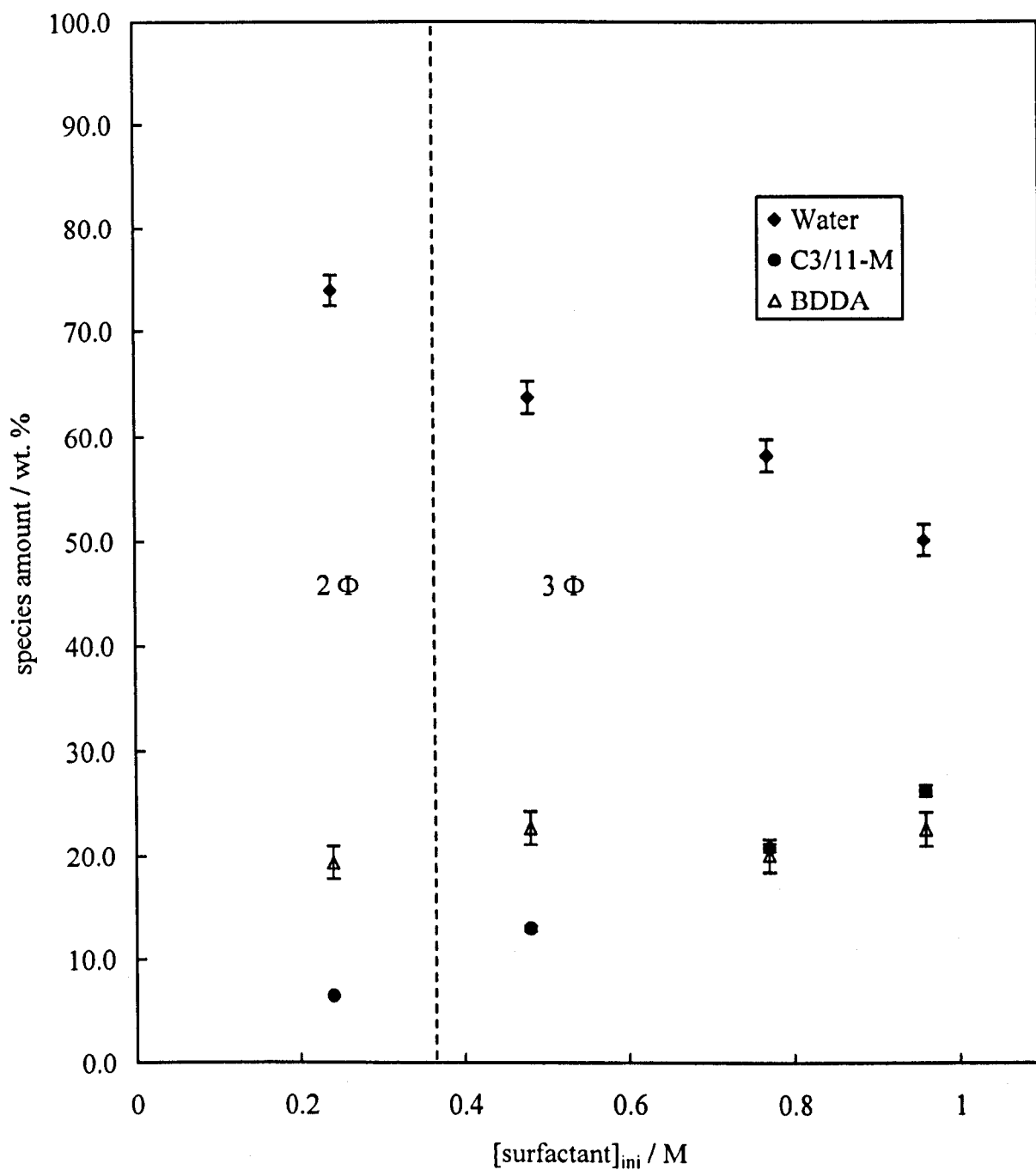


Figure 4.22. Composition of middle equilibrium phase vs. surfactant concentration in initial aqueous phase ( $[\text{surfactant}]_{\text{ini}}$ ) for system containing  $\text{C}_{3/11}\text{-M}$ , BDDA and  $\text{D}_2\text{O}$ .  $\phi_0 = 0.5$ ,  $T = 25^\circ\text{C}$



**Figure 4.23. Composition of lower equilibrium phase vs. surfactant concentration in initial aqueous phase ( $[\text{surfactant}]_{\text{ini}}$ ) for system containing  $\text{C}_{3/11}\text{-M}$ , BDDA and  $\text{D}_2\text{O}$ .  $\phi_0 = 0.5$ ,  $T = 25\text{ }^\circ\text{C}$**



### **C<sub>3/11-M</sub>, DPGDA, D<sub>2</sub>O:**

Figure 4.24 shows that the equilibrium [surfactant] in the upper phase increases with increasing [surfactant]<sub>ini</sub>, as does the equilibrium water content, while the equilibrium oil content decreases with increasing [surfactant]<sub>ini</sub>. These trends become more pronounced from ~ 0.8 M initial surfactant. This shows that aggregate structures are forming in the oil phase at high [surfactant]<sub>ini</sub>. This agrees with the phase trends seen in Figure 4.11, which shows a possible phase inversion occurring with increasing [surfactant]<sub>ini</sub>. The sample with highest [surfactant]<sub>ini</sub> is a two-phase system. Figure 4.25 shows the composition of the middle equilibrium phases. It shows that as [surfactant]<sub>ini</sub> is increased, the equilibrium [surfactant] increases. The oil content increases up to a maximum at ~ 0.77 M [surfactant]<sub>ini</sub>, then decreases. The equilibrium water content follows the opposite trend. This is not unexpected as Figure 4.11 does show a dramatic change in appearance of the third phase between 0.77 M and 0.96 M [surfactant]<sub>ini</sub>. Figure 4.26 shows that as [surfactant]<sub>ini</sub> is increased, equilibrium [surfactant] and oil content increase in the lower equilibrium phase as equilibrium water content decreases. The system at 0.96 M [surfactant]<sub>ini</sub> has a markedly different composition to the other lower phases and this sample (as seen in Figure 4.11) is approaching a two-phase system. Control of water content with [surfactant]<sub>ini</sub> is more difficult but not impossible in this system.

### **C<sub>10</sub>, HDDA, D<sub>2</sub>O:**

Figure 4.27 shows that the upper phase consists of an excess oil phase (with low concentrations of water and surfactant), which agrees with the equilibrium

Figure 4.24. Composition of upper equilibrium phase vs. surfactant concentration in initial aqueous phase ( $[\text{surfactant}]_{\text{ini}}$ ) for system containing  $\text{C}_{3/11\text{-M}}$ , DPGDA and  $\text{D}_2\text{O}$ .  $\phi_0 = 0.5$ ,  $T = 25\text{ }^\circ\text{C}$

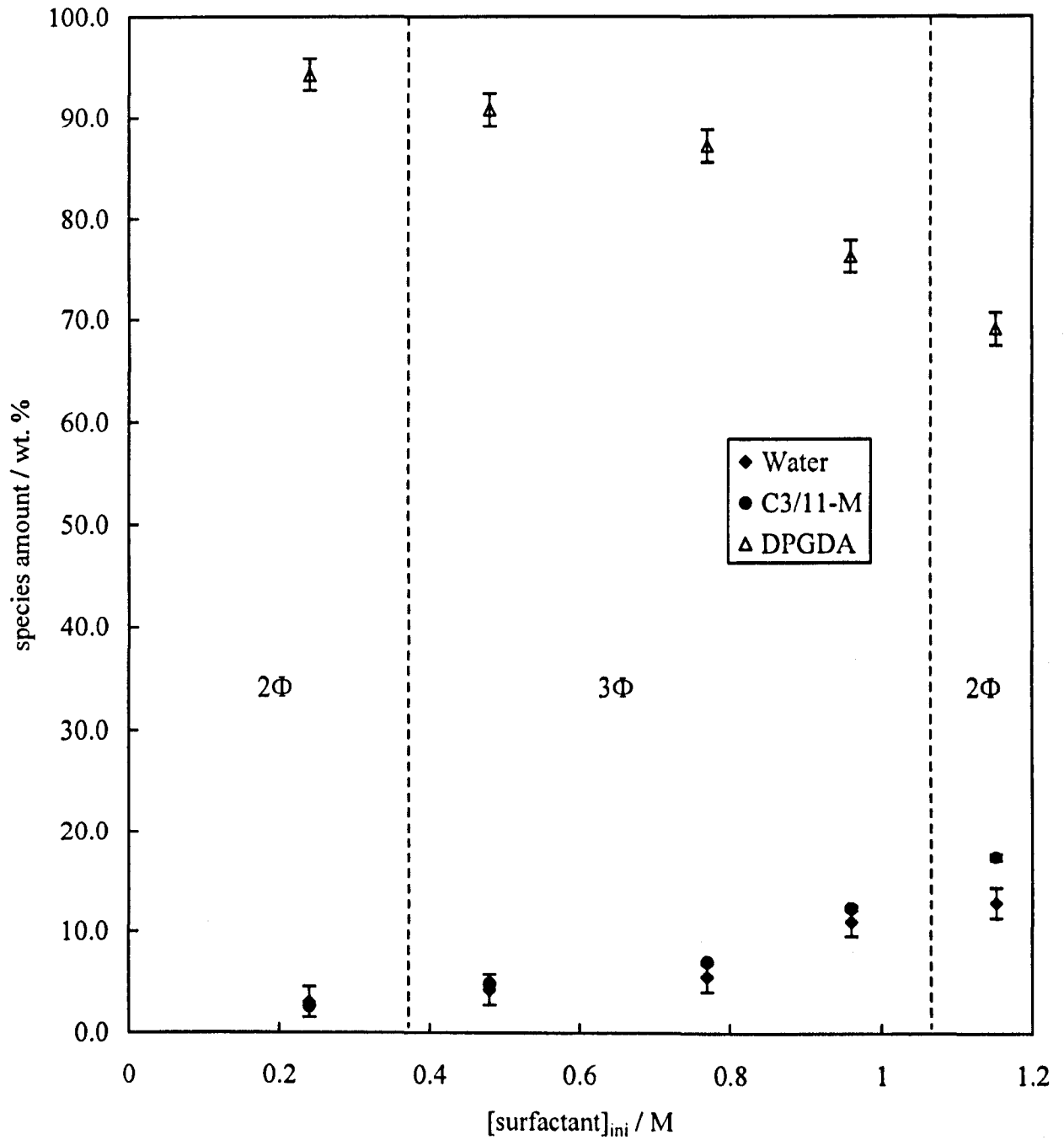


Figure 4.25. Composition of middle equilibrium phase vs. surfactant concentration in initial aqueous phase ( $[\text{surfactant}]_{\text{ini}}$ ) for system containing  $\text{C}_{3/11}\text{-M}$ , DPGDA and  $\text{D}_2\text{O}$ .  $\phi_0 = 0.5$ ,  $T = 25^\circ\text{C}$

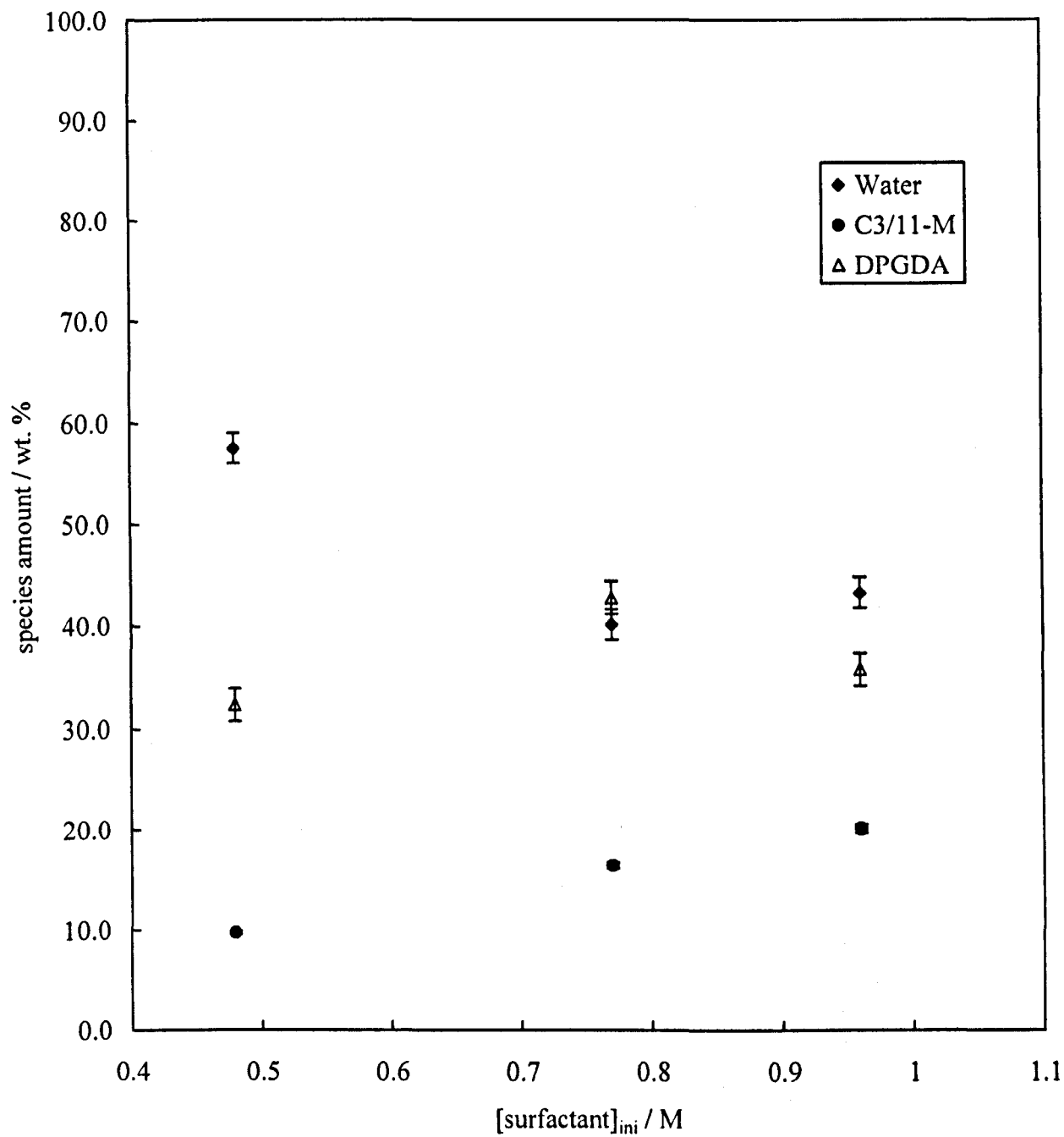




Figure 4.26. Composition of lower equilibrium phase vs. surfactant concentration in initial aqueous phase ( $[\text{surfactant}]_{\text{ini}}$ ) for system containing C<sub>3/11</sub>-M, DPGDA and D<sub>2</sub>O.  $\phi_0 = 0.5$ ,  $T = 25^\circ\text{C}$

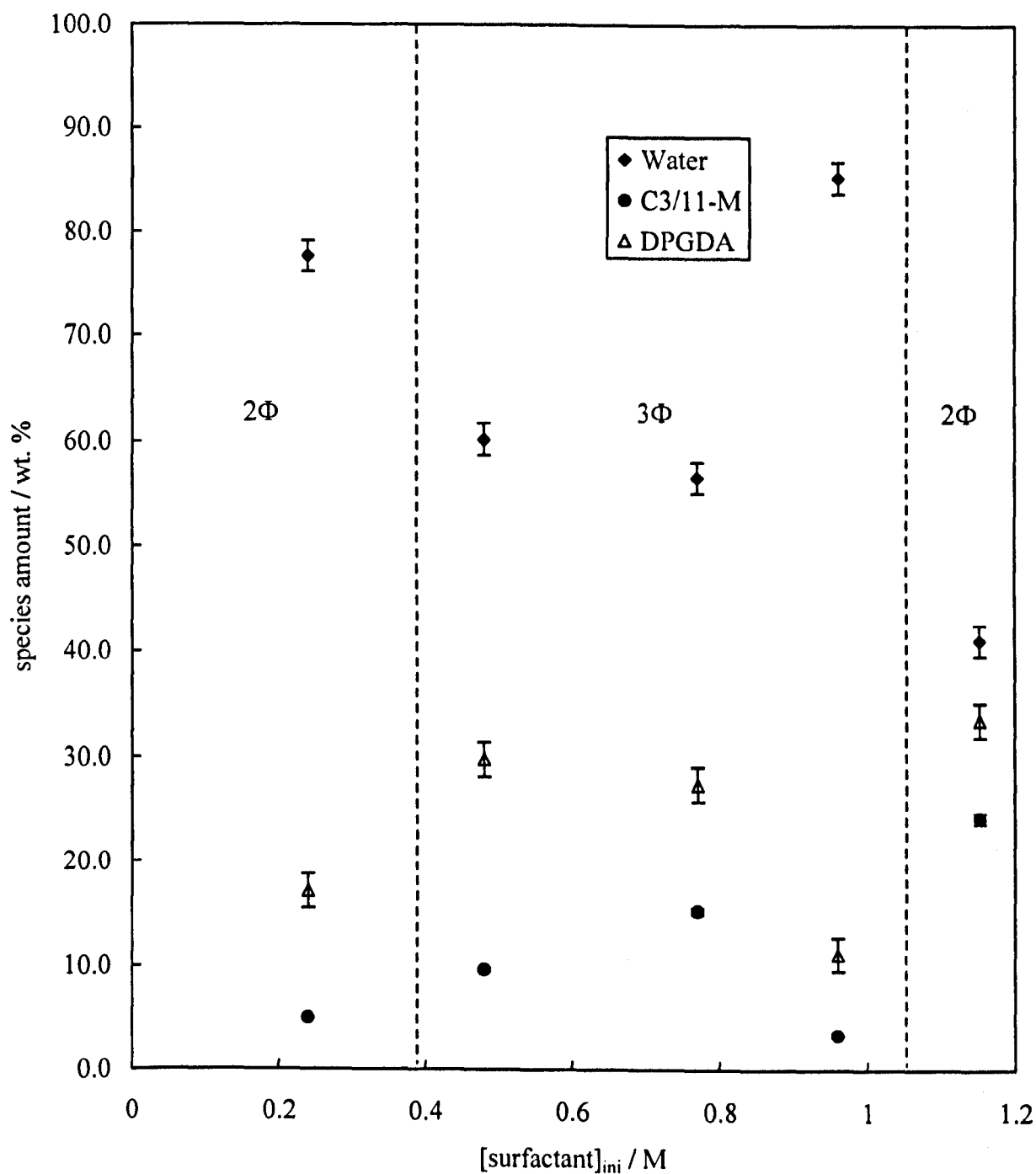


Figure 4.27. Composition of upper equilibrium phase vs. initial surfactant concentration in system ( $[\text{surfactant}]_{\text{ini}}$ ) for system containing C<sub>10</sub>, HDDA and D<sub>2</sub>O.  $\phi_0 = 0.5$ ,  $T = 25\text{ }^\circ\text{C}$

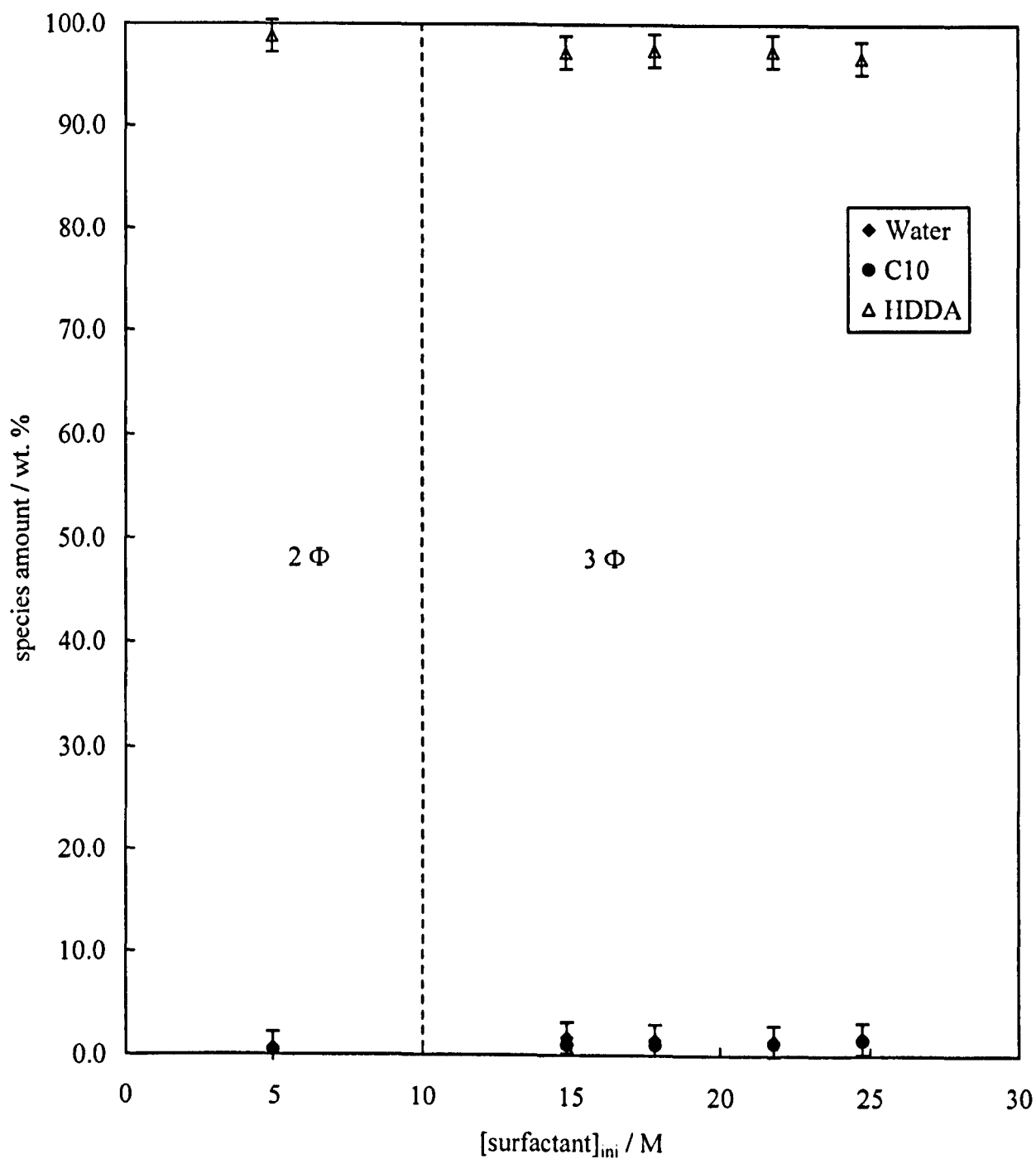


Figure 4.28. Composition of middle equilibrium phase vs. initial surfactant concentration in system ( $[\text{surfactant}]_{\text{ini}}$ ) for system containing  $\text{C}_{10}$ , HDDA and  $\text{D}_2\text{O}$ .  $\phi_0 = 0.5$ ,  $T = 25^\circ\text{C}$

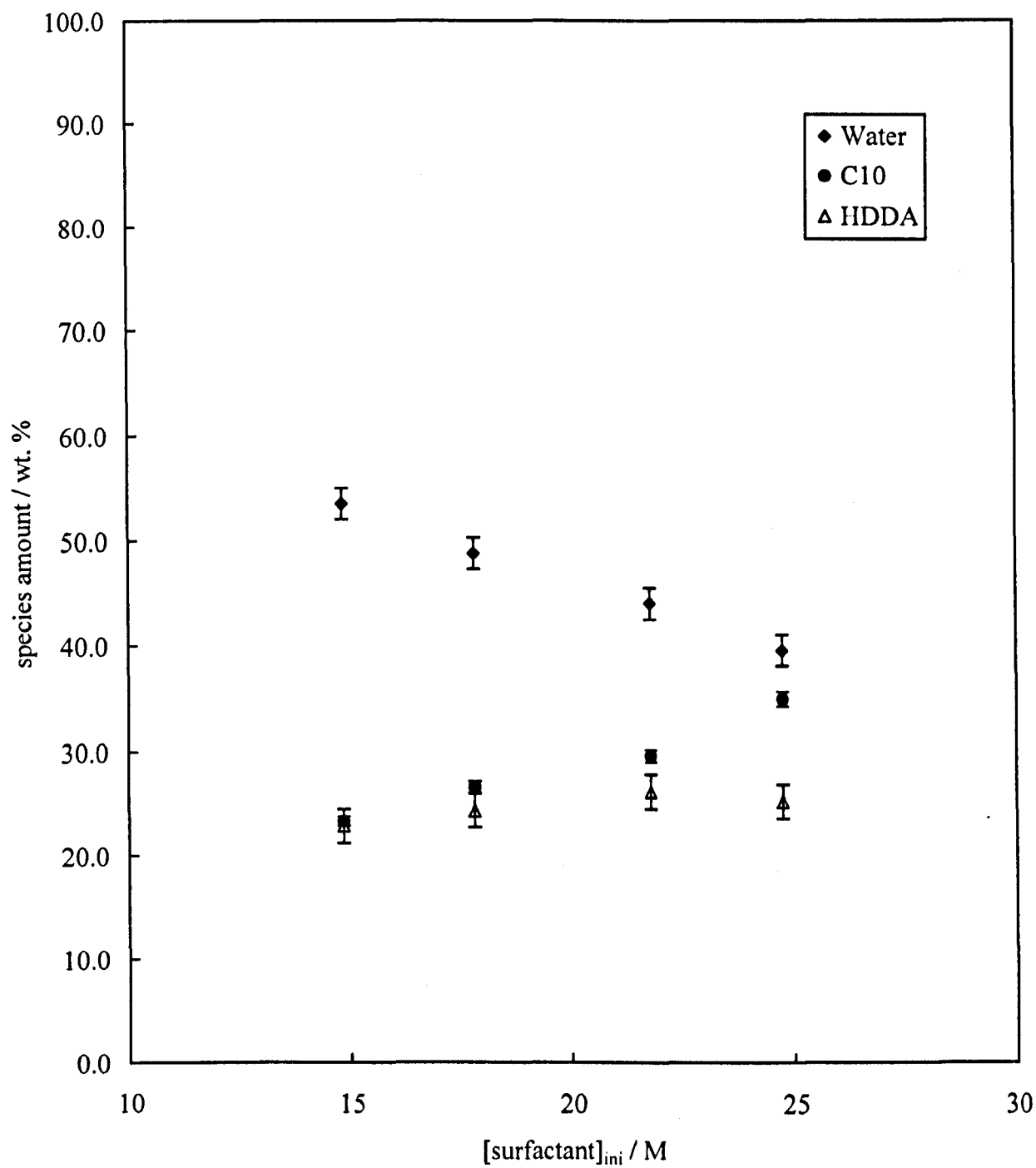
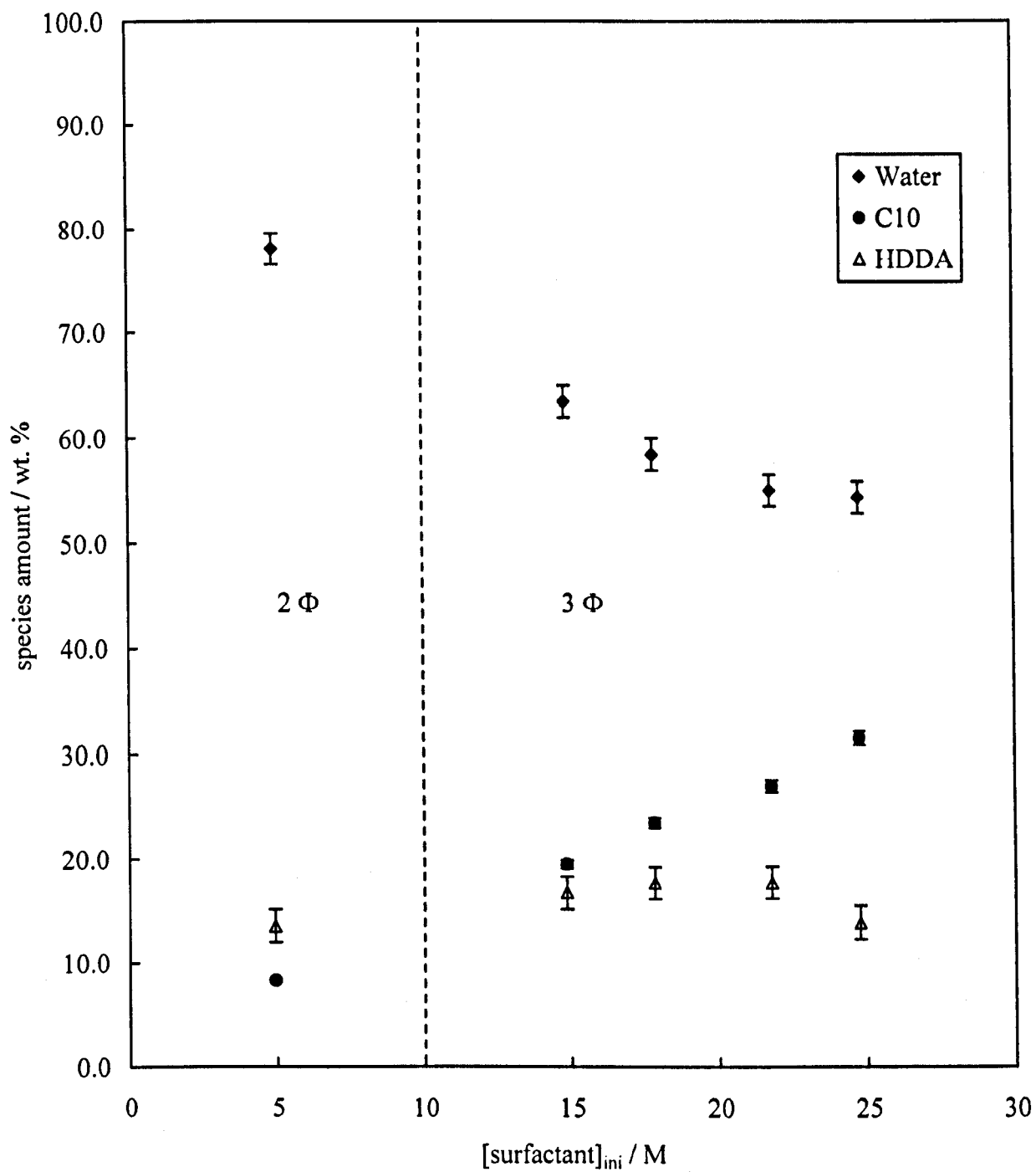


Figure 4.29. Composition of lower equilibrium phase vs. initial surfactant concentration in system ( $[\text{surfactant}]_{\text{ini}}$ ) for system containing C<sub>10</sub>, HDDA and D<sub>2</sub>O.  $\phi_0 = 0.5$ ,  $T = 25^\circ\text{C}$



[surfactant] data shown in Figure 4.12. Figure 4.28 shows a similar relationship between  $[\text{surfactant}]_{\text{ini}}$  and equilibrium [surfactant], oil and water contents in the middle phase of this system to that seen in the lower phase of the  $\text{C}_{3/11}\text{-M}$ , BDDA,  $\text{D}_2\text{O}$  system (Figure 4.23) although the oil and water contents are closer in Figure 4.28 than in Figure 4.23. As surfactant content increases, the oil content remains fairly constant and water content decreases. Figure 4.29 shows a very similar trend in the lower phase of this system to that seen in Figure 4.23. The similar trends in composition with  $[\text{surfactant}]_{\text{ini}}$  between these two systems are expected because the phase equilibration behaviour is very similar as shown in Figures 4.10 and 4.12. Figures 4.28 and 4.29 show that equilibrium [surfactant] increases linearly with  $[\text{surfactant}]_{\text{ini}}$  in both aggregate-containing phases in this system. Water content in both aggregate-containing phases can be controlled by  $[\text{surfactant}]_{\text{ini}}$ .

#### **$\text{C}_{10}$ , BDDA, $\text{D}_2\text{O}$ :**

Figure 4.30 shows that in the upper equilibrium phase of this system as  $[\text{surfactant}]_{\text{ini}}$  is increased, equilibrium [surfactant] increases along with the equilibrium water content as the equilibrium oil content decreases. This signifies aggregate-containing phases with increasing solubilisation of water into w/o aggregates. The oil content remains significantly higher than that of water or surfactant. Figure 4.31 shows that in the middle equilibrium phase, also an aggregate-containing phase, as  $[\text{surfactant}]_{\text{ini}}$  is increased the equilibrium [surfactant] increases only slightly as does that of water. The oil content decreases to a greater extent such that the concentrations of surfactant, oil and water approach equal values with the oil content always higher than the water content. Figure 4.32 shows a slight maximum in

**Figure 4.30. Composition of upper equilibrium phase vs. initial surfactant concentration in system ( $[\text{surfactant}]_{\text{ini}}$ ) for system containing  $\text{C}_{10}$ , BDDA and  $\text{D}_2\text{O}$ .  $\phi_0 = 0.5$ ,  $T = 25^\circ\text{C}$**

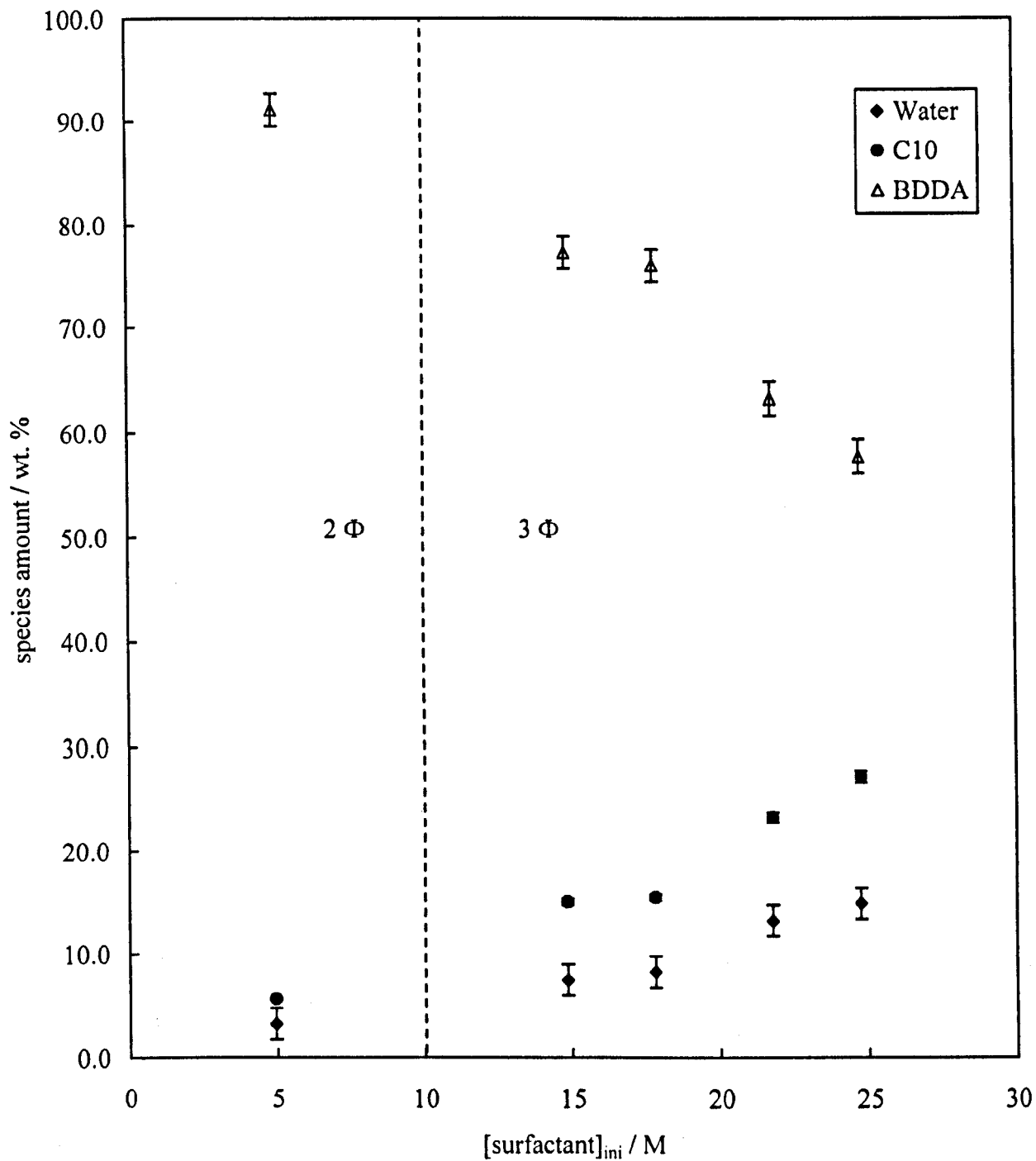
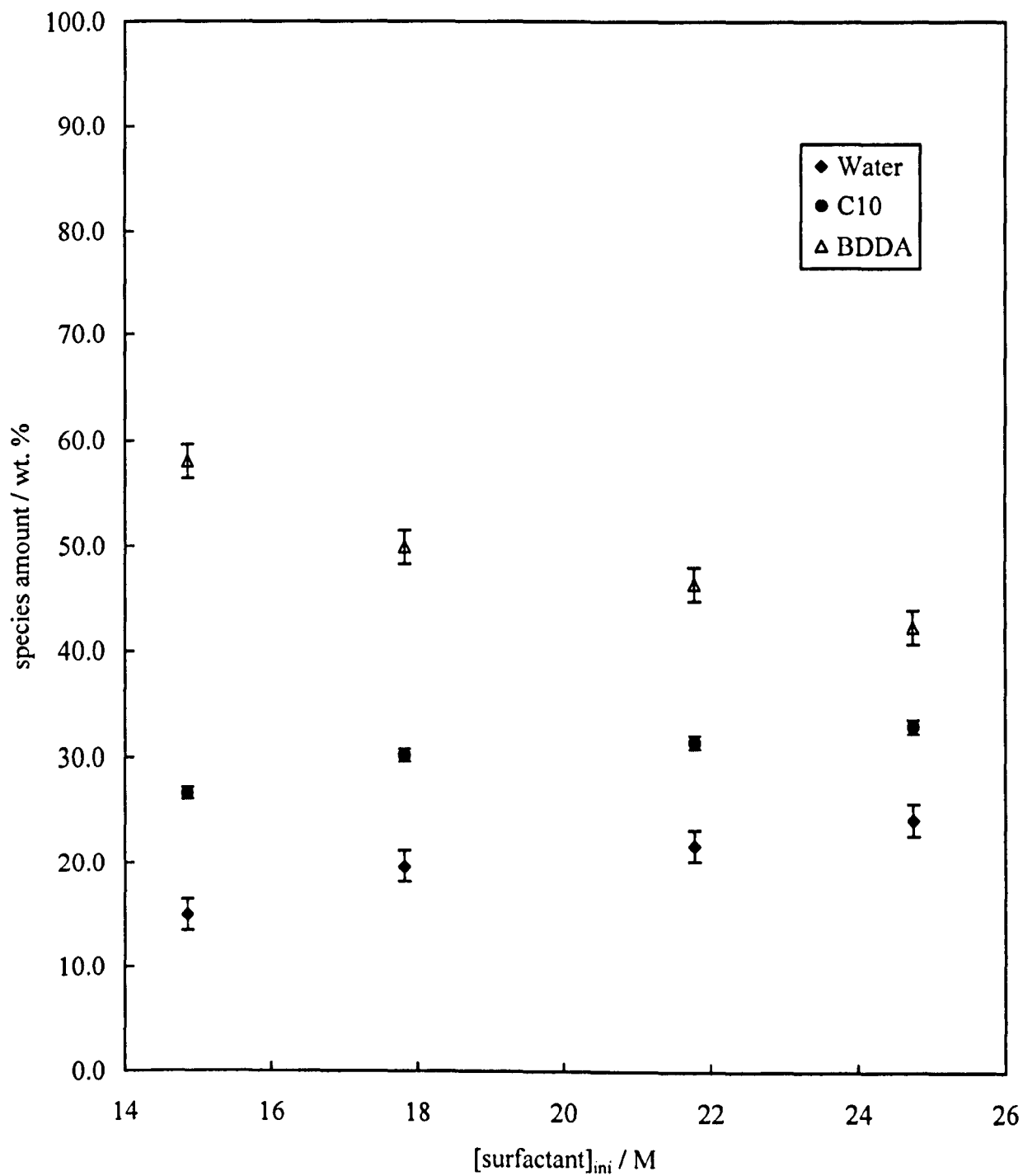
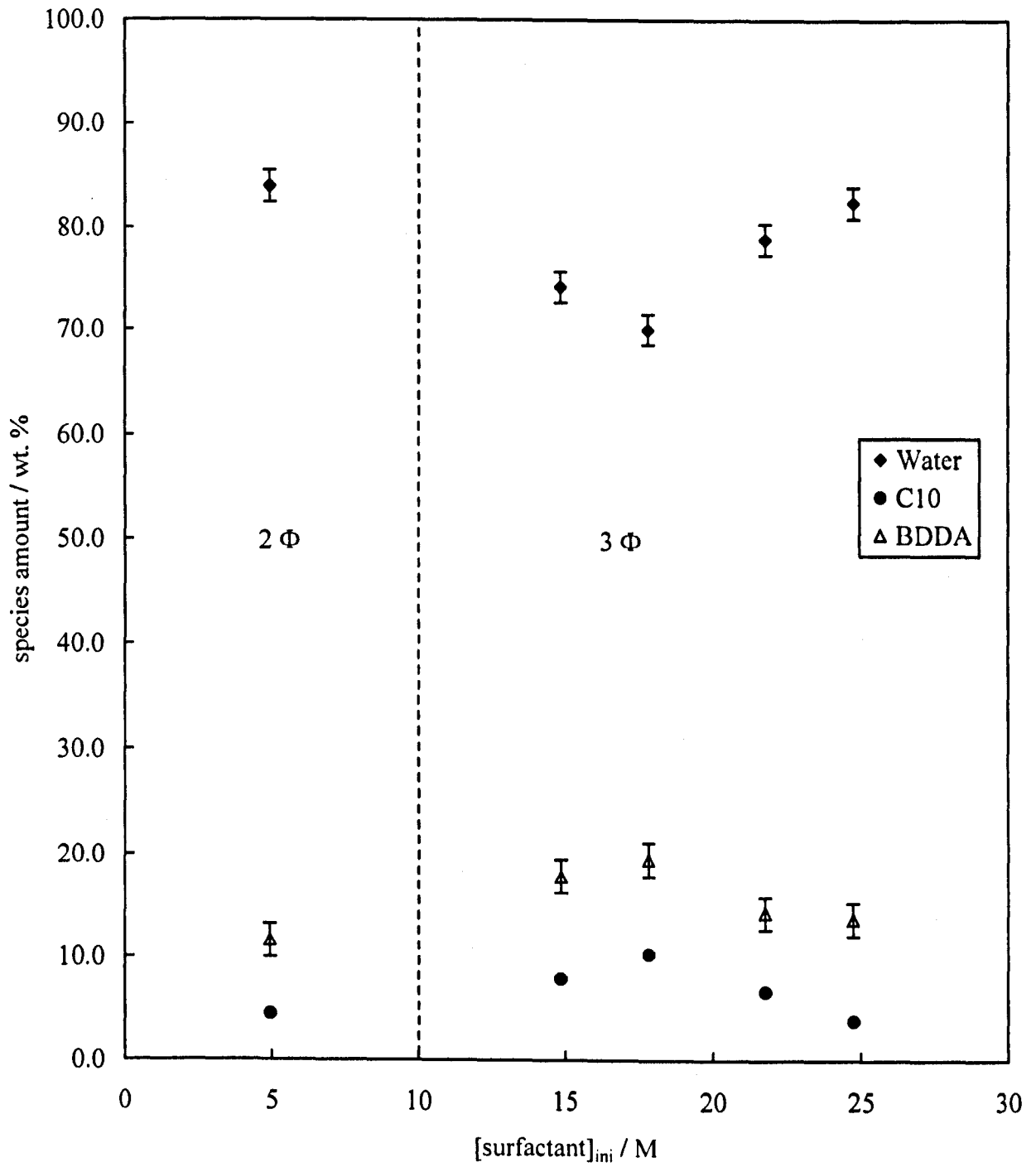


Figure 4.31. Composition of middle equilibrium phase vs. initial surfactant concentration in system ( $[\text{surfactant}]_{\text{ini}}$ ) for system containing  $\text{C}_{10}$ , BDDA and  $\text{D}_2\text{O}$ .  $\phi_0 = 0.5$ ,  $T = 25^\circ\text{C}$



**Figure 4.32. Composition of lower equilibrium phase vs. initial surfactant concentration in system ( $[\text{surfactant}]_{\text{ini}}$ ) for system containing  $\text{C}_{10}$ , BDDA and  $\text{D}_2\text{O}$ .  $\phi_0 = 0.5$ ,  $T = 25\text{ }^\circ\text{C}$**





the equilibrium [surfactant] and oil content accompanied by a slight minimum in the equilibrium water content in the lower phase. This may signify a different type of phase relationship developing at higher [surfactant]<sub>ini</sub> content and the continuous phase drop test results shown in Figure 4.13 show that indeed this may be the case as the continuous phase of the middle equilibrium phase is seen to change from possible bicontinuous to aqueous continuous. Figures 4.30 to 4.32 show that this system exhibits a more complex relation between [surfactant]<sub>ini</sub> and equilibrium water content suggesting that accurate control of equilibrium water content by adjusting the [surfactant]<sub>ini</sub> may be very difficult in this system.

#### **C<sub>10</sub>, DPGDA, D<sub>2</sub>O:**

Figure 4.33 shows a very similar compositional trend with increasing [surfactant]<sub>ini</sub> in the upper phase of this system to that seen in the upper phase of the C<sub>10</sub>, BDDA, D<sub>2</sub>O system (Figure 4.30). This would be expected as Figures 4.13 and 4.14 show some similarities in phase behaviour trends in the two systems. Figure 4.34 shows a similar trend with [surfactant]<sub>ini</sub> to that of Figure 4.31 in that the composition of the middle equilibrium phase changes very little with [surfactant]<sub>ini</sub>. The relative proportions of water and oil in the two systems are quite different however with the water content almost double that of oil in the system shown in Figure 4.34. Both oil and water contents decrease with increasing [surfactant]<sub>ini</sub> as the equilibrium [surfactant] increases. Figure 4.35 shows a similar trend for the lower phase to that seen in Figure 4.32. The water and oil contents are closer in Figure 4.35 and a greater change in composition with increasing [surfactant]<sub>ini</sub> is seen. Again the relationship

Figure 4.33. Composition of upper equilibrium phase vs. initial surfactant concentration in system ( $[\text{surfactant}]_{\text{ini}}$ ) for system containing  $\text{C}_{10}$ , DPGDA and  $\text{D}_2\text{O}$ .  $\phi_0 = 0.5$ ,  $T = 25\text{ }^\circ\text{C}$

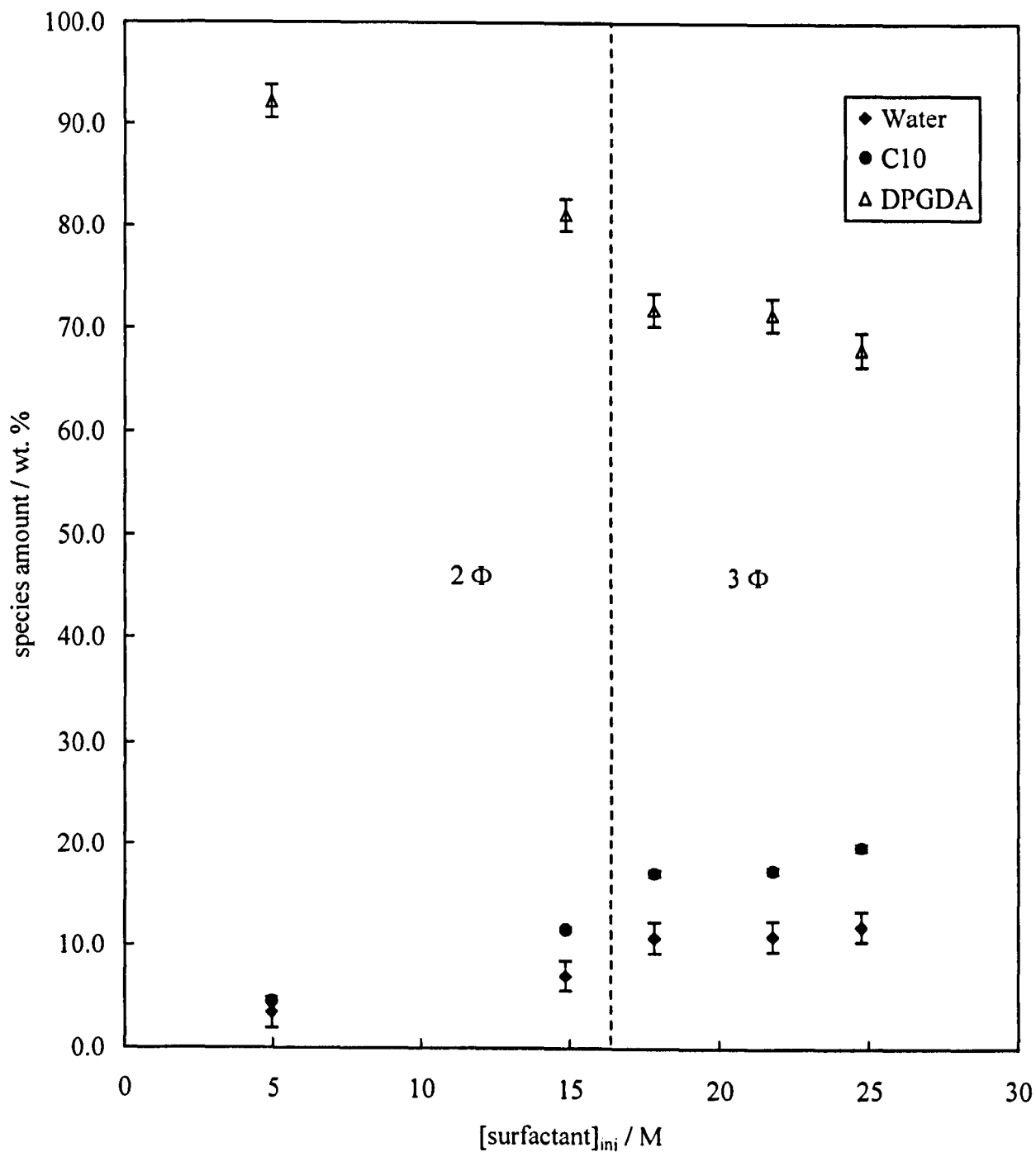


Figure 4.34. Composition of middle equilibrium phase vs. initial surfactant concentration in system ( $[\text{surfactant}]_{\text{ini}}$ ) for system containing  $\text{C}_{10}$ , DPGDA and  $\text{D}_2\text{O}$ .  $\phi_0 = 0.5$ ,  $T = 25\text{ }^\circ\text{C}$

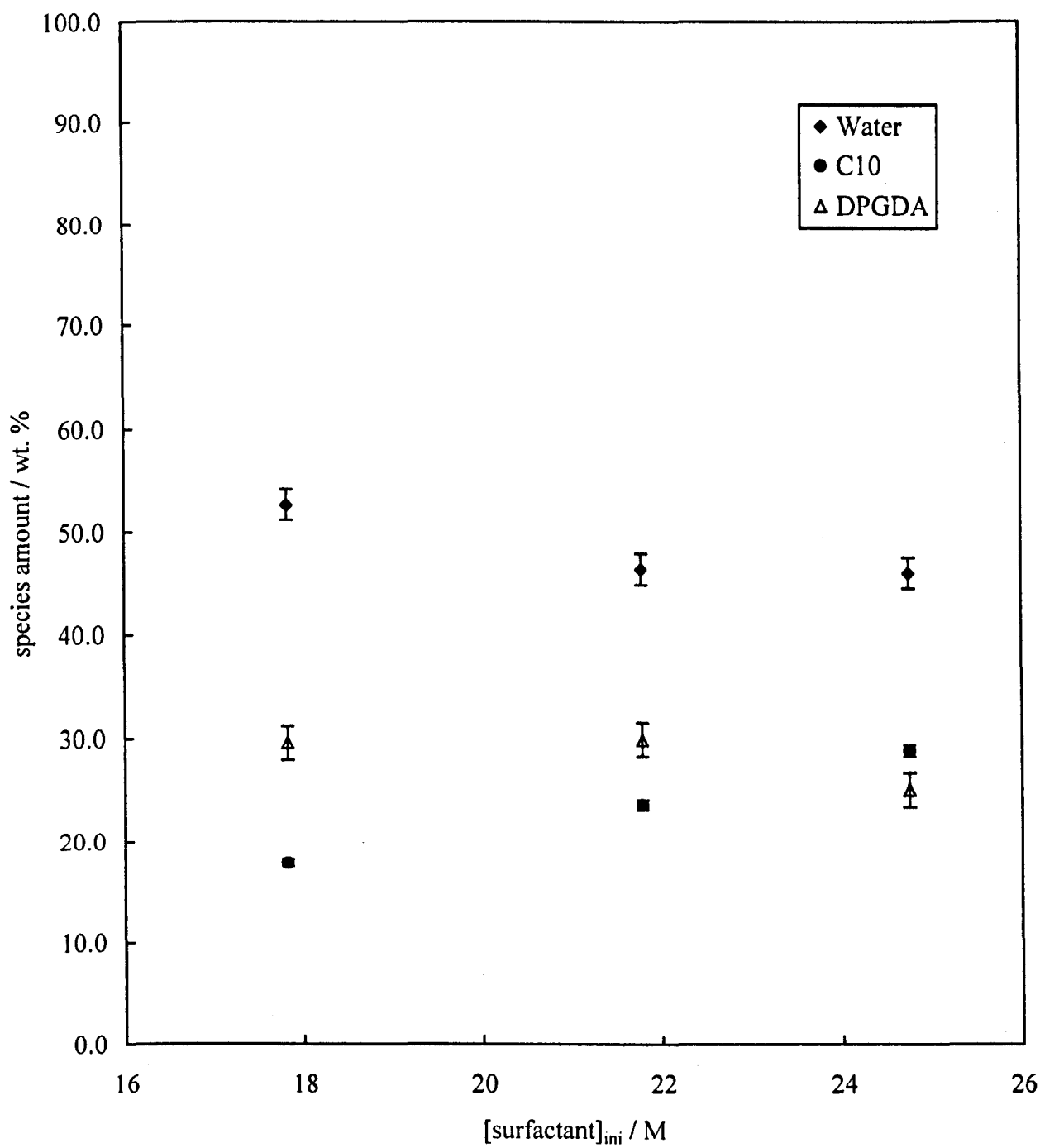
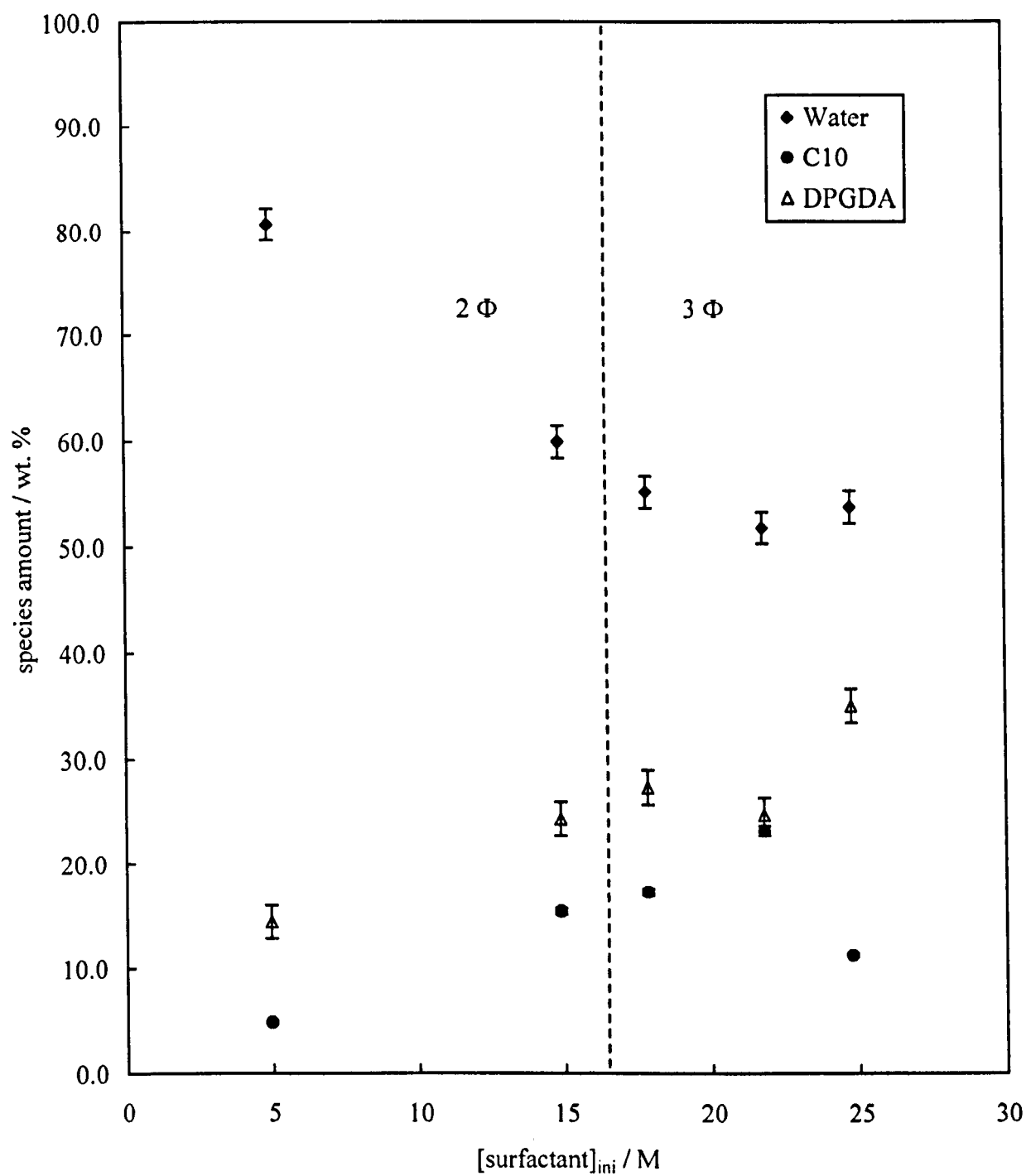


Figure 4.35. Composition of lower equilibrium phase vs. initial surfactant concentration in system ( $[\text{surfactant}]_{\text{ini}}$ ) for system containing  $\text{C}_{10}$ , DPGDA and  $\text{D}_2\text{O}$ .  $\phi_0 = 0.5$ ,  $T = 25\text{ }^\circ\text{C}$



between  $[\text{surfactant}]_{\text{ini}}$  and equilibrium water content is complex making it difficult to accurately control equilibrium water content with  $[\text{surfactant}]_{\text{ini}}$  in this system.

### **C<sub>12</sub>, HDDA, D<sub>2</sub>O:**

Figure 4.36 shows that as  $[\text{surfactant}]_{\text{ini}}$  is increased, the concentration of surfactant in the upper equilibrium phase increases, the water content remains minimal and the oil content decreases slightly. This would be expected from Figure 4.15, which shows the phase behaviour of the system and indicates that at high  $[\text{surfactant}]_{\text{ini}}$  the upper oil phase does show an increase in equilibrium  $[\text{surfactant}]$ . Figure 4.37 shows that as  $[\text{surfactant}]_{\text{ini}}$  is increased, the equilibrium  $[\text{surfactant}]$  in the middle phase also increases but very gradually. The oil content rises steeply and the water content decreases steeply with increasing  $[\text{surfactant}]_{\text{ini}}$ . The relative oil and water contents reverse at  $\sim 22$  wt. %  $[\text{surfactant}]_{\text{ini}}$ . The continuous phase was seen to change at around 20 wt. %  $[\text{surfactant}]_{\text{ini}}$  as seen in Figure 4.15. The compositional analysis seen in Figure 4.37 supports this observation and the relative proportions of water and oil cross at around this  $[\text{surfactant}]_{\text{ini}}$ . A dramatic change in composition is seen with only a slight increase in equilibrium  $[\text{surfactant}]$  in this phase. Figure 4.38 shows an abrupt change in compositional trend with increasing  $[\text{surfactant}]_{\text{ini}}$  in the lower phase at  $\sim 15$  wt. %  $[\text{surfactant}]_{\text{ini}}$ . The gradient of the increase in equilibrium  $[\text{surfactant}]$  with  $[\text{surfactant}]_{\text{ini}}$  decreases greatly and the relative concentrations of water and oil become much closer which signifies a change in phase behaviour at this  $[\text{surfactant}]_{\text{ini}}$ . This is shown in the appearance of the equilibrium phases shown in Figure 4.15. Control of equilibrium water content with  $[\text{surfactant}]_{\text{ini}}$  in this system is possible, but difficult at high  $[\text{surfactant}]_{\text{ini}}$  in the lower phase.

Figure 4.36. Composition of upper equilibrium phase vs. initial surfactant concentration in system ( $[\text{surfactant}]_{\text{ini}}$ ) for system containing  $\text{C}_{12}$ , HDDA and  $\text{D}_2\text{O}$ .  $\phi_0 = 0.5$ ,  $T = 25\text{ }^\circ\text{C}$

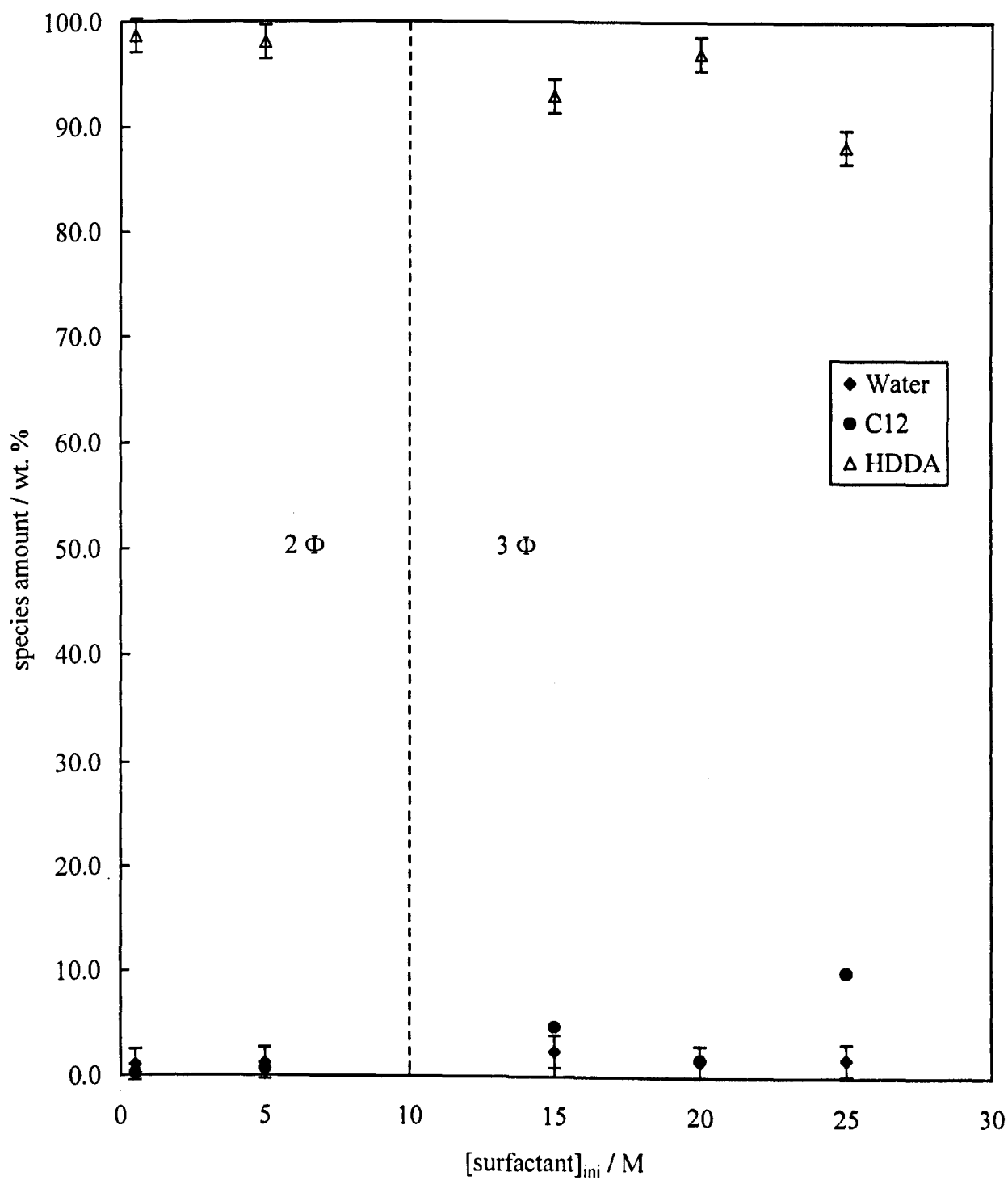
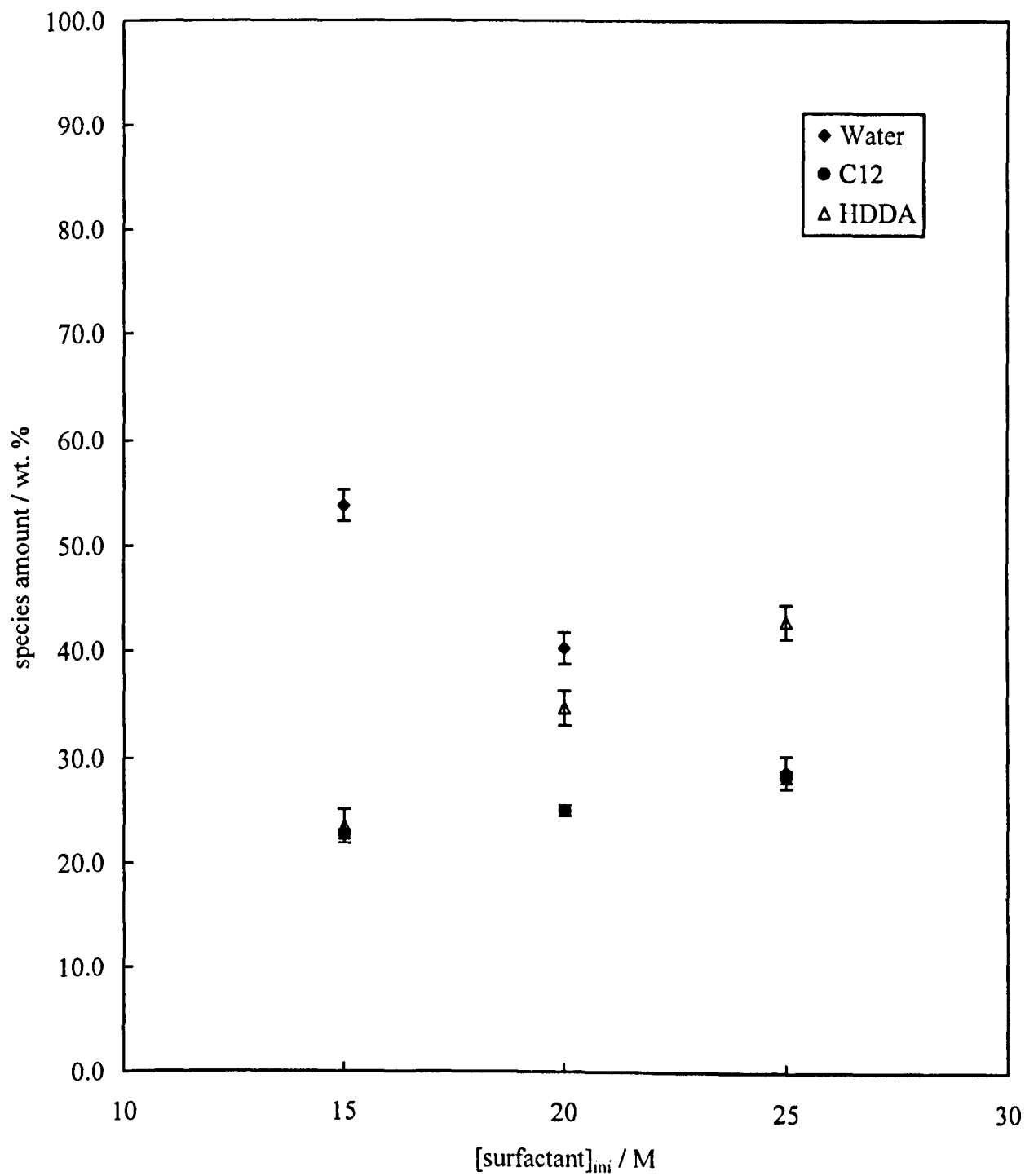
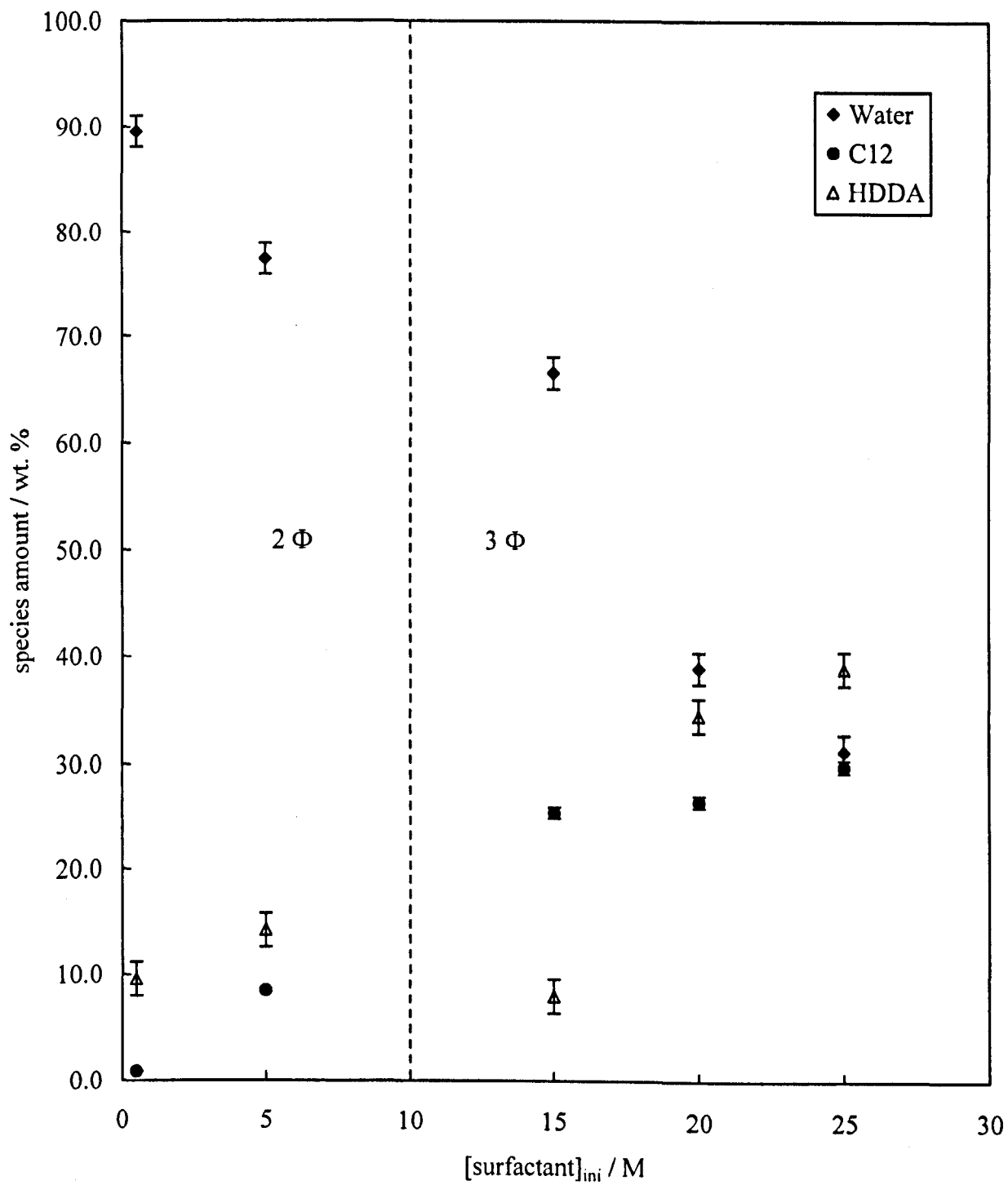


Figure 4.37. Composition of middle equilibrium phase vs. initial surfactant concentration in system ( $[\text{surfactant}]_{\text{ini}}$ ) for system containing  $\text{C}_{12}$ , HDDA and  $\text{D}_2\text{O}$ .  $\phi_0 = 0.5$ ,  $T = 25^\circ\text{C}$



**Figure 4.38. Composition of lower equilibrium phase vs. initial surfactant concentration in system ( $[\text{surfactant}]_{\text{ini}}$ ) for system containing  $\text{C}_{12}$ , HDDA and  $\text{D}_2\text{O}$ .  $\phi_0 = 0.5$ ,  $T = 25^\circ\text{C}$**





### **C<sub>12</sub>, BDDA, D<sub>2</sub>O:**

Figure 4.39 shows that as  $[\text{surfactant}]_{\text{ini}}$  is increased, the equilibrium  $[\text{surfactant}]$  also increases in the upper oil phase. This is accompanied by an increase in water content and a sharp decrease in oil content confirming that this phase is an aggregate-containing phase. The drop-test results seen in Figure 4.16 show that these are w/o aggregates. This is expected, as Figure 4.16 suggests that as  $[\text{surfactant}]_{\text{ini}}$  increases the system behaves like a Winsor II-like system. Figure 4.40 shows a very similar trend in the middle phase to that seen in Figure 4.39 which again is expected from the phase behaviour shown in Figure 4.16. Figure 4.41 shows that as  $[\text{surfactant}]_{\text{ini}}$  is increased the equilibrium  $[\text{surfactant}]$  actually decreases in the lower phase, as this phase starts to become an excess water phase. The oil content does however remain fairly high at  $\sim 12$  wt. % and the water content remains unchanged at  $\sim 85$  wt. %. Figures 4.39 to 4.41 show that this system is quite different to the others so far observed, as almost complete phase inversion from WI at a few times cmc  $[\text{surfactant}]_{\text{ini}}$  (see Chapter 3) to a WII like system at very high  $[\text{surfactant}]_{\text{ini}}$ . In the aggregate-containing phases, control of equilibrium water content with  $[\text{surfactant}]_{\text{ini}}$  can be achieved.

### **C<sub>12</sub>, DPGDA, D<sub>2</sub>O:**

Figure 4.42 shows a very similar trend to that seen in Figure 4.39, which is expected, as Figures 4.16 and 4.17 show very similar trends in microemulsion phase behaviour. Figure 4.43, although containing data from only two middle phases, suggests a similarly small change in middle phase composition with  $[\text{surfactant}]_{\text{ini}}$  to

Figure 4.39. Composition of upper equilibrium phase vs. initial surfactant concentration in system ( $[\text{surfactant}]_{\text{ini}}$ ) for system containing  $\text{C}_{12}$ , BDDA and  $\text{D}_2\text{O}$ .  $\phi_0 = 0.5$ ,  $T = 25^\circ\text{C}$

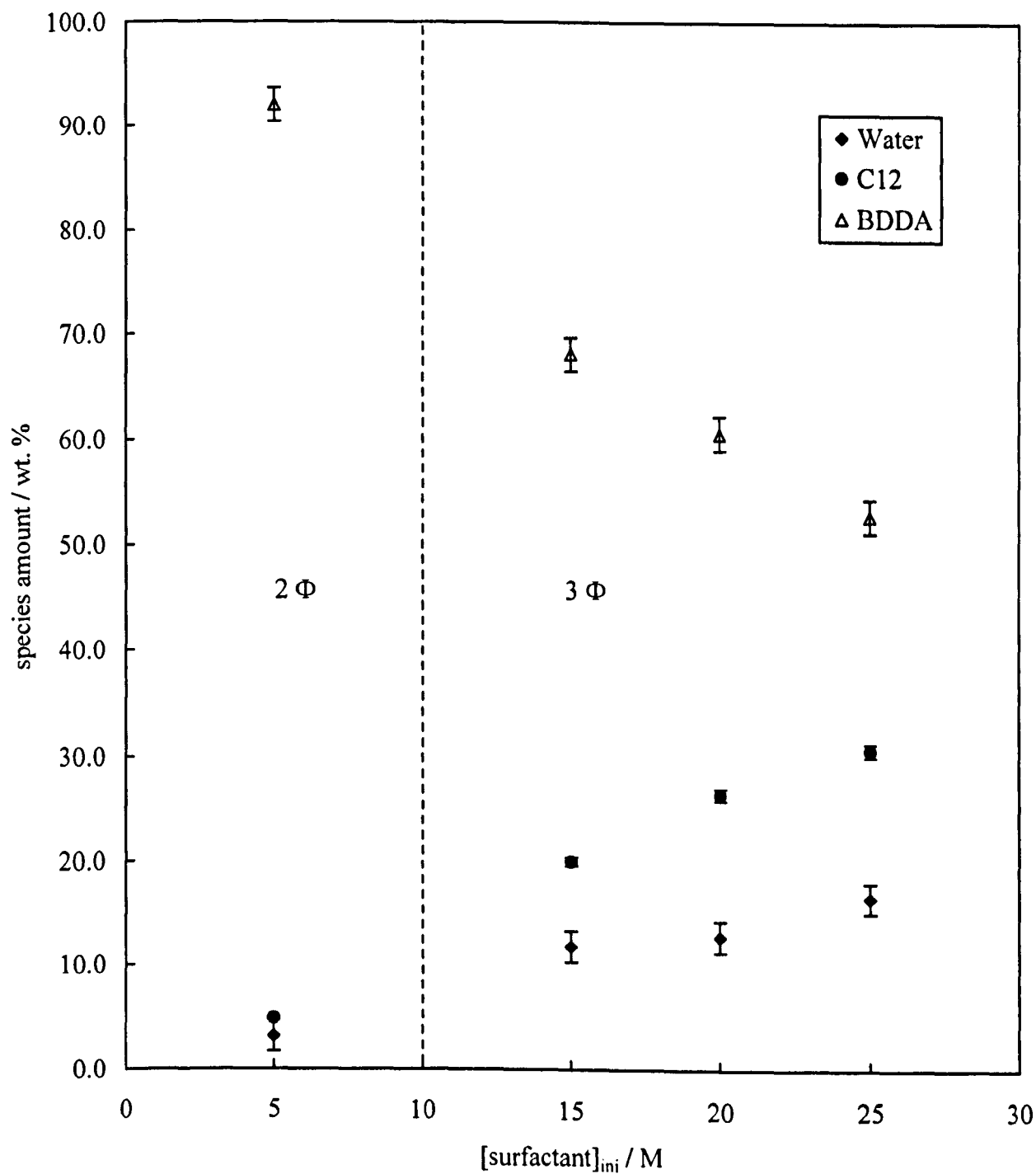


Figure 4.40. Composition of middle equilibrium phase vs. initial surfactant concentration in system ( $[\text{surfactant}]_{\text{ini}}$ ) for system containing  $\text{C}_{12}$ , BDDA and  $\text{D}_2\text{O}$ .  $\phi_0 = 0.5$ ,  $T = 25^\circ\text{C}$

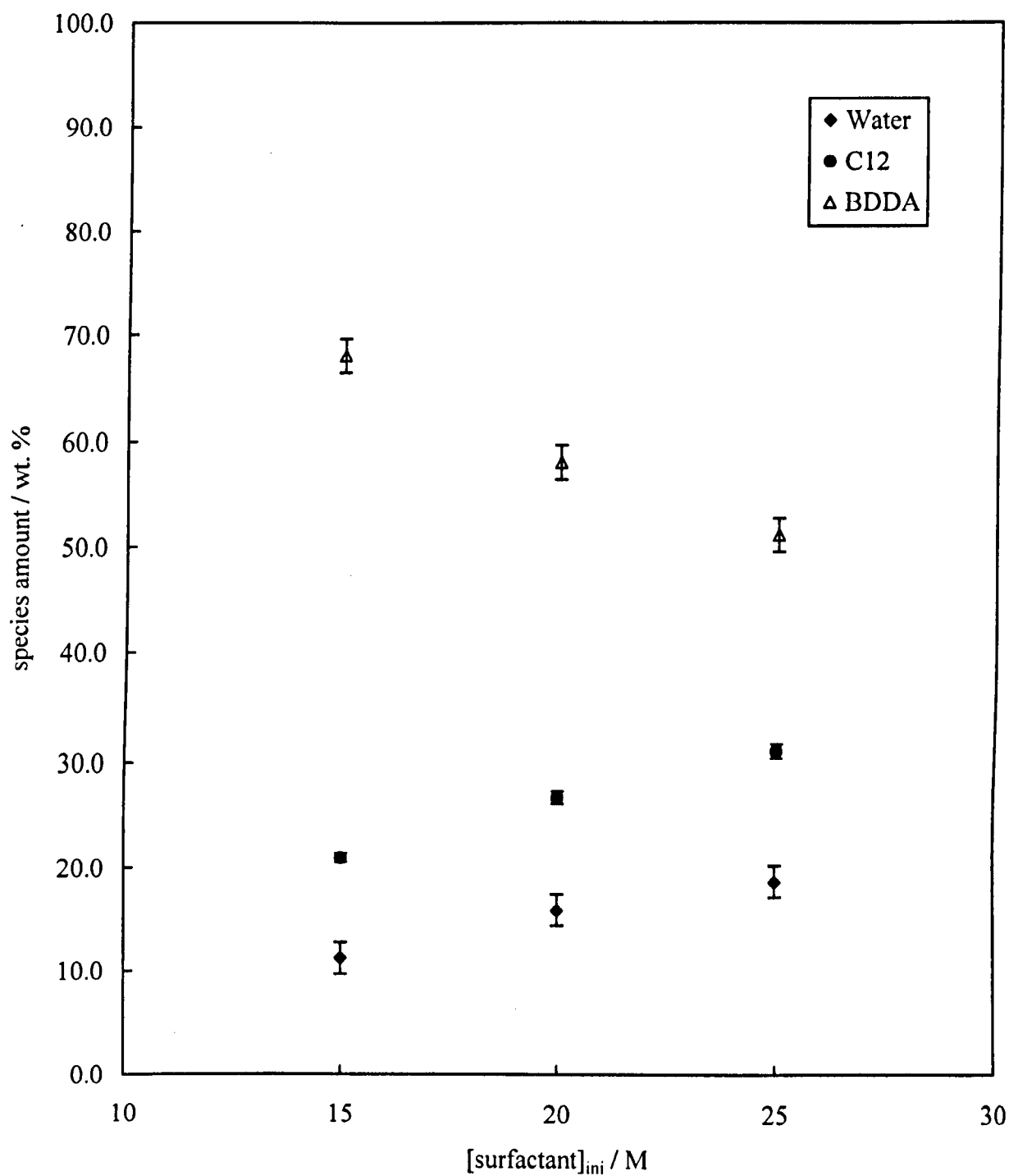


Figure 4.41. Composition of lower equilibrium phase vs. initial surfactant concentration in system ( $[\text{surfactant}]_{\text{ini}}$ ) for system containing  $\text{C}_{12}$ , BDDA and  $\text{D}_2\text{O}$ .  $\phi_0 = 0.5$ ,  $T = 25^\circ\text{C}$

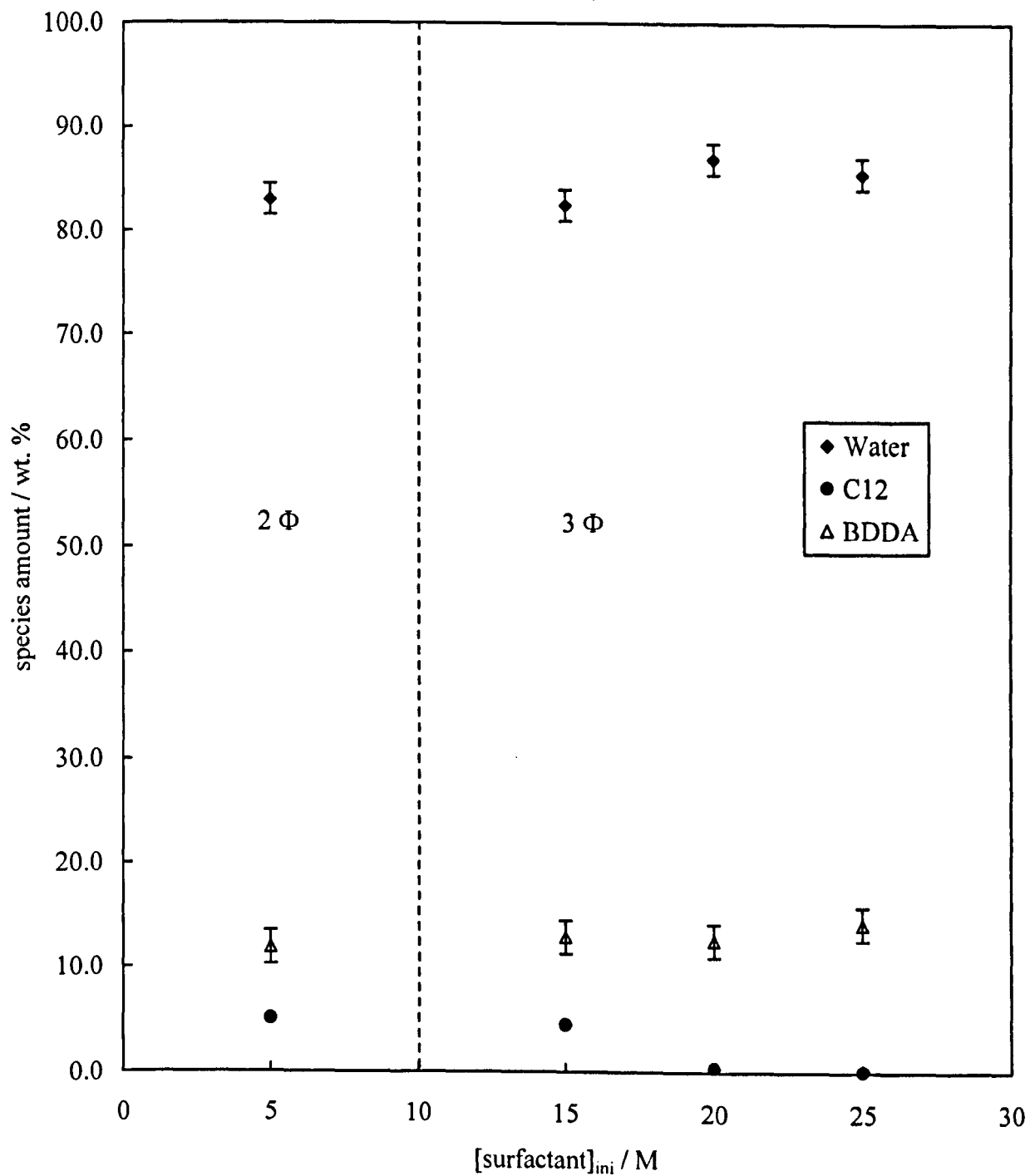


Figure 4.42. Composition of upper equilibrium phase vs. initial surfactant concentration in system ( $[\text{surfactant}]_{\text{ini}}$ ) for system containing C<sub>12</sub>, DPGDA and D<sub>2</sub>O.  $\phi_0 = 0.5$ , T = 25 °C

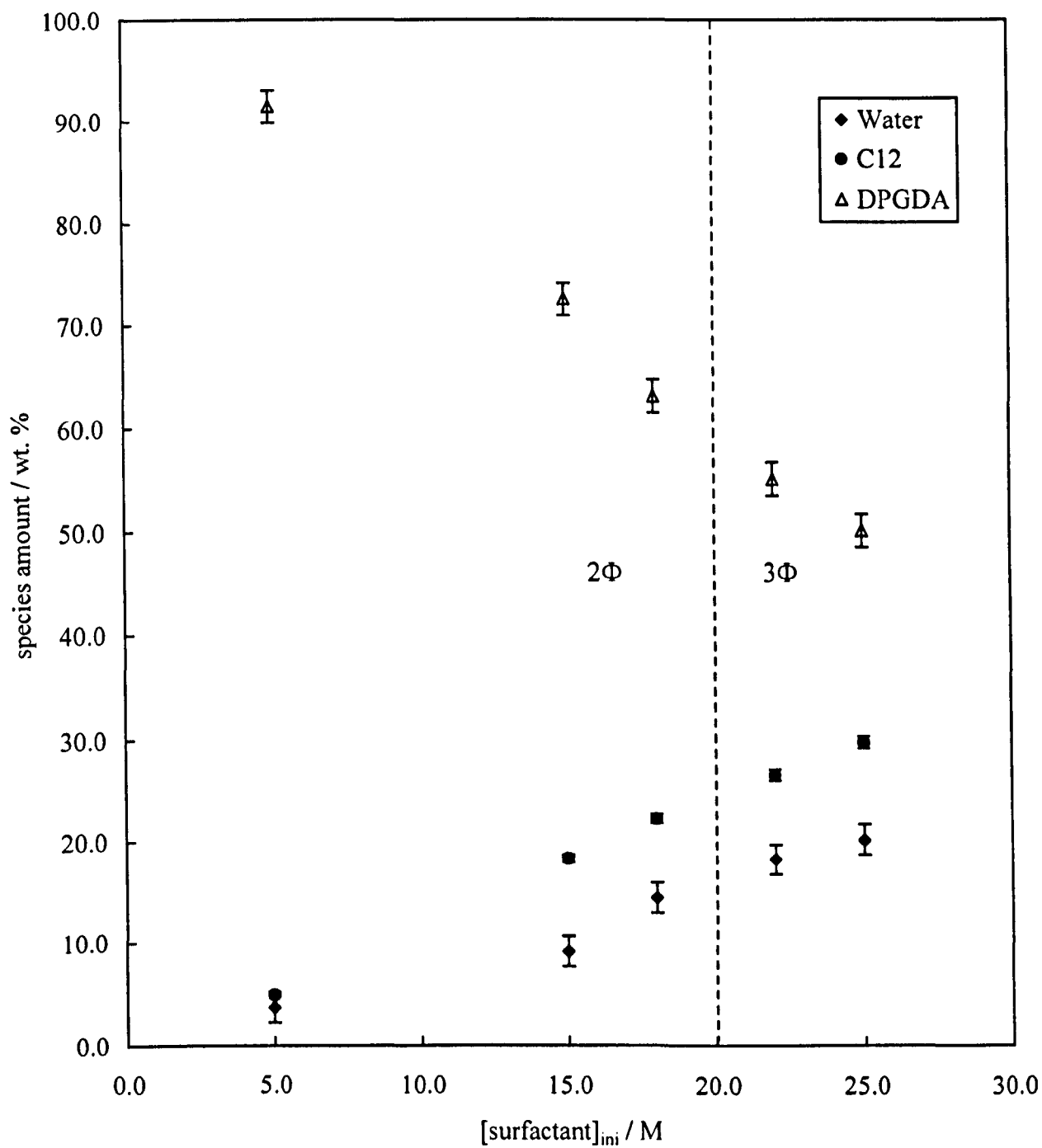


Figure 4.43. Composition of middle equilibrium phase vs. initial surfactant concentration in system ( $[\text{surfactant}]_{\text{ini}}$ ) for system containing C<sub>12</sub>, DPGDA and D<sub>2</sub>O.  $\phi_0 = 0.5$ , T = 25 °C

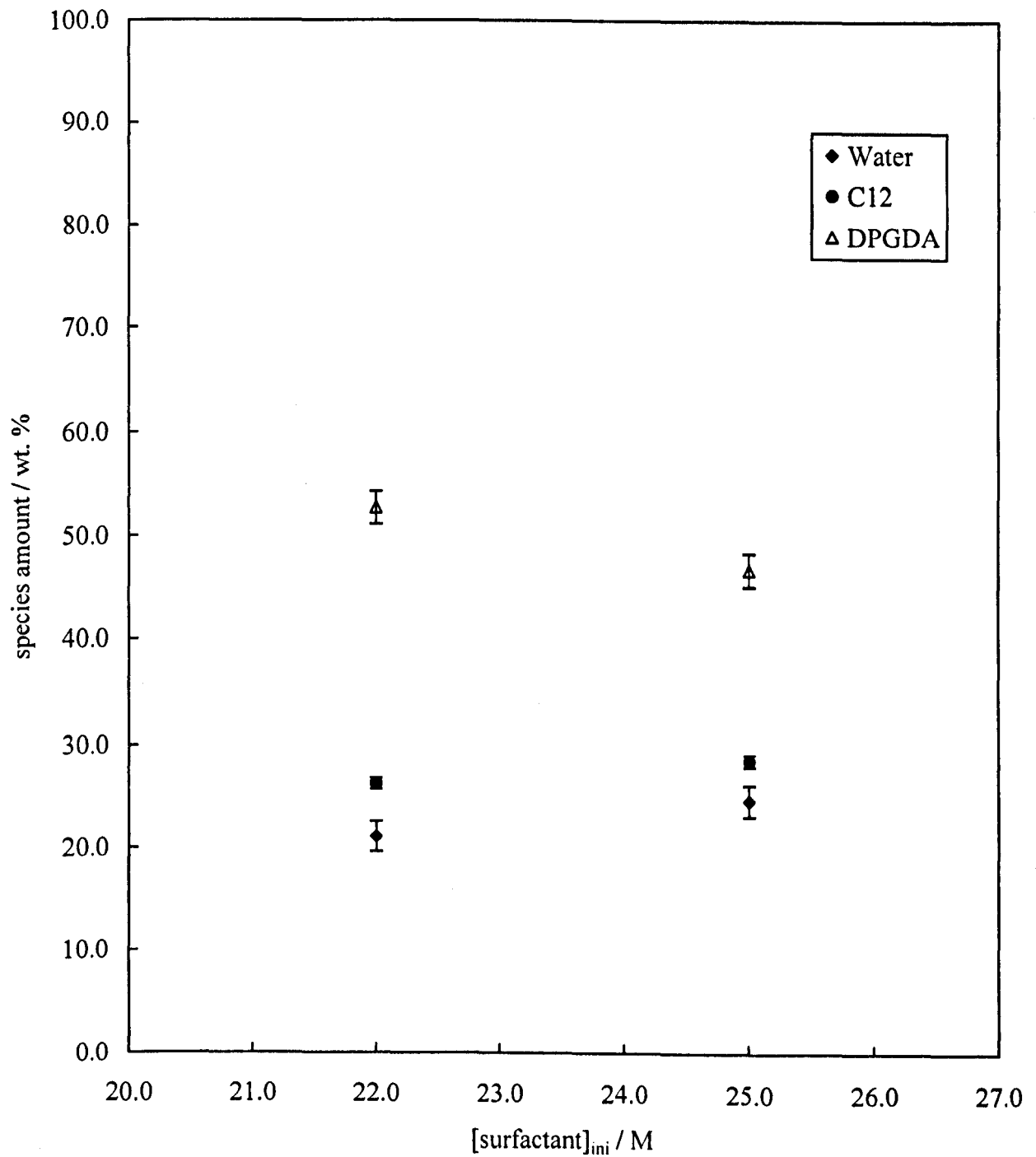
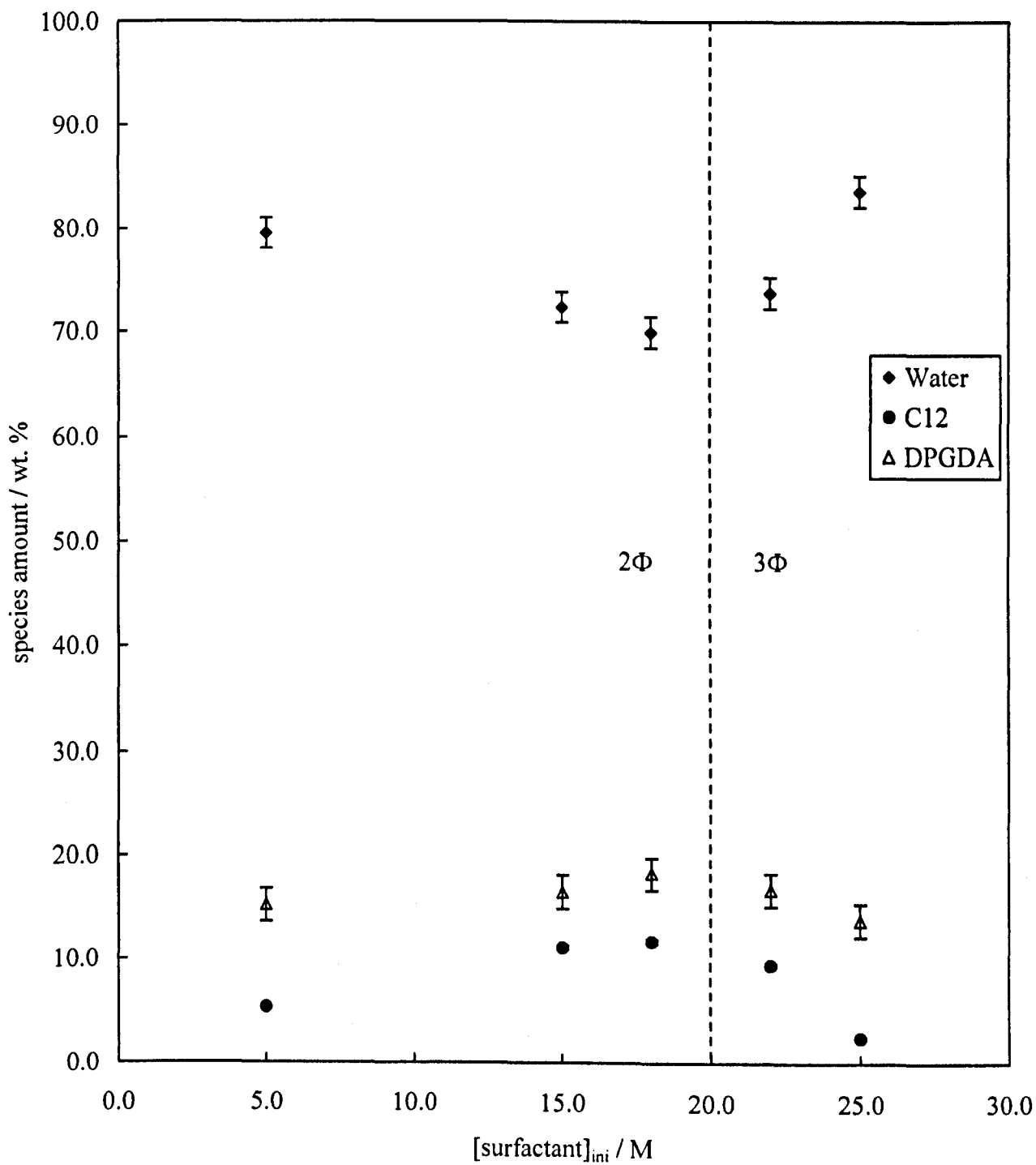


Figure 4.44. Composition of lower equilibrium phase vs. initial surfactant concentration in system ( $[\text{surfactant}]_{\text{ini}}$ ) for system containing  $\text{C}_{12}$ , DPGDA and  $\text{D}_2\text{O}$ .  $\phi_0 = 0.5$ ,  $T = 25^\circ\text{C}$



that seen in Figure 4.40. Figure 4.44 shows that in the lower phase, the compositional trend depends on whether one is in the two or three phase region of  $[\text{surfactant}]_{\text{ini}}$ . In the two-phase region, as  $[\text{surfactant}]_{\text{ini}}$  is increased, the oil content is seen to increase slightly along with equilibrium  $[\text{surfactant}]$  as the water content decreases. In the three-phase region, equilibrium  $[\text{surfactant}]$  and oil contents decrease with increasing  $[\text{surfactant}]_{\text{ini}}$  and equilibrium water content increases. Figures 4.42 to 4.44 show another system with a complex relationship between  $[\text{surfactant}]_{\text{ini}}$  and equilibrium water content of the microemulsion phases. Again, evidence of phase inversion with increasing  $[\text{surfactant}]_{\text{ini}}$  is seen. While the control of water content of the equilibrium microemulsion with  $[\text{surfactant}]_{\text{ini}}$  is difficult, control of the microemulsion aggregate type with  $[\text{surfactant}]_{\text{ini}}$  may be achievable.

Figures 4.18 to 4.44 show that the structures of the surfactant and oil used in each system clearly affect the phase behaviour of the system and self phase inversion with  $[\text{surfactant}]_{\text{ini}}$  is seen in some systems. In all WI\* systems, the equilibrium  $[\text{surfactant}]$  in all aggregate-containing phases increases linearly with  $[\text{surfactant}]_{\text{ini}}$ . In these systems, as  $[\text{surfactant}]_{\text{ini}}$  is increased, the number of aggregates in the aggregate-containing phases increases, allowing greater solubilisation of the oil phase, but the preferred surfactant monolayer curvature and partitioning of surfactant into oil is not changed by the electrolytic effect of the surfactant. In the WI<sup>1</sup> systems, the equilibrium  $[\text{surfactant}]$  does not increase linearly with  $[\text{surfactant}]_{\text{ini}}$  as in these systems the electrolytic effect of the surfactant changes the partitioning of the surfactant and surfactant monolayer curvature, leading to increasing surfactant partitioning into oil and aggregate formation in the oil phase above a particular  $[\text{surfactant}]_{\text{ini}}$ . This leads to a kink in the increase in equilibrium  $[\text{surfactant}]$  with



$[\text{surfactant}]_{\text{ini}}$  in the aqueous/ bicontinuous aggregate-containing phases. Table 4.4 summarises all the systems.

**Table 4.4. Relation between system, equilibrium system type and ability to control equilibrium water content with  $[\text{surfactant}]_{\text{ini}}$**

System (surfactant / oil)	Equilibrium phase type	Control of equilibrium water content with $[\text{surfactant}]_{\text{ini}}$
C <sub>3/11-M</sub> / HDDA	WI*	✓
C <sub>3/11-M</sub> / BDDA	WI*	✓
C <sub>3/11-M</sub> / DPGDA	WI <sup>i</sup>	X
C <sub>10</sub> / HDDA	WI*	✓
C <sub>10</sub> / BDDA	WI <sup>i</sup>	X
C <sub>10</sub> / DPGDA	WI <sup>i</sup>	X
C <sub>12</sub> / HDDA	WI*	✓
C <sub>12</sub> / BDDA	WII*	✓
C <sub>12</sub> / DPGDA	WI <sup>i</sup>	X

Table 4.4 shows that:-

- i.) HDDA forms WI\* systems independent of surfactant type, in which the control of equilibrium water content is possible with  $[\text{surfactant}]_{\text{ini}}$
- ii.) BDDA forms a range of systems dependent on surfactant type. C<sub>12</sub> with BDDA is the only example of a WII\* system and control of equilibrium water content with  $[\text{surfactant}]_{\text{ini}}$  is possible in this system.

iii.) DPGDA forms WI<sup>i</sup> systems independent of surfactant type, in which the control of equilibrium water content is not possible with [surfactant]<sub>ini</sub>.

This suggests that the more polar DPGDA oil increases the dissociation constant of the surfactant therefore increasing its electrolytic effect and allowing self-inversion of surfactant monolayer curvature at high enough [surfactant]<sub>ini</sub>. However, the most extreme example of self-inversion is seen with the less polar BDDA oil with C<sub>10</sub> surfactant. However, BDDA also produces a WI\* system (with C<sub>3/11-M</sub> surfactant). The oil polarity and electrolytic effect of the surfactant together must therefore form the driving force for self-inversion as discussed in Chapter 3.

## 4.4 Conclusions

Equilibrium microemulsion phases have been prepared with increasing  $[\text{surfactant}]_{\text{ini}}$  for each system in the absence of salt. The equilibrium phase volumes, location of aggregates and phase compositions have been studied. The aim was to determine the effects of surfactant and oil structure on microemulsion phase behaviour characteristics including microemulsion type, equilibrium  $[\text{surfactant}]$ , oil content and water content of the equilibrium phases.

(a) Surfactant C<sub>3/11-M</sub> was found to contain a high level of impurities resulting in irreproducible phase behaviour when preparing microemulsions with a high  $[\text{surfactant}]_{\text{ini}}$ . A method of purification has been supplied by Avecia and with modifications has resulted in the reproducible preparation of microemulsion phases.

(b) The structures of the surfactant and oil affect the microemulsion phase equilibration and formation. A broad range of phase types can be prepared from Winsor I-like water continuous phases thru bicontinuous to Winsor II-like oil continuous phases by selection of suitable surfactants and oils. Self-inversion was exhibited by all of the surfactants, the extent of inversion depending on the particular surfactant-oil combination. Definite Winsor III systems have not been prepared.

(c) The structures of the surfactant and oil affect the phase behaviour of the system resulting in several trends in equilibrium water content with  $[\text{surfactant}]_{\text{ini}}$ .

- Self-phase inversion with surfactant content occurs in all systems containing DPGDA oil independent of surfactant type, in which control of equilibrium water content is not possible with  $[\text{surfactant}]_{\text{ini}}$ .
- All systems containing HDDA oil are WI-like systems with two aggregate-containing water continuous phases (WI\*), in which the control of equilibrium water content is possible with  $[\text{surfactant}]_{\text{ini}}$ .
- The type of phase produced with BDDA oil is dependent on the surfactant type. BDDA with C<sub>10</sub> produces fully inverted WI-like systems in which control of equilibrium water content with  $[\text{surfactant}]_{\text{ini}}$  is possible.

## 4.5 References

- <sup>1</sup> M. Sasthav and H. M. Chung, *Langmuir*, **7**, 1378 (1991).
- <sup>2</sup> L. M. Gan, T. D. Li, C. H. Chew, W. K. Teo, and L. H. Gan, *Langmuir*, **11**, 3316 (1995).
- <sup>3</sup> T. D. Li, L. M. Gan, C. H. Chew, W. K. Teo and L. H. Gan, *Langmuir*, **12**, 5863 (1996).
- <sup>4</sup> T. H. Chieng, L. M. Gan, C. H. Chew, S. C. Ng and K. L. Pey, *Polymer*, **37**, 4823 (1996).
- <sup>5</sup> C. H. Chew, L. M. Gan, L. H. Ong, K. Zhang, T. D. Li, T. P. Loh and P. M. MacDonald, *Langmuir*, **13**, 2917 (1997).
- <sup>6</sup> T. D. Li, L. M. Gan, C. H. Chew, W. K. Teo and L. H. Gan, *Journal of Membrane Science*, **133**, 177 (1997).
- <sup>7</sup> C. H. Chew, T. D. Li, L. H. Gan, C. H. Queck and L. M. Gan, *Langmuir*, **14**, 6068 (1998).
- <sup>8</sup> W. R. Palaini Raj, M. Sasthav and H. M. Chung, *Langmuir*, **7**, 2586 (1991).
- <sup>9</sup> F. M. Menger, T. Tsuio and G. S. Hammond, *J. Am. Chem. Soc.*, **112**, 1263 (1990).
- <sup>10</sup> M. Summers and J. Eastoe, *Adv. Coll. Int. Sci.*, **100**, 137 (2003).
- <sup>11</sup> W. Jahn and R. Strey, *J. Phys. Chem.*, **92**, 2294 (1988).
- <sup>12</sup> R. Strey, W. Jahn, G. Porte and P. Bassereau, *Langmuir*, **6**, 1635 (1990).
- <sup>13</sup> R. Aveyard, B. P. Binks and P. D. I. Fletcher, in E. Wyn-Jones and D. Bloor (Eds.), 'Structure, Dynamics and Equilibrium Properties of Colloidal systems', Kluwer, Amsterdam, pp. 557 (1990).
- <sup>14</sup> B. P. Binks, *Chemistry and Industry*, 19<sup>th</sup> July 1993, pp. 537.

- <sup>15</sup> L. M. Gan, W. Xu, K. S. Siow, Z. Gao, S. Y. Lee and P. Chow, *Langmuir*, **15**, 4812 (1999).
- <sup>16</sup> R. Aveyard, B. P. Binks, S. Clark, P. D. I. Fletcher, H. Giddings, P. A. Kingston and A. Pitt, *Colloids and Surfaces*, **59**, 97 (1991).
- <sup>17</sup> F. Candau, in C. M. Paleos (Ed.) 'Polymerisation in Organised Media', Gordon & Breach, Philadelphia, pp. 215 (1992).
- <sup>18</sup> P. D. I. Fletcher, *J. Chem. Soc. Faraday Trans. I*, **83**, 1493 (1987).
- <sup>19</sup> P. A. Winsor, 'Solvent Properties of Amphiphilic Compounds', Butterworths, London (1954).
- <sup>20</sup> A. M. Bellocq, *Langmuir*, **14**, 3730 (1998).
- <sup>21</sup> I. Javierre, A. M. Bellocq and F. Nallet, *Langmuir*, **17**, 5417 (2001).
- <sup>22</sup> E. Staples, I. Tucker, J. Penfold, N. Warren and R. K. Thomas, *Langmuir*, **18**, 5139 (2002).
- <sup>23</sup> E. Staples, I. Tucker, J. Penfold, N. Warren, R. K. Thomas and D. J. F. Taylor, *Langmuir*, **18**, 5147 (2002).
- <sup>24</sup> B. Jakobs, T. Sottmann, R. Strey, J. Allgaier, L. Willner and D. Richter, *Langmuir*, **15**, 6707 (1999).
- <sup>25</sup> T. Sottmann, *Curr. Op. Coll. Int. Sci.*, **7**, 57 (2002).
- <sup>26</sup> R. Aveyard, B. P. Binks, P. D. I. Fletcher, C. E. Rutherford, P. J. Dowding and B. Vincent, *Phys. Chem. Chem. Phys.*, **1**, 1971 (1999).
- <sup>27</sup> J. H. Clint, 'Surfactant Aggregation', Blackie, London (1992).

# *CHAPTER 5*

# CHAPTER 5

## CHARACTERISATION OF POLYMER FILMS PREPARED BY POLYMERISATION OF EQUILIBRIUM MICROEMULSION PHASES

### 5.1 Introduction

The equilibrium microemulsion phases characterised in Chapter 4 were polymerised and the polymer films analysed by visual appearance and electron microscopy and for pore volume fraction. This allows the effects of various features of the parent microemulsion (e.g. surfactant and oil type, Winsor phase equilibration, continuous phase type and equilibrium phase composition) on the characteristics of the polymer film to be determined. The effects of continuous phase, surfactant type and equilibrium water content of the parent microemulsion were of particular interest. The continuous phase of the microemulsion (in relation to aggregate type), has been shown to have a large effect on the structure<sup>1-5</sup> and opacity<sup>2,4</sup> of the resulting polymer and several microemulsion phase types have been successfully polymerised<sup>2,4,6,7</sup> yielding opaque,<sup>2,4,6,8-10</sup> cloudy<sup>4,8,9</sup> and optically transparent<sup>2,4,7,8,10-14</sup> polymer films. The structure of the surfactant has also been shown to affect the polymer structure and porosity,<sup>10</sup> especially in relation to the position of the polymerizable species on the surfactant molecule.<sup>15-19</sup> There are two types of polymerizable surfactant used in this study: The first has the polymerizable group located on the end of the surfactant tail



(C<sub>3/11-M</sub>). This type of polymerizable surfactant is sometimes referred to as T-type.<sup>18</sup> The second type has the polymerizable group located on the surfactant head group (C<sub>10</sub> and C<sub>12</sub>). This type of polymerizable surfactant is sometimes referred to as H-type.<sup>18</sup> The equilibrium water content of the parent microemulsion also has an effect on the structure, appearance and porosity of the polymer as has been shown in several studies.<sup>7,8,9,11-14</sup> One of the main aims of this work is to correlate the equilibrium water content of the parent microemulsion with the pore volume fraction of the polymer. This will provide a method of preparing polymer films with desirable optical and structural properties by selection of surfactant type at particular initial concentration and oil type of the parent polymerizable microemulsion. A method of preparing polymer films of reproducible physical dimensions and microstructure by the process of polymerisation by photoinitiation of microemulsion phases has been developed which enables the structural characteristics of the polymer films to be determined accurately.

## **5.2 Polymerisation by photoinitiation**

From many available methods of microemulsion polymerisation, photoinitiation was selected as the method to be used in this work as it is rapid, comparatively non-destructive of microemulsion equilibria<sup>20</sup> (cf. thermal) and is well suited to acrylate and methacrylate polymerisation.

### 5.2.1 Polymerisation of HDDA oil

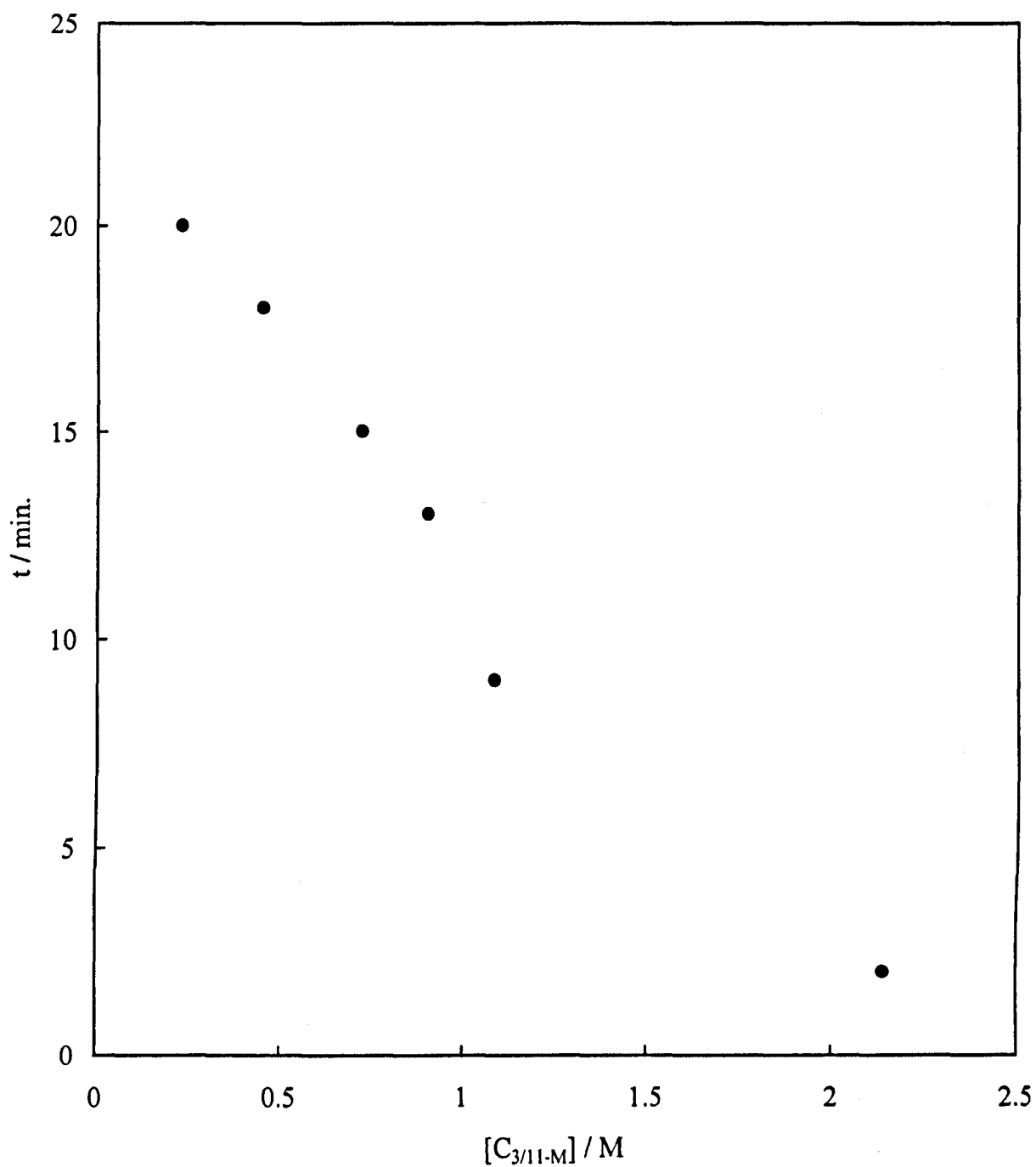
Before polymerisation of microemulsion phases was studied, polymerisation by photoinitiation was used with pure HDDA oil along with a suitable UV initiator. Darocur 1173 was used as the initiator and UV exposure times were varied from 2.0 to 0.1 minutes on drops of oil containing 1 – 4 wt. % initiator in the set-up shown in Chapter 2, section 2.9.1, Figure 2.3. For each sample, the minimum time of exposure to UV needed was 0.1 min. This was the shortest exposure time possible using the SCL1-2 automatic shutter. It was concluded that 1 wt. % of initiator was sufficient to enable polymerisation of the oil. The resulting polymer films were all transparent and fairly pliable. Some liquid residue was found in each case and it was thought this may be due to premature termination of the polymerisation by oxygen from the atmosphere as oxygen has been shown to cause termination reactions during the polymerisation of acrylate monomers.<sup>21-24</sup> In order to test this, a rubber ring 2 mm deep positioned on a glass slide was filled with 2 wt. % Darocur-in-HDDA, thus greatly reducing the surface area to volume ratio and reducing the effect of atmospheric oxygen compared to the previous experiment. This was irradiated with UV as above for 0.2 min. It was found that a hard disc of polymer was produced with very little residue confirming that oxygen does inhibit the polymerisation reaction.

### 5.2.2 Polymerisation of C<sub>3/11-M</sub> aqueous solutions

Following the polymerisation of HDDA diacrylate oil using Darocur 1173 initiator, the monomethacrylate surfactant C<sub>3/11-M</sub> was polymerised using the same initiator. This would enable the polymerisation characteristics of an acrylate oil and a

methacrylate surfactant to be compared prior to polymerisation of microemulsion phases containing both oil and surfactant. A 2 wt. % solution of Darocur in C<sub>3/11-M</sub> was prepared and a small droplet placed on top of a single glass slide. Prior to this an attempt to polymerise the surfactant between two glass slides was made to try to minimise the terminating effects of oxygen on the polymerisation process. It was found however that the glass slides could not be prised apart following polymerisation so the resulting polymer could not be examined. Pure C<sub>3/11-M</sub> with 2 wt. % initiator was polymerised followed by a series of solutions of surfactant in Milli-Q water also containing 2 wt. % Darocur. The [surfactant] present in these solutions was: 0.23, 0.45, 0.72, 0.90 and 1.08 M. Pure C<sub>3/11-M</sub> has a concentration equivalent to 2.4 M. Figure 5.1 shows the change in total time taken for polymerisation versus [surfactant]. As [surfactant] present in the initial solution droplet increases, the total curing time required for polymerisation decreases. This is explained by the emulsion polymerisation process model developed by Smith and Ewart,<sup>25</sup> which assumes polymerisation in a micelle is propagated by a radical diffusing into the micelle and only one active radical is present in the micelle at any one time. The radical propagates a polymerisation reaction with rate  $v_p$ , resulting in the growth of a polymer chain until another radical enters the micelle and comes into contact with the growing chain end and terminates it. This cycle of propagation followed by termination is repeated resulting in a 'start-stop' polymerisation reaction within any one micelle, which can contain either one or no radical at any one time. Due to the random nature of radical entry into a micelle, there is a 50 % chance that a micelle will be 'active' and contain a growing polymer chain at any one time. Therefore, if there are N micelles in a system then N/2 will be active during the course of the complete polymerisation reaction so the rate  $v_p$  will be proportional to the concentration of

**Figure 5.1. Time taken for complete polymerisation ( $t$  / min) vs. concentration of surfactant ( $[C_{3/11-M}] / M$ ) in aqueous solution using the UV Spot Cure instrument at 20 °C. Concentration of Darocur 1173 initiator = 2 wt. %**



monomer in the micelle [M] (approximately constant for an aqueous solution of polymerizable surfactant above cmc in the absence of polymerizable oil) and the number of active micelles  $N/2$  according to:

$$v_p = k_p [M] [N/2] \quad (5.1)$$

where  $k_p$  is the rate constant of  $v_p$  and is also equal to the rate of polymerisation within a single micelle. Therefore, an increase in [surfactant] causes an increase in the polymerisation rate. As [surfactant] in the surfactant solution increases it was observed that polymerisation appears to start less from the edges of the droplet (0.23 and 0.45 M surfactant) and more from the bulk of the droplet (0.90 and 1.08 M surfactant). Polymerisation within the bulk of the droplet is observed where the droplet becomes more viscous during curing until a very thick gel-like substance is formed just prior to complete polymerisation to rubbery semi-solid. The toughness of the resulting polymer (tested by scraping a needle through the polymer) is seen to increase with [surfactant] in the solution droplet prior to polymerisation. It is possible that the reason polymerisation starts at the edges and works inwards in the lower surfactant concentration samples is due to the effects of evaporation of water. Evaporation of water is higher at the edges of a droplet due to the higher surface area:volume ratio of water exposed. This will make the [surfactant] at the edges higher relative to the bulk and thus will increase the rate of polymerisation in this area. Once polymerisation has started at a particular point in a solution, further polymerisation may occur more preferably from this polymerised area as oligomer radicals interact with more monomers. This may also explain the increase in viscosity seen in higher surfactant concentration samples. As polymer 'droplets' form and grow

in size and number with some cross-linking, a gel-like structure is formed, which retards movement through the solution. As the surfactant concentration in each solution is far above the cmc, micelles will be present in the droplets prior to polymerisation. These will polymerise with limited cross-linking of micelles which may also explain the increase in viscosity with curing time due to cross-linking between micelles and monomer surfactant present in the solution.

There is only one methacrylate group present on the  $C_{3/11-M}$  molecule compared to two acrylate groups present on the HDDA molecule. This means there will be a less rigid structure of the resulting surfactant polymer compared to the HDDA and microemulsion polymers as less bonding between molecules can occur. This will result in a polymer with little or no cross-linking in the pure  $C_{3/11-M}$  polymer compared to a polymer with extensive cross-linking in the HDDA and microemulsion polymers. The position of the polymerizable group on the  $C_{3/11-M}$  molecule (on the tail) will also lead to increased viscosity as the micelles polymerise to form a concentrated solution of polymer droplets, which although increasing the viscosity of the solution, does not polymerise to a solid polymer. This accounts for the semi-solid properties of the surfactant polymer compared with the rigid polymers produced in the cases of pure HDDA and microemulsion polymers reported in the literature.

### **5.2.3 Polymerisation cell**

Following the polymerisation of HDDA oil and  $C_{3/11-M}$  surfactant solutions it was decided to construct a polymerisation cell which would not only reduce the effects of atmospheric oxygen on the polymerisation process but would also produce

polymer films of reproducible thickness, determined by the thickness of a suitable spacer material. If the dimensions of a polymer film can be controlled accurately then useful information based on the volume of the film can be determined, e.g. pore volume fraction. A glass slide was used for the base of the cell with a second glass slide or cover slip on top of this, separated by the spacer material, into which a hole would be cut for the polymerisable material. This would provide a cheap, disposable, reproducible method of preparing polymer films of precise dimensions.

### ***5.2.3.1 Absorbance of UV by glass***

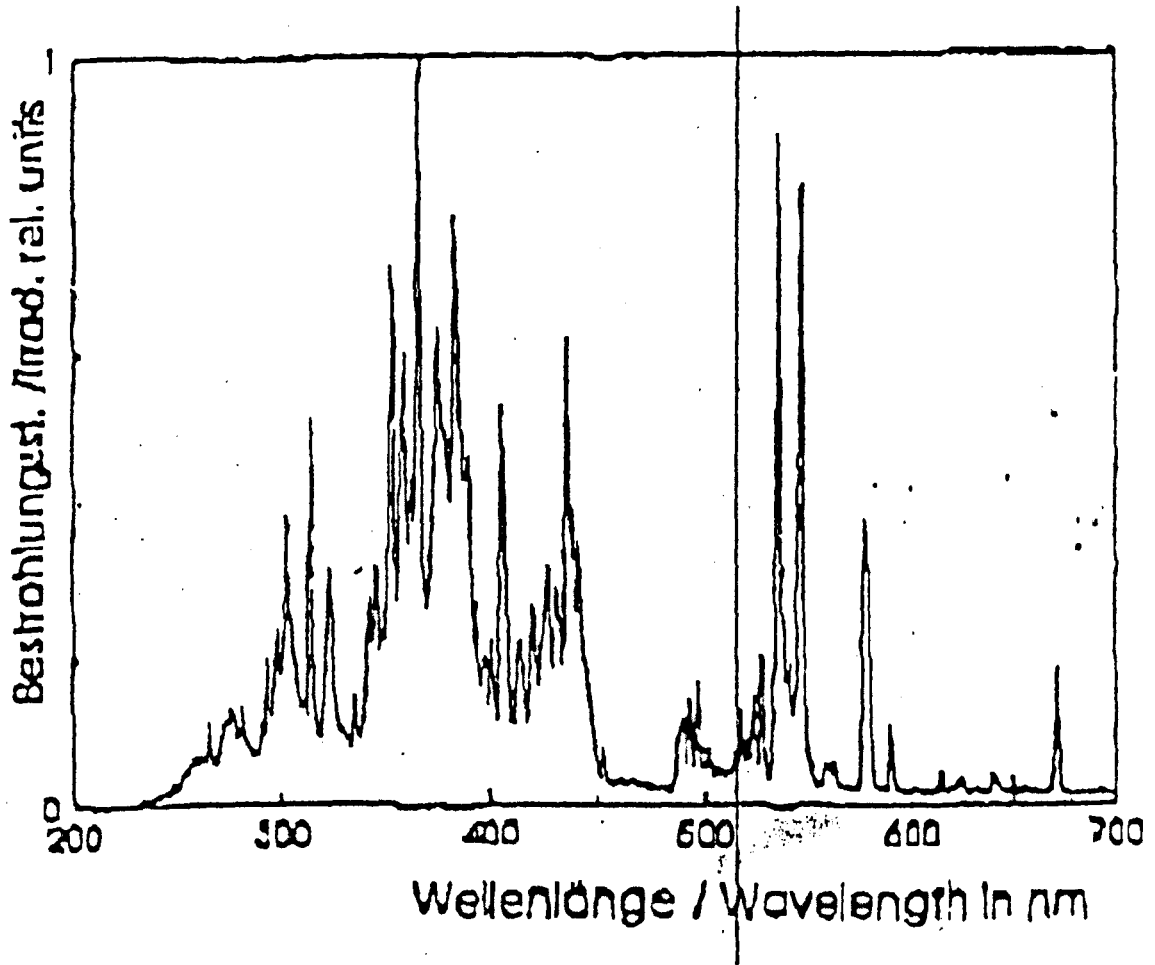
The UV absorption spectrum of two brands of glass slide and a cover slip was measured so that a glass for the top cover could be selected which would absorb as little of the UV radiation emitted by the spot cure instrument as possible. The UV transmission spectrum of the instrument was obtained from the manufacturer and is shown in Figure 5.2. The UV absorption spectra of the glass slides and cover slip are shown in Figure 5.3. It can be seen from the spectra that glass slide 1 (Menzel-Glaser extra- white glass slide) is the more suitable slide as this absorbs the least UV radiation. The cover slip performs least well of all so glass slide 1 was used in the cell.

### ***5.2.3.2 Polymerisation cell design***

Aluminium foil was used as the spacer material as it is cheap and disposable and of constant thickness (12  $\mu\text{m}$ ). A 10 mm x 10 mm hole was cut into a piece of foil. This was sandwiched between two glass slides held together as shown in Figure 5.4. This was positioned 25 mm under the UV wand giving complete coverage of the

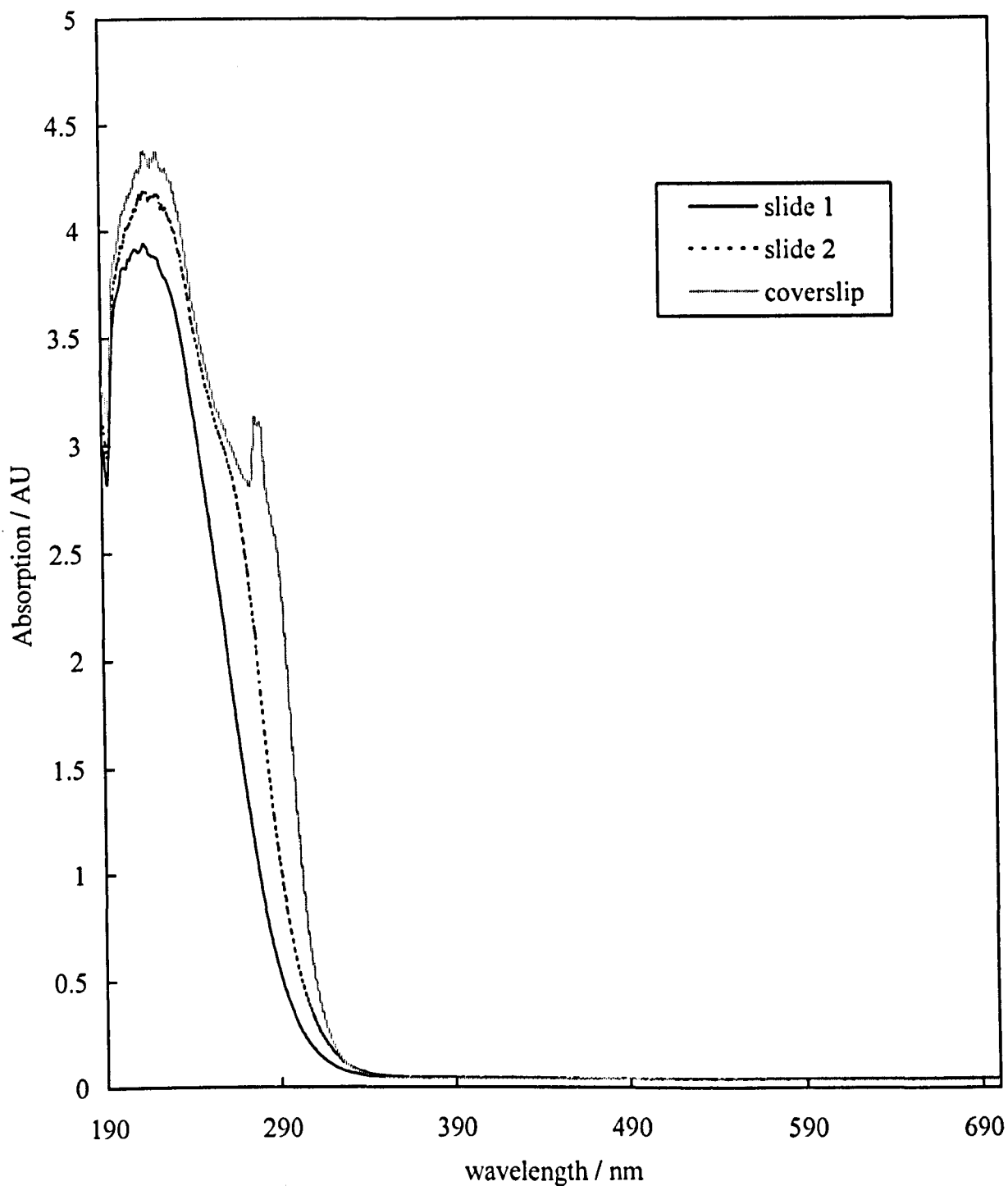
Figure 5.2. UV emission spectrum of UVP Spot Cure SCL1-2 lamp.

Spectrum obtained from manufacturer

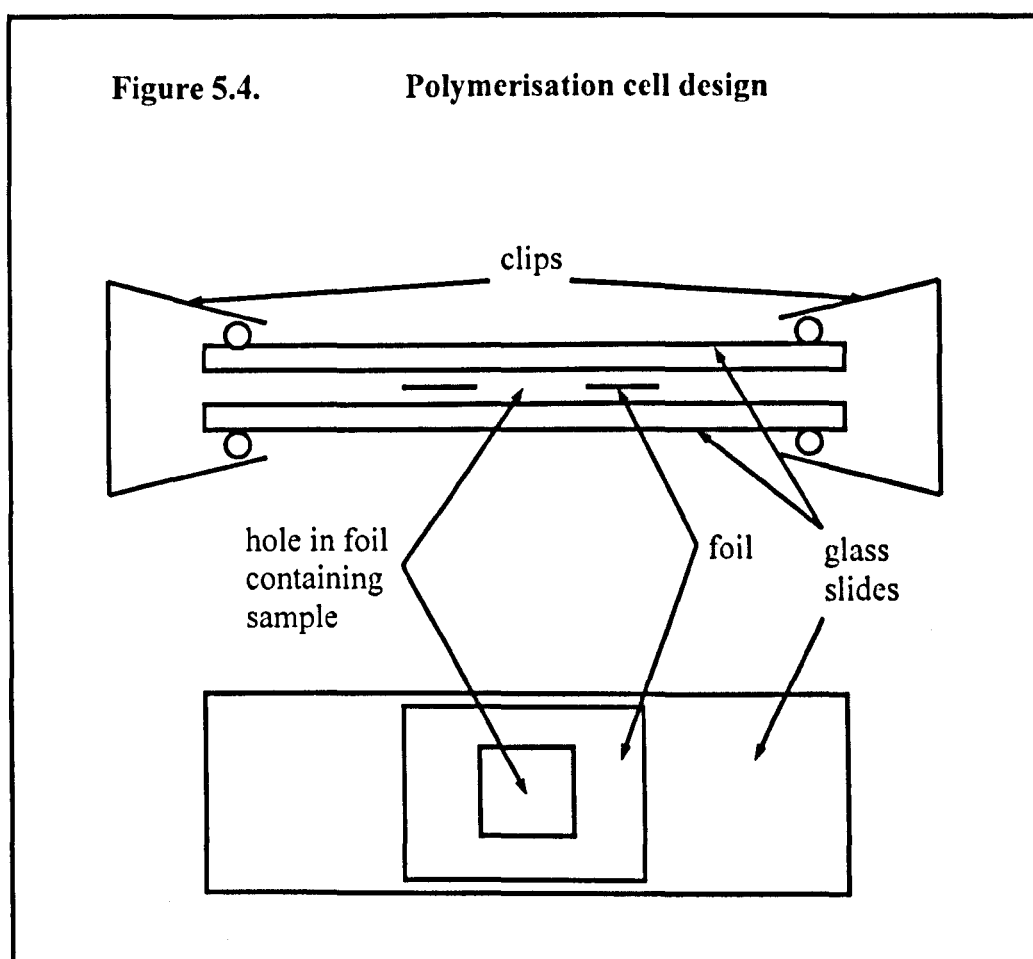




**Figure 5.3. Absorption spectra of glass slides and coverslip for use in polymerisation cell from 190 to 700 nm. Baseline measured against air**



sample by the UV beam. Samples of HDDA containing 1 wt. % initiator were irradiated for 0.1 min. using this system and found to give reproducible films  $13 \pm 1$   $\mu\text{m}$  thick using foil  $12 \pm 1$   $\mu\text{m}$  thick. This was repeated using multiple layers of foil and found to give reproducible clear polymer films rising in  $\sim 12$   $\mu\text{m}$  intervals up to five layers of foil giving a film thickness of  $61 \pm 1$   $\mu\text{m}$ . If thicker films are required, 50  $\mu\text{m}$  foil can be used as above.



### ***5.2.3.3 Absorbance of incident UV by polymerisation cell containing HDDA oil with initiator***

In order to determine the variation in incident UV on the upper and lower surfaces of the microemulsion film and the UV absorption of the cell, a polymerisation cell with a 50  $\mu\text{m}$  spacer was filled with HDDA oil containing 1 wt. % Darocur 1173. The UV/Vis absorption spectrum was measured from 190 to 700 nm. The instrument was zeroed with air in the sample and reference beams. This was repeated with an empty polymerisation cell and this spectrum subtracted from the filled cell spectrum. The absorption spectra of the empty cell and the absorption of UV by HDDA with 1 wt. % Darocur are shown in Figure 5.5. Using the following equations, the amount of UV absorbed by the glass slides and the HDDA with Darocur sample can be calculated and expressed as % of incident UV:

$$T = I / I_0 \quad (5.2)$$

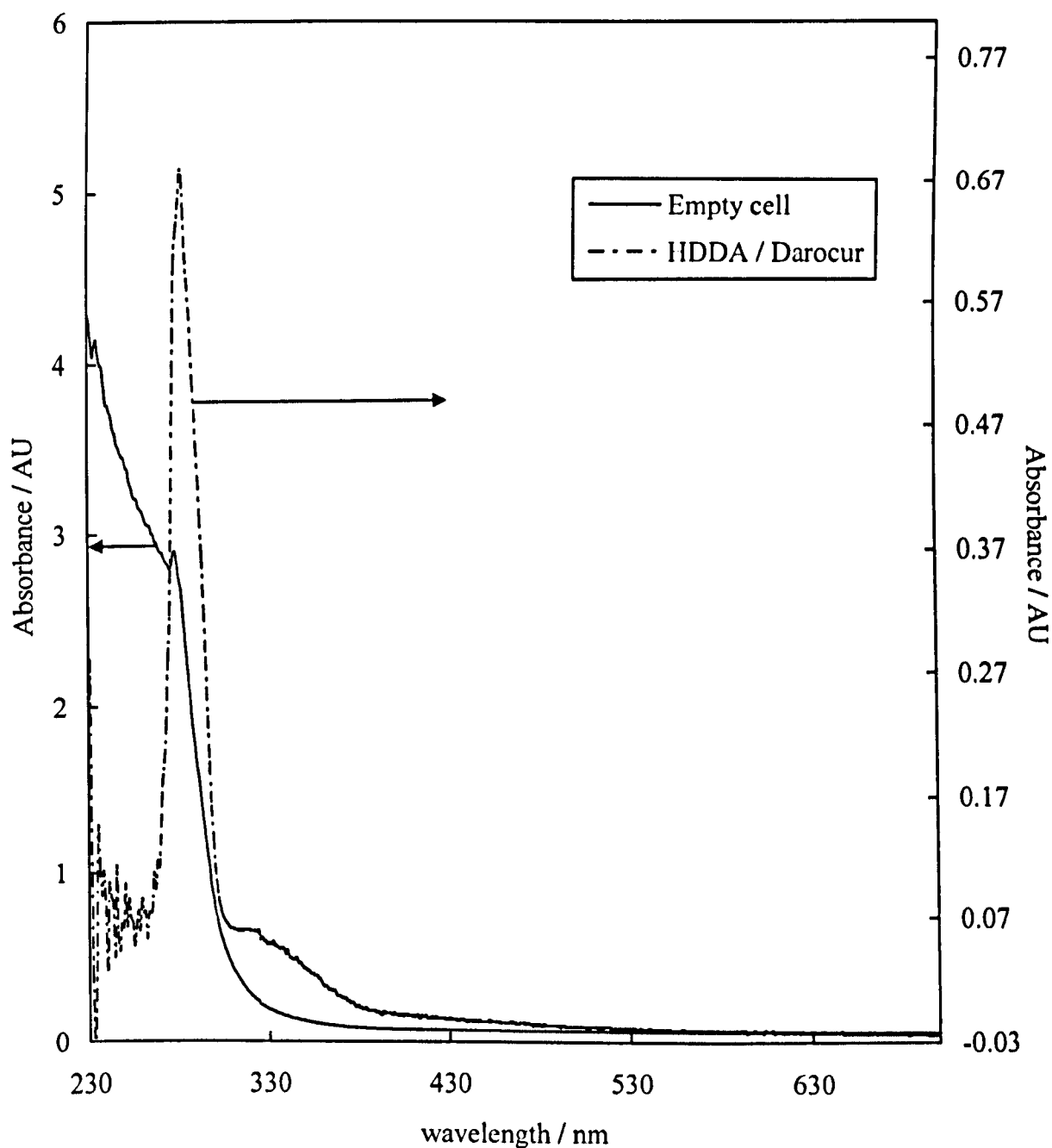
$$A = -\log_{10} (I / I_0) = -\log_{10} T \quad (5.3)$$

$$\therefore T = 10^{-A} \quad (5.4)$$

where T = transmission, I = intensity of bottom surface of sample,  $I_0$  = intensity of top surface of sample and A = absorbance (AU).

Figure 5.5 shows that at 280 nm which is where the main absorption peak of HDDA with Darocur occurs, the absorbance of the empty cell, i.e. of two glass slides,

**Figure 5.5.** Absorption spectra of empty polymerisation cell and of HDDA with 1 wt. % Darocur 1173 (subtracted from filled cell absorption spectrum) for a 50  $\mu\text{m}$  path-length. The spectra were measured with air in the reference beam



is 2 AU, therefore the absorbance of the top glass slide of the cell is 1 AU. This corresponds to 10 % of the incident light on the top surface of the glass slide reaching the top surface of the sample in the cell. The absorption peak by HDDA and Darocur is at 280 nm with an absorbance of 0.67 AU, corresponding to 21 % of the incident light on the top surface of the sample reaching the bottom surface of the sample (2.1 % of the total light incident on the cell) i.e. there is a factor of five difference between the intensities of the UV light incident on the top and bottom surfaces of the sample. This may not affect the polymerisation and resulting microstructure of the polymer films if the power of UV radiation incident on the bottom surface of the microemulsion film is such that maximum effect of incident photons is achieved.

### **5.3 Appearance and strength of polymer films**

One of the main aims is to prepare clear, colourless films which can be used as absorbing coatings for ink deposition. The appearance of the polymer film is therefore of importance. The appearance of the polymerised films after drying in relation to the equilibrium water content of the parent microemulsion is described.

The opacity of films from microemulsions containing  $C_{3/11-M}$  surfactant with HDDA or BDDA increases from fairly clear to opaque with increasing water content of the equilibrium microemulsion. The strength of the films decreases with increasing water content. Most films from microemulsions containing  $C_{3/11-M}$  surfactant with DPGDA were cloudy, though not completely opaque, and strong. These properties did not change with increasing water content of the equilibrium microemulsion. All films prepared from microemulsions containing  $C_{10}$  with surfactant HDDA were opaque.

The strength of the films decreased slightly with increasing water content of the equilibrium microemulsions. All films prepared from microemulsions containing C<sub>10</sub> surfactant with BDDA from both the upper and middle phases were hard but brittle when bent. Films from the upper phase increased in opacity with increasing water content. All films from the middle phase were opaque. Films prepared from microemulsions containing C<sub>10</sub> surfactant with DPGDA varied depending on the equilibrium phases from which the films were prepared. All films prepared from the upper phases were clear and strong. All films from the middle phases were opaque with the strength decreasing with increasing water content. Only phases with the higher initial surfactant concentrations produced polymer films from the lower phase. All the films from this phase were opaque and weak. Most films prepared from microemulsions containing C<sub>12</sub> surfactant with HDDA, BDDA or DPGDA were found to be opaque and strong. Films from microemulsions containing DPGDA were less opaque than those from microemulsions containing HDDA or BDDA.

The opacity is seen to be greater for films prepared from microemulsions with a higher water content and most water continuous microemulsions produce opaque or cloudy films. In the system containing surfactant C<sub>3/11-M</sub> with HDDA oil, water continuous microemulsion phases did produce clear films but these were at lower equilibrium water contents. The strength of the polymer films decreases with increasing water content of the equilibrium microemulsion and in general, microemulsions with very high water contents either do not polymerise or produce very weak films. Most films however are strong but brittle if bent excessively.

## 5.4 Microstructure of polymer films

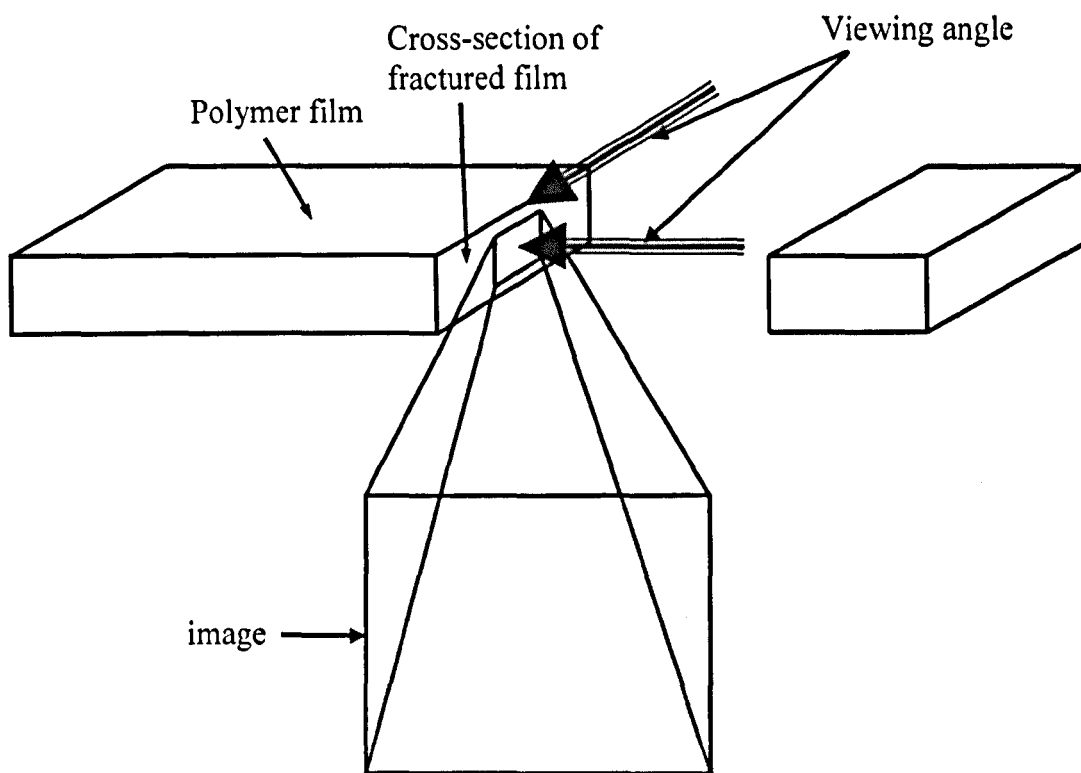
### 5.4.1 Appearance of films by electron microscopy

The microstructure of a polymerised microemulsion film is dependent on the composition of the liquid microemulsion before polymerisation and can vary according to the aggregate type of the parent microemulsion. Thus, determination of the microstructure of the polymer film can provide information about the effects of water content and surfactant and oil type of the parent microemulsion on the microstructure of the polymer film. The films were fractured in air and carbon coated prior to viewing. Figure 5.6 shows the viewing angle of the fractured surface of the films. Figures 5.7 to 5.78 show the SEM images of the polymer films with the surfactant and oil types of the parent microemulsion. The  $[\text{surfactant}]_{\text{ini}}$ , the equilibrium phase polymerised (i.e. upper, middle or lower phase), the equilibrium water content (wt. %) and the continuous phase (where oil = oil, aq = water and b = bicontinuous) of the parent equilibrium microemulsion phase are also indicated. They show three main microstructure types: i) Nano structures (e.g. Figures 5.11, 5.26 and 5.72) which other than fracture marks appear almost featureless, as the microstructure cannot be resolved by the SEM instrument used; ii) micrometer sized closed pores (e.g. Figures 5.41, 5.53 and 5.63). These occur only with  $C_{10}$  and  $C_{12}$  surfactants and are seen in polymers from both oil and water continuous microemulsions. Higher water contents of the equilibrium microemulsion generally results in a larger number of closed pores; iii) open porous/ spherical aggregates (e.g. Figures 5.8, 5.31, 5.51 and 5.61). These structures are found only with polymers from water continuous microemulsions, predominantly in HDDA systems. Generally,  $C_{3/11-M}$  surfactant,

containing the polymerizable group on the tail, forms nano featured films with some open spherical structure with HDDA and BDDA systems. C<sub>10</sub> and C<sub>12</sub> surfactants, with the polymerizable group located on the head group, form nano featured films with the presence of micrometer sized closed pores contained within the polymer film. These vary in size between 0.2 – 10 µm and increase in number and size with increasing water content of the parent equilibrium microemulsion. The oil type is also seen to have an effect as HDDA systems polymerise to form open porous spherical aggregate structures which could be an indication of significant swelling of micelles during the polymerisation process. This is possible as the reaction kinetics of polymerisation is very much slower than that of surfactant monomer exchange in a micelle, allowing a polymer core to grow within a micelle as surfactant monomers orient themselves around the growing oil polymer core.<sup>26,27</sup> The reaction rate of polymerisation of the acrylate groups present on HDDA is also much quicker than that of the methacrylate groups present on the surfactants, assisting in the micelle core growth model of micelle polymerisation. This model is more likely with the surfactant methacrylate groups present on the head group, making co-polymerisation with the oil more difficult than if they were present on the tail and therefore residing in the oil during polymerisation. Comparison of Figures 5.7 to 5.78 with Table 4.4 (Chapter 4) shows that WI\* systems tend to form the open porous, spherical aggregate structures whereas WI<sup>i</sup> and WII\* systems form nano structured polymers. The water content of the parent equilibrium microemulsion also affects the microstructure of the polymer film as phases with <35 wt. % water polymerise to form nano porous polymers, whereas those with >35 wt. % water form open porous spherical aggregate structured polymers.

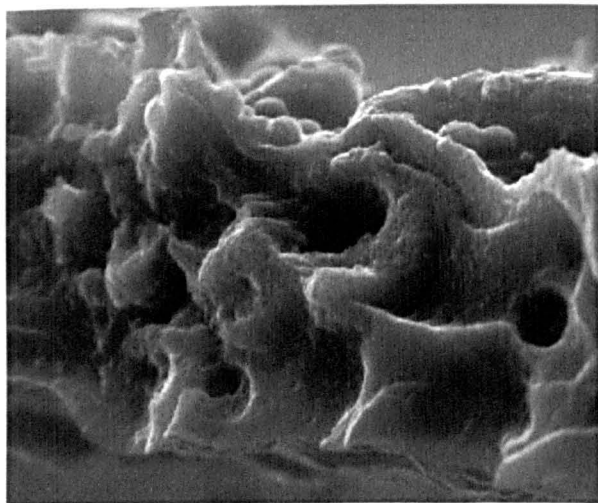


**Figure 5.6** Viewing angle of SEM images in relation to polymer film



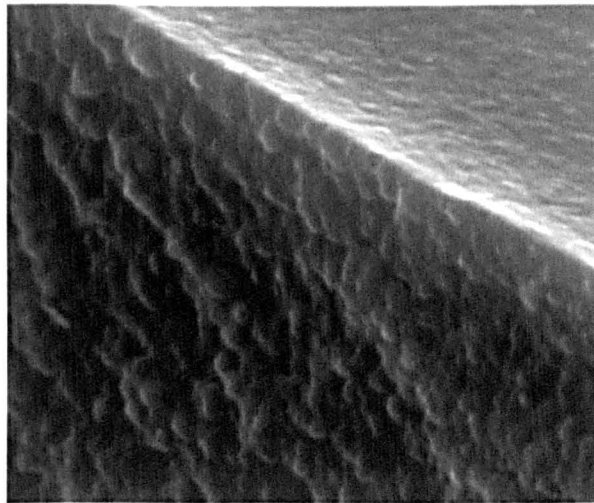
**Figure 5.7.** 0.24 M  $[C_{3/11-M}]_{ini}$  / HDDA,  
lower phase, 72 wt. %, aq

5  $\mu$ m



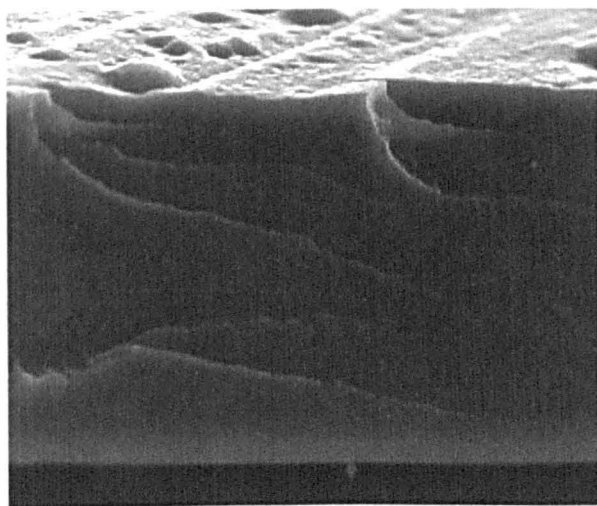
**Figure 5.8.** 0.48 M  $[C_{3/11-M}]_{ini}$  / HDDA,  
middle phase, 50 wt. %, aq

2  $\mu$ m



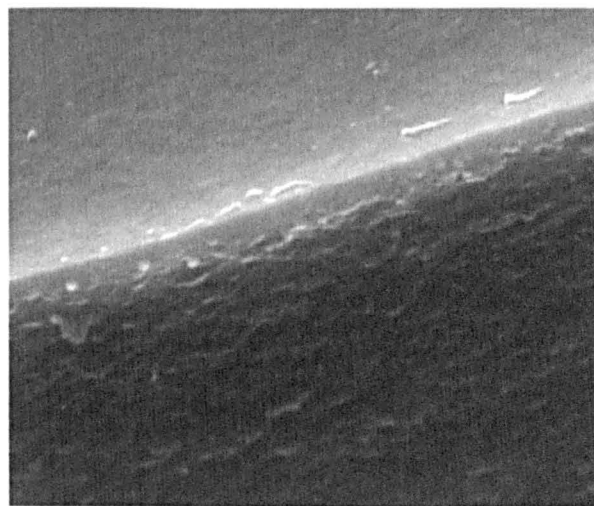
**Figure 5.9.** 0.48 M  $[C_{3/11-M}]_{ini}$  / HDDA,  
lower phase, 72 wt. %, aq

10  $\mu$ m



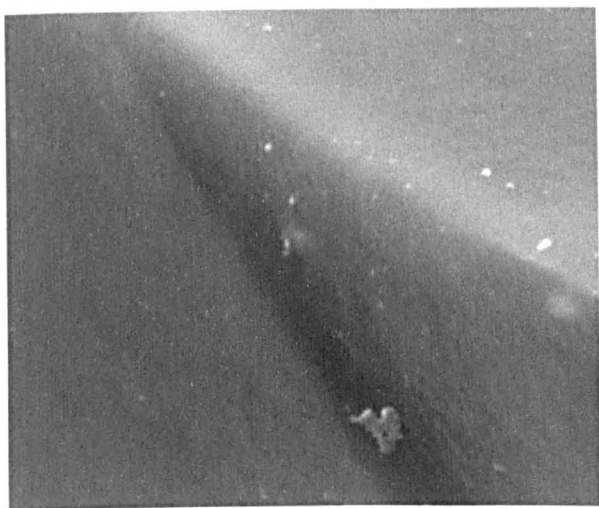
**Figure 5.10.** 0.77 M  $[C_{3/11-M}]_{ini}$  / HDDA,  
middle phase, 35 wt. %, aq

2  $\mu$ m



**Figure 5.11.** 0.77 M  $[C_{3/11-M}]_{ini}$  / HDDA, lower phase, 62 wt. %, aq

2  $\mu$ m



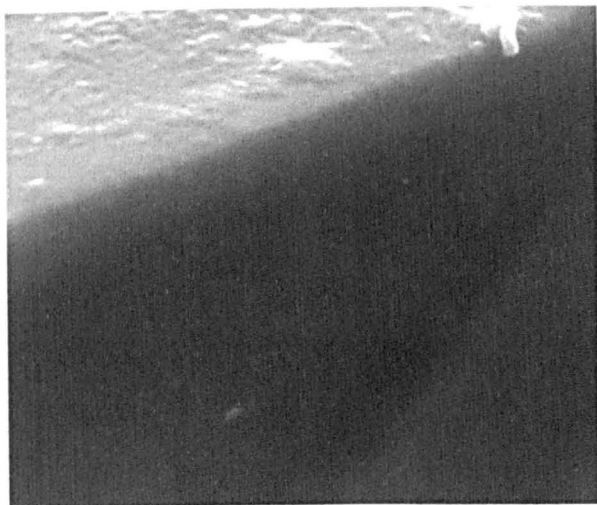
**Figure 5.12.** 0.96 M  $[C_{3/11-M}]_{ini}$  / HDDA, middle phase, 33 wt. %, aq

2  $\mu$ m



**Figure 5.13.** 0.96 M  $[C_{3/11-M}]_{ini}$  / HDDA, lower phase, 55 wt. %, aq

2  $\mu$ m



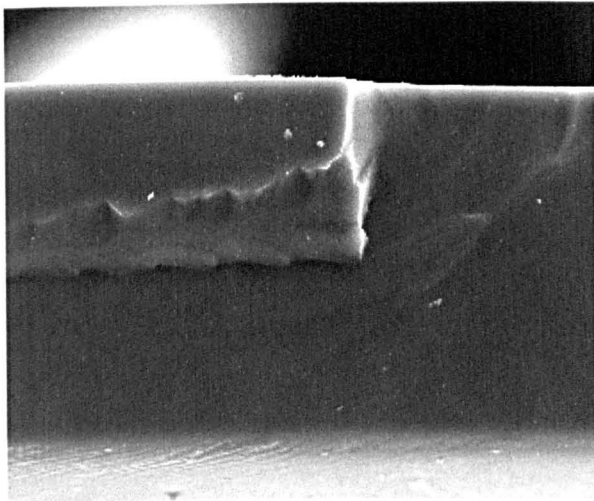
**Figure 5.14.** 1.15 M  $[C_{3/11-M}]_{ini}$  / HDDA, middle phase, 29 wt. %, aq

2  $\mu$ m



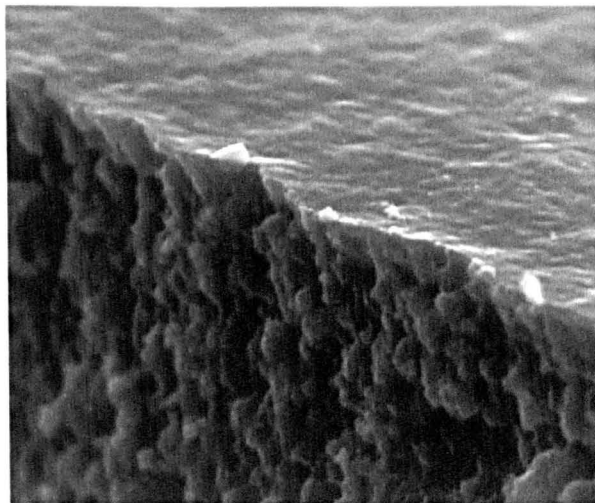
**Figure 5.15.** 1.15 M  $[C_{3/11-M}]_{ini}$  / HDDA,  
lower phase, 49 wt. %, aq

20  $\mu\text{m}$



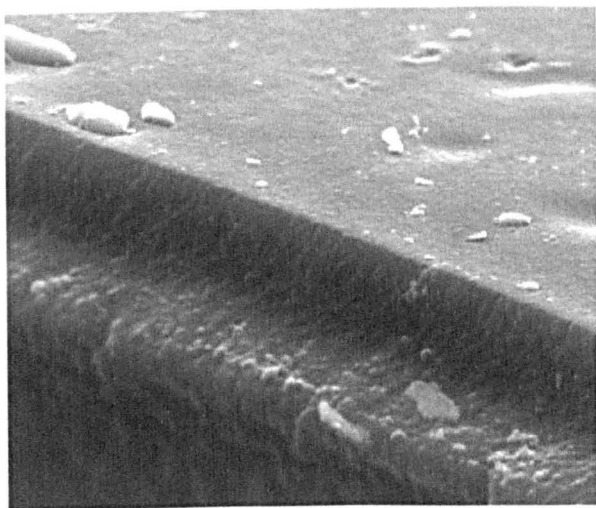
**Figure 5.16.** 0.48 M  $[C_{3/11-M}]_{ini}$  / BDDA,  
middle phase, 46 wt. %, aq/ b

5  $\mu\text{m}$



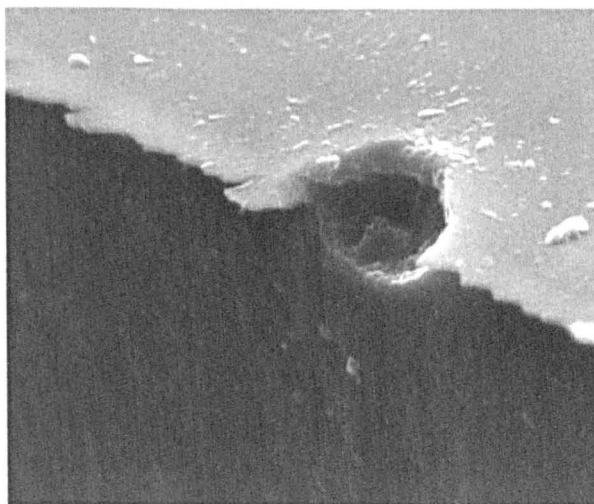
**Figure 5.17.** 0.48 M  $[C_{3/11-M}]_{ini}$  / BDDA,  
lower phase, 64 wt. %, aq

5  $\mu\text{m}$

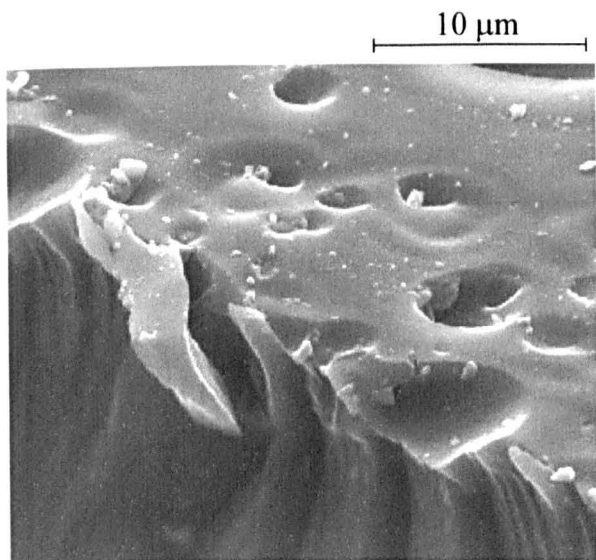


**Figure 5.18.** 0.77 M  $[C_{3/11-M}]_{ini}$  / BDDA,  
middle phase, 37 wt. %, aq/ b

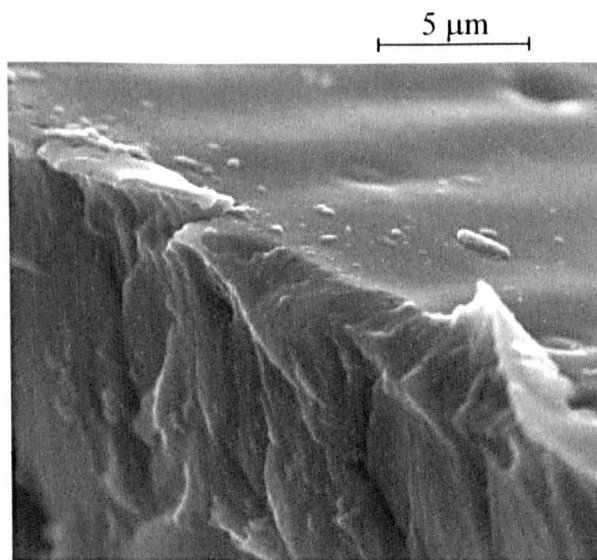
5  $\mu\text{m}$



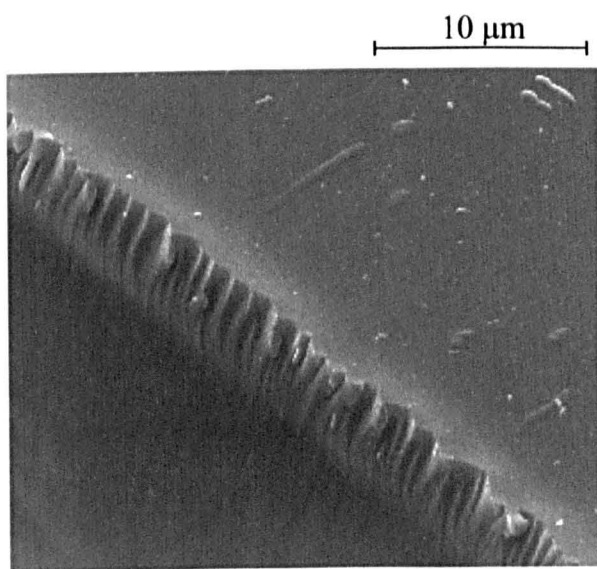
**Figure 5.19.** 0.96 M [C<sub>3/11-M</sub>]<sub>ini</sub> / BDDA, middle phase, 29 wt. %, aq/ b



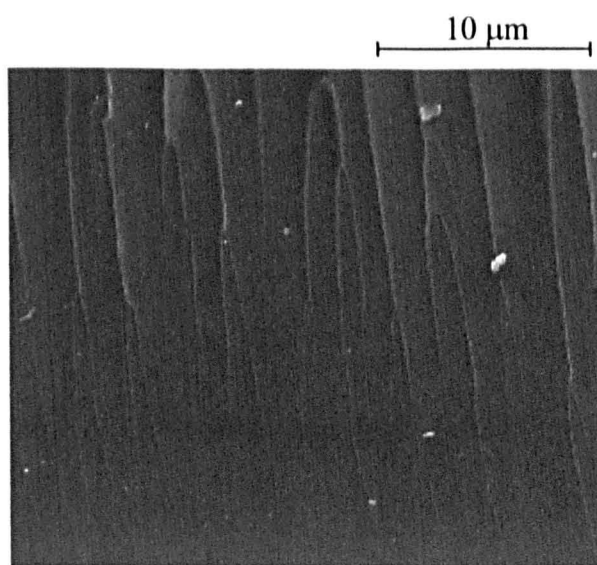
**Figure 5.20.** 0.96 M [C<sub>3/11-M</sub>]<sub>ini</sub> / BDDA, lower phase, 50 wt. %, aq



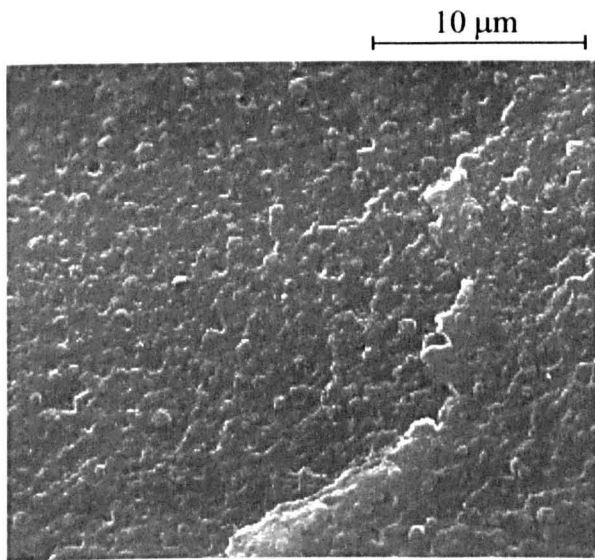
**Figure 5.21.** 0.24 M [C<sub>3/11-M</sub>]<sub>ini</sub> / DPGDA, upper phase, 3 wt. %, oil



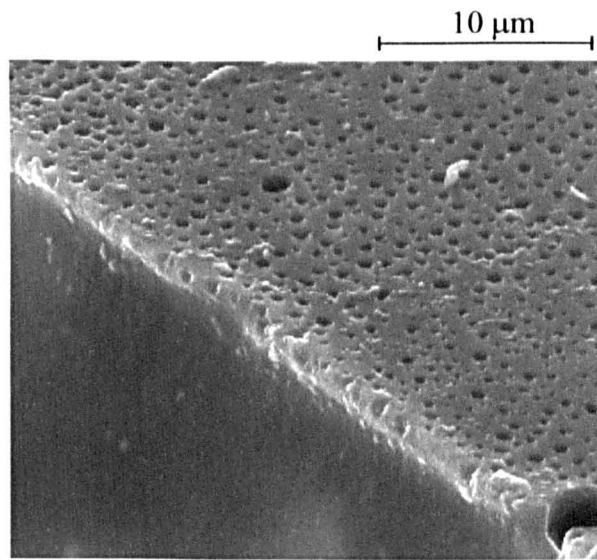
**Figure 5.22.** 0.48 M [C<sub>3/11-M</sub>]<sub>ini</sub> / DPGDA, upper phase, 4 wt. %, oil



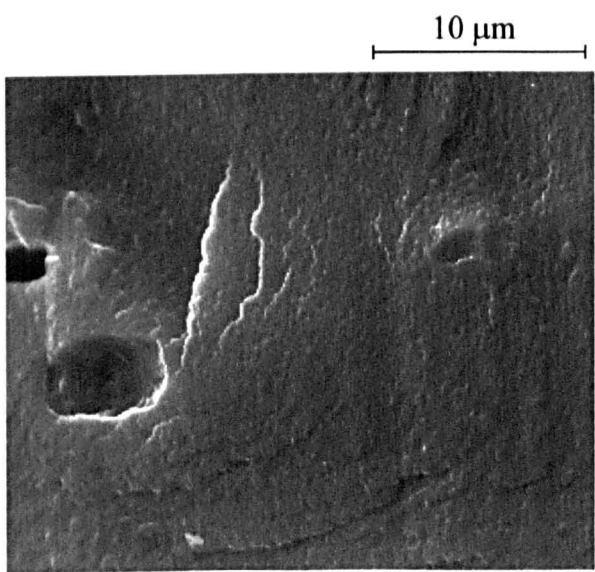
**Figure 5.23.** 0.48 M  $[C_{3/11-M}]_{ini}$  / DPGDA,  
middle phase, 58 wt. %, aq



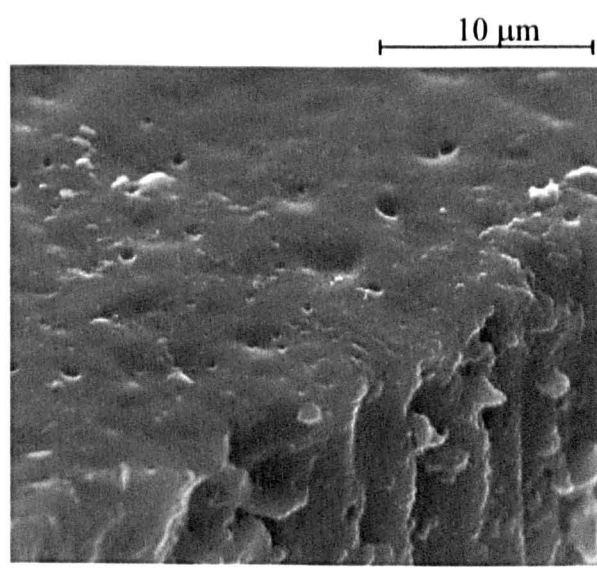
**Figure 5.24.** 0.77 M  $[C_{3/11-M}]_{ini}$  / DPGDA,  
upper phase, 6 wt. %, oil



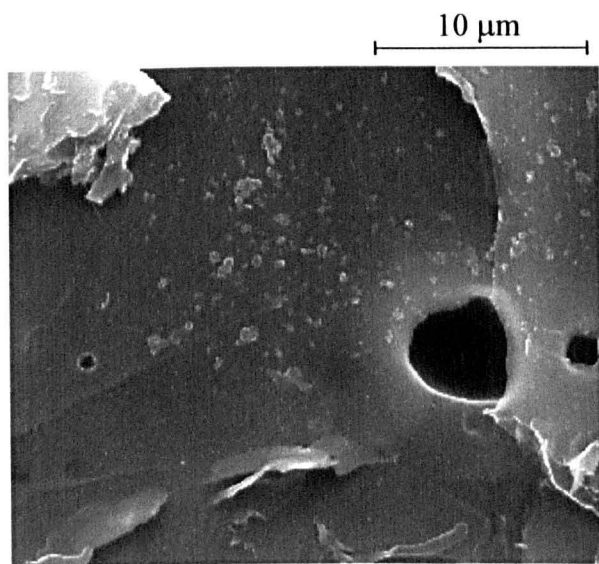
**Figure 5.25.** 0.77 M  $[C_{3/11-M}]_{ini}$  / DPGDA,  
middle phase, 40 wt. %, aq



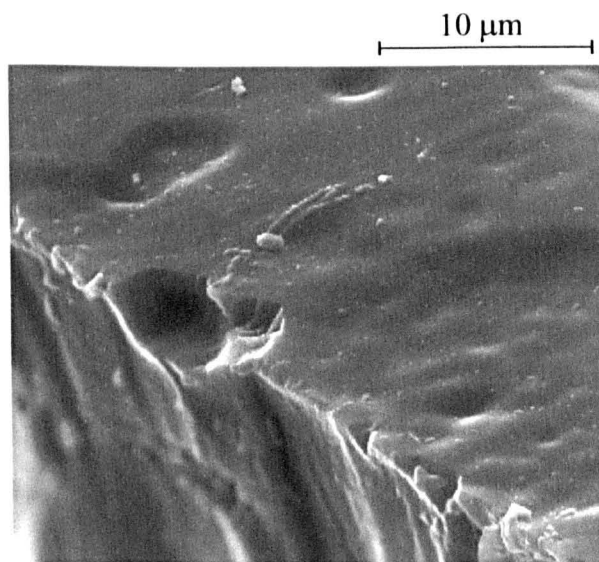
**Figure 5.26.** 0.77 M  $[C_{3/11-M}]_{ini}$  / DPGDA,  
lower phase, 57 wt. %, aq



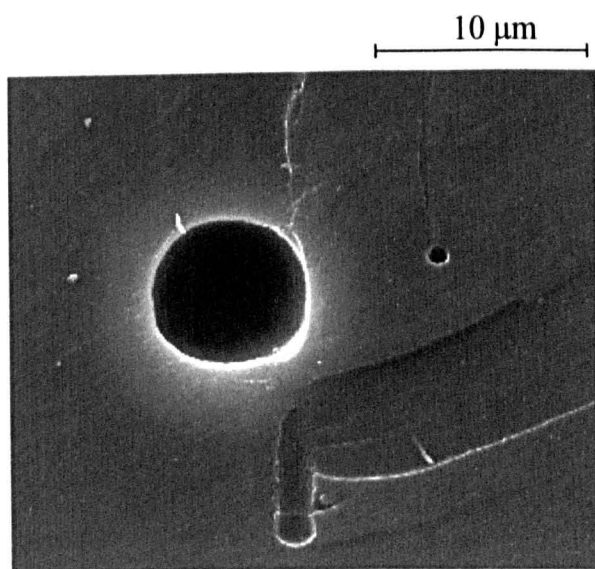
**Figure 5.27.** 0.96 M [C<sub>3/11-M</sub>]<sub>ini</sub> / DPGDA, upper phase, 11 wt. %, oil



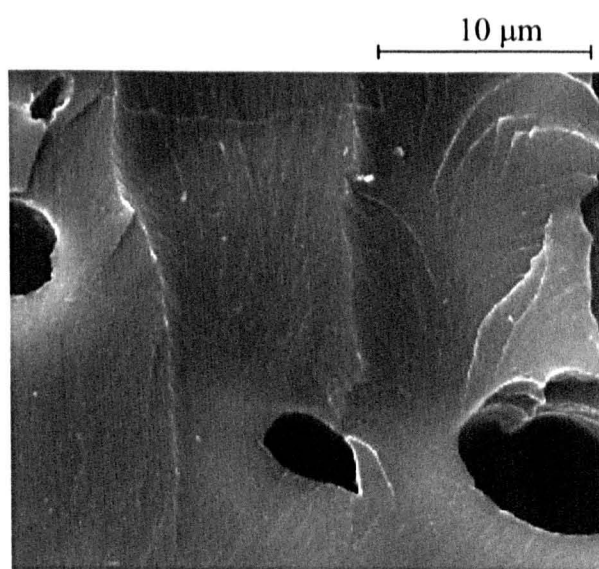
**Figure 5.28.** 0.96 M [C<sub>3/11-M</sub>]<sub>ini</sub> / DPGDA, middle phase, 43 wt. %, aq



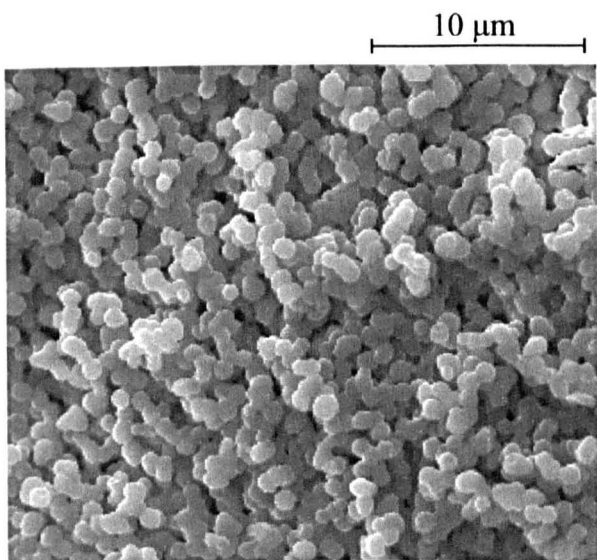
**Figure 5.29.** 1.15 M [C<sub>3/11-M</sub>]<sub>ini</sub> / DPGDA, upper phase, 13 wt. %, oil



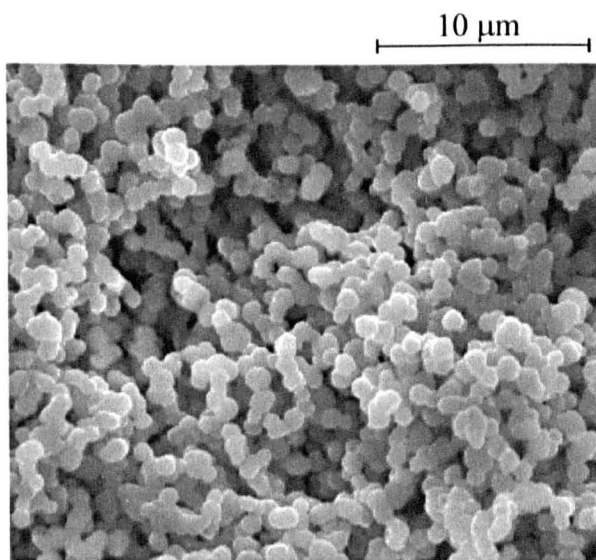
**Figure 5.30.** 1.15 M [C<sub>3/11-M</sub>]<sub>ini</sub> / DPGDA, lower phase, 41 wt. %, aq



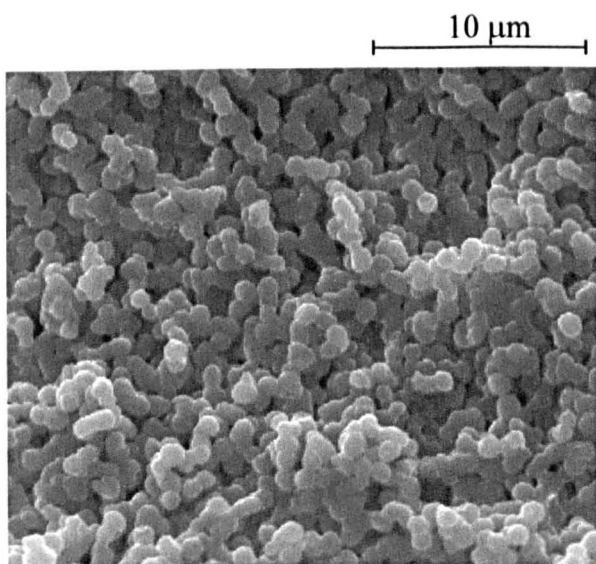
**Figure 5.31.** 15.0 wt. %  $[C_{10}]_{ini}$  / HDDA,  
middle phase, 54 wt. %, aq/ b



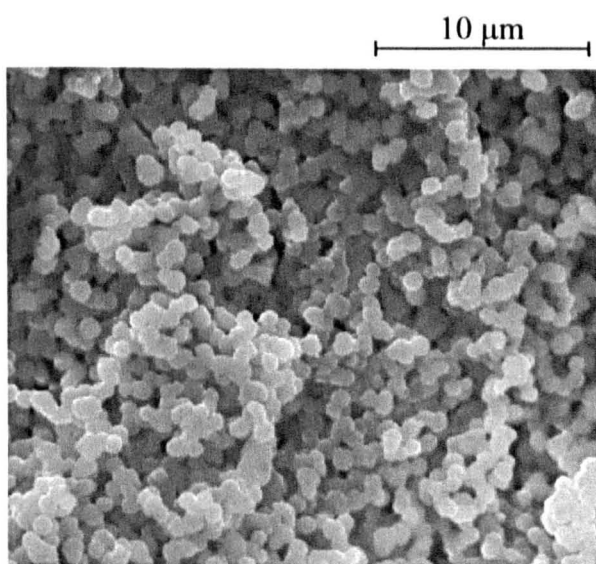
**Figure 5.32.** 15.0 wt. %  $[C_{10}]_{ini}$  / HDDA,  
lower phase, 63 wt. %, aq/ b



**Figure 5.33.** 18.0 wt. %  $[C_{10}]_{ini}$  / HDDA,  
middle phase, 49 wt. %, aq/ b

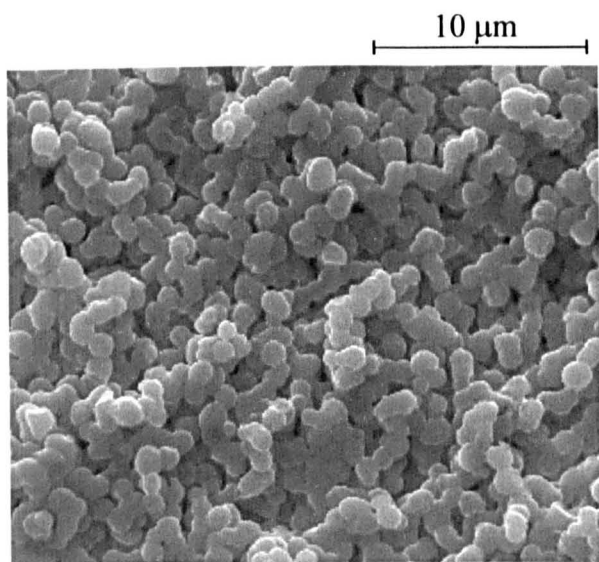


**Figure 5.34.** 18.0 wt. %  $[C_{10}]_{ini}$  / HDDA,  
lower phase, 58 wt. %, aq/ b

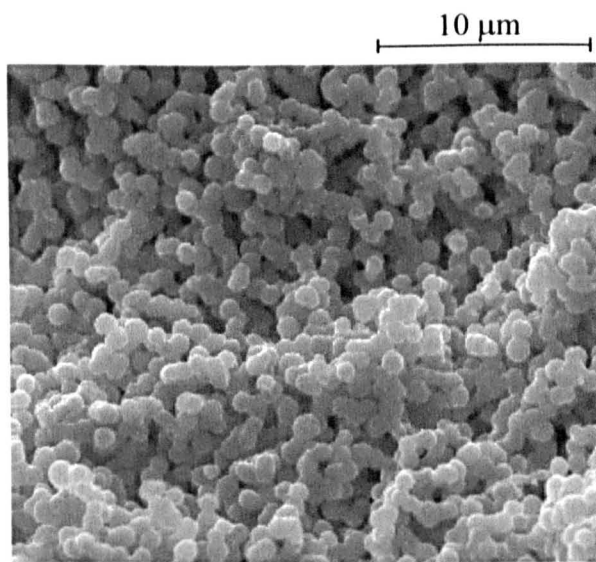




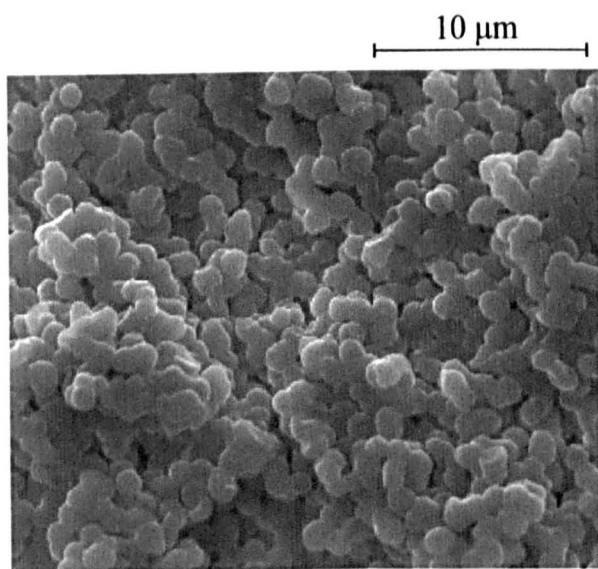
**Figure 5.35.** 22.0 wt. % [C<sub>10</sub>]<sub>ini</sub> / HDDA,  
middle phase, 44 wt. %, aq/ b



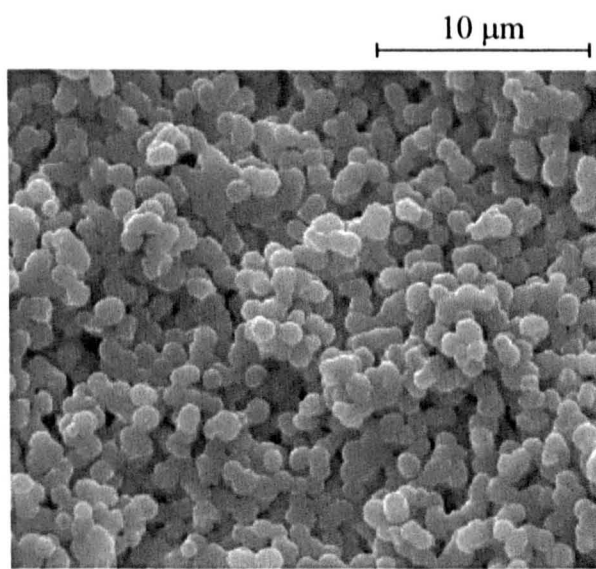
**Figure 5.36.** 22 wt. % [C<sub>10</sub>]<sub>ini</sub> / HDDA,  
lower phase, 55 wt. %, aq/ b



**Figure 5.37.** 25.0 wt. % [C<sub>10</sub>]<sub>ini</sub> / HDDA,  
middle phase, 40 wt. %, aq/ b

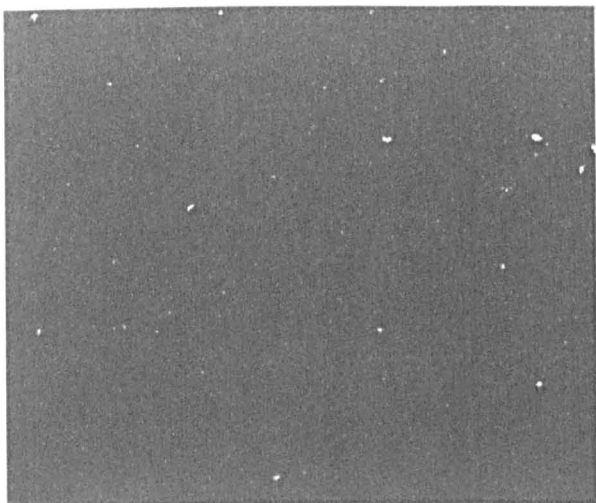


**Figure 5.38.** 25.0 wt. % [C<sub>10</sub>]<sub>ini</sub> / HDDA,  
lower phase, 54 wt. %, aq/ b



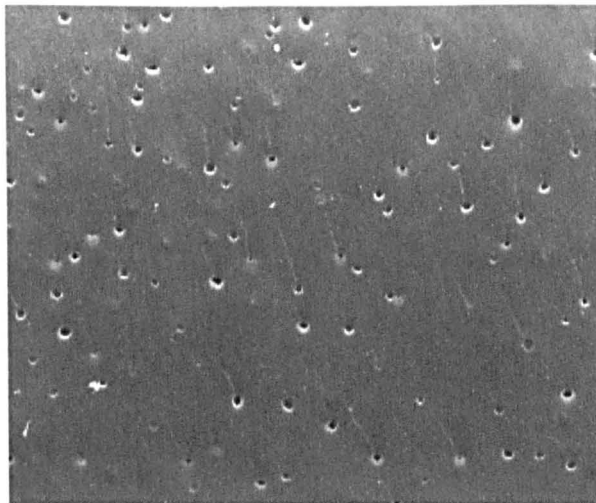
**Figure 5.39.** 5.0 wt. %  $[C_{10}]_{ini}$  / BDDA, upper phase, 3 wt. %, oil

10  $\mu$ m



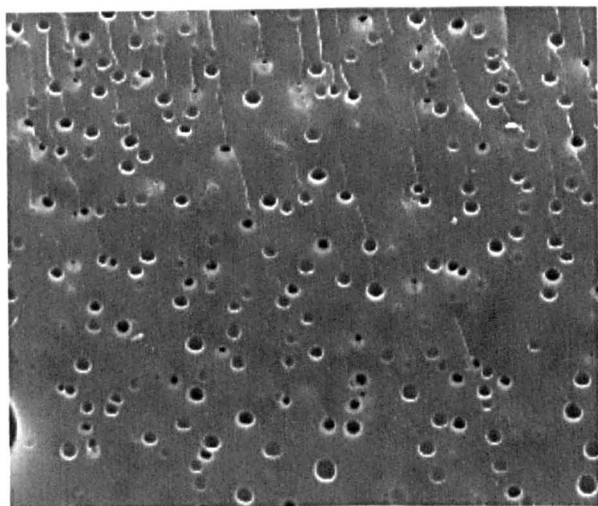
**Figure 5.40.** 15.0 wt. %  $[C_{10}]_{ini}$  / BDDA, upper phase 8 wt. %, oil

10  $\mu$ m



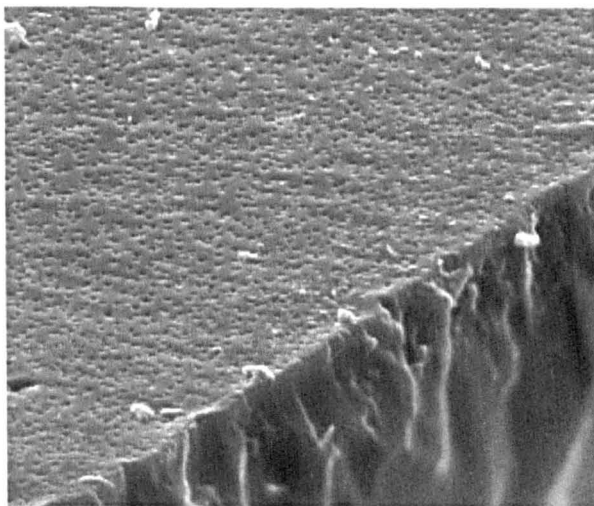
**Figure 5.41.** 15.0 wt. %  $[C_{10}]_{ini}$  / BDDA, middle phase, 15 wt. %, aq/ b

10  $\mu$ m

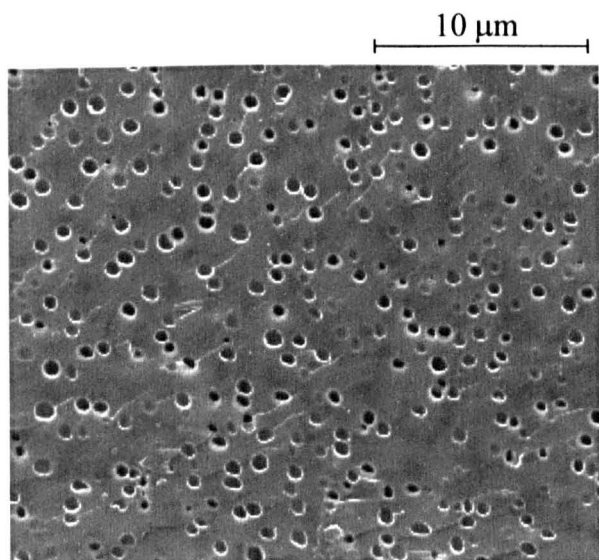


**Figure 5.42.** 18.0 wt. %  $[C_{10}]_{ini}$  / BDDA, upper phase, 8 wt. %, oil

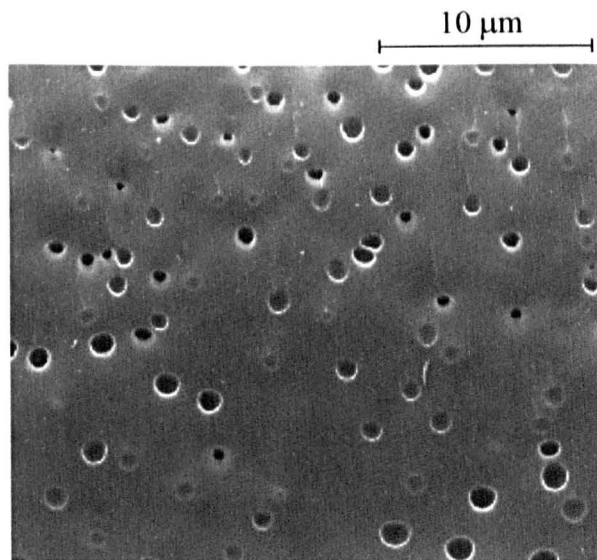
10  $\mu$ m



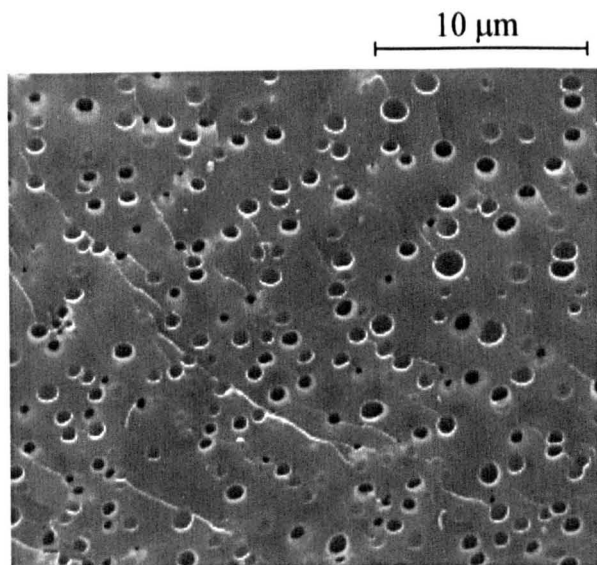
**Figure 5.43.** 18.0 wt. %  $[C_{10}]_{ini}$  / BDDA, middle phase, 20 wt. %, aq/ b



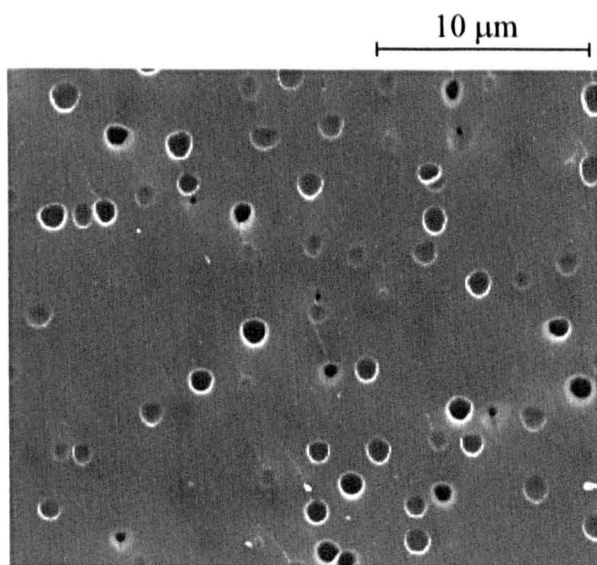
**Figure 5.44.** 22.0 wt. %  $[C_{10}]_{ini}$  / BDDA, upper phase, 13 wt. %, oil



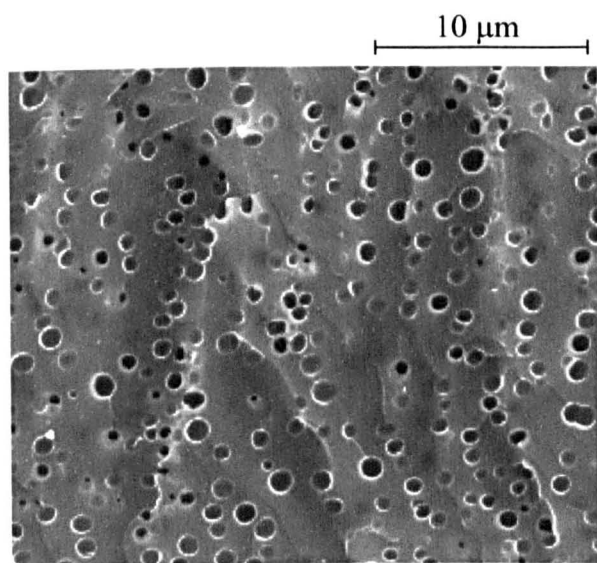
**Figure 5.45.** 22.0 wt. %  $[C_{10}]_{ini}$  / BDDA, middle phase, 22 wt. %, aq



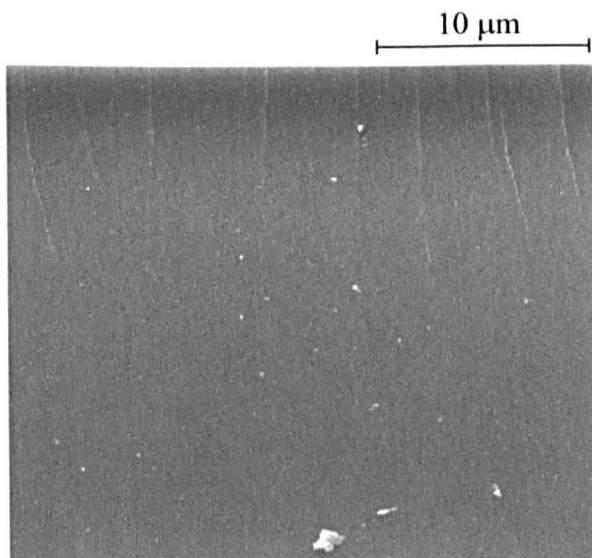
**Figure 5.46.** 25.0 wt. %  $[C_{10}]_{ini}$  / BDDA, upper phase, 15 wt. %, oil



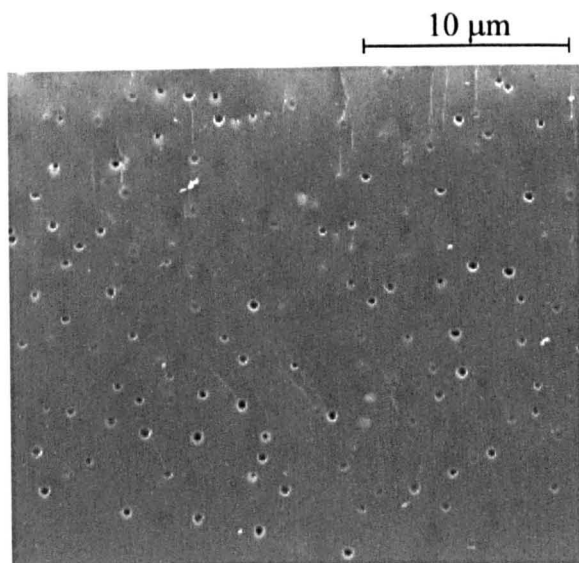
**Figure 5.47.** 25.0 wt. %  $[C_{10}]_{ini}$  / BDDA,  
middle phase, 24 wt. %, aq



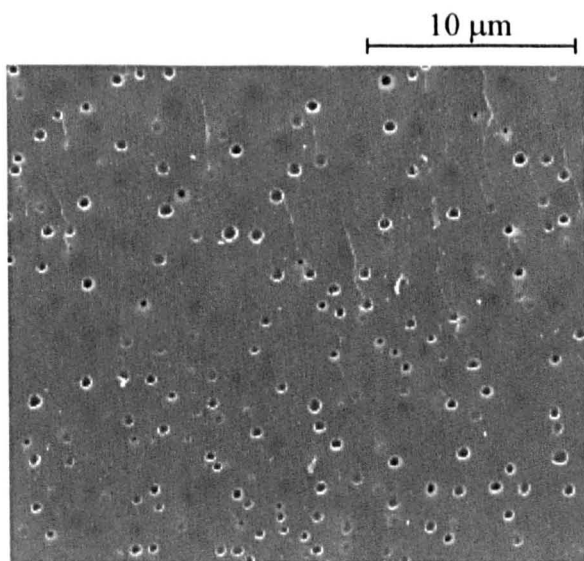
**Figure 5.48.** 5.0 wt. %  $[C_{10}]_{ini}$  / DPGDA,  
upper phase, 3 wt. %, oil



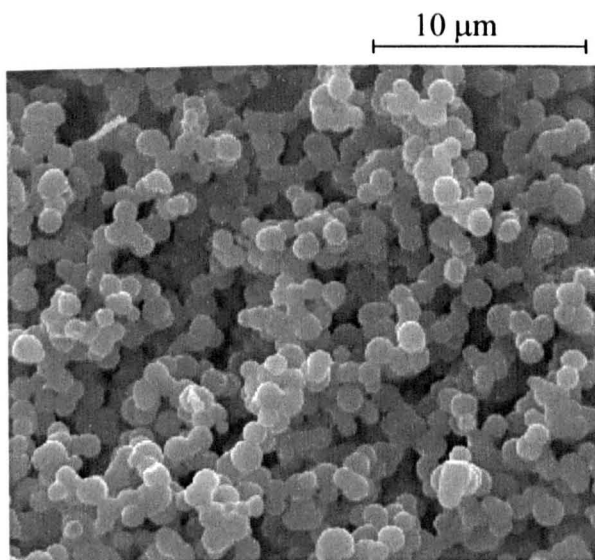
**Figure 5.49.** 15.0 wt. %  $[C_{10}]_{ini}$  / DPGDA,  
upper phase, 7 wt. %, oil



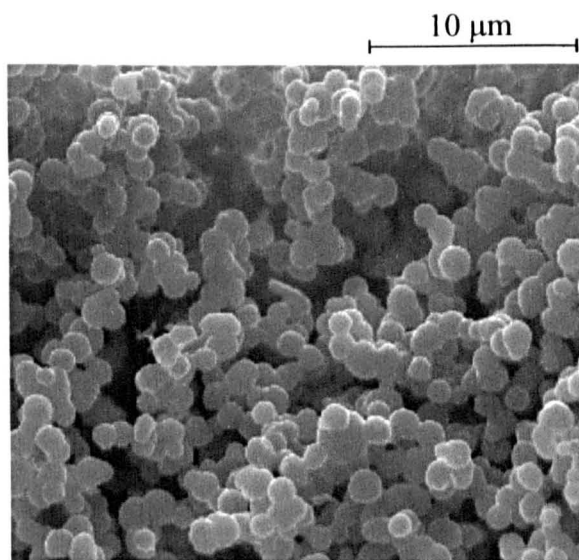
**Figure 5.50.** 18.0 wt. %  $[C_{10}]_{ini}$  / DPGDA,  
upper phase, 11 wt. %, oil



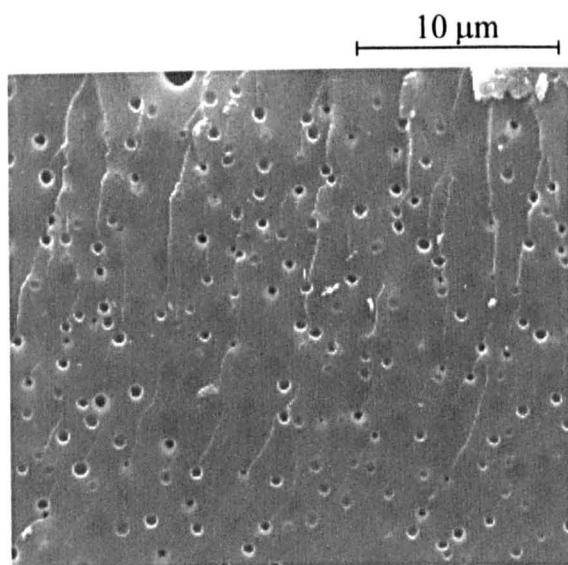
**Figure 5.51.** 18.0 wt. % [C<sub>10</sub>]ini / DPGDA,  
middle phase, 53 wt. %, aq/ b



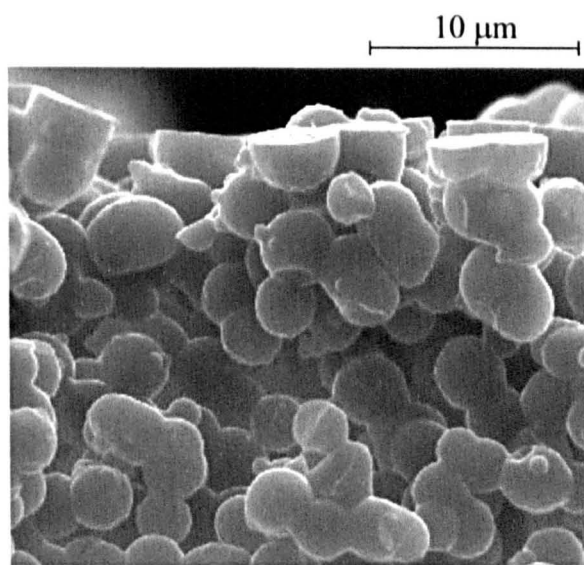
**Figure 5.52.** 18.0 wt. % [C<sub>10</sub>]ini / DPGDA,  
lower phase, 55 wt. %, aq/ b



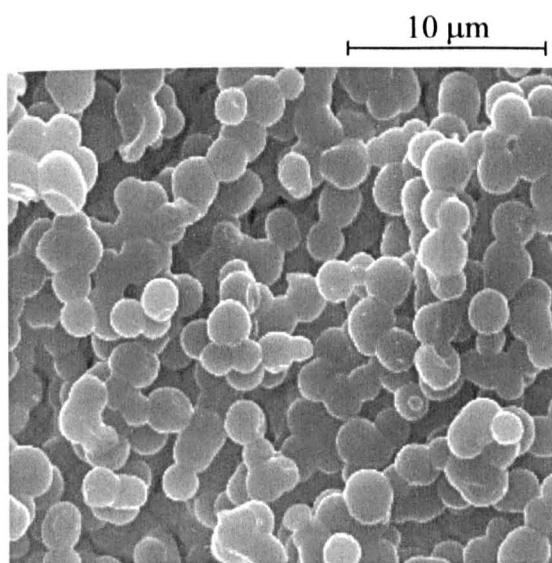
**Figure 5.53.** 22.0 wt. % [C<sub>10</sub>]ini / DPGDA,  
upper phase, 11 wt. %, oil



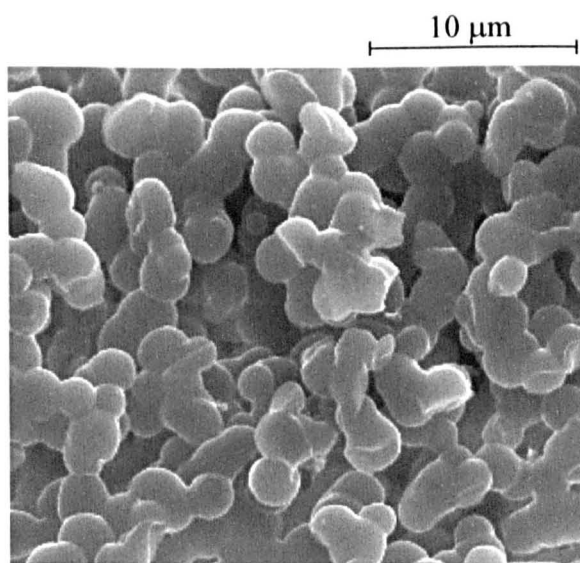
**Figure 5.54.** 22.0 wt. % [C<sub>10</sub>]ini / DPGDA,  
middle phase, 46 wt. %, aq/ b



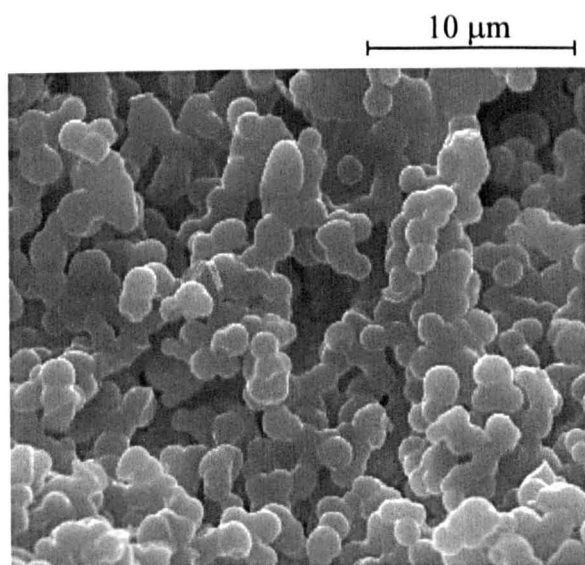
**Figure 5.55.** 22.0 wt. % [C<sub>10</sub>]<sub>ini</sub> / DPGDA,  
lower phase, 52 wt. %, aq/ b



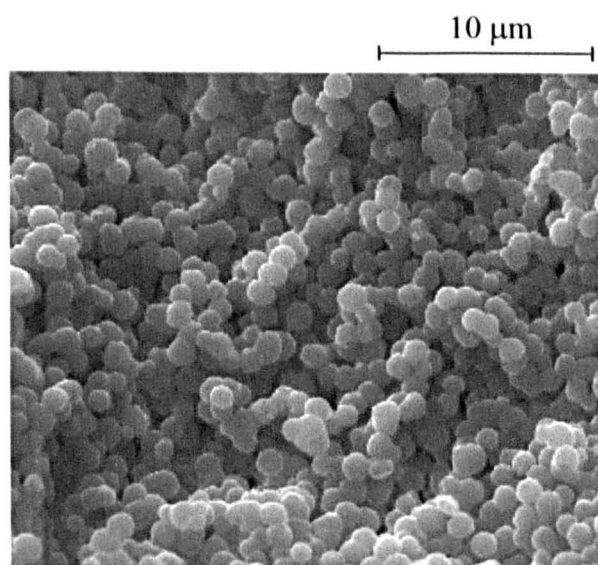
**Figure 5.56.** 25.0 wt. % [C<sub>10</sub>]<sub>ini</sub> / DPGDA,  
middle phase, 46 wt. %, aq/ b



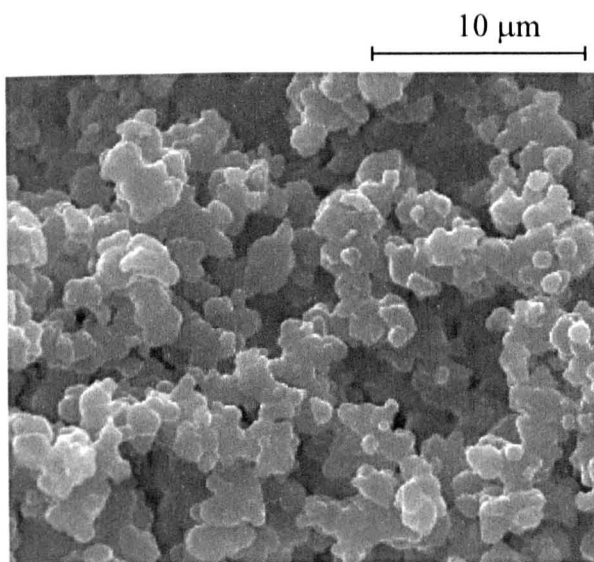
**Figure 5.57.** 25.0 wt. % [C<sub>10</sub>]<sub>ini</sub> / DPGDA,  
lower phase, 54 wt. %, aq/ b



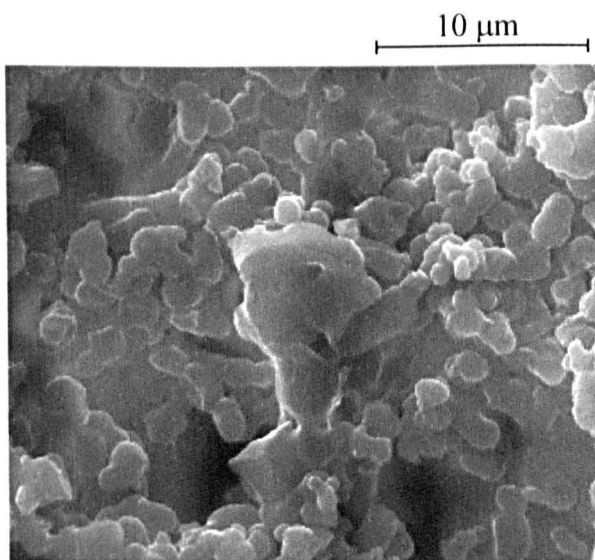
**Figure 5.58.** 15.0 wt. % [C<sub>12</sub>]<sub>ini</sub> / HDDA,  
middle phase, 54 wt. %, aq



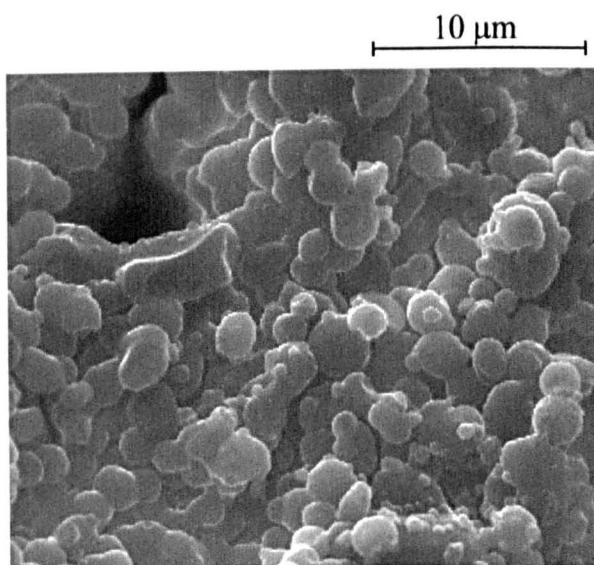
**Figure 5.59.** 15.0 wt. % [C<sub>12</sub>]<sub>ini</sub> / HDDA,  
lower phase, 67 wt. %, aq



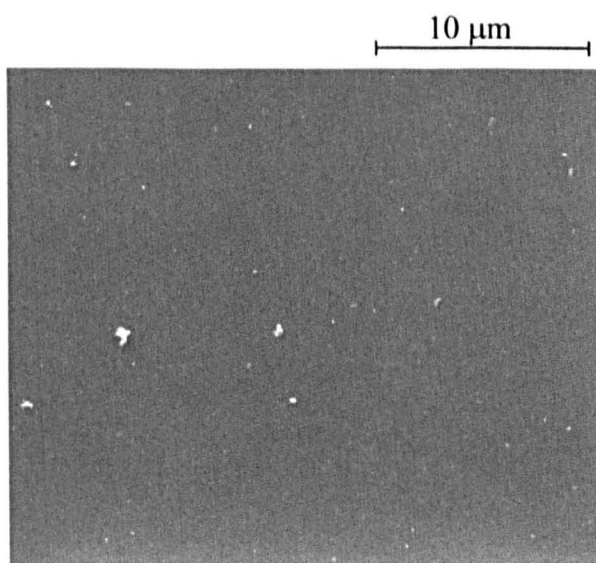
**Figure 5.60.** 20.0 wt. % [C<sub>12</sub>]<sub>ini</sub> / HDDA,  
middle phase, 40 wt. %, aq/ b



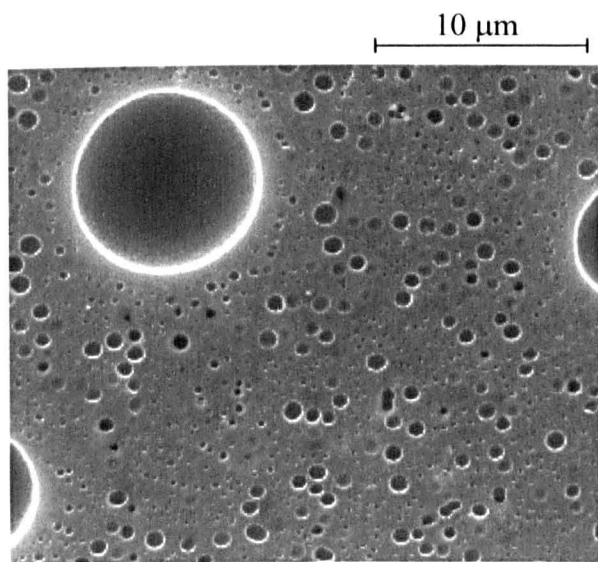
**Figure 5.61.** 20.0 wt. % [C<sub>12</sub>]<sub>ini</sub> / HDDA,  
lower phase, 39 wt. %, aq



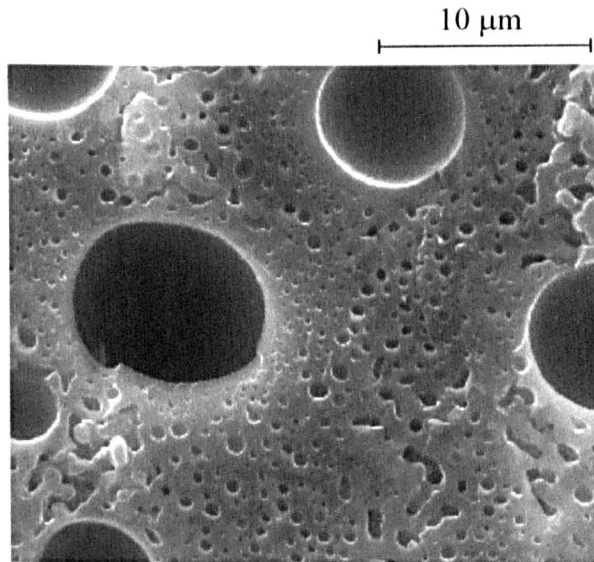
**Figure 5.62.** 25.0 wt. % [C<sub>12</sub>]<sub>ini</sub> / HDDA,  
upper phase, 2 wt. %, oil



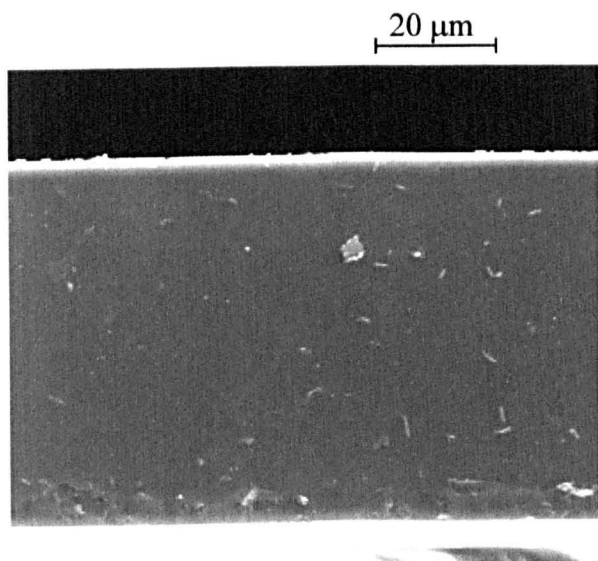
**Figure 5.63.** 25.0 wt. %  $[C_{12}]_{ini}$  / HDDA, middle phase, 29 wt. %, aq/ b



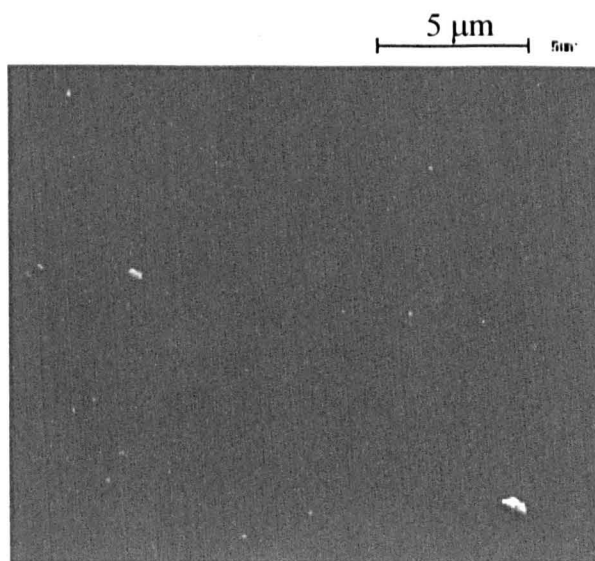
**Figure 5.64.** 25.0 wt. %  $[C_{12}]_{ini}$  / HDDA, lower phase, 31 wt. %, aq



**Figure 5.65.** 5.0 wt. %  $[C_{12}]_{ini}$  / BDDA, upper phase, 3 wt. %, oil

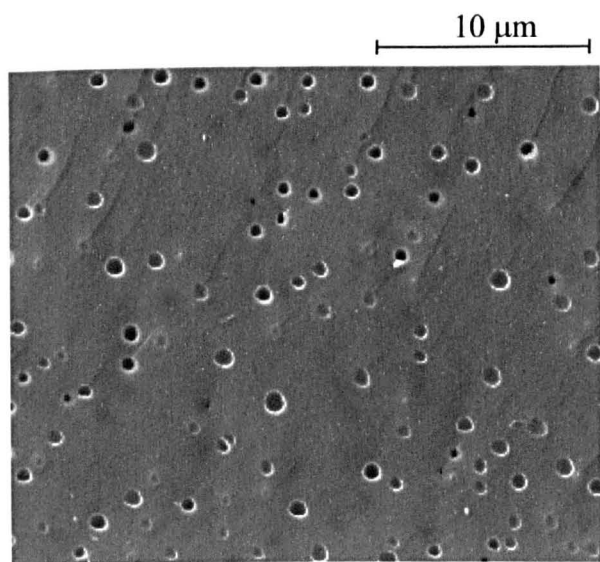


**Figure 5.66.** 15.0 wt. %  $[C_{12}]_{ini}$  / BDDA, upper phase, 12 wt. %, oil

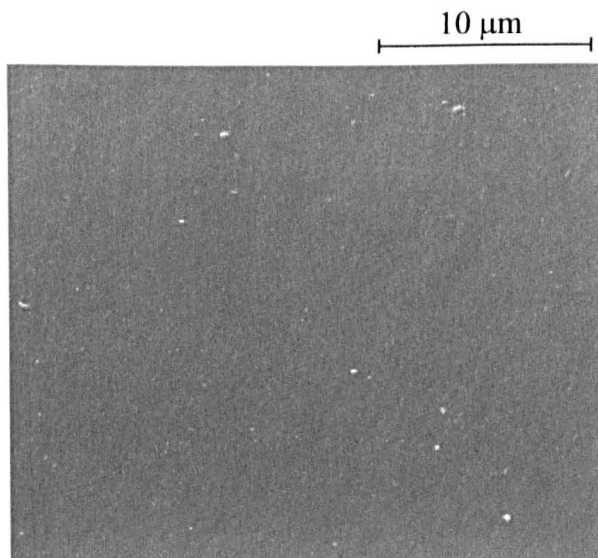




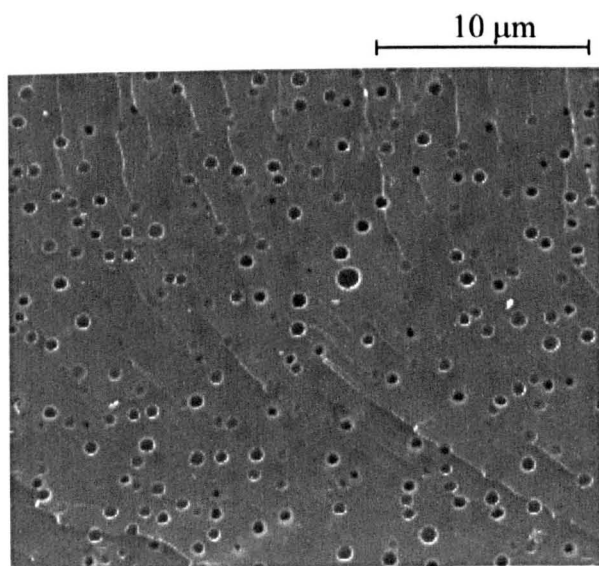
**Figure 5.67.** 15.0 wt. %  $[C_{12}]_{ini}$  / BDDA, middle phase, 11 wt. %, oil



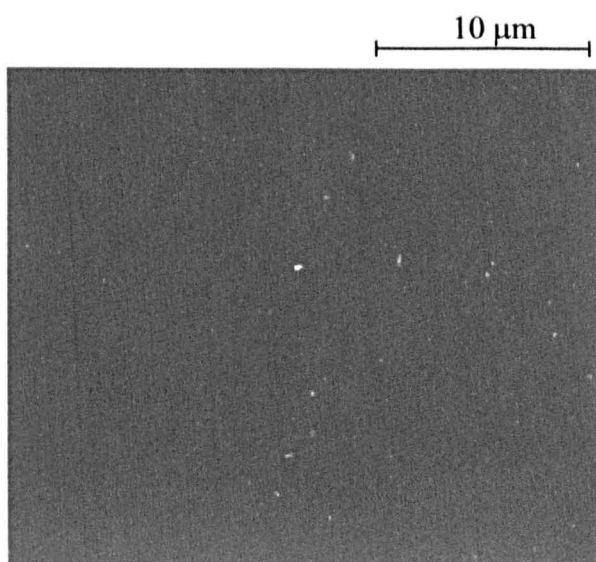
**Figure 5.68.** 20.0 wt. %  $[C_{12}]_{ini}$  / BDDA, upper phase, 13 wt. %, oil



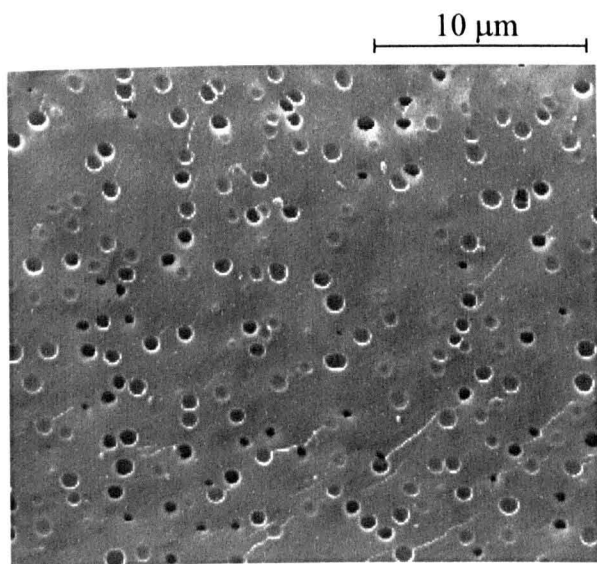
**Figure 5.69.** 20.0 wt. %  $[C_{12}]_{ini}$  / BDDA, middle phase, 16 wt. %, oil



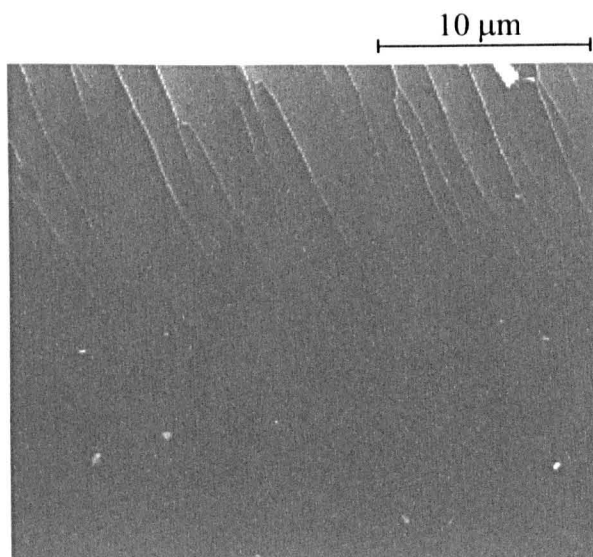
**Figure 5.70.** 25.0 wt. %  $[C_{12}]_{ini}$  / BDDA, upper phase, 17 wt. %, oil



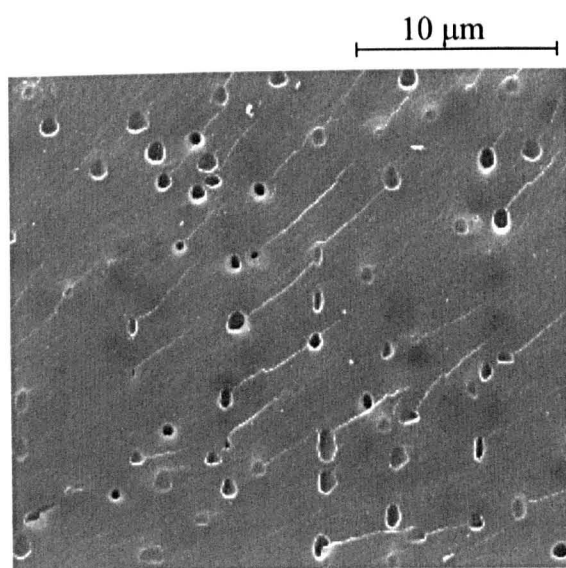
**Figure 5.71.** 25.0 wt. %  $[C_{12}]_{ini}$  / BDDA, middle phase, 19 wt. %, oil



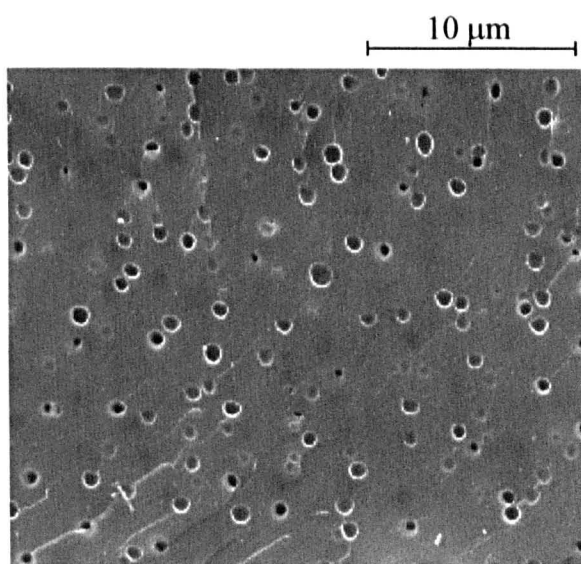
**Figure 5.72.** 5.0 wt. %  $[C_{12}]_{ini}$  / DPGDA, upper phase, 4 wt. %, oil



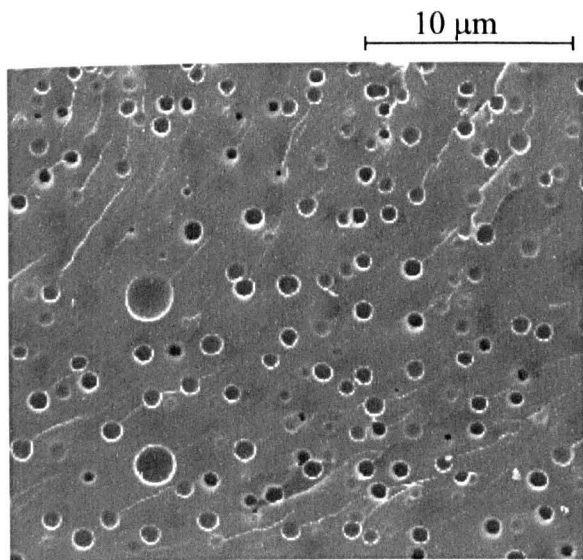
**Figure 5.73.** 15.0 wt. %  $[C_{12}]_{ini}$  / DPGDA, upper phase, 9 wt. %, oil



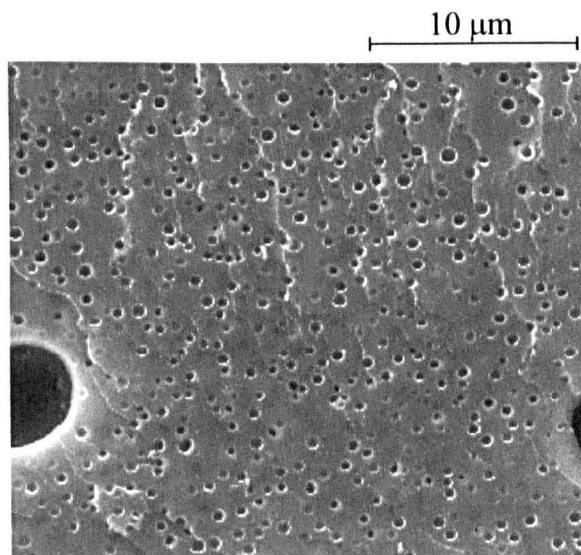
**Figure 5.74.** 18.0 wt. %  $[C_{12}]_{ini}$  / DPGDA, upper phase, 15 wt. %, oil



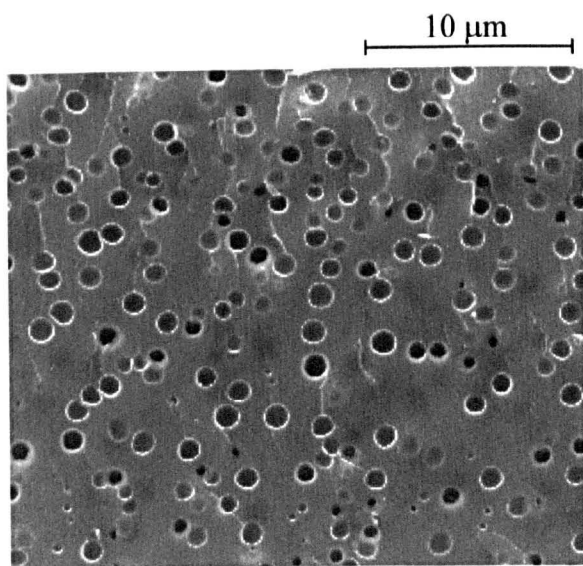
**Figure 5.75.** 22.0 wt. %  $[C_{12}]_{ini}$  / DPGDA,  
upper phase, 18 wt. %, oil



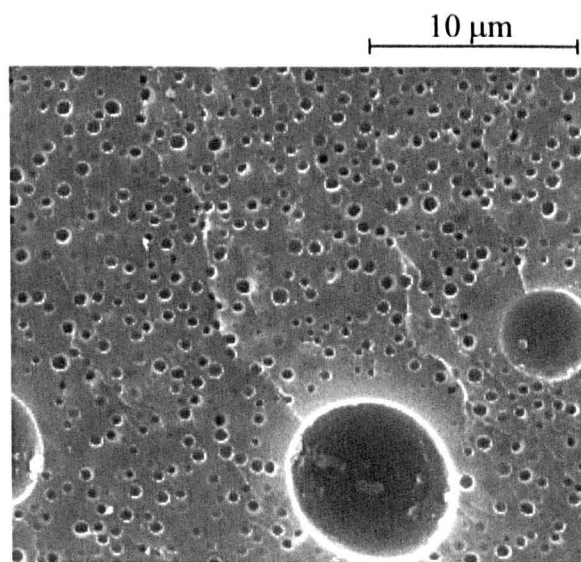
**Figure 5.76.** 22.0 wt. %  $[C_{12}]_{ini}$  / DPGDA,  
middle phase, 21 wt. %, aq/ b



**Figure 5.77.** 25.0 wt. %  $[C_{12}]_{ini}$  / DPGDA,  
upper phase, 20 wt. %, oil



**Figure 5.78.** 25.0 wt. %  $[C_{12}]_{ini}$  / DPGDA,  
middle phase, 25 wt. %, aq/ b

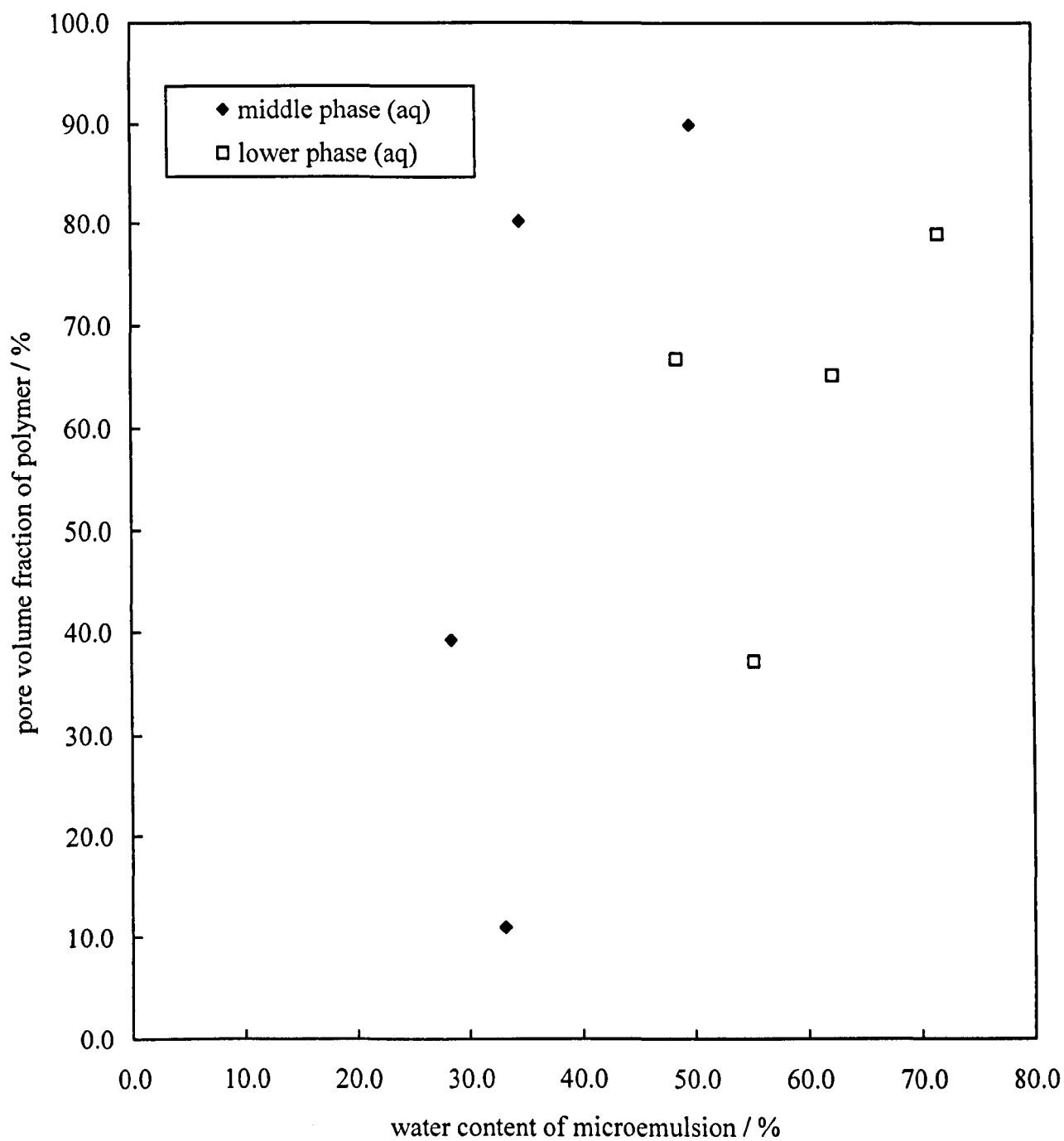


#### 5.4.2 Pore volume fraction of polymer films by water absorption

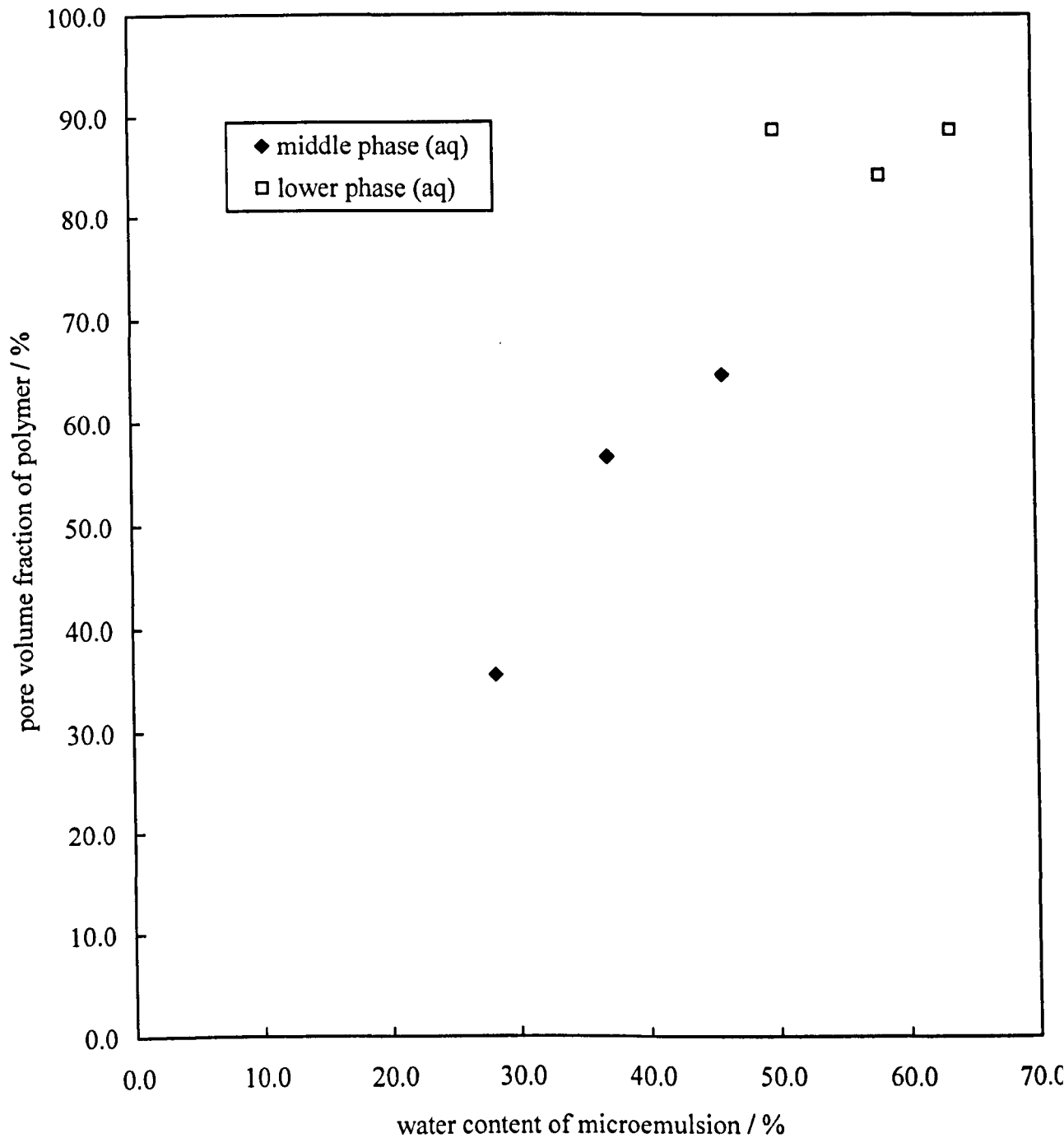
An important parameter of the polymer films produced by polymerisation of the microemulsion phases is the pore volume fraction, i.e. the fraction of the total volume of the polymer that is pore (empty) space. This affects the extent of liquid (e.g. ink) uptake in the films. The pore volume fraction of the polymer films was measured by water absorption. It was found that on soaking in water, films formed from water or bicontinuous microemulsion phases swelled with water uptake to a certain degree. The pore volume fraction in these cases is quoted as volume fraction of the wet (i.e. swollen) films. The pore volume fraction of the solid polymer films was related to the equilibrium water content of the parent liquid microemulsions. This provides a useful method of controlling the pore volume fraction and hence liquid uptake of the polymer films.

Figures 5.79 to 5.87 show the pore volume fraction of each film versus the water content of the equilibrium microemulsion from which they were prepared. Figures 5.79 and 5.80 show that for the films prepared from aggregate containing phases (middle and lower) in the systems containing  $C_{3/11-M}$  and HDDA or BDDA, the pore volume fraction increases with increasing water content of the equilibrium microemulsion. In the case of BDDA, the lower phase (higher water content) produces polymer films with a much higher pore volume fraction than those from the middle phase. The pore volume fraction of the films from both middle and lower phases is higher than the corresponding microemulsion water content. The films from the upper equilibrium microemulsion phases were measured and found to be of very low pore volume fraction (typically <1 %). This is expected as the upper phase is an

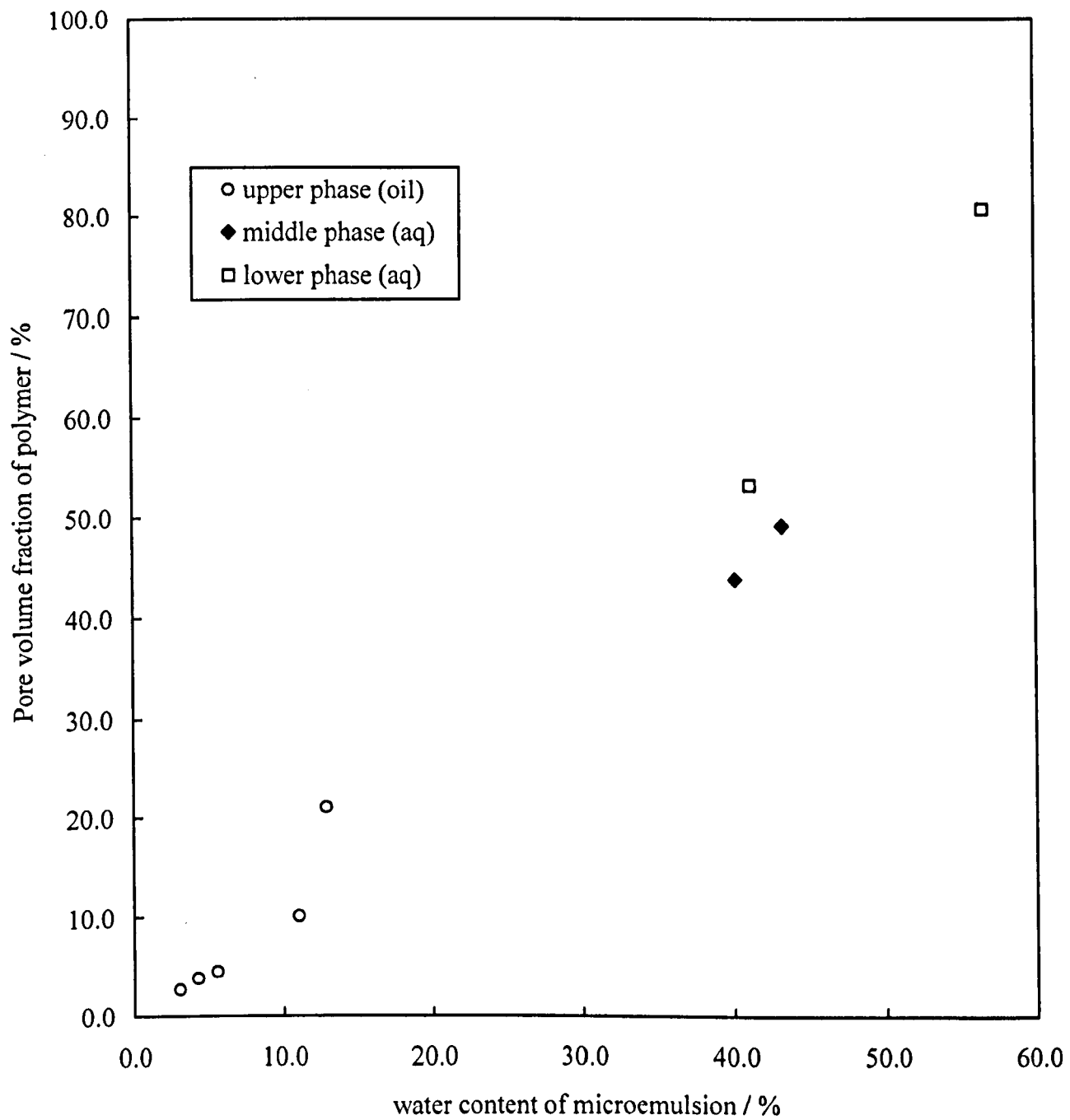
**Figure 5.79. Pore volume fraction of polymer film vs. water content of equilibrium microemulsion phase for microemulsions containing C<sub>3/11-M</sub>, D<sub>2</sub>O and HDDA. Continuous phase of microemulsion is indicated in legend**



**Figure 5.80. Pore volume fraction of polymer film vs. water content of equilibrium microemulsion phase for microemulsions containing C<sub>3/11</sub>-M, D<sub>2</sub>O and BDDA. Continuous phase of microemulsion is indicated in legend**



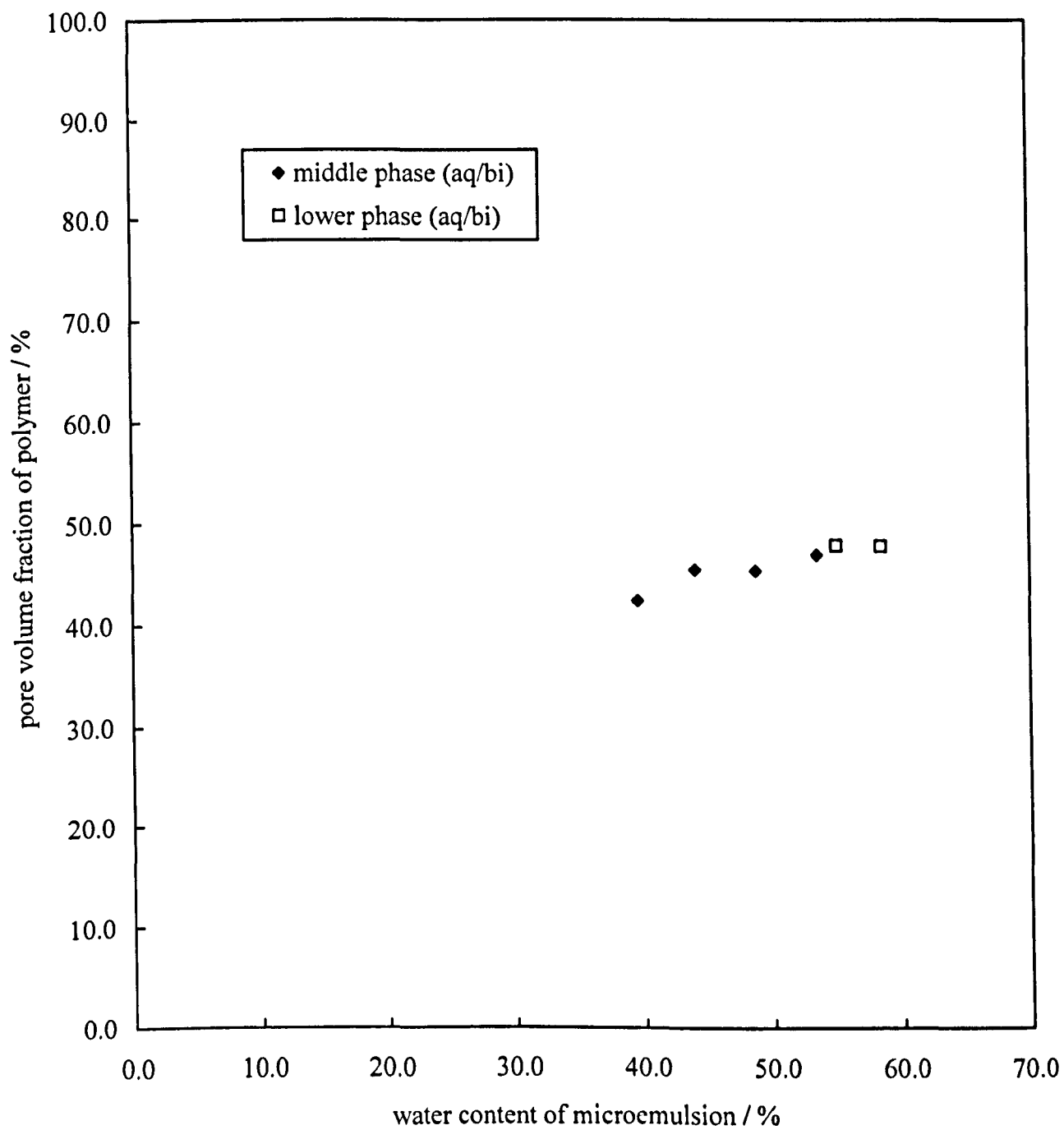
**Figure 5.81. Pore volume fraction of polymer film vs. water content of equilibrium microemulsion phase for microemulsions containing  $C_{3/11-M}$ ,  $D_2O$  and DPGDA. Continuous phase of microemulsion is indicated in legend**



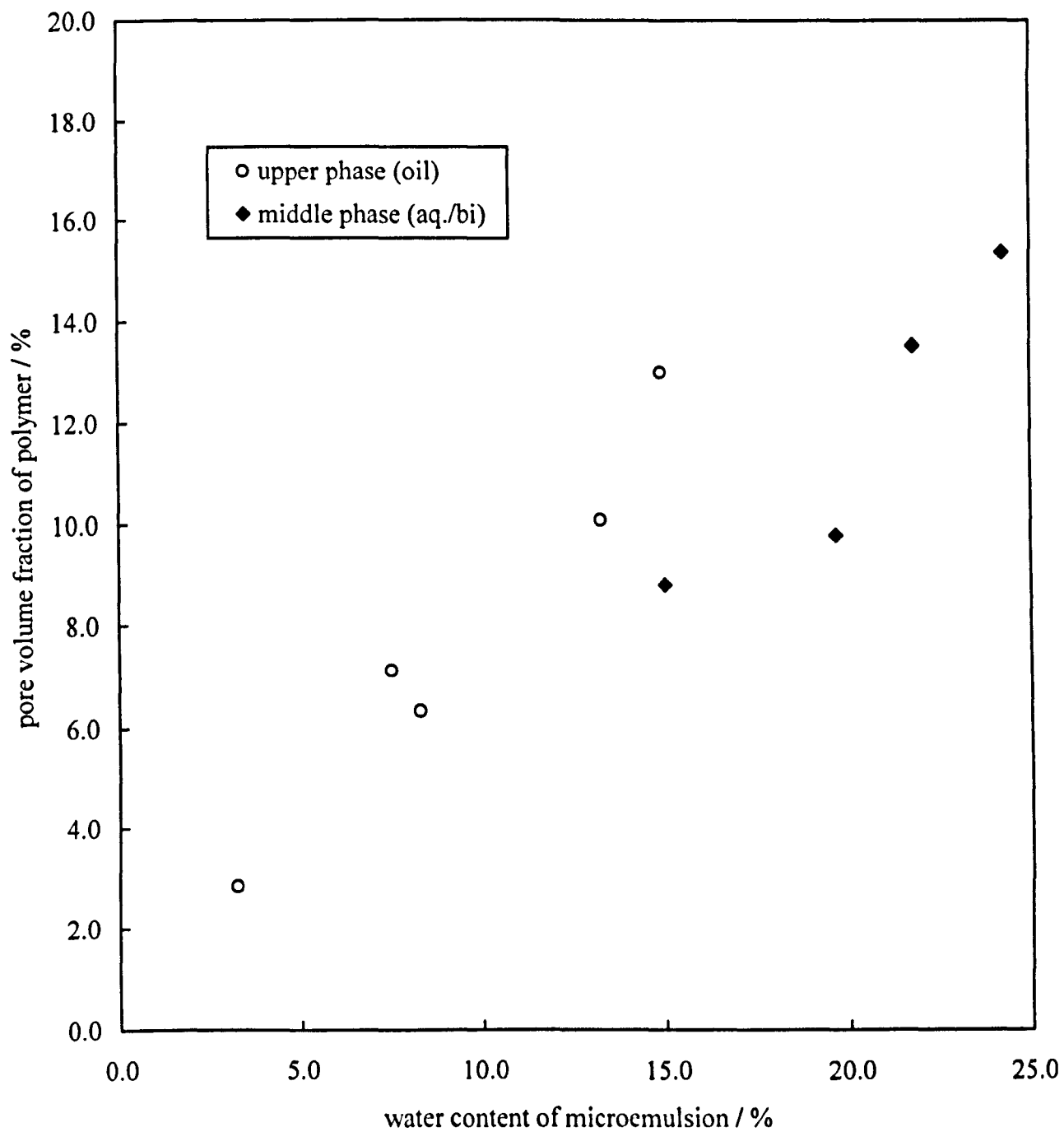
excess oil phase. Figure 5.81 shows that in systems containing  $C_{3/11-M}$  and DPGDA, for all three phases as the equilibrium water content of the microemulsion increases, the pore volume fraction of the corresponding polymer film increases. In this case, porous films are observed from both oil and water continuous microemulsion phases with both phases containing aggregates. The films from oil continuous microemulsions however have a much lower pore volume fraction than those from the water continuous microemulsions, due to their much lower water content. The pore volume fraction of films from oil continuous microemulsions increases rapidly with increasing water content beyond the phase inversion seen in Figure 4.11 (Chapter 4). Pore volume fractions are higher than the equilibrium water content of the corresponding microemulsions. It is seen that films prepared from microemulsions containing surfactant  $C_{3/11-M}$  are generally highly porous with the pore volume fraction increasing approximately linearly with equilibrium water content of microemulsion. Figure 5.82 shows that for the films prepared from aggregate containing phases (middle and lower) in the system containing  $C_{10}$  and HDDA, the pore volume fraction increases only fractionally with increasing water content of the equilibrium microemulsion. The excess oil phases do not produce porous films. Figure 5.83 shows that both the upper (oil continuous) and middle (aqueous/bicontinuous) microemulsion phases in the system containing  $C_{10}$  with BDDA produce porous polymer films. The films from the middle phases reach higher pore volume fractions than those from the upper phase as the parent microemulsions have higher equilibrium water contents. In both cases the water content is higher than the corresponding pore volume fraction and the pore volume fractions (and equilibrium water contents) are lower than those observed in previous systems. The lower microemulsion phase did not polymerise to produce films. Figure 5.84 shows that the



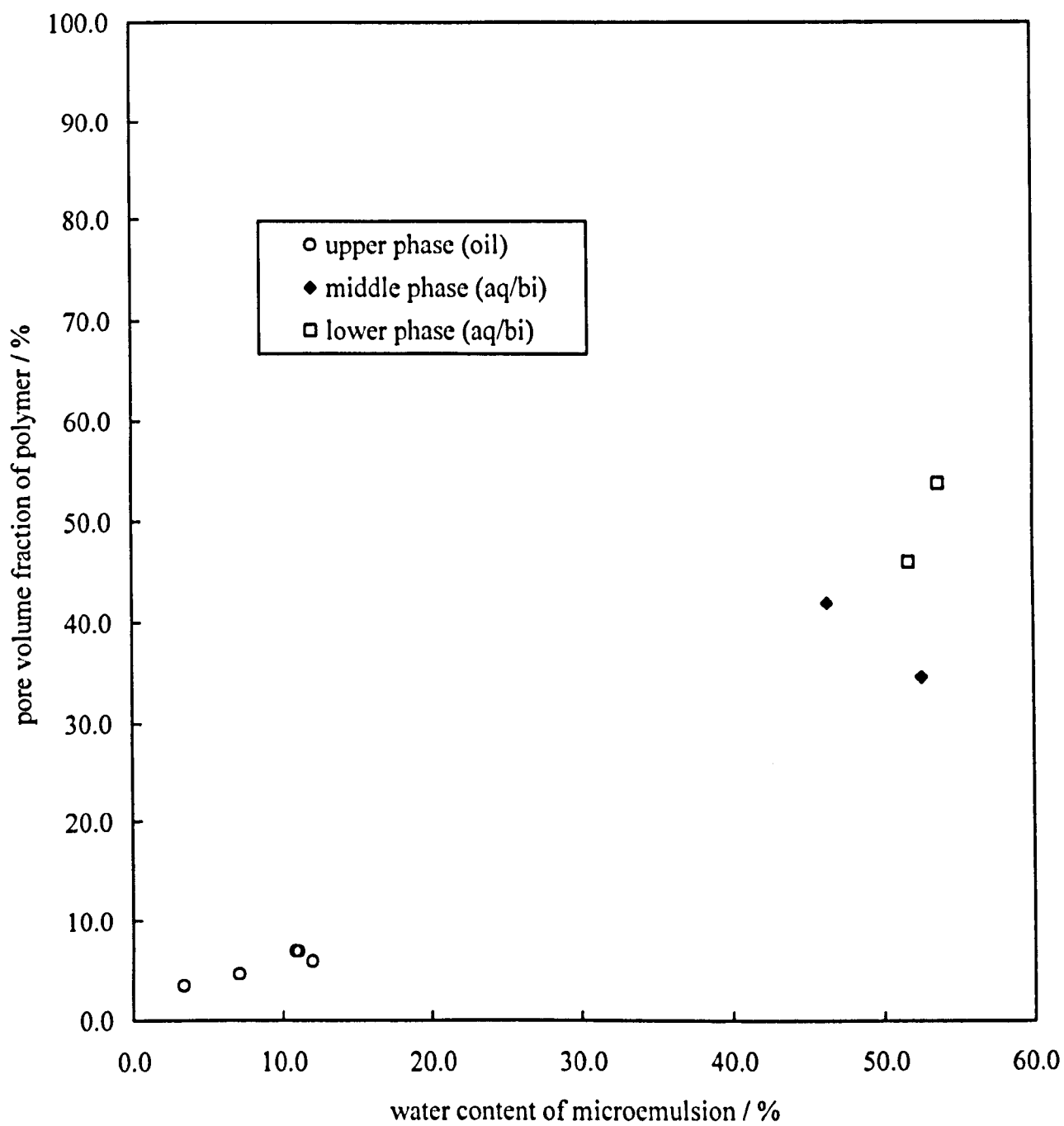
**Figure 5.82. Pore volume fraction of polymer film vs. water content of equilibrium microemulsion phase for microemulsions containing C<sub>10</sub>, D<sub>2</sub>O and HDDA. Continuous phase of microemulsion is indicated in legend**



**Figure 5.83. Pore volume fraction of polymer film vs. water content of equilibrium microemulsion phase for microemulsions containing C<sub>10</sub>, D<sub>2</sub>O and BDDA. Continuous phase of microemulsion is indicated in legend**

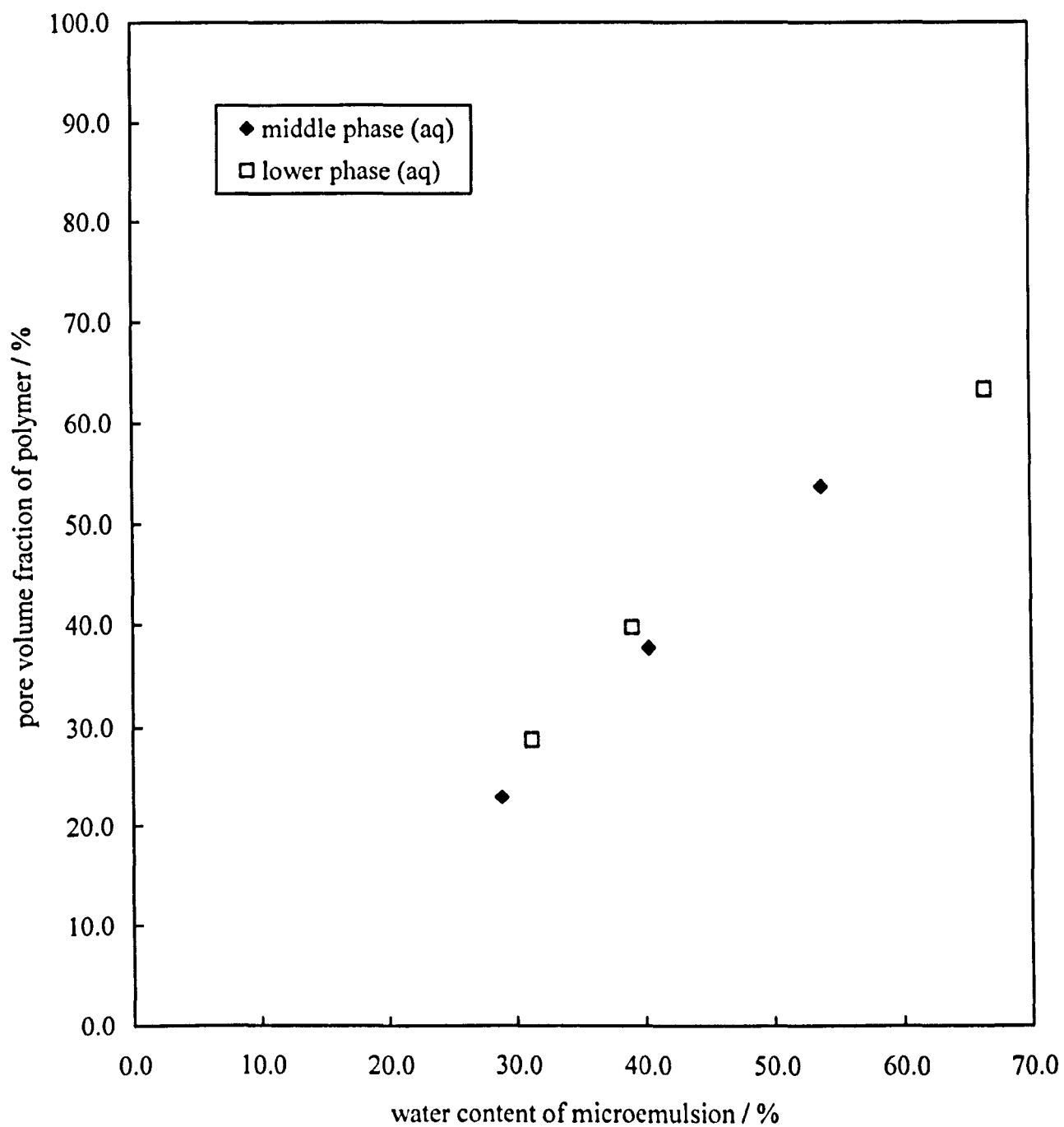


**Figure 5.84. Pore volume fraction of polymer film vs. water content of equilibrium microemulsion phase for microemulsions containing C<sub>10</sub>, D<sub>2</sub>O and DPGDA. Continuous phase of microemulsion is indicated in legend**

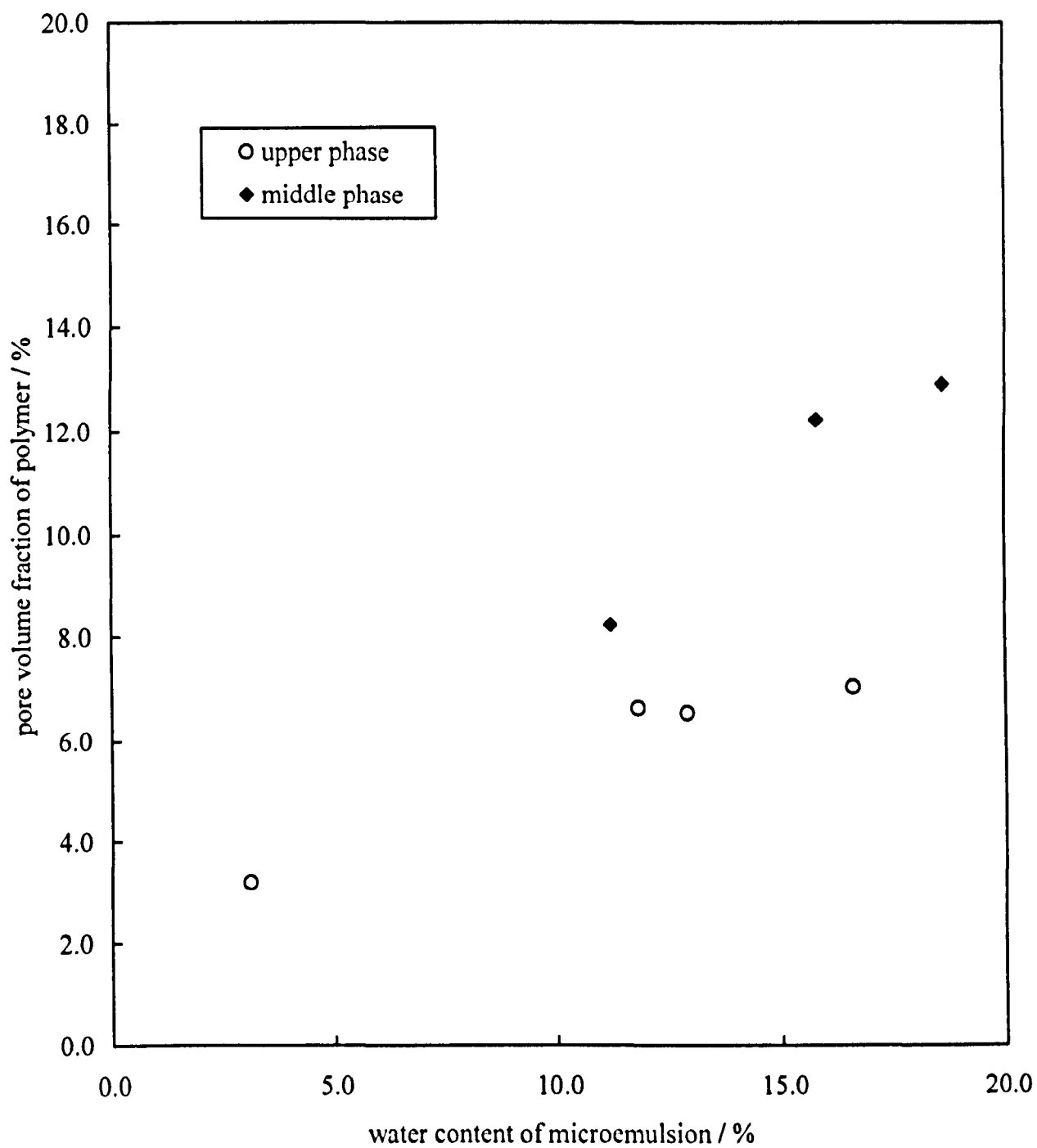


middle and lower microemulsion phases (aqueous/ bicontinuous) in the system containing C<sub>10</sub> with DPGDA produce highly porous polymer films with the pore volume fraction closely related to the microemulsion water content. It is difficult to see a definite trend as some of the phases did not produce stable polymer films, but it appears that the pore volume fraction increases with equilibrium water content. The upper microemulsion phase also produces films with a pore volume fraction which increases with increasing water content of the microemulsion phase but both the water content and pore volume fraction are low. Figure 5.85 shows that the middle and lower microemulsion phases (aqueous continuous) in the system containing C<sub>12</sub> and HDDA produce highly porous films with the pore volume fraction increasing with equilibrium water content of the microemulsion. The pore volume fraction is almost directly proportional to the equilibrium water content of the microemulsion. The upper (oil continuous) phase, which in most cases is an excess oil phase containing surfactant and very little water did not produce porous films. Figure 5.86 shows the pore volume fraction versus water content of the equilibrium microemulsion phase for the upper and middle phases (both oil continuous) for the system containing C<sub>12</sub> and BDDA. In both cases the pore volume fraction increases with equilibrium water content with the pore volume fraction lower than the equilibrium water content. In the upper phase the pore volume fraction is around half the value of the water content. In both cases the water contents and pore volume fractions are fairly low. Figure 5.87 shows that the pore volume fraction of the polymer films prepared from the system containing C<sub>12</sub> with DPGDA increases approximately linearly with increasing equilibrium water content of the microemulsion phases for the upper and middle (oil continuous) phases. As seen previously with films from oil continuous aggregate containing phases, both the water contents and pore volume fractions are low.

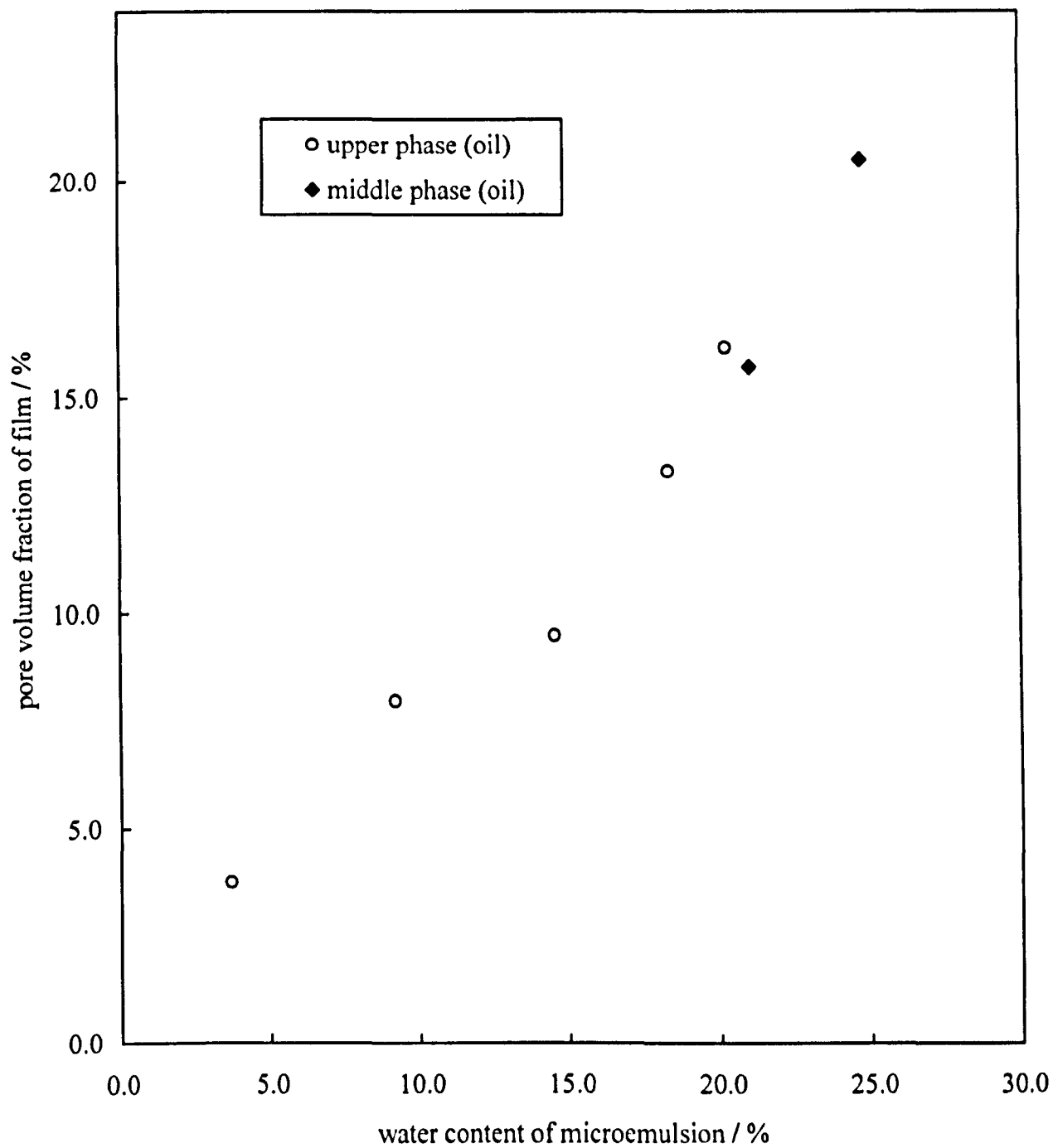
**Figure 5.85. Pore volume fraction of polymer film vs. water content of equilibrium microemulsion phase for microemulsions containing C<sub>12</sub>, D<sub>2</sub>O and HDDA. Continuous phase of microemulsion is indicated in legend**



**Figure 5.86. Pore volume fraction of polymer film vs. water content of equilibrium microemulsion phase for microemulsions containing C<sub>12</sub>, D<sub>2</sub>O and BDDA. Continuous phase of microemulsion is indicated in legend**



**Figure 5.87. Pore volume fraction of polymer film vs. water content of equilibrium microemulsion phase for microemulsions containing C<sub>12</sub>, D<sub>2</sub>O and DPGDA. Continuous phase of microemulsion is indicated in legend**



Figures 5.79 to 5.87 show that in general films from aqueous/ bicontinuous phases (which have a high water content) produce films that have a high pore volume fraction, which increases with water content of the equilibrium microemulsion. Films from oil continuous aggregate containing phases (which have a low water content) produce films with a low pore volume fraction, which also increases with increasing water content of the equilibrium microemulsion. Films which have open-porous spherical aggregate microstructures, generally have higher pore volume fractions than those polymers with nano featured microstructures. The proportion of highly porous films from aqueous continuous microemulsion phases to low porosity films from oil continuous microemulsions increases with surfactant type from C<sub>12</sub> to C<sub>10</sub> to C<sub>3/11-M</sub> and with oil type from BDDA to DPGDA to HDDA. Almost all films from C<sub>3/11-M</sub> surfactant and all films from HDDA oil systems have a high pore volume fraction. Comparing this data to Table 4.4 (Chapter 4), one concludes that systems exhibiting WI\* phase equilibration produce aggregate containing phases which can be polymerised. The pore volume fraction of the resulting polymers is dependent on the equilibrium water content of the phases which is itself dependent on the [surfactant]<sub>ini</sub> of the phases. Therefore, the pore volume fraction of films of polymerised WI\* aggregate containing phases can be controlled by the [surfactant]<sub>ini</sub> in the parent microemulsion system.

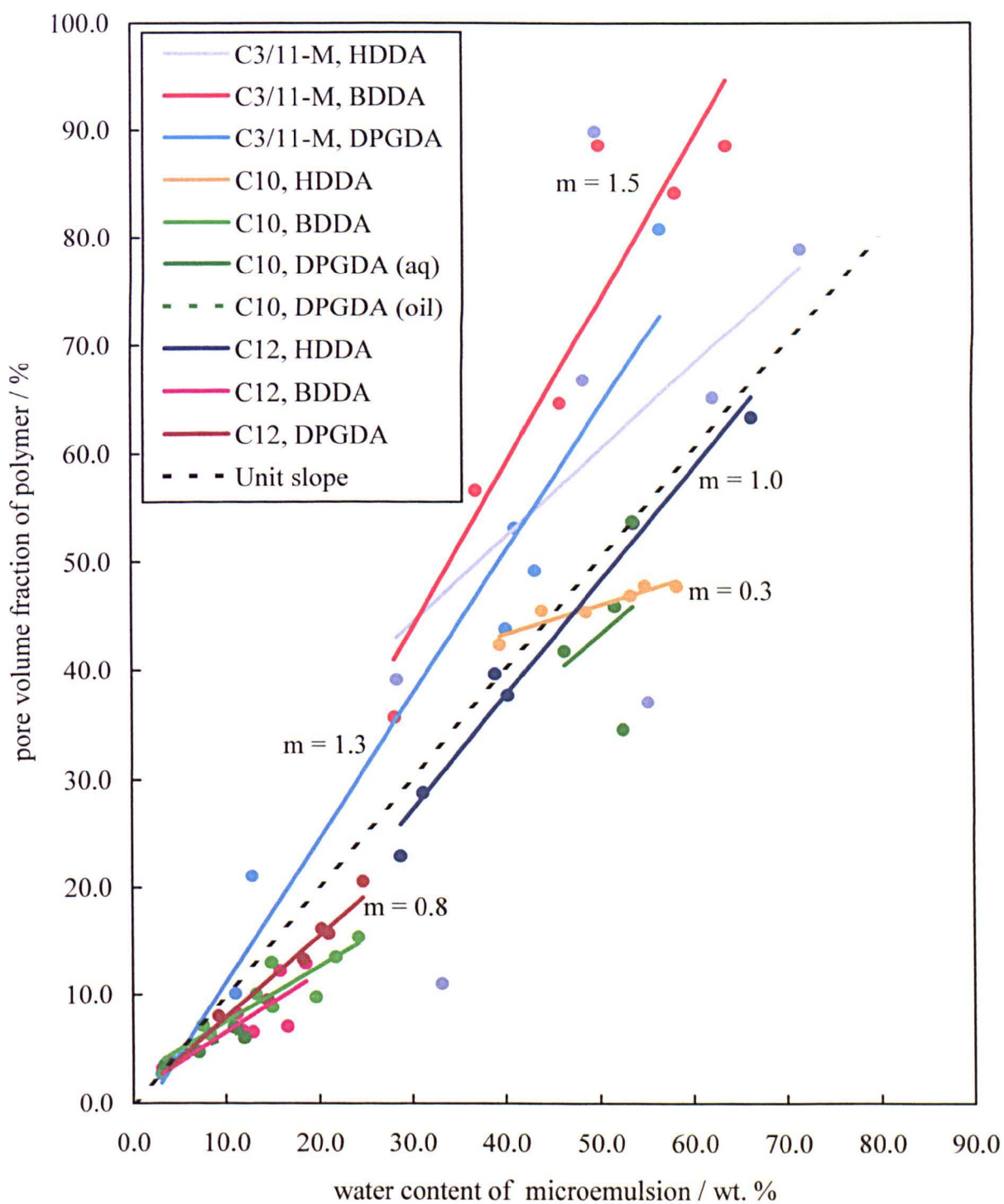
The structures of the surfactant and oil molecules affect not only the microemulsion phase equilibration and therefore the pore volume fraction of the resulting polymer films, but also the relation between increase in equilibrium water content of the microemulsion and the associated increase in pore volume fraction of



the polymer films. The gradient of the slope of pore volume fraction of the polymer films against equilibrium water content of the microemulsion phases can be used to attach a value to this relation. Figure 5.88 shows the pore volume fraction of the polymer films versus the equilibrium water content of the respective microemulsion phases and gives the gradient of the slope for five of the systems. Accurate values for the gradient could not be obtained for the other systems due to the extent of deviation of data points from the best-fit slope resulting in low  $R^2$  values for the best fit slope for these systems.

Figure 5.88 shows that the gradient is affected by the surfactant and oil molecular structures. The gradient increases with surfactant type from  $C_{10}$  to  $C_{12}$  to  $C_{3/11-M}$  with the more polar oil system having a slightly lower gradient for a particular surfactant type. The unit slope denotes pore volume fraction equal to equilibrium water content of the pre-cursor microemulsion. If the data points for a system lie above this slope, then the pore volume fraction is larger than the equilibrium water content of the microemulsion and so film swelling must have occurred during the polymerisation process. If the points lie below the unit slope then the pore volume fraction is lower than the equilibrium water content of the microemulsion and therefore films shrinkage must occur during the polymerisation process. With films prepared from microemulsions containing  $C_{3/11-M}$  surfactant, film expansion occurs during the polymerisation process. With films prepared from microemulsions containing  $C_{10}$  or  $C_{12}$  surfactants, film shrinkage occurs during the polymerisation process. This could be due to the location of the polymerisable methacrylate group on the surfactant molecule. This group is located on the headgroup with  $C_{10}$  and  $C_{12}$  surfactants, but is present on the end of the tail group in  $C_{3/11-M}$ . The position of the

**Figure 5.88. Pore volume fraction of films vs. equilibrium water content of microemulsion for films prepared from aggregate containing phases.**



polymerizable group on the surfactant molecule has been shown to affect the structure of the resulting polymer,<sup>17-19</sup> although the model proposed in refs. 18-20 does not hold with these systems as both surfactant types form solid porous films.

## 5.5 Conclusions

Polymerisation by photoinitiation was selected as a suitable method to prepare solid polymer films from liquid equilibrium microemulsion phases containing polymerizable surfactants and polymerizable oils. Work was carried out to ensure that the polymerisation of microemulsion systems would yield reproducible polymer films with controlled dimensions. Polymer films have been prepared from equilibrium microemulsion phases containing polymerizable surfactant and oil using a polymerisation cell. These films have been characterised by visual inspection and handling, electron microscopy and pore volume fraction. The following conclusions summarise the characteristics of films from the nine microemulsion systems studied.

- (a) Transparent, pliable polymer films can be produced using 1 wt. % Darocur 1173 initiator with HDDA oil irradiated with UV for 0.1 minutes.
- (b) C<sub>3/11-M</sub> surfactant has been polymerised using UV light with Darocur 1173 both as pure surfactant and surfactant solution yielding soft, semi-solid polymers.
- (c) A polymerisation cell was constructed which reduces the effects of atmospheric oxygen, which was found to inhibit the polymerisation reaction by rapid termination of the polymerisation process. Polymer films of reproducible thickness were prepared, with the film thickness determined by the thickness of a spacer material. Glass slides are used for the top and base with aluminium foil used as the spacer. This provides a simple, disposable design and enables the preparation of polymer films of consistent reproducible dimensions.

(d) Opacity is greater for films prepared from microemulsions with a higher water content. Most water continuous microemulsions produce opaque or cloudy films. The strength of the polymer films decreases with increasing water content of the equilibrium microemulsion and in general, microemulsions with very high water contents either do not polymerise or produce very weak films. Most films are strong but brittle if bent excessively.

(e) Three different microstructures of polymers were observed, which depend on the surfactant and oil type and Winsor phase type of the parent microemulsion. WI\* systems polymerise to form open porous spherical aggregate structures which may form as a result of micelle swelling during the polymerisation process. WI<sup>I</sup> and WII\* systems polymerise to form nano structured porous polymers. Surfactants with the polymerizable group located on the head group form polymers which contain micrometer sized holes. These holes were absent in the films prepared from microemulsion phases containing the surfactant with the polymerizable group located on the tail.

(f) Films from aqueous/ bicontinuous phases (which have a high water content) produce films that have a high pore volume fraction, which increases with water content of the equilibrium microemulsion. Films from oil continuous aggregate containing phases (which have a low water content) produce films with a low pore volume fraction, which also increases with increasing water content of the equilibrium microemulsion.

(g) The pore volume fraction of a polymerised WI\* microemulsion phase can be controlled via the equilibrium water content of the microemulsion by adjusting the  $[\text{surfactant}]_{\text{ini}}$ .

(h) The gradient of pore volume fraction vs. equilibrium water content is affected by the surfactant and oil molecular structures. Both film swelling and film shrinkage during the polymerisation process has been observed and is dependent on the location of the surfactant polymerisable group.

## 5.6 References

- <sup>1</sup> F. M. Menger, T. Tsuno and G. S. Hammond, *J. Am. Chem. Soc.*, **112**, 1263 (1990).
- <sup>2</sup> W. Palani Raj, M. Sasthav and H. M. Chung, *Langmuir*, **7**, 2586 (1991).
- <sup>3</sup> M. Antonietti, R. Basten and F. Gröhn, *Langmuir*, **10**, 2498 (1994).
- <sup>4</sup> L. M. Gan, T. D. Li, C. H. Chew and W. K. Teo, *Langmuir*, **11**, 3316 (1995).
- <sup>5</sup> A. Aguiar, S. González-Villegas, M. Rabelero, E. Mendezabal, J. E. Ping, J. M. Dominguez and I. Katime, *Macromolecules*, **32**, 6767 (1999).
- <sup>6</sup> M. Sasthav and H. M. Chung, *Langmuir*, **7**, 1378 (1991).
- <sup>7</sup> T. H. Chieng, L. M. Gan, C. H. Chew, L. Lee, S. C. Ng, K. L. Pey and D. Grant, *Langmuir*, **11**, 3321 (1995).
- <sup>8</sup> T. H. Chieng, L. M. Gan, C. H. Chew, S. C. Ng and K. L. Pey, *Langmuir*, **12**, 319 (1996).
- <sup>9</sup> W. Xu, K. S. Siow, Z. Gao, S. Y. Lee, P. Y. Chow and L. M. Gan, *Langmuir*, **15**, 4812 (1999).
- <sup>10</sup> T. D. Li, L. M. Gan, C. H. Chew, W. K. Teo and L. H. Gan, *Langmuir*, **12**, 5863 (1996).
- <sup>11</sup> C. H. Chew, L. M. Gan, L. H. Ong, K. Zhang, T. D. Li, T. P. Loh and P. M. MacDonald, *Langmuir*, **13**, 2917 (1997).
- <sup>12</sup> J. Lui, L. M. Gan, C. H. Chew, W. K. Teo and L. H. Gan, *Langmuir*, **13**, 6421 (1997).
- <sup>13</sup> T. D. Li, L. M. Gan, C. H. Chew, W. K. Teo and L. H. Gan, *Journal of Membrane Science*, **133**, 177 (1997).
- <sup>14</sup> C. H. Chew, T. D. Li, L. H. Gan, C. H. Queck and L. M. Gan, *Langmuir*, **14**, 6068 (1998).

- <sup>15</sup> T. H. Chieng, L. M. Gan, W. K. Teo and K. L. Pey, *Polymer*, **37**, 5917 (1996).
- <sup>16</sup> T. H. Chieng, L. M. Gan, C. H. Chew, S. C. Ng and K. L. Pey, *Polymer*, **37**, 4823 (1996).
- <sup>17</sup> M. Dreja and B. Tieke, *Macromol. Rapid Commun.*, **17**, 825 (1996).
- <sup>18</sup> M. Dreja, W. Pyckhout-Hintzen and B. Tieke, *Macromolecules*, **31**, 272 (1998).
- <sup>19</sup> M. Pyrasch and B. Tieke, *Colloid Polym. Sci.*, **278**, 375 (2000).
- <sup>20</sup> C. Larpent and T. F. Tadros, *Colloid and Polymer Science*, **269**, 1171 (1991).
- <sup>21</sup> V. A. Bhaau and K. Kilshore, *Chem. Rev. Am. Chem. Soc.*, **91**, 99 (1991).
- <sup>22</sup> C. Decker and K. Moussa, *Makromol. Chem.*, **189**, 2381 (1988).
- <sup>23</sup> L. Lecamp, B. Youssef, C. Bunel and P. Lebaudy, *Polymer*, **40**, 6313 (1999).
- <sup>24</sup> H. De Bruyn, R. G. Gilbert and B. S. Hankett, *Polymer*, **41**, 8633 (2000).
- <sup>25</sup> J. M. G. Cowie, 'Polymers: Chemistry and Physics of Modern Materials', 2nd Ed., Blackie, New York (1991).
- <sup>26</sup> K. Jajima and T. Aida, *Chem. Commun.*, 2399 (2000).
- <sup>27</sup> M. Summers and J. Eastoe, *Adv. Coll. Int. Sci.*, **100-102**, 137 (2003).



# *CHAPTER 6*

# CHAPTER 6

## CONCLUSIONS

This thesis was concerned with the microemulsion phase behaviour of polymerizable surfactants with polymerizable oils and water, and the resulting structure of solid polymer materials formed by polymerisation of the parent liquid polymerizable microemulsions. Many of the objectives described in the aims of the thesis have been resolved. The main conclusions derived from this work are provided in the following sections.

### **6.1 Phase behaviour of polymerizable methacrylate surfactants with polymerizable acrylate oils**

The preparation and characterisation of emulsions, microemulsions and surfactant solutions of the nine systems using the three surfactants and the three oils has been described. The effects of temperature and added electrolyte on the macroemulsions and the effects of added electrolyte and initial concentration of surfactant on the partitioning of surfactant between the two phases in microemulsion systems were studied and it was found that:

- (a) All surfactants are most soluble in water with the solubility in the three oils being similar for each surfactant. In general, the order of extent to which the

surfactants dissolve in each solvent is:  $\text{H}_2\text{O} \gg \text{DPGDA} > \text{BDDA} > \text{HDDA}$ . The order of solubility of the surfactants in each solvent is:  $\text{C}_{3/11-\text{M}} > \text{C}_{10} > \text{C}_{12}$ .

(b) Stable o/w emulsions can be produced in all nine systems and no phase inversion occurs with temperature up to  $55^\circ\text{C}$  in any system.

(c) Oil-in-water emulsion breaking occurs at high salt concentrations in all systems with phase inversion to produce w/o emulsions occurring in all systems containing  $\text{C}_{3/11-\text{M}}$  and all systems containing HDDA.

(d) At a certain concentration of salt, the partitioning of surfactant between oil and water changes from mostly in water to mostly in oil in all systems as the preferred curvature of surfactant changes from positive to negative.

(e) The  $\text{C}_{3/11-\text{M}}$  surfactant itself was found to act as a weak salt, lowering the [added salt] required to effect phase inversion and increasing the amount of surfactant that partitions into oil.

(f) Winsor I microemulsion systems were prepared at low salt concentration and Winsor II systems were observed at high salt concentration for systems containing HDDA or DPGDA for each of the three surfactants.

(g) Increasing surfactant chain length increases the monomer partition coefficient  $P$ . Low salt, Winsor I systems show non-ideal surfactant partitioning post-cmc whereas high salt systems show ideal surfactant partitioning post-cmc.

(h) The cmc in water of the surfactants was seen to decrease by a factor of  $\sim 2$  for each additional  $\text{CH}_2$  group on the hydrophobic surfactant chain.  $\text{Cmc}_{\text{water}}$  for a particular surfactant increases with increasing polarity of the oil used for low salt systems but decreases with increasing polarity of the oil used for high salt systems. Increasing [electrolyte] decreases  $\text{cmc}_{\text{water}}$  in all systems.

(i) Increasing polarity of the oil increases  $\text{cmc}_{\text{oil}}$  for a particular surfactant. The effect of increasing [electrolyte] on  $\text{cmc}_{\text{oil}}$  is dependent on the polarity of the oil.

## **6.2 Phase equilibration in high surfactant concentration polymerizable surfactant and oil systems**

Equilibrium microemulsion phases were prepared with increasing  $[\text{surfactant}]_{\text{ini}}$  for each of nine surfactant/ oil systems studied in all. The equilibrium phase volumes, location of aggregates and phase compositions were studied and related to the surfactant and oil molecular structures.

(a) Surfactant  $\text{C}_{3/11-\text{M}}$  was found to contain a high level of impurities resulting in irreproducible phase behaviour when preparing microemulsions with a high  $[\text{surfactant}]_{\text{ini}}$ . A method of purification for surfactant  $\text{C}_{3/11-\text{M}}$  has resulted in the reproducible preparation of microemulsion phases.

(b) The structures of the surfactant and oil affect the microemulsion phase equilibration and formation. A broad range of phase types can be prepared from Winsor I like water continuous phases, through bicontinuous and on to Winsor II like

oil continuous phases by selection of suitable surfactants and oils. Self-inversion was exhibited by all of the surfactants, the extent of inversion depending on the particular surfactant-oil combination. Definite Winsor III systems have not been prepared.

(c) The structures of the surfactant and oil affect the phase behaviour of the system and several trends in equilibrium water content with  $[\text{surfactant}]_{\text{ini}}$  were observed.

- Self-phase inversion with surfactant content occurs in all systems containing DPGDA oil independent of surfactant type, in which control of equilibrium water content is not possible with  $[\text{surfactant}]_{\text{ini}}$ .
- All systems containing HDDA oil, independent of surfactant type are WI-like systems with two aggregate containing water continuous phases (WI\*), in which the control of equilibrium water content is possible with  $[\text{surfactant}]_{\text{ini}}$ .
- The type of phase produced with BDDA oil is dependent on the surfactant type. BDDA with C<sub>10</sub> produces fully inverted WII-like systems in which control of equilibrium water content with  $[\text{surfactant}]_{\text{ini}}$  is possible.

### **6.3 Characteristics of polymer films from microemulsions containing polymerizable surfactants and oils**

Solid polymer films were prepared from liquid equilibrium microemulsion phases containing polymerizable surfactants and polymerizable oils using a photo-initiation polymerisation method. A polymerisation cell was designed and used to prepare reproducible polymer films with controlled dimensions. The films were characterised by visual inspection and handling, electron microscopy and pore volume

fraction. The following conclusions summarise the characteristics of films from the nine microemulsion systems studied.

(a) Transparent, pliable polymer films can be produced using 1 wt. % Darocur 1173 initiator with HDDA oil irradiated with UV for 0.1 minutes.

(b) C<sub>3/11-M</sub> surfactant has been polymerised using UV light with UV initiator Darocur 1173 both as pure surfactant and surfactant solution yielding soft semi-solid polymers.

As surfactant concentration in the droplet prior to polymerisation increases:-

- i) Total time required for polymerisation decreases
- ii) Polymerisation occurs more in bulk than at edges
- iii) Strength / rigidity of polymer increases

(c) Opacity is greater for films prepared from microemulsions with a higher water content. Most water continuous microemulsions produce opaque or cloudy films. The strength of the polymer films decreases with increasing water content of the equilibrium microemulsion and in general, microemulsions with very high water contents either do not polymerise or produce very weak films. Most films are strong but brittle if bent excessively.

(d) Three different microstructures of polymers were observed, which depend on the surfactant and oil type and Winsor phase type of the parent microemulsion. WI\* microemulsion aggregate phases polymerise to form open porous spherical aggregate structures which may form as a result of micelle swelling during the polymerisation

process. WI<sup>i</sup> and WII\* microemulsion aggregate phases polymerise to form nano structured porous polymers. Surfactants with the polymerizable group located on the head group form polymers which contain micrometer sized holes within the nano structured film. These holes were absent in the films prepared from microemulsion phases containing the surfactant with the polymerizable group located on the tail.

(e) Films from aqueous/ bicontinuous phases (which have a high water content) produce films that have a high pore volume fraction, which increases with water content of the equilibrium microemulsion. Films from oil continuous aggregate containing phases (which have a low water content) produce films with a low pore volume fraction, which also increases with increasing water content of the equilibrium microemulsion.

(f) The pore volume fraction of a polymerised WI\* microemulsion phase can be controlled via the equilibrium water content of the microemulsion by adjusting the  $[\text{surfactant}]_{\text{ini}}$ .

(g) The gradient of pore volume fraction vs. equilibrium water content is affected by the surfactant and oil molecular structures. Both film swelling and film shrinkage during the polymerisation process have been observed and are dependent on the location of the surfactant polymerisable group.

# FUTURE WORK

A number of techniques could be used to complement the work described in this thesis and provide a more detailed picture of various aspects of the work which has been discussed. These techniques can be separated into two main areas according to the substrates on which they can provide information: microemulsion phase characterisation and polymer film characterisation. The following section provides a brief description of the information the techniques can provide.

## a) Microemulsion phase characterisation

Although microemulsion continuous phase was determined by the drop test and complete phase compositional analysis was performed, detailed analysis on the fine structure of the microemulsions would yield useful information on the effects of the constituent species on the structure of the resulting microemulsions. This could also be correlated to the microstructure of the resulting polymers, which would yield information on the structural changes occurring during polymerisation. This may allow a more detailed mechanism of polymerisation in these systems to be developed.

### i. Self-diffusion NMR

Nuclear Magnetic Resonance (NMR) can be used to gain information on microemulsion structure. Fourier Transform Pulsed-Gradient Spin-Echo NMR (FT PGSE NMR) can measure the diffusion of solvent molecules in a liquid microemulsion. The diffusion path of solvent molecules in a microemulsion system



depends on the physical structure of the domains in which the solvent molecules are located. Measurement of the self-diffusion coefficients by FT PGSE NMR allows the domain structure (i.e. droplets, bicontinuous etc.) and domain size to be determined.

## ii. Neutron Scattering

Small Angle Neutron Scattering (SANS) is a powerful technique which involves measuring the extent (angle) of neutrons scattered by an object (e.g. micelle). The scattered angle and intensity of neutrons from a microemulsion phase can provide detailed information about size and structure of the microemulsion domains. In addition to this, information about the structure of micelles, such as the thickness and orientation of a surfactant monolayer in an aggregate is possible. Various parts of the aggregate can be studied separately using a technique called contrast matching, allowing the micelle core or bicontinuous domain size to be distinguished from the surfactant monolayer.

## b) Polymer film characterisation

Porosity by pore volume fraction has been measured for each of the polymer films prepared, providing a useful quantity to characterise the films. Another quantity which would be useful to measure is the pore size distribution. The rate of water (and ink) uptake by the polymer films will be affected by the size of the pores in the polymer. This may affect the drying rate of the films once deposited on acetate sheets. This is an important parameter in the ink-jet printing industry as acceptable drying times are in a fairly narrow range. Mercury porosimetry (used for thin films) would enable measurement of pore size in open pore polymer films.

# *APPENDIX 1*

# APPENDIX 1

## DATA PRESENTED IN CHAPTER 3

Data presented in Figures 3.1 to 3.4

[C <sub>3/11-m</sub> ] / wt. %	solvent and temperature of dissolution / °C			
	Water	DPGDA	BDDA	HDDA
0.2	23.1	23.1	22.5	27.5
0.5	23.1	27.5	22.5	27.5
1	23.1	32.5	27.5	32.5
2	23.1	37.5	32.5	37.5
5	23.1	42.5	37.5	42.5

Data presented in Figure 3.5

Oil	Temp / °C	$\kappa / \mu\text{Scm}^{-1}$	Oil	Temp / °C	$\kappa / \mu\text{Scm}^{-1}$
HDDA	10	419	DPGDA	10	360
HDDA	15	483	DPGDA	15	433
HDDA	20	540	DPGDA	20	495
HDDA	25	593	DPGDA	25	548
HDDA	30	646	DPGDA	30	608
HDDA	35	710	DPGDA	35	660
HDDA	40	783	DPGDA	40	723
HDDA	45	846	DPGDA	45	769
HDDA	50	923	DPGDA	50	822
HDDA	55	984	DPGDA	55	885
BDDA	10	386			
BDDA	15	422			
BDDA	20	463			
BDDA	25	505			
BDDA	30	549			
BDDA	35	588			
BDDA	40	649			
BDDA	45	698			
BDDA	50	758			

BDDA	55	817
------	----	-----

**Data presented in Figures 3.6 to 3.8**

HDDA		BDDA		DPGDA	
[NaBr] / M	$\kappa / \mu\text{S cm}^{-1}$	[NaBr] / M	$\kappa / \mu\text{S cm}^{-1}$	[NaBr] / M	$\kappa / \mu\text{S cm}^{-1}$
1.00E-03	600	1.00E-03	485	1.00E-03	550
1.00E-02	924	5.00E-03	605	5.00E-03	590
2.00E-02	1260	1.00E-02	805	1.00E-02	818
3.00E-02	1630	2.00E-02	1150	2.00E-02	850
4.00E-02	1976	3.00E-02	1430	2.50E-02	880
5.00E-02	2500	4.00E-02	1873	3.00E-02	890
5.50E-02	2400	4.50E-02	2020	4.00E-02	1000
6.00E-02	3	5.00E-02	20	4.50E-02	1300
1.00E-01	3	1.00E-01	17	5.00E-02	1892
				6.00E-02	60
				1.00E-01	60

**Data presented in Figure 3.10**

[NaBr] / M	[C <sub>3/11-M</sub> ] / mM	[C <sub>3/11-M</sub> ] / mM
	Aqueous	HDDA
0.005	15.91	3.40
0.01	14.70	3.92
0.02	14.63	4.88
0.03	13.73	5.19
0.04	13.46	6.29
0.05	12.01	7.11
0.06	11.88	7.96
0.07	9.73	9.24
0.10	7.83	15.64
0.08	7.30	10.27
0.09	4.96	14.68
0.12	4.20	14.91
0.14	3.55	14.95
0.16	3.36	15.03
0.18	3.26	15.11
0.20	3.15	15.19
0.23	3.03	15.23

**Data presented in Figure 3.12**

[NaBr] / M	[C <sub>3/11-M</sub> ] / mM Aqueous	[C <sub>3/11-M</sub> ] / mM BDDA
0.00	15.33	6.25
0.005		7.81
0.01	11.47	9.69
0.02	8.03	12.56
0.03	6.25	14.43
0.04	4.94	15.31
0.05	4.22	16.03
0.06	3.94	16.42
0.07	3.47	17.16
0.10	2.54	17.63
0.09	3.52	17.80
0.12	3.36	17.88
0.13	3.25	17.96

**Data presented in Figure 3.14**

[NaBr] / M	[C <sub>3/11-M</sub> ] / mM Aqueous	[C <sub>3/11-M</sub> ] / mM HDDA
0.00	63.10	28.40
0.02	48.40	42.00
0.04	28.30	60.50
0.05	16.90	72.00
0.06	14.90	74.00
0.07	8.88	76.00
0.08	8.16	77.00
0.10	6.40	78.50
0.12	5.26	80.50
0.14	4.50	81.00
0.16	4.00	81.25

**Data presented in Figure 3.16**

[C <sub>3/11-M</sub> ] / mM Aqueous	[C <sub>3/11-M</sub> ] / mM HDDA
4.06	1.18
5.85	1.76
7.32	2.06
9.08	2.98
10.96	3.36
12.66	3.80
14.75	3.80
19.45	3.86
24.25	3.76
28.30	3.78
37.55	3.76

**Data presented in Figure 3.17**

[C <sub>3/11-M</sub> ] / mM Aqueous	[C <sub>3/11-M</sub> ] / mM HDDA
0.61	3.64
0.91	6.24
0.98	7.57
1.16	10.81
1.30	13.60
1.31	14.70
1.31	15.66
1.31	20.30
1.31	23.95
1.33	21.42

**Data presented in Figure 3.18**

[C <sub>10</sub> ] / mM Aqueous	[C <sub>10</sub> ] / mM HDDA
16.55	2.81
24.60	4.43
33.18	4.70
41.97	4.76
51.44	5.00
56.22	5.08
62.07	5.43
71.74	5.54
4.78	0.78
8.71	1.02
12.73	1.52
18.98	3.38
21.91	4.24
17.76	2.34

**Data presented in Figure 3.19**

[C <sub>10</sub> ] / mM Aqueous	[C <sub>10</sub> ] / mM HDDA
1.58	1.44
2.27	2.86
2.45	3.33
2.61	3.93
2.76	4.63
2.95	5.02
3.26	6.19
3.38	9.51
3.42	14.15
3.36	19.03
3.41	23.03
3.36	25.18
3.37	29.28
3.36	34.55

**Data presented in Figure 3.20**

[C <sub>12</sub> ] / mM Aqueous	[C <sub>12</sub> ] / mM HDDA
1.66	1.58
2.82	2.56
3.60	3.62
4.46	3.92
6.16	4.28
10.94	4.50
16.00	4.78
20.25	4.82
25.20	5.00
30.35	4.88
35.05	5.30

**Data presented in Figure 3.21**

[C <sub>12</sub> ] / mM Aqueous	[C <sub>12</sub> ] / mM HDDA
0.14	0.79
0.22	3.36
0.33	6.78
0.38	15.60
0.36	17.67
0.36	27.62
0.36	31.33

**Data presented in Figure 3.22**

[C <sub>3/11-M</sub> ] / mM Aqueous	[C <sub>3/11-M</sub> ] / mM DPGDA
1.88	3.01
4.81	4.48
5.44	7.10
9.16	7.58
12.00	11.65
12.95	15.00
15.40	17.60
17.80	20.45
20.00	26.50
26.00	28.90
40.20	32.90
54.40	36.20

**Data presented in Figure 3.23**

[C <sub>3/11-M</sub> ] / mM Aqueous	[C <sub>3/11-M</sub> ] / mM DPGDA
0.20	4.60
0.35	8.48
0.61	13.05
0.62	16.60
0.62	22.05
0.61	25.70
0.66	29.85
0.68	33.50

**Data presented in Figure 3.24**

[C <sub>10</sub> ] / mM Aqueous	[C <sub>10</sub> ] / mM DPGDA
3.96	1.79
7.06	3.07
11.08	5.05
12.30	6.96
14.50	8.04
19.60	10.82
22.90	12.18
25.50	13.66
25.00	21.50
27.00	31.00
29.50	36.00
34.50	41.00
41.25	55.00
49.5	65.25
63.75	77.5

**Data presented in Figure 3.25**

[C <sub>10</sub> ] / mM Aqueous	[C <sub>10</sub> ] / mM DPGDA
0.78	4.74
1.12	9.06
1.57	13.35
2.12	17.10
2.14	18.50
2.14	26.40
2.16	31.05
2.16	35.10

**Data presented in Figure 3.26**

[C <sub>12</sub> ] / mM Aqueous	[C <sub>12</sub> ] / mM DPGDA
2.64	3.72
3.46	5.16
6.40	8.86
9.10	11.80
11.00	14.40
12.00	20.75
14.05	24.75
14.95	29.45
15.20	36.00
18.6	40.25
28.30	48.75
38.25	58.00

**Data presented in Figure 3.27**

[C <sub>12</sub> ] / mM Aqueous	[C <sub>12</sub> ] / mM DPGDA
0.06	4.90
0.13	9.74
0.18	11.42
0.24	14.63
0.27	19.05
0.26	24.85
0.26	30.20
0.26	34.65
0.26	38.10



**Data presented in Figure 3.28**

Partition coefficient	Carbon chain length
22.228	11
64.767	12

**Data presented in Figure 3.29**

HDDA NaBr / M	cmc <sub>water</sub> / mM	Surf. chain length
0.01	23.0	10
	12.3	11
	4.8	12
0.5	3.4	10
	1.3	11
	0.4	12
DPGDA [NaBr] / M	cmc <sub>water</sub> / mM	Surf. chain length
0.01	25.5	10
	22.7	11
	17.0	12
0.5	2.1	10
	0.6	11
	0.3	12

# *APPENDIX 2*

## APPENDIX 2

### DATA PRESENTED IN CHAPTER 4

Data presented in Figures 4.18 to 4.20

Phase	$[C_{3/11-M}]_{ini} / M$	water / wt. %	$C_{3/11-M} / wt. \%$	HDDA / wt. %
upper	0.24	1.1	0.4	98.5
	0.48	0.7	0.4	98.9
	0.76	0.2	0.4	99.3
	0.95	1.0	0.4	98.5
	1.14	1.2	0.4	98.3
middle	0.48	49.7	17.5	31.3
	0.76	34.6	23.2	40.2
	0.95	33.2	27.4	37.1
	1.14	28.5	30.3	38.6
lower	0.24	72.0	7.0	20.4
	0.48	71.6	13.9	13.3
	0.76	62.4	22.4	13.3
	0.95	55.3	29.2	13.0
	1.14	48.5	37.3	10.9

Data presented in Figures 4.21 to 4.23

Phase	$[C_{3/11-M}]_{ini} / M$	water / wt. %	$C_{3/11-M} / wt. \%$	BDDA / wt. %
upper	0.24	2.0	1.6	96.4
	0.48	1.7	1.7	96.6
	0.77	2.0	1.7	96.2
	0.96	1.6	1.2	97.2
middle	0.48	46.0	12.8	40.7
	0.77	37.0	19.6	42.5
	0.96	28.2	22.0	48.9
lower	0.24	73.9	6.5	19.4
	0.48	63.7	13.0	22.7
	0.77	58.2	20.8	20.1
	0.96	50.1	26.2	22.6

**Data presented in Figures 4.24 to 4.26**

Phase	$[C_{3/11-M}]_{ini} / M$	water / wt. %	$C_{3/11-M} / wt. \%$	DPGDA / wt. %
upper	0.24	3.0	2.6	94.2
	0.48	4.2	4.8	90.7
	0.77	5.6	7.0	87.1
	0.96	11.0	12.3	76.2
	1.152	12.9	17.5	68.9
middle	0.48	57.5	9.8	32.3
	0.77	40.1	16.4	42.8
	0.96	43.3	20.2	35.7
lower	0.24	77.6	5.0	17.2
	0.48	60.2	9.7	29.7
	0.77	56.6	15.3	27.4
	0.96	85.3	3.4	11.2
	1.152	41.2	24.3	33.5

**Data presented in Figures 4.27 to 4.29**

Phase	$[C_{10}]_{ini} / M$	water / wt. %	$C_{10} / wt. \%$	HDDA / wt. %
upper	4.95	0.7	0.5	98.8
	14.85	1.7	1.1	97.2
	17.82	1.5	1.0	97.5
	21.78	1.4	1.2	97.4
	24.75	1.7	1.5	96.8
middle	14.85	53.5	23.4	22.9
	17.82	48.7	26.6	24.4
	21.78	44.0	29.5	26.2
	24.75	39.5	34.9	25.3
lower	4.95	78.1	8.3	13.5
	14.85	63.4	19.6	16.8
	17.82	58.4	23.6	17.8
	21.78	55.0	26.9	17.8
	24.75	54.3	31.5	13.9

**Data presented in Figures 4.30 to 4.32**

Phase	[C <sub>10</sub> ] <sub>ini</sub> / M	Water / wt. %	C <sub>10</sub> / wt. %	BDDA / wt. %
upper	4.95	3.2	5.6	91.1
	14.85	7.5	15.0	77.3
	17.82	8.3	15.5	76.1
	21.78	13.3	23.3	63.2
	24.75	14.9	27.1	57.7
middle	14.85	15.0	26.7	58.0
	17.82	19.7	30.1	49.9
	21.78	21.8	31.5	46.4
	24.75	24.3	33.0	42.4
lower	4.95	84.0	4.5	11.6
	14.85	74.2	7.9	17.9
	17.82	70.0	10.3	19.5
	21.78	78.9	6.7	14.3
	24.75	82.4	3.9	13.7

**Data presented in Figures 4.33 to 4.35**

Phase	[C <sub>10</sub> ] <sub>ini</sub> / M	Water / wt. %	C <sub>10</sub> / wt. %	DPGDA / wt. %
upper	4.95	3.4	4.4	92.2
	14.85	7.1	11.6	81.2
	17.82	10.9	17.2	71.7
	21.78	11.0	17.5	71.3
	24.75	12.0	19.8	68.0
middle	17.82	52.6	17.8	29.5
	21.78	46.4	23.6	29.8
	24.75	46.0	28.7	25.0
lower	4.95	80.7	4.9	14.4
	14.85	59.9	15.6	24.4
	17.82	55.1	17.4	27.3
	21.78	51.8	23.3	24.7
	24.75	53.7	11.3	34.9

**Data presented in Figures 4.36 to 4.38**

Phase	$[C_{12}]_{ini} / M$	Water / wt. %	$C_{12} / wt. \%$	HDDA / wt. %
upper	0.5	1.1	0.3	98.7
	5	1.2	0.7	98.1
	15	2.3	4.7	93.0
	20	1.4	1.6	97.0
	25	1.7	10.1	88.2
middle	15	53.8	22.7	23.5
	20	40.3	25.1	34.6
	25	28.8	28.3	42.9
lower	0.5	89.6	0.9	9.6
	5	77.4	8.4	14.2
	15	66.5	25.5	8.0
	20	39.0	26.5	34.5
	25	31.2	29.8	39.0

**Data presented in Figures 4.39 to 4.41**

Phase	$[C_{12}]_{ini} / M$	Water / wt. %	$C_{12} / wt. \%$	BDDBA / wt. %
upper	5	3.1	4.8	92.0
	15	11.8	20.1	68.0
	20	12.9	26.5	60.6
	25	16.6	30.6	52.8
middle	15	11.2	21.0	67.8
	20	15.8	26.5	57.7
	25	18.6	30.6	50.9
lower	5	83.1	5.1	11.9
	15	82.5	4.6	12.9
	20	87.0	0.4	12.6
	25	85.6	0.2	14.2

**Data presented in Figures 4.42 to 4.44**

Phase	$[C_{12}]_{ini} / M$	Water / wt. %	$C_{12} / wt. \%$	DPGDA / wt. %
upper	5.0	3.7	4.8	91.5
	15.0	9.2	18.3	72.5
	18.0	14.5	22.3	63.1
	22.0	18.3	26.6	55.1
	25.0	20.3	29.6	50.1
middle	22.0	21.1	26.3	52.7
	25.0	24.7	28.5	46.8
lower	5.0	79.6	5.3	15.2
	15.0	72.4	11.1	16.5
	18.0	69.9	11.7	18.3
	22.0	73.8	9.5	16.7
	25.0	83.7	2.4	13.8

# *APPENDIX 3*



# APPENDIX 3

## DATA PRESENTED IN CHAPTER 5

**Data presented in Figure 5.1**

t / min	[C <sub>3/11-M</sub> ] / M
20	0.23
18	0.45
15	0.72
13	0.9
9	1.08
2	2.14

**Data presented in Figure 5.79**

Phase	PVF / %	Water content / wt. %
middle	89.9	49.7
	80.3	34.6
	11.0	33.2
	39.1	28.5
lower	79.0	71.6
	65.1	62.4
	37.0	55.3
	66.7	48.5

**Data presented in Figure 5.80**

Phase	PVF / %	Water content / wt. %
middle	64.6	46.0
	56.6	37.0
	35.5	28.2
	88.6	63.7
lower	84.2	58.2
	88.6	50.1

**Data presented in Figure 5.81**

Phase	PVF / %	Water content / wt. %
middle	43.8	40.1
	49.1	43.3
lower	80.8	56.6
	53.1	41.2

**Data presented in Figure 5.82**

Phase	PVF / %	Water content / wt. %
middle	46.9	53.5
	45.3	48.7
	45.4	44.0
	42.3	39.5
lower	47.7	58.4
	47.7	55.0

**Data presented in Figure 5.83**

Phase	PVF / %	Water content / wt. %
upper	2.8	3.2
	7.1	7.5
	6.3	8.3
	10.1	13.3
	13.0	14.9
middle	8.8	15.0
	9.8	19.7
	13.5	21.8
	15.4	24.3

**Data presented in Figure 5.84**

Phase	PVF / %	Water content / wt. %
upper	3.5	3.4
	4.7	7.1
	7.0	10.9
	6.9	11.0
	6.0	12.0
middle	34.5	52.6
	41.7	46.4
lower	45.9	51.8
	53.7	53.7

**Data presented in Figure 5.85**

Phase	PVF / %	Water content / wt. %
middle	53.6	53.8
	37.6	40.3
	22.9	28.8
lower	63.3	66.5
	39.6	39.0
	28.7	31.2

**Data presented in Figure 5.86**

Phase	PVF / %	Water content / wt. %
upper	3.2	3.1
	6.6	11.8
	6.5	12.9
	7.0	16.6
middle	8.2	11.2
	12.2	15.8
	12.9	18.6

**Data presented in Figure 5.87**

Phase	PVF / %	Water content / wt. %
upper	3.8	3.7
	8.0	9.2
	9.5	14.5
	13.3	18.3
	16.1	20.3
middle	15.7	21.1
	20.5	24.7

Data presented in Figure 5.88

C <sub>3/11-M</sub> / HDDA		C <sub>3/11-M</sub> / BDDA		C <sub>3/11-M</sub> / DPGDA	
PVF / %	Water content / wt. %	PVF / %	Water content / wt. %	PVF / %	Water content / wt. %
89.9	49.72	64.6	46.0	2.7	3.0
80.3	34.61	56.6	37.0	3.8	4.2
11.0	33.17	35.5	28.2	4.5	5.6
39.1	28.46	88.6	63.7	10.1	11.0
79.0	71.58	84.2	58.2	21.0	12.9
65.1	62.36	88.6	50.1	43.8	40.1
37.0	55.28			49.1	43.3
66.7	48.52			80.8	56.6
				53.1	41.2
C <sub>10</sub> / HDDA		C <sub>10</sub> / BDDA		C <sub>10</sub> / DPGDA	
PVF / %	Water content / wt. %	PVF / %	Water content / wt. %	PVF / %	Water content / wt. %
46.9	53.5	2.8	3.2	3.5	3.4
45.3	48.7	7.1	7.5	4.7	7.1
45.4	44.0	6.3	8.3	7.0	10.9
42.3	39.5	10.1	13.3	6.9	11.0
47.7	58.4	13.0	14.9	6.0	12.0
47.7	55.0	8.8	15.0	34.5	52.6
		9.8	19.7	41.7	46.4
		13.5	21.8	45.9	51.8
		15.4	24.3	53.7	53.7
C <sub>12</sub> / HDDA		C <sub>12</sub> / BDDA		C <sub>12</sub> / DPGDA	
PVF / %	Water content / wt. %	PVF / %	Water content / wt. %	PVF / %	Water content / wt. %
53.6	53.8	3.2	3.1	3.8	3.7
37.6	40.3	6.6	11.8	8.0	9.2
22.9	28.8	6.5	12.9	9.5	14.5
63.3	66.5	7.0	16.6	13.3	18.3
39.6	39.0	8.2	11.2	16.1	20.3
28.7	31.2	12.2	15.8	15.7	21.1
		12.9	18.6	20.5	24.7